Masaharu Ishii
Satoshi Wakai *Editors*

Electron-Based Bioscience and Biotechnology

Springer

Electron-Based Bioscience and Biotechnology

Masaharu Ishii • Satoshi Wakai
Editors

Electron-Based Bioscience and Biotechnology

Springer

Editors
Masaharu Ishii
Department of Biotechnology
Graduate School of Agricultural and Life Sciences, The University of Tokyo
Bunkyo-ku, Tokyo, Japan

Satoshi Wakai
Institute for Extra-cutting-edge Science and Technology Avant-garde Research (X-star)
Japan Agency for Marine-Earth Science and Technology (JAMSTEC)
Yokosuka, Japan

ISBN 978-981-15-4762-1 ISBN 978-981-15-4763-8 (eBook)
https://doi.org/10.1007/978-981-15-4763-8

This Springer imprint is published by the registered company Springer Nature Singapore Pte Ltd.
The registered company address is: 152 Beach Road, #21-01/04 Gateway East, Singapore 189721, Singapore

Preface

Living organisms use electron in various biological reactions for energy conversion and signal transduction. For example, electron transport chain in respiration is well characterized, and biological component, which can transfer electrons, is also identified. In addition, various technologies using these electron-transferring properties have been developed, for example, microbial fuel cells and electrochemical biosensors.

On the other hand, novel phenomena related to living organisms and electron have recently been discovered, e.g., novel types of electron bifurcation processes, electrochemically active microorganisms, electrotrophic metabolisms, and metal corrosion by electron-consuming microorganisms. To deeply understand these novel phenomena, we must study using not only traditional biochemical methods, which are biologist friendly, but also electrochemical methods, which are non-friendly for biologists.

This book covers the novel findings and latest knowledge related to "living organisms and electron" as reviewed by experts consisting of senior and young scientists. Especially, this book is composed of three parts: Part I, Electron-Based Bioscience; Part II, Electron-Based Biotechnology; and Part III, Electron-Based Biocorrosion. Each part contains some chapters, and these chapters describe historical information, latest knowledge, and future application of each research field.

We believe that this book will help in deep understanding of relationship between living organisms and electron through detailed description of the electron flow during metabolic process in (micro)organisms and introduction of the development toward resolution of social issues and probable application. We named eBioX as a subtitle of this book. It means electron-based Bio*science*, Bio*technology*, and Bio*corrosion*. We hope that many scientists and students connect to each other through this book, and each research field would be fused and advanced in the near future.

Bunkyo-ku, Tokyo, Japan — Masaharu Ishii
Yokosuka, Japan — Satoshi Wakai

Contents

Part I
Electron Based Bioscience

Chapter 1
Latest Knowledge of Electromicrobiology

Satoshi Wakai

1.1 Introduction

Electrons and living cells are strongly related, particularly in terms of the electron transport chain of respiration and photosynthesis. In the electron transport chain, electrons move via various biomolecules from an electron donor to an electron acceptor. For example, in the mitochondrial electron transport chain, NADH dehydrogenase, quinone, cytochrome bc_1 complex, cytochrome *c*, and cytochrome *c* oxidase are involved in electron transfer from NADH as an electron donor to oxygen as an electron acceptor. Such electron transfer among biomolecules is effective for biological energy conversion because the process is directly connected to each other without diffusion of the reacting substances into water fraction, cytosol and extracellular solvent. Electron transfer in the field of biology is common. However, little is known about inter- and intramolecular electron transfer, although many studies in related fields have been performed.

Recently, novel types of electron bifurcation systems and electron transfer systems such as extracellular electron transfer have been reported. The first study of an electron bifurcation system was performed using cytochrome bc_1 complex, which is a member of the electron transport chain in respiration (Mitchell 1975, 1976); additionally, novel types of flavin- and metal-based electron bifurcation systems in various energy metabolism processes were recently discovered (Li et al. 2008; Peters et al. 2019; Yuly et al. 2019). Similarly, various extracellular electron transfer systems such as outer membrane multi-heme cytochrome, electron conductive pili, and diffusible mediator have recently been characterized. Studies of microbial fuel cells would contribute to the understanding and utilization of these microbial energy

S. Wakai (✉)
Institute for Extra-cutting-edge Science and Technology Avant-garde Research (X-star), Japan Agency for Marine-Earth Science and Technology (JAMSTEC), Yokosuka, Japan
e-mail: wakais@jamstec.go.jp

M. Ishii, S. Wakai (eds.), *Electron-Based Bioscience and Biotechnology*,
https://doi.org/10.1007/978-981-15-4763-8_1

metabolism processes. Thus, "electron-based bioscience" and "electron-based biotechnology" have progressed together.

Recent progress in the fields of electron-based bioscience and biotechnology may be related to increased studies of electromicrobiology in microbiology. This chapter focuses on the progression of electromicrobiology studies in microbiology field.

1.2 Brief History of Electromicrobiology

Although studies related to electromicrobiology have greatly advanced in recent years, conceptual research was performed a long time ago. In 1911, Potter reported that yeast and bacteria can produce electric currents during their metabolism (Potter 1911). After that, many studies have been conducted for a long time, but the production of electric currents by microbial metabolism remained small (Fig. 1.1). In 1988, two different research groups reported two different iron- and manganese-reducing bacteria, *Geobacter* sp. and *Shewanella* sp., which are currently used as model microorganisms in the electromicrobiology field (Myers and Nealson 1988; Lovley and Phillips 1988). Both bacteria can consume organic acids and reduce iron oxide or manganese oxide; electrons liberated from the oxidation of organic acids are transported to extracellular insoluble materials as terminal electron acceptors. These studies were the first demonstration of extracellular electron transport.

This discovery of extracellular electron transport established the field of "electromicrobiology" and greatly contributed to the progression of microbial fuel cell research, as the current produced by electrochemically active microorganisms was notably higher than previously known (Kim et al. 1999; Logan et al. 2006; Lovley 2006). In these microorganisms, electrons flow from the cytosol outward to the extracellular space. Inward electron flow also occurs. A simple model of electron flow is iron and sulfur oxidation in the acidophile *Acidithiobacillus ferrooxidans* (Wakai 2019). Although this electron flow connects extracellular molecules and intracellular metabolism, studies have not focused on *A. ferrooxidans* as an electrochemically active microorganism for a long time. However, this microorganism contributed to the development of an electrochemical cultivation method. In this system, iron-oxidizing bacterium uses ferrous ion reduced by an external power supply and can grow to higher densities compared to in conventional batch culture (Matsumoto et al. 1999). Although this simple approach involved indirect electrochemical cultivation, the situation changed dramatically in 2015.

Ishii et al. demonstrated that the iron- and sulfur-oxidizing *A. ferrooxidans* can grow by consuming electrons directly from an electrode, known as electrolithoautotrophic growth (Ishii et al. 2015). The chemolithotrophic growth of this bacterium was demonstrated in 1951 (Temple and Colmer 1951), prior to the discovery of *Shewanella* and *Geobacter*. Extracellular electron transfer during metabolism in *A. ferrooxidans* has not been recently studied, but can be used as a model of electrotrophic metabolism. The term "electrotrophy" was firstly used in 2011 (Lovley 2011), although electrotrophic metabolism has not been well-defined.

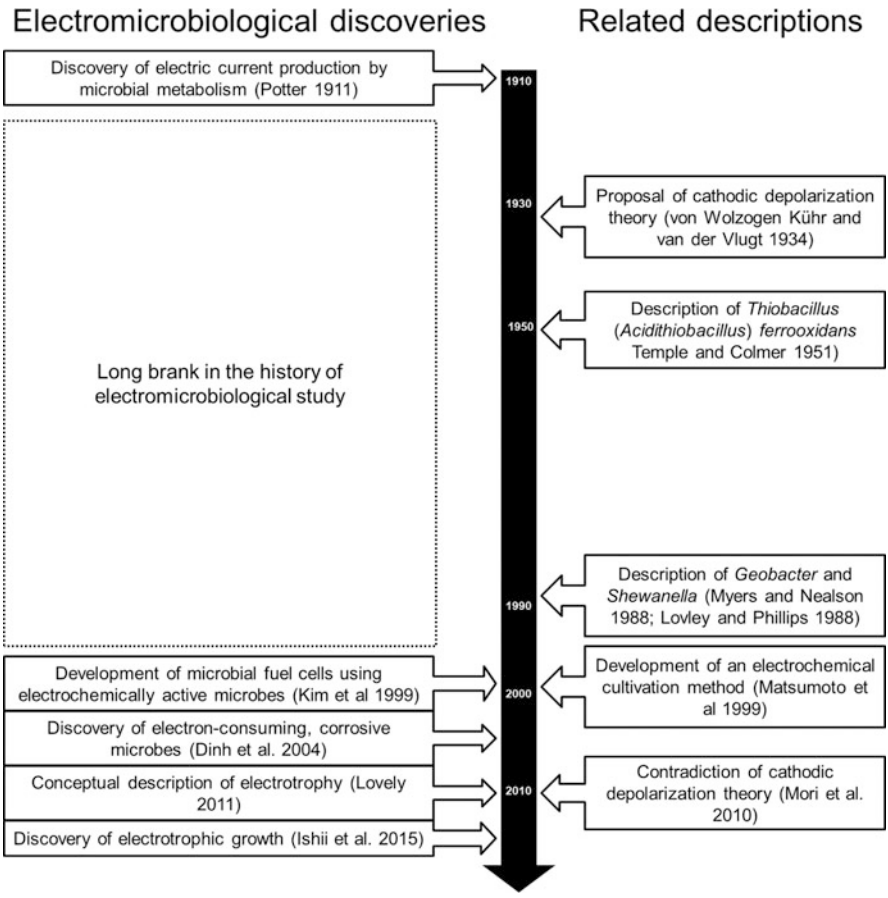

Fig. 1.1 Brief chronological table of electromicrobiology studies

Previously, electrotrophy-like metabolism was reported in iron-corrosive microorganisms (Dinh et al. 2004). Although the term electrotrophy was not evaluated by Dinh et al. (2004), it has been reported that novel types of sulfate-reducing bacteria and methane-producing archaea can corrode metallic iron (Fe^0) by directly consuming electrons in solid-state Fe^0. In 1934, cathodic depolarization theory, which is the concept of iron corrosion by hydrogen-consuming sulfate-reducing bacteria, was reported (von Wolzogen Kühr and van der Vlugt 1934); since then, it has been thought that hydrogen-consuming microorganisms can corrode metal materials by consuming atomic and molecular hydrogen generated chemically on the cathodic area. However, almost all hydrogen-consuming microorganisms excepting for part of iron-corrosive microorganisms do not accelerate corrosion (Mori et al. 2010). In addition, Mori et al. demonstrated the presence of true iron-corrosive microbe from clearly accelerated iron dissolution (2010). Namely, the cathodic depolarization theory cannot explain corrosion mechanism by hydrogen-consuming bacteria, and

the reports of iron-corrosive microorganisms as electrotrophs have changed current thinking about the corrosive microorganisms.

Studies of electromicrobiology have progressed in various fields. Various types of electrochemically active microorganisms and energy metabolism processes have been discovered, and these discoveries can contribute to the development of new technology such as electrobiosynthesis, that is, established by combined research microbial fuel cells and electrotrophy.

1.3 Biological Molecules of Electrochemically Active Microorganisms

Microorganisms capable of transferring directly electrons to extracellular substances or acquiring electrons from extracellular substances are referred to as electrochemically active microorganisms. This unique ability is named as extracellular electron transfer, which differs from the electron transport chain that is completely on the inner membrane. The extracellular electron transfer system can be broadly divided into two modes, direct electron transfer and mediated electron transfer (Fig. 1.2).

Shewanella and *Geobacter* use direct electron transfer which involves biological molecules, with multi-heme cytochromes and cytochrome network as the key components (Nealson and Rowe 2016). This electron transfer process has been well-studied (Santos et al. 2015; Edwards et al. 2017). Recently, in addition to *Shewanella* and *Geobacter*, direct electron transfer systems were demonstrated in the iron-corrosive, sulfate-reducing bacteria *Desulfovibrio ferrophilus* and *Desulfobacterium corrodens* (Deng et al. 2015; Beese-Vasbender et al. 2015). Additionally, iron-corrosive methanogen *Methanococcus maripaludis* KA1 can corrode metallic iron by acquiring electrons from a metal surface (see Chap. 14), but does not contain a cytochrome system and likely possesses other biological molecules for this purpose.

Shewanella oneidensis MR-1 uses not only a direct electron transfer system but also a mediated electron system (Nealson and Rowe 2016; Gralnick 2012; Gross and El-Naggar 2015). In the mediated electron transfer in *Shewanella*, multi-heme cytochromes are cellular components, and diffusible flavin is an extracellular component. In addition to flavin, a menaquinone derivative and phenazine derivative have been reported as biological electron mediators (Newman and Kolter 2000; Rabaey et al. 2005). Flavin-based extracellular electron transfer systems are found in gram-positive bacteria (Light et al. 2018), which have a thick cell wall compared to gram-negative bacteria such as *Shewanella*, *Geobacter*, and iron-corrosive sulfate-reducing bacteria. Thus, their extracellular electron transfer system remained unknown for a long time. These findings further extend the distribution of extracellular electron transfer abilities in microbiology.

Furthermore, the concept of electron conductive biofilms has been reported (Lovley 2008). Direct extracellular electron transfer is ineffective because only

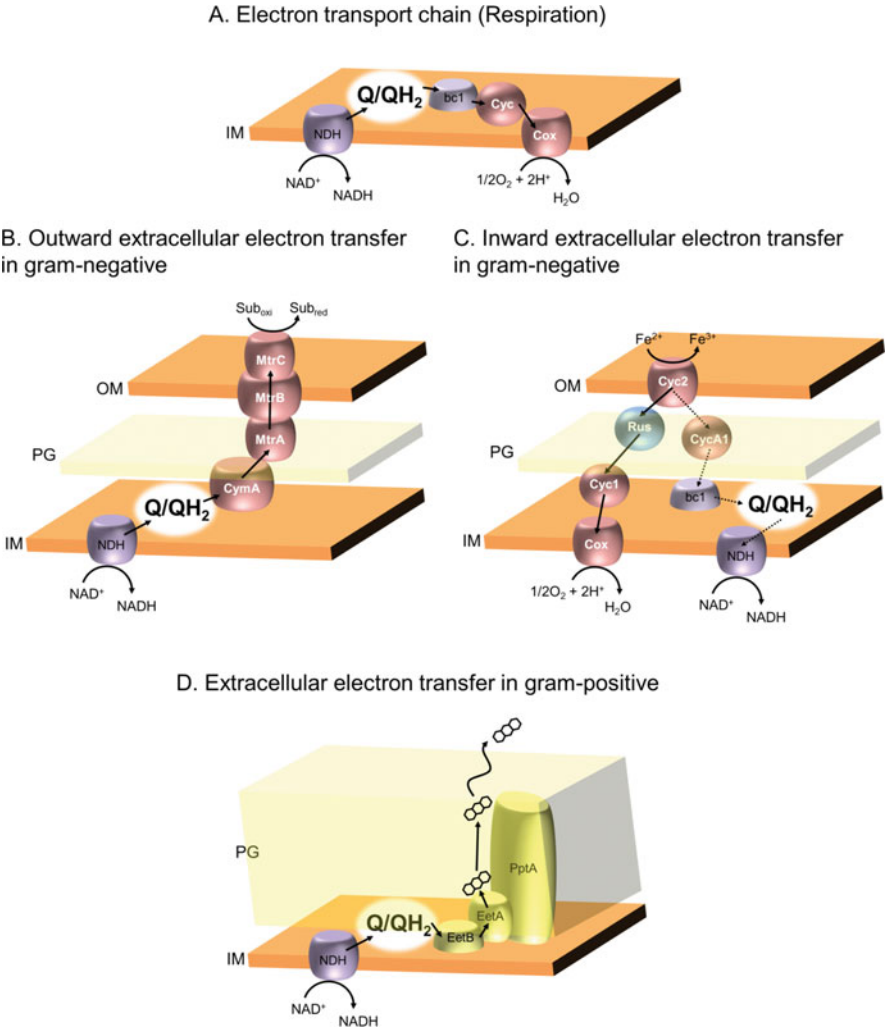

Fig. 1.2 Various electron transfer systems. (**a**) Mitochondrial electron transport chain in respiration. This is not extracellular transfer system because electron transfer complete on the inner membrane. (**b**, **c**) Outward and inward electron transport chains in gram-negative bacteria. Outward type is multi-heme cytochrome type of extracellular electron transfer. Inward type is iron-oxidizing model in *A. ferrooxidans*. (**d**) Extracellular electron transfer using flavin in gram-positive bacteria

single-layered cells on the substrate surface acquire electrons. Mediated extracellular electron transfer proves ineffective because electron mediators are discrete in the natural environment. Also, several microbial cells survive by forming biofilms. The concept of electron conductive biofilms, comprising a combination of direct and mediated extracellular electron transfer systems, is reasonable because these systems effectively use limited substrate surface.

1.4 Application of Electrochemically Active Microorganisms

Studies of electrochemically active microorganisms have mainly focused on *Shewanella* and *Geobacter*. These bacteria can transfer electrons from organic matter to electrodes in microbial fuel cells. Specifically, the energy metabolism of *Shewanella* and *Geobacter* can generate electric current, and hence these bacteria are known as "electric bacteria," "electricigens," and so on. However, the production of electric current is insufficient to replace thermal and nuclear power generation, and the technology of microbial fuel cells has been applied to waste water treatment. Its application in waste water treatment contributes to the reduction of solid waste materials and methane during operation.

On the other hand, these bacteria can transfer electrons in the opposite direction by controlling the potential. Specifically, electrons from an external power source can be transferred to molecules in the microbial cells. This allows the production of a variety of chemicals from CO_2 and small volatile fatty acids; this technology is known as electrobiosynthesis and microbial electrosynthesis. Recently, similar studies were carried out, and various volatile fatty acids such as acetate, propionate, butyrate, valerate, caproate, and succinate were successfully produced (Andersen et al. 2015; Prochaska et al. 2018; Prévoteau et al. 2019). Although low productivities and sources of external power in these systems pose challenging, this technology would contribute to reduce the emission of carbon dioxide.

In addition to microbial fuel cells and chemical production, there have been recent developments in the field of bioremediation using electrochemically active microorganisms. For example, soluble, toxic metal ions such as chromium and uranium could be reduced and deposited as nontoxic metal hydroxides (Hsu et al. 2012). Similarly, the possibility of electrobiochemical reduction of arsenate, selenate, and selenite has been reported (Kato 2015). Furthermore, the effective removal of nitrobenzene by the combination of *Shewanella* sp. and a mediator-modified matrix has been reported (Wang et al. 2013). The applications of electrochemically active microorganisms and their biological components are expected to expand.

1.5 Important Techniques in Modern Microbiology

1.5.1 Development of Sequencing Technologies

In the recent development of microbiology, next-generation sequencing technology has made a significant contribution. Microbial community analysis by meta-16S analysis has revealed several uncultured microorganisms and contributed to our understanding of microbial dynamics in the field of ecology. Metagenomic analyses have revealed the genomic structure of uncultured microorganisms in natural environments, including extreme environments, and discovered several novel and useful

enzymes by heterologous expression of homologous genes and unknown function genes. Metatranscriptomic analyses have revealed the functional dynamics of environmental microorganisms, including uncultured microorganisms. In the past decade, the equipment for next-generation sequencing has become a familiar research tool, and many researchers have been able to use the technology and related services on a daily basis. It is suggested that this technology has accelerated research on environmental microorganisms.

Although next-generation sequencing is a technique for analyzing a large amount of short reads, the technique of long-read analysis has become widespread recently and has become an indispensable technique for whole-genome analysis (Loman and Pallen 2015). Furthermore, as one of the nanopore sequencers that can perform long-read analysis, MinION has been developed, which can be used for fieldwork and can be carried out in the field of view; it is also called the fourth-generation sequencer. Its versatility is also being reported, including applications of whole-genome analysis performed using data from only this nanopore sequencer (Loman et al. 2015), metagenomic analysis (Moss et al. 2020), meta-16S analysis (Gonçalves et al. 2020), and metatranscriptome analysis (Semmouri et al. 2020). I has also succeeded in analyzing a tandem repeat structure (50–100 kbp in length), which is difficult for short-read sequencer analysis, by using it for genome resequencing analysis of genetically engineered filamentous fungi (unpublished).

The handy-type nanopore sequencer is claimed to be useful in field work, and will be in demand for onboard analysis in long-term research cruises. In addition, in technical fields using microbial communities such as microbial fuel cells, it may be possible to use on-site microbial communities for quality control.

1.5.2 Novel Cultivation System

In the field of electromicrobiology, the technology of electrochemical cultivation has been established, and with developments in the field of microbial fuel cells, the electrochemical activities of various microorganisms have been revealed. The concept of electrotrophy as the third energy acquisition system of life has also emerged from this field. Electrochemical cultivation systems have become an essential tool for the isolation of electrotrophs and understanding of their physiology. Therefore, the departure from Koch's established culture technology and the design of a novel culture technology needs to be explored further for the development of microbiology. In fact, several microorganisms are still uncultivable at present, and a technique for culturing them is required for discovering new biochemical phenomena and analyzing functions of genes with unknown functions.

1.6 Concluding Remarks

The relationship between life phenomena and electrons is not a novel discovery in the history of biology. In the field of microbiology, extensive research and development has occurred in electromicrobiology. This may be owing to contributions from applied research on the development of microbial fuel cells and the basic science of proposing a new concept of electrotrophy. In addition, the recent development of genome analysis tools has made a significant contribution to visualizing the whole picture of microorganisms. However, despite the revelation of the phylogenetic position of novel microorganisms and their genomic information, several aspects remain unelucidated. For further development of microbiology in the future, it is necessary to link vast genomic information to biological functions. For this, it will be necessary to stably culture huge amounts of uncultured microorganisms. On the other hand, culturing these dark matter microorganisms would remain impossible if we rely on traditional culture techniques alone; there is a need to establish a culture method based on a novel concept.

References

Andersen SJ, Candry P, Basadre T, Khor WC, Roume H, Hernandez-Sanabria E, Coma M, Rabaey K (2015) Electrolytic extraction drives volatile fatty acid chain elongation through lactic acid and replaces chemical pH control in thin stillage fermentation. Biotechnol Biofuels 8:221

Beese-Vasbender PF, Nayak S, Erbe A, Stratmann M, Mayrhofer KJJ (2015) Electrochemical characterization of direct electron uptake in electrical microbially influenced corrosion of iron by the lithoautotrophic SRB *Desulfopila corrodens* strain IS4. Electrochim Acta 167:321–329

Deng X, Nakamura R, Hashimoto K, Okamoto A (2015) Electron extraction from an extracellular electrode by *Desulfovibrio ferrophilus* strain IS5 without using hydrogen as an electron carrier. Electrochemistry 83:529–531

Dinh HT, Kuever J, Mussmann M, Hassel AW, Stratmann M, Widdel F (2004) Iron corrosion by novel anaerobic microorganisms. Nature 427:829–832

Edwards MJ, Gates AJ, Butt JN, Richardson DJ, Clarke TA (2017) Comparative structure-potentio-spectroscopy of the *Shewanella* outer membrane multiheme cytochromes. Curr Opin Electrochem 4:199–205

Gonçalves AT, Collipal-Matamal R, Valenzuela-Muñoz V, Nuñez-Acuña G, Valenzuela-Miranda-D, Gallardo-Escárate C (2020) Nanopore sequencing of microbial communities reveals the potential role of sea lice as a reservoir for fish pathogens. Sci Rep 10:2895

Gralnick JA (2012) On conducting electron traffic across the periplasm. Biochem Soc Trans 40:1178–1180

Gross BJ, El-Naggar MY (2015) A combined electrochemical and optical trapping platform for measuring single cell respiration rates at electrode interfaces. Rev Sci Instrum 86:064301

Hsu L, Masuda SA, Nealson KH, Pirbazari M (2012) Evaluation of microbial fuel cell Shewanella biocathodes for treatment of chromate contamination. RSC Adv 2:5844–5855

Ishii T, Kawaichi S, Nakagawa H, Hashimoto K, Nakamura R (2015) From chemolithoautotrophs to electrolithoautotrophs: CO2 fixation by Fe(II)-oxidizing bacteria coupled with direct uptake of electrons from solid electron sources. Front Microbiol 6:994

Kato S (2015) Biotechnological aspects of microbial extracellular electron transfer. Microbes Environ 30:133–139

Kim BH, Kim HJ, Hyun MS, Park DH (1999) Direct electrode reaction of Fe (III)-reducing bacterium, *Shewanella putrefaciens*. J Microbiol Biotechnol 9:127–131
Li F, Hinderberger J, Seedorf H, Zhang J, Buckel W, Thauer RK (2008) Coupled ferredoxin and crotonyl coenzyme A (CoA) reduction with NADH catalyzed by the butyryl-CoA dehydrogenase/Etf complex from Clostridium kluyveri. J Bacteriol 190:843–850
Light SH, Su L, Rivera-Lugo R, Cornejo JA, Louie A, Iavarone AT, Ajo-Franklin CM, Portnoy DA (2018) A flavin-based extracellular electron transfer mechanism in diverse Gram-positive bacteria. Nature 562:140–144
Logan BE, Hamelers B, Rozendal R, Schröder U, Keller J, Freguia S, Aelterman P, Verstraete W, Rabaey K (2006) Microbial fuel cells: methodology and technology. Environ Sci Technol 40:5181–5192
Loman NJ, Pallen MJ (2015) Twenty years of bacterial genome sequencing. Nat Rev Microbiol 13:787–794
Loman NJ, Quick J, Simpson JT (2015) A complete bacterial genome assembled de novo using only nanopore sequencing data. Nat Methods 12:733–735
Lovley DR (2006) Bug juice: harvesting electricity with microorganisms. Nat Rev Microbiol 4:497–508
Lovley DR (2008) The microbe electric: conversion of organic matter to electricity. Curr Opin Biotechnol 19:564–571
Lovley DR (2011) Powering microbes with electricity: direct electron transfer from electrodes to microbes. Environ Microbiol Rep 3:27–35
Lovley DR, Phillips EJ (1988) Novel mode of microbial energy metabolism: organic carbon oxidation coupled to dissimilatory reduction of iron or manganese. Appl Environ Microbiol 54:1472–1480
Matsumoto N, Nakasono S, Ohmura N, Saiki H (1999) Extension of logarithmic growth of Thiobacillus ferrooxidans by potential controlled electrochemical reduction of Fe(III). Biotechnol Bioeng 64:716–721
Mitchell P (1975) The protonmotive Q cycle: a general formulation. FEBS Lett 59:137–139
Mitchell P (1976) Possible molecular mechanisms of the protonmotive function of cytochrome systems. J Theor Biol 62:327–367
Mori K, Tsurumaru H, Harayama S (2010) Iron corrosion activity of anaerobic hydrogen-consuming microorganisms isolated from oil facilities. J Biosci Bioeng 110:426–430
Moss EL, Maghini DG, Bhatt AS (2020) Complete, closed bacterial genomes from microbiomes using nanopore sequencing. Nat Biotechnol. https://doi.org/10.1038/s41587-020-0422-6. [Epub ahead of print]
Myers CR, Nealson KH (1988) Bacterial manganese reduction and growth with manganese oxide as the sole electron acceptor. Science 240:1319–1321
Nealson KH, Rowe AR (2016) Electromicrobiology: realities, grand challenges, goals and predictions. Microb Biotechnol 9:595–600
Newman DK, Kolter R (2000) A role for excreted quinones in extracellular electron transfer. Nature 405:94–97
Peters JW, Beratan DN, Bothner B, Dyer RB, Harwood CS, Heiden ZM, Hille R, Jones AK, King PW, Lu Y, Lubner CE, Minteer SD, Mulder DW, Raugei S, Schut GJ, Seefeldt LC, Tokmina-Lukaszewska M, Zadvornyy OA, Zhang P, Adams MW (2019) A new era for electron bifurcation. Curr Opin Chem Biol 47:32–38
Potter MC (1911) Electrical effects accompanying the decomposition of organic compounds. Proc R Soc B Biol Sci 84:260–276
Prévoteau A, Carvajal-Arroyo JM, Ganigué R, Rabaey K (2019) Microbial electrosynthesis from CO_2: forever a promise? Curr Opin Biotechnol 62:48–57
Prochaska K, Antczak J, Regel-Rosocka M, Szczygiełda M (2018) Removal of succinic acid from fermentation broth by multistage process (membrane separation and reactive extraction). Sep Purif Technol 192:360–368

Rabaey K, Boon N, Höfte M, Verstraete W (2005) Microbial phenazine production enhances electron transfer in biofuel cells. Environ Sci Technol 39:3401–3408

Santos TC, Silva MA, Morgado L, Dantas JM, Salgueiro CA (2015) Diving into the redox properties of Geobacter sulfurreducens cytochromes: a model for extracellular electron transfer. Dalton Trans 44:9335–9344

Semmouri I, De Schamphelaere KAC, Mees J, Janssen CR, Asselman J (2020) Evaluating the potential of direct RNA nanopore sequencing: Metatranscriptomics highlights possible seasonal differences in a marine pelagic crustacean zooplankton community. Mar Environ Res 153:104836

Temple KL, Colmer AR (1951) The autotrophic oxidation of iron by a new bacterium, Thiobacillus ferrooxidans. J Bacteriol 62:605–611

von Wolzogen Kühr CAH, van der Vlugt LS (1934) The graphitization of cast iron as an electrochemical process in anaerobic soil. Water 18:147–165

Wakai S (2019) Biochemical and thermodynamic analyses of energy conversion in extremophiles. Biosci Biotechnol Biochem 83:49–64

Wang J, Lu H, Zhou Y, Song Y, Liu G, Feng Y (2013) Enhanced biotransformation of nitrobenzene by the synergies of *Shewanella* species and mediator-functionalized polyurethane foam. J Hazard Mater 252–253:227–232

Yuly JL, Lubner CE, Zhang P, Beratan DN, Peters JW (2019) Electron bifurcation: progress and grand challenges. Chem Commun (Camb) 55:11823–11832

Chapter 2
Importance of Electron Flow in Microbiological Metabolism

Masafumi Kameya, Hiroyuki Arai, and Masaharu Ishii

2.1 Introduction

Many types of oxidative and reductive reactions occur within individual microbial cells to mediate intracellular metabolism and biological activities. These reactions are diverse, with more than 1800 Enzyme Commission (EC) number entries categorized in the oxidoreductases class (EC 1) in the ENZYME database (Bairoch 2000) till date (October 2019). These redox reactions coordinate to accomplish various physiological demands, such as energy conservation, anabolic biosynthesis, maintenance of cellular redox homeostasis, and antioxidant defense. Intracellular electrons flow through coordinated redox reactions arranged in complicated chains and networks. Understanding the regulated electron flow can form the basis for studies on electron-based bioscience, biotechnology, and biocorrosion as discussed in this book.

With this premise, we elaborate on the biological electron carriers operative in cellular metabolism (Sect. 2.2) and the redox reactions and pathways that govern the total electron flow in microbes (Sect. 2.3). Further, we discuss the ubiquitous energy synthesis system through the respiratory chain (Sect. 2.4). Finally, we will shed light on the unconventional mechanisms of electron transfer carried out by electron bifurcation systems (Sect. 2.5).

M. Kameya · H. Arai
Department of Biotechnology, Graduate School of Agricultural and Life Sciences, The University of Tokyo, Bunkyo-ku, Tokyo, Japan

Collaborative Research Institute for Innovative Microbiology (CRIIM), The University of Tokyo, Bunkyo-ku, Tokyo, Japan

M. Ishii (✉)
Department of Biotechnology, Graduate School of Agricultural and Life Sciences, The University of Tokyo, Bunkyo-ku, Tokyo, Japan
e-mail: amishii@mail.ecc.u-tokyo.ac.jp

M. Ishii, S. Wakai (eds.), *Electron-Based Bioscience and Biotechnology*,
https://doi.org/10.1007/978-981-15-4763-8_2

2.2 Biological Electron Carriers

Biological electron transfers are mediated by many kinds of biomolecules, including quinone/quinol, cytochromes, flavins (FMN and FAD), and disulfides. In this section, nicotinamide nucleotide coenzymes (Sect. 2.2.1) and ferredoxin (Sect. 2.2.2) are reviewed as primary electron carriers.

2.2.1 Nicotinamide Nucleotide Coenzymes: NAD(H) and NADP(H)

Among the various biological electron carriers, NAD(H) and NADP(H) serve as the primary electron acceptor/donor and contribute ubiquitously to most metabolic pathways. Because these two share a similar structure except for the presence/absence of an additional phosphate group, their redox potentials are comparable to each other ($E'_0 = -320$ mV). The oxidized forms, NAD^+ and $NADP^+$, get reduced by the transfer of a hydride ion (H^-) onto the nicotinamide ring. Due to this reaction mechanism, their oxidation and reduction require a simultaneous transfer of two electrons. The importance of this feature would be discussed in further detail for understanding two-electron/one-electron switch in the flavin-based bifurcation system (Sect. 2.5).

Several physiological differences exist between NAD(H) and NADP(H). One of them is their redox ratio; while NADP(H) is generally maintained in a reduced state, NAD(H) remains in a more oxidized state. It is reported that in bacterial cells, $NADPH/NADP^+$ ratio ranges from 1.1 to 59, whereas $NADH/NAD^+$ ratio is lower (between 0.032 and 0.27) (Spaans et al. 2015). Another difference occurs in the metabolic pathways in which these two coenzymes work; while NAD(H) is involved in catabolism and a wide range of metabolisms, NADPH works as an electron donor in anabolic and biosynthetic pathways such as photosynthesis and fatty acid synthesis (Spaans et al. 2015; Agledal et al. 2010). The highly reduced state of NADP(H) can promote biosynthetic metabolism by driving the NADPH-dependent reduction reactions. The difference in the redox balance between NAD(H) and NADP(H) also forms a key factor for an electron bifurcation system (NADH-dependent reduced ferredoxin: $NADP^+$ oxidoreductase in Sect. 2.5.3) in which NADPH and NAD^+ serve as an electron donor and acceptor, respectively.

2.2.2 Ferredoxin

Ferredoxin (Fd) is a small metalloprotein harboring Fe–S cluster(s) as the redox center. Fd can be classified based on the structure of its Fe–S cluster, such as [2Fe–2S], [4Fe–4S], [3Fe–4S], and [7Fe–8S]. In contrast to NAD(H) and NADP(H), an Fe–S

cluster in Fd physiologically transfers only one electron at a time. Due to its simple structure and wide distribution among organisms, Fd is presumed to be one of the evolutionarily oldest proteins and to be even more primitive than NAD(H) (Eck and Dayhoff 1966; Hall et al. 1971; Daniel and Danson 1995).

Another characteristic of Fd as an electron carrier is its low redox potential. Although Fds are diverse in their redox potentials ranging from −500 to −340 mV, many of them are around −420 mV (Valentine 1964; Tagawa and Arnon 1962; Buckel and Thauer 2018b), significantly lower than those of NAD(P)H. Thus, reduced Fd can provide a reducing power strong enough to drive energetically unfavored reactions that cannot be driven by NAD(P)H, such as H_2 production, CO_2 fixation, and nitrogen fixation.

2.3 Redox Reactions in Metabolism

2.3.1 Carbon Metabolism

2.3.1.1 Glycolysis

Conversion of one molecule of glucose to two pyruvate molecules is accompanied by the generation of reducing equivalents ($4e^-$). In the Embden-Meyerhof pathway in many bacteria, the reducing equivalents are transferred to NAD^+ by glyceraldehyde-3-phosphate dehydrogenase (EC 1.2.1.12), followed by the NADH re-oxidation coupled to the respiratory chain (see Sect. 2.4). In bacteria where respiration is not functional, NADH is oxidized by the donation of electrons to glycolysis products, resulting in fermentation products such as ethanol and lactate. Another type of glycolytic pathway, the Entner-Doudoroff pathway, is operative in some microbes (Chen et al. 2016). This pathway donates electrons not only to NAD^+ but also to $NADP^+$, providing one NADH and one NADPH per one glucose oxidized. Instead of these pathways, glucose can be metabolized also through the pentose phosphate pathway (Stincone et al. 2015). It should be noted that the provision of NADPH for cellular biosynthetic reactions is one of the important roles of the pentose phosphate pathway because electrons are donated not to NAD^+ but only to $NADP^+$ in this pathway.

In archaea, some NAD-reducing reactions in glycolysis are replaced by Fd-reducing reactions. Glyceraldehyde-3-phosphate Fd oxidoreductase (EC 1.2.7.6) substitutes (or coexists with) NAD-dependent glyceraldehyde-3-phosphate dehydrogenase with the concomitant reduction of ferredoxin in archaeal species, including *Pyrococcus furiosus*, *Pyrobaculum aerophilum*, and *Methanococcus maripaludis* (Reher et al. 2007; Mukund and Adams 1995; Costa et al. 2013). As another example, pyruvate:Fd oxidoreductase (POR; EC 1.2.7.1) substitutes NAD-depending pyruvate dehydrogenase complex (PDH; EC 1.2.4.1, 2.3.1.12, 1.8.1.4), catalyzing oxidative decarboxylation of pyruvate to acetyl-CoA (Furdui and Ragsdale 2000). Fd reduced

by these reactions is used for hydrogenation as an electron sink or for driving methanogenesis in these archaea living in anaerobic environments.

2.3.1.2 Tricarboxylic Acid Cycle

The tricarboxylic acid (TCA) cycle is a major source of NADH and electron equivalents in many aerobic organisms. In this cycle, NAD^+ is reduced to NADH by isocitrate dehydrogenase (EC 1.1.1.42), 2-oxoglutarate dehydrogenase (OGDH) complex (OGOR; EC 1.2.4.2, 2.3.1.61, 1.8.1.4), and malate dehydrogenase (EC 1.1.137). In the other oxidative reaction catalyzed by succinate dehydrogenase (EC 1.3.5.1), electrons are transferred not to NAD^+ but to quinone because the reducing power provided by the oxidation of succinate to fumarate is weak (E'_0 = 33 mV) (Thauer et al. 1977).

The TCA cycle produces reducing equivalents ($8e^-$ per 1 acetyl-CoA oxidized), but an electron sink is often unavailable in organisms grown in anaerobic environments. In these organisms, an incomplete TCA cycle functions in a "horseshoe" structure, being divided into two halves: an oxidative half cycle leading to 2-oxoglutarate and a reductive half cycle to fumarate (Jahn et al. 2007; Marco-Urrea et al. 2011). This incomplete cycle still provides TCA cycle metabolites as important precursors for various biosynthetic processes without producing excess electrons.

2.3.1.3 Carbon Fixation

To date, six metabolic pathways have been found to fix CO_2 in autotrophic organisms (Montoya et al. 2012; Berg and Ivanovskii 2009; Berg et al. 2010). All of the fixing pathways require reductants to convert CO_2 into metabolites. While Fd is used in three pathways (including the acetyl-CoA pathway and the reductive TCA cycle) out of the six, the other three pathways (including the Calvin cycle) rely only on NAD(P)H. Because the reduced Fd can more strongly drive the reaction due to its low redox potential than that of NAD(P)H, the Fd-dependent pathways require less ATP equivalents than the Fd-independent pathways.

The reductive TCA cycle is known as a "reversed" version of the TCA cycle, and the two cycles share homologous enzymes and reaction steps. However, the difference between them surfaces especially when they are analyzed from the perspective of electron carriers. Whereas PDH and OGDH in the TCA cycle use NAD^+ as the electron acceptor, the reverse reactions in the reductive TCA cycle are catalyzed by POR and OGOR using reduced Fd as the electron donor (Ikeda et al. 2010; Yamamoto et al. 2010). This difference is feasible because the carboxylation reactions catalyzed by POR and OGOR are energetically unfavorable and require strong reductants with a low redox potential. In addition, while succinate oxidation in the TCA cycle donates electrons to quinone, *Hydrogenobacter thermophilus* is reported

to reduce fumarate using NADH as the reductant and not quinol (Miura et al. 2008). Considering that the redox potentials of NAD^+/NADH are significantly lower than those of fumarate/succinate and quinone/quinol, the use of NADH is advantageous to drive the fumarate/succinate conversion irreversibly in the direction of the reductive TCA cycle.

2.3.2 Nitrogen Metabolism

Nitrogen forms a constituent of inorganic compounds with various redox states: +5 in nitrate (NO_3^-), +3 in nitrite (NO_2^-), +2 in nitric oxide (NO), +1 in nitrous oxide (N_2O), 0 for dinitrogen (N_2), −1 in hydroxylamine (NH_2OH), and −3 in ammonium (NH_4^+). Organisms utilize these compounds/intermediates as electron donors or acceptors in energy synthesis processes known as denitrification, anammox, and nitrification, as already reviewed elsewhere (Canfield et al. 2010; Stein and Klotz 2016; Kuypers et al. 2018).

Besides energy synthesis, reduction of inorganic nitrogen compounds occurs in cellular anabolism. Organisms can assimilate nitrogen only in the form of NH_4^+, thereby necessitating the reduction of the oxidized forms of nitrogen to NH_4^+ before assimilation. Assimilatory nitrate reductase (aNar) and nitrite reductase (aNir) catalyze the reduction of NO_3^- into NH_4^+ in their coupling reaction. NH_4^+ is incorporated into Glu by the coupling reaction of Gln synthetase and Glu synthase (GOGAT) (Kameya et al. 2006). While many bacterial aNar and GOGAT are NAD(P)H-dependent, cyanobacteria and chloroplast possess Fd-dependent aNar and GOGAT, which had been considered to be "plant-type" enzymes. However, recent studies discarded this paradigm by reporting Fd-dependent aNar and GOGAT in non-phototrophs, such as hydrogen-oxidizing bacteria and haloarchaea (Martinez-Espinosa et al. 2001; Kameya et al. 2007; Zafrilla et al. 2011; Pire et al. 2014; Kameya et al. 2017).

Nitrogen fixation is a process where N_2 is reduced to NH_4^+ by nitrogenase (EC 1.18.6.1) with the aid of ATP hydrolysis and electron supply from Fd (Buckel and Thauer 2018b). Because ammonification of N_2 is energetically unfavorable, the use of Fd with a low redox potential is the most suitable resort to drive the reaction, as for the carboxylation reactions discussed above.

2.3.3 Sulfur Metabolism

As with nitrogen, sulfur forms various inorganic species at different redox states, for instance, −2 in thiosulfate ($S_2O_3^{2-}$), 0 in elemental sulfur, +4 in sulfite (SO_3^{2-}), and +6 in sulfate (SO_4^{2-}). Many microbes use sulfur species for electron transfer during energy synthesis and redox metabolism.

Oxidation of sulfur compounds is catalyzed by the coupling of several enzymes and systems, such as the sulfur-oxidizing (Sox) enzyme system, heterodisulfide reductase (Hdr)-like system, sulfide:quinone oxidoreductase (EC 1.8.5.4), and sulfur oxygenase reductase (EC 1.13.11.55) (Friedrich et al. 2005; Wang et al. 2018). Electrons produced through these oxidizing reactions are transferred to quinone, which can be linked to the electron transport chain to produce energy.

Sulfate-reducing bacteria anaerobically oxidize organic compounds to synthesize energy and carbon skeletons, and the electrons produced through this oxidation are donated to the terminal electron acceptor, sulfate (Qian et al. 2019). Sulfate reduction is also ecologically important to maintain the activity of anaerobic methane-oxidizing archaea (ANME) because symbiotic sulfate-reducing bacteria accept and consume electrons produced by methane oxidation, thus allowing a continuum (McGlynn et al. 2015).

Sulfur is one of the primary elements of all organisms and is contained in many biomolecules, such as Cys, Met, glutathione, and proteins harboring Fe–S clusters. In general with sulfur anabolism, inorganic sulfur compounds are incorporated to produce Cys, and the Cys serves as a sulfur donor for biosynthetic reactions of sulfur-containing metabolites. Sulfate and sulfite are reduced to sulfide before being incorporated into Cys, where NAD(P)H and electron carrier proteins (thioredoxin and glutaredoxin) serve as electron donors (Sekowska et al. 2000).

2.4 Respiratory Electron Transport Pathway

2.4.1 Branched Bacterial Respiratory Chain

In the presence of oxygen, aerobic and facultative anaerobic bacteria produce most of the energy required for cellular function, such as anabolic metabolism, ion homeostasis, or motility, through aerobic respiration like that of mitochondria in eukaryotic cells. Mitochondrial respiratory chain consists of four complexes, NADH dehydrogenase (complex I), succinate dehydrogenase (complex II), a cytochrome bc_1 complex (complex III), and a cytochrome *c* oxidase (complex IV). Protons are pumped across the inner mitochondrial membrane during electron transfer through complexes I, III, and IV, producing a transmembrane chemiosmotic gradient. The generated proton motive force (PMS) drives ATP synthesis by F_0F_1-ATP synthase. This entire process of PMS generation and subsequent ATP synthesis is called oxidative phosphorylation. Many bacteria have more complex and flexible respiratory electron transfer pathways because they use a variety of electron donors and acceptors for oxidative phosphorylation (Anraku 1988).

Bacterial respiratory chains are composed of primary dehydrogenases that feed electrons to the quinone/quinol pool from low-potential substrates and terminal oxidoreductases that reduce the high-potential electron acceptors. Respiratory substrates, such as NADH, succinate, lactate, malate, and hydrogen, are used as electron donors. Among them, NADH, generated by the TCA cycle, is the most common

substrate for aerobic respiration. *Escherichia coli* is known to have a multicomponent NADH dehydrogenase corresponding to the mitochondrial complex I, which has proton-pumping activity, and a single-subunit-type flavin-containing enzyme, which does not couple the redox reaction to proton translocation (Calhoun et al. 1993). Some bacteria such as *Vibrio cholerae* have a sodium-pumping NADH:ubiquinone oxidoreductase (Steuber et al. 2015). The electrochemical potential generated by sodium excretion is also used for oxidative phosphorylation.

Oxygen is used as the terminal electron acceptor for aerobic respiration. The enzymes that catalyze the four-electron reduction of oxygen to water at the end of the aerobic respiratory chain are called terminal oxidases. They can be divided into two groups, cytochrome *c* oxidases and quinol oxidases. The former receives electrons from quinol via the cytochrome bc_1 complex and *c*-type cytochromes, while the latter receives electrons directly from quinol (Garcia-Horsman et al. 1994). Most bacteria have more than one terminal oxidase with different features that are used differentially depending on the growth conditions. The branched respiratory pathways of *Pseudomonas aeruginosa* and *Rhodobacter sphaeroides* are shown in Fig. 2.1 for reference.

2.4.2 Heme-Copper Oxidases for Aerobic Respiration

Cytochrome *c* oxidases and most quinol oxidases are membrane-bound multisubunit enzymes belonging to the heme-copper oxidase superfamily. Although they have a variation in heme types and subunit composition, their catalytic subunits (subunit I) commonly contain 12 core transmembrane helices and are characterized by the presence of a six-coordinated low-spin heme and a binuclear catalytic center composed of a high-spin heme and a copper ion, Cu_B. The second subunit (subunit II) of most cytochrome *c* oxidases has a binuclear copper center, Cu_A, that receives electrons from cytochromes *c* and passes them to the catalytic subunit. The Cu_A site is absent in quinol oxidases.

The heme-copper oxidases, irrespective of cytochrome *c* oxidases and quinol oxidases, are proposed to be divided into three major types, A, B, and C, based on the constituents of their proton channels. The classification is also in good accordance with their phylogenetic relationship (Pereira et al. 2001; Sousa et al. 2012). Type A includes the mitochondrial complex IV and is distributed in many bacteria and some archaea. The type A oxidases have two proton-conducting channels, named D- and K-channel, according to specific aspartate and lysine residues present in the channels, respectively. Type A can be divided into two subfamilies, A1 and A2, according to the conserved motif in the helix VI at the hydrophobic end of the D-channel. The motif sequences are –XGHPEV– and –YSHPXV– for the types A1 and A2, respectively (Pereira et al. 2001).

The aa_3 cytochrome *c* oxidases from *Paracoccus denitrificans* and *Rhodobacter sphaeroides* and the bo_3 quinol oxidase from *E. coli* are type A enzymes. These

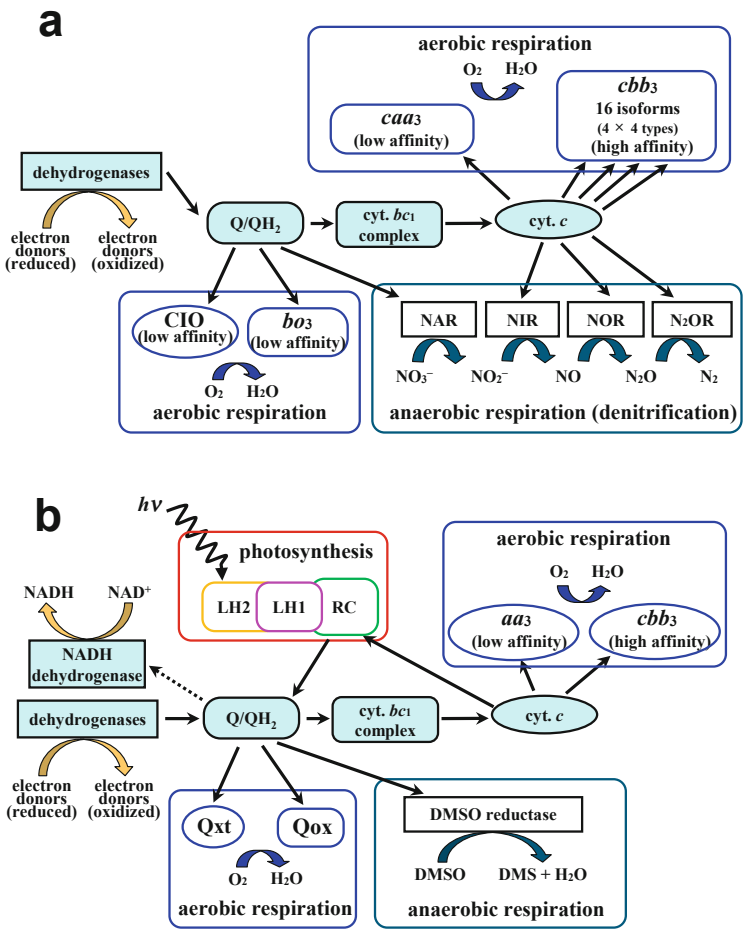

Fig. 2.1 Schematic representation of the branched respiratory electron transport pathway in *Pseudomonas aeruginosa* PAO1 (**a**) and *Rhodobacter sphaeroides* 2.4.1 (**b**). *P. aeruginosa* produces sixteen isoforms of the cbb_3 cytochrome *c* oxidase, which can be divided into four types. Two quinol oxidases of the heme-copper oxidase superfamily (Qox) and the cyanide-insensitive oxidase (CIO)-type (Qxt) are encoded in the genome of *R. sphaeroides*. Arrows indicate electron flow. The "uphill" reverse electron flow that regenerates NADH under the anaerobic photosynthetic conditions is indicated by a dotted arrow. Q/QH_2 ubiquinone-ubiquinol pool, *hν* light irradiation, *LH1*, *LH2* light harvesting complexes, *RC* photosynthetic reaction center

oxidases have low affinity for oxygen and are utilized under high oxygen conditions. The proton-pumping stoichiometry (H^+/e^- ratio) of the type A oxidases has been reported to be 0.75–1 (Pereira et al. 2008). The aa_3-like oxidases, which have C-terminal extension of subunit II containing one or two heme *c* binding motifs, have been found in many bacterial species such as *Thermus thermophilus*, *P. aeruginosa*, and *Shewanella oneidensis* (Lyons et al. 2012; Osamura et al.

2017; Le Laz et al. 2016). These enzymes are referred to as caa_3 or $ccaa_3$. The caa_3 oxidase of *P. aeruginosa* and the $ccaa_3$ oxidase of *S. oneidensis* have been reported to be expressed under starvation conditions (Kawakami et al. 2010; Le Laz et al. 2016).

Type B is mainly distributed in Crenarchaeota and thermophilic bacteria. A catalytic tyrosine residue in helix VI, which is covalently linked to a copper-binding histidine, is conserved both in the type A and type B enzymes. The type B oxidases are thought to have only one proton-conducting channel. The three-dimensional structure of the ba_3 oxidase of *T. thermophilus* indicated three possible proton-conducting pathways (Soulimane et al. 2000). One of these is an alternative of the K-channel of the type A enzymes, although some amino acid residues are substituted. The other two are not conserved in other type B enzymes and might not be functional (Sousa et al. 2012).

Type C is found only in bacteria, mainly in Proteobacteria. The cbb_3 cytochrome *c* oxidase is the only member of this type. The cbb_3 oxidases are encoded by the *ccoNOQP* (or *fixNOQP*) genes. CcoN is the core catalytic subunit corresponding to the subunit I of the other types. CcoO and CcoP are membrane-bound monoheme and diheme cytochromes *c*, respectively. CcoQ is known to affect the stability of the cbb_3 complex (Ekici et al. 2012; Buschmann et al. 2010). The position of the catalytic tyrosine residue is different from that of the type A and B enzymes and located in helix VII of CcoN. The cbb_3 oxidases do not have the Cu_A center. The electrons are thought to be received by the distal heme group of CcoP from the electron donor cytochromes *c*. The electrons are transferred to the catalytic center in CcoN via the proximal heme of CcoP and the heme group of CcoO. The cbb_3 oxidases have only one proton-conducting channel, which is an alternative of the K-channel, but its amino acid composition is different from those of the type A and B enzymes (Buschmann et al. 2010). The H^+/e^- ratios of the type B and C enzymes are reported to be 0.5–0.75 and 0.2–0.4, respectively, which is lower than those of the type A enzymes (Pereira et al. 2008). The lower values are thought to result from the lack of the D-channel. It is has been recently reported that the stoichiometry is close to unity among the three types if there is no proton leak under the optimal experimental conditions (Rauhamäki and Wikström 2014).

The cbb_3 oxidases have a very high affinity for oxygen with K_m values ranging from 6.5 to 40 nM and are usually utilized under low oxygen conditions (Arai et al. 2014; Mouncey and Kaplan 1998; Otten et al. 2001). Many *Pseudomonas* species have two tandemly located *ccoNOQP* gene clusters. In *P. aeruginosa*, one of the clusters is expressed constitutively, and the other is induced under low oxygen conditions (Kawakami et al. 2010). *P. aeruginosa* also has two additional orphan *ccoNQ* gene clusters and can produce sixteen cbb_3 oxidase isoforms via combinations of four CcoN, two CcoO, and two CcoP isosubunits (Hirai et al. 2016). The isoforms derived from the orphan clusters confer resistance to nitrite and cyanide under low oxygen conditions.

2.4.3 Non-Heme-Copper Oxidases for Aerobic Respiration

The heme-copper oxidases are very sensitive to cyanide; however, many bacteria have cyanide-resistant respiration pathways that use non-heme-copper oxidases. Two major types of quinol oxidases, the cytochrome *bd* oxidase and the alternative oxidase (AOX), are known as the cyanide-resistant respiratory oxygen reductases. The *bd* oxidase is a two-subunit enzyme containing a low-spin heme b_{558} and a binuclear center consisting of a high-spin heme b_{595} and a heme *d*. The *bd* oxidase does not pump protons, but it generates proton gradient across the cell membrane by proton extrusion from quinol oxidation at the periplasmic side and proton uptake from the cytoplasm for oxygen reduction (Safarian et al. 2016).

The cyanide-insensitive oxidase (CIO) is known as a subfamily of the *bd* oxidase. CIO is homologous with but phylogenetically distinct from the canonical *bd* oxidases. The conserved sequence of the hydrophilic loop (Q-loop), which contains the putative quinol-oxidizing site, is shorter in CIOs than in the canonical *bd* oxidases (Cunningham et al. 1997). CIO contains the hemes b_{558}, b_{595}, and *d* but shows very weak spectroscopic features of heme b_{595} and heme *d* (Miura et al. 2013; Mogi et al. 2009). The canonical *bd* oxidases have high affinity for oxygen and are generally utilized under low oxygen conditions such as in *E. coli* (Jünemann 1997). However, CIOs of *Campylobacter jejuni*, *Gluconacetobacter oxydans*, and *P. aeruginosa* have been reported to have a low affinity (Arai et al. 2014; Jackson et al. 2007; Miura et al. 2013).

AOX is a non-heme di-iron protein found in all higher plants and certain eukaryotes including some algae, fungi, and protists (Moore and Albury 2008). The crystal structure of AOX from a protozoan parasite *Trypanosoma brucei*, which causes human African sleeping sickness, has been reported (Shiba et al. 2013). The genes encoding AOX have also been identified in the genomes of some bacteria, especially those inhabiting marine environments, such as *Vibrio fischeri* and *R. denitrificans* (Dunn 2018; Swingley et al. 2007). AOX does not create proton gradient across the membrane and supports the oxidative phosphorylation only when coupled with proton-translocating NADH dehydrogenase.

AOX is responsible for the production of heat in thermogenic plants. It also contributes to stress resistance by maintaining redox and metabolic homeostasis in plant cells (Saha et al. 2016). When the parasite *T. brucei* lives in the bloodstream of its mammalian host, the glycolytic pathway is the major source of ATP, and the oxidative phosphorylation using cytochromes is not operative. Because AOX is required for re-oxidation of NADH accumulated during glycolysis in the bloodstream form of the parasite, it is expected to be a drug target for the infectious disease (Shiba et al. 2013). The function of bacterial AOX was only reported in *V. fischeri*. The gene encoding AOX is regulated by an NO-sensing regulator, NsrR, and involved in reducing stress during exposure of the bacterium to NO (Dunn 2018). Our preliminary investigation has indicated that AOX is required for the growth of the photosynthetic bacterium *R. denitrificans* under low temperature conditions.

2.4.4 Respiratory Protection by High-Affinity Oxidases

The *bd* quinol oxidase and the cbb_3 cytochrome *c* oxidase have a very high affinity for oxygen. These high-affinity oxidases are thought to have a role in protecting oxygen-sensitive enzymes or processes by scavenging oxygen. The protective role of the *bd* oxidase was initially proposed in a free-living nitrogen-fixing bacterium *Azotobacter vinelandii*, in which oxygen scavenging by the *bd* oxidase is thought to be required for the oxygen-sensitive nitrogenase activity (Poole and Hill 1997), although the role is still arguable (Oelze 2000). The *bd* oxidase has also been reported to be involved in conferring resistance to oxidative and nitrosative stresses in bacteria such as *E. coli* and *Mycobacterium tuberculosis* (Giuffrè et al. 2014).

Some chemolithoautotrophic bacteria such as *Hydrogenophilus thermoluteolus* and *Hydrogenovibrio marinus*, which fix carbon dioxide by ribulose-1,5-bisphosphate carboxylase/oxygenase (RuBisCO) in the Calvin-Benson-Bassham cycle, have the cbb_3 oxidase as the only terminal oxidase for aerobic respiration (Arai et al. 2018; Arai and Ishii 2019). The oxygenase reaction of RuBisCO is accompanied by wastage of energy and fixed carbon. Scavenging oxygen by the cbb_3 oxidase might minimize the futile oxygenase reaction and be advantageous for the autotrophic growth of these chemolithotrophs under aerobic conditions.

2.4.5 Anaerobic Electron Transport Pathways

In the absence of oxygen, many bacterial species utilize alternative electron acceptors for the oxidative phosphorylation by anaerobic respiration. Many organic and inorganic compounds and metal ions, such as fumarate, dimethyl sulfoxide (DMSO), trimethylamine *N*-oxide (TMAO), nitrogen oxides, sulfate, elemental sulfur, ferric iron, and arsenate, are known to be utilized for anaerobic respiration. These compounds and ions are reduced by specific reductases that receive electrons from the respiratory chain.

E. coli uses nitrate or fumarate as the terminal electron acceptor for anaerobic respiration. Nitrate is catabolically reduced to ammonium via nitrite, and the process is called ammonification. Because oxygen is a preferred electron acceptor for oxidative phosphorylation, the genes for anaerobic respiration enzymes are usually repressed under aerobic conditions. The induction of these genes under the anaerobic conditions is regulated by an oxygen-sensing global regulator FNR (fumarate and nitrate reductase regulator) (Gunsalus and Park 1994).

Some facultative anaerobic bacteria such as *P. aeruginosa* reduce nitrate to dinitrogen via nitrite, NO, and N_2O by the process called denitrification (Arai 2011) (Fig. 2.1a). The four steps of the denitrification pathway are each catalyzed by metalloenzymes, which receive electrons from quinol, cytochromes *c*, or copper proteins in the respiratory chain. Among the denitrification enzymes, NO reductase (NOR) is phylogenetically related to the terminal oxidases of the heme-copper

oxidase superfamily; however, it lacks the proton-pumping activity. The catalytic binuclear center of NOR contains a non-heme iron, Fe_B, instead of Cu_B (Shiro 2012). In some pathogenic bacteria, NOR also has a function for detoxification of NO produced by the host immune defense system. Expression of the denitrification genes under the anaerobic conditions is regulated by an oxygen-sensing regulator ANR (anaerobic regulation of arginine deiminase and nitrate reduction), which is the analog of *E. coli* FNR, and a NO-sensing regulator DNR (dissimilatory nitrate respiration regulator) in *P. aeruginosa* (Arai et al. 1997; Kuroki et al. 2014).

Photosynthesis is another system to produce ATP using the proton gradient by a mechanism similar to oxidative phosphorylation. In contrast to the oxygenic photosynthesis of plants and cyanobacteria, photosynthetic bacteria, such as *R. sphaeroides*, perform anoxygenic photosynthesis under anaerobic conditions in the presence of light (Mackenzie et al. 2007). The process of ATP production in anoxygenic photosynthesis is called cyclic photophosphorylation. In this process, low-energy electrons in the reaction center bacteriochlorophyll are excited by light energy. The excited electrons are transferred through cyclic electron transport chain composed of quinones and cytochromes and return to the bacteriochlorophyll (Fig. 2.1b). PMS is generated during the electron transport, and ATP is produced using PMS, akin to oxidative phosphorylation. Some photosynthetic bacteria, such as the *Roseobacter* clade, produce the anoxygenic photosynthetic apparatus even under aerobic conditions (Rathgeber et al. 2004). Because photosynthetic and respiratory pathways share a common electron transfer chain, regulation of electron flow in the diverse electron transport pathways is more important in these photosynthetic bacteria.

2.4.6 Regulation of the Electron Transport Pathway

Aerobic respiration is a preferred ATP synthesis system, and the anaerobic respiration and anoxygenic respiration genes are generally induced in the absence of oxygen. As described above, the oxygen-sensing regulator FNR and its homologs function as global regulators for the expression of the anaerobic respiratory enzymes in several facultative anaerobes. They are also involved in the expression of anoxygenic photosynthesis apparatus in photosynthetic bacteria.

The ambient oxygen tension and the redox status of the respiratory chain form important signals for the regulation of multiple terminal oxidases. The FNR-type regulators also regulate the expression of the high-affinity *bd* oxidase and cbb_3 oxidase in response to oxygen depletion. The *fnr* gene is often clustered with the *ccoNOQP* and *hemN* genes, which encode the cbb_3 oxidase and the oxygen-independent coproporphyrinogen III oxidase, respectively. The latter is used for heme biosynthesis under hypoxic or anoxic conditions.

The redox status of the respiratory chain is predicted to be sensed by two-component regulatory systems. In *E. coli*, the ArcBA two-component system regulates many genes for energy metabolism, including those for the *bd* oxidase, in

combination with FNR, by monitoring the redox status of the quinone pool (Gunsalus and Park 1994). The PrrBA/RegBA/RoxSR-type two-component systems, which are predicted to sense the redox status of the respiratory chain, either by the redox status of the quinone pool or by the electron flow through terminal oxidases, are found in several Proteobacteria. PrrBA or RegBA regulate the expression of the genes responsible for photosynthesis, carbon dioxide fixation, nitrogen fixation, and many other functions in photosynthetic bacteria of the *Rhodobacter* species (Mackenzie et al. 2007). In *P. aeruginosa*, five terminal oxidase gene clusters are directly or indirectly regulated by RoxSR (Kawakami et al. 2010; Arai 2011). Because quinones are located at the pivotal point of the divergent electron transport chain of aerobic and anaerobic respiration and photosynthesis (Fig. 2.1), the redox status of the quinone pool serves as a critical leverage on the trafficking of electrons.

2.5 Electron Bifurcation

In several biochemical reactions, an electron carrier with a higher energy level gets reduced by an electron carrier with a lower energy level. Such instances are mediated by electron bifurcation, unless membrane potential is used. In the biochemical field, quinone-based electron bifurcation and flavin-based electron bifurcation have been verified. In this section, a brief history, the current research status, and future prospects of electron bifurcation have been discussed.

2.5.1 What Is Electron Bifurcation?

In electron bifurcation process, a pair of electrons with the same energy level is essentially converted to two electrons with different energy status (Buckel and Thauer 2018a). That is, one electron is converted to one with higher energy level, and the other electron is converted to one with lower energy level. Usually, the first electron leaves as one with the lower energy level, and the second electron comes out as one with the higher energy level. Therefore, by adopting electron bifurcation process, it becomes possible to reduce an electron carrier with higher energy level (lower redox potential) by an electron carrier with a lower energy (higher redox potential).

In view of the history of biochemistry, electron bifurcation process was firstly found in complex III (cytochrome bc_1 complex) (Mitchell 1976). Still, it was about 40 years later, when the existence of another type of electron bifurcation system, flavin-based electron bifurcation, was discovered (Li et al. 2008). Nowadays, metal-based electron bifurcation has also been suggested (Peters et al. 2018).

2.5.2 Quinone-Based Electron Bifurcation

As mentioned above, electron bifurcation is operative in cytochrome bc_1 complex. In the complex, quinol is converted to semiquinone by transferring one electron to Fe–S protein. This first electron is with low energy. Then, the generated semiquinone state with higher energy level than the quinol state is able to discharge an electron with high energy. Further, with the aid of large conformational changes in the cytochrome bc_1 complex, the semiquinone makes a contact with cytochrome *b* and reduces it through electron transfer (Crofts et al. 2017). Here, it may be emphasized that quinone has three redox states, oxidized state (quinone state), one-electron-reduced state (semiquinone state), and two-electron-reduced state (quinol state), and is therefore capable of harboring two electrons simultaneously.

2.5.3 Flavin-Based Electron Bifurcation

As mentioned above, flavin-based electron bifurcation was discovered around 40 years after the discovery of the quinone-based electron bifurcation system (Li et al. 2008). Since the first discovery of flavin-based electron bifurcation, many metabolic systems with such electron bifurcation have been reported (Buckel and Thauer 2018b). Similar to quinone, flavin also displays three states, which forms the theoretical basis for electron bifurcation. It should be considered that flavin can adopt neutral or anionic structures under the three redox states, oxidized, semiquinone, and reduced, which might explain the limited clarification of mechanism for flavin-based electron bifurcation metabolic reactions.

A detailed structural analysis has been performed on the NADH-dependent reduced ferredoxin: $NADP^+$ oxidoreductase (Nfn) from *Pyrococcus furiosus* (Lubner et al. 2017). Nfn is an enzyme that catalyzes the following reaction: $2NADPH + NAD^+ + 2Fd_{ox} \rightarrow 2NADP^+ + NADH + 2Fd_{red}$.

The bifurcating flavin in this enzyme has an electrochemical potential difference of +359 mV between HQ (hydroquinone state) and ASQ (anionic semiquinone state) and −911 mV ASQ/OX (oxidized state). For electron bifurcation, flavin is converted to a fully reduced state (hydroquinone state). The first electron, which comes out between HQ and ASQ, reduces NAD. The second electron, which is released between ASQ and OX, reduces ferredoxin. The electron generated between ASQ and OX does not reduce NAD. However, unlike cytochrome bc_1 complex, a large conformational change has not been detected. Although physical distance between flavin and [2Fe–2S]-type ferredoxin (14.1 Å) is minutely larger than the distance between flavin and [4Fe–4S]-type ferredoxin (7.5 Å), this is not enough to explain the high specificity of the second electron transfer. The reason can be explained by including the Marcus theory (Marcus and Sutin 1985) in addition to physical distance.

The Marcus theory states the energy gap law. In chemical reactions, it is reasonable to consider that the lower the free energy of the final state, the higher would be the electron transfer rate. However, according to Marcus theory, there exists a reversal region, wherein after a threshold energy difference is crossed, the speed of electron transfer would decrease. This theory is now used to explain the mechanism by which the second electron reduces ferredoxin, and not NAD.

2.5.4 Metal-Based Electron Bifurcation

Any redox cofactor that can receive at least two electrons and can then donate them sequentially can serve as a candidate for the essential catalytic part of electron bifurcation. Indeed, redox-factor architecture similar to that of Nfn is found in tungsten-containing formate dehydrogenase, [FeFe]-hydrogenase, and [NiFe]-hydrogenase. For this reason, these enzymes have been proposed to bear electron bifurcation capacity (Peters et al. 2018).

2.5.5 Future Prospects of Electron Bifurcation

Since the discovery of flavin-based electron bifurcation, several findings are accumulating that precisely explain the theoretical basis of electron bifurcation through physics and structural information. Efforts ensue to develop electron bifurcation systems using biotechnological advances. This would require the construction of protein structures and/or peptide stretches, which would hold the bifurcating carriers and recruit electron acceptors. To this end, detailed understanding of the molecular machinery and biochemistry of the existing quinone-based, flavin-based, and metal-based bifurcation reactions is critical. Such studies would enable the control of metabolism on the basis of energetics.

Also, because electron bifurcation system has been identified from the microorganisms with old lineage (Schut and Adams 2009), biochemical analyses of these systems might provide avenues for generating insights on the emergence of life.

2.6 Conclusions

We may appreciate that microorganisms take up external energy to convert it into bioenergy and utilize the bioenergy to conduct various life activities such as proliferation, metabolism, and survival. The entire process of transforming external energy into bioenergy is governed by the flow of electrons. Therefore, electron transfer in microorganisms is a key facet to understand their metabolism and survival tactics.

Although there are unconventional instances such as an apparent uphill reaction during electron bifurcation, the flow of electrons is generally downhill. Since the electrons can be accepted by various molecules, microorganisms have evolved mechanisms to tightly regulate electron flow to ensure smooth functioning of all biological processes. In this light, microorganisms fine-tune the energy conservation systems so that electrons are received by the most appropriate redox systems. Yet, instances of erroneous transfer of electrons exist, which ultimately lead to the production of reactive oxygen species (ROS). The microorganisms utilize detoxification systems to ameliorate these conditions and use additional electrons for that.

Together, microorganisms orchestrate a highly complex system of handling electrons while sensing and responding to their external environment and cell-intrinsic cues.

References

Agledal L, Niere M, Ziegler M (2010) The phosphate makes a difference: cellular functions of NADP. Redox Rep 15(1):2–10. https://doi.org/10.1179/174329210X12650506623122

Anraku Y (1988) Bacterial electron transport chains. Annu Rev Biochem 57:101–132

Arai H (2011) Regulation and function of versatile aerobic and anaerobic respiratory metabolism in *Pseudomonas aeruginosa*. Front Microbiol 2:103

Arai H, Ishii M (2019) Complete genome sequence of a mesophilic obligately chemolithoautotrophic hydrogen-oxidizing bacterium, *Hydrogenovibrio marinus* MH-110. Microbiol Resour Announc 8:e01132–e01119

Arai H, Kodama T, Igarashi Y (1997) Cascade regulation of the two CRP/FNR-related transcriptional regulators (ANR and DNR) and the denitrification enzymes in *Pseudomonas aeruginosa*. Mol Microbiol 25:1141–1148

Arai H, Kawakami T, Osamura T, Hirai T, Sakai Y, Ishii M (2014) Enzymatic characterization and *in vivo* function of five terminal oxidases in *Pseudomonas aeruginosa*. J Bacteriol 196:4206–4215

Arai H, Shomura Y, Higuchi Y, Ishii M (2018) Complete genome sequence of a moderately thermophilic facultative chemolithoautotrophic hydrogen-oxidizing bacterium, *Hydrogenophilus thermoluteolus* TH-1. Microbiol Resour Announc 7:e00857–e00818

Bairoch A (2000) The ENZYME database in 2000. Nucleic Acids Res 28(1):304–305. https://doi.org/10.1093/nar/28.1.304

Berg IA, Ivanovskii RN (2009) Enzymes of the citramalate cycle in *Rhodospirillum rubrum*. Mikrobiology 78(1):16–24

Berg IA, Kockelkorn D, Ramos-Vera WH, Say RF, Zarzycki J, Hugler M, Alber BE, Fuchs G (2010) Autotrophic carbon fixation in archaea. Nat Rev Microbiol 8(6):447–460. https://doi.org/10.1038/nrmicro2365

Buckel W, Thauer RK (2018a) Flavin-based electron bifurcation, a new mechanism of biological energy coupling. Chem Rev 118(7):3862–3886. https://doi.org/10.1021/acs.chemrev.7b00707

Buckel W, Thauer RK (2018b) Flavin-based electron bifurcation, ferredoxin, flavodoxin, and anaerobic respiration with protons (Ech) or NAD(+) (Rnf) as electron acceptors: a historical review. Front Microbiol 9:401. https://doi.org/10.3389/fmicb.2018.00401

Buschmann S, Warkentin E, Xie H, Langer JD, Ermler U, Michel H (2010) The structure of cbb_3 cytochrome oxidase provides insights into proton pumping. Science 329:327–330

Calhoun MW, Oden KL, Gennis RB, Teixeira de Mattos MJ, Neijssel OM (1993) Energetic efficiency of *Escherichia coli*: effects of mutations in components of the aerobic respiratory chain. J Bacteriol 175:3020–3025

Canfield DE, Glazer AN, Falkowski PG (2010) The evolution and future of earth's nitrogen cycle. Science 330(6001):192–196. https://doi.org/10.1126/science.1186120

Chen X, Schreiber K, Appel J, Makowka A, Fahnrich B, Roettger M, Hajirezaei MR, Sonnichsen FD, Schonheit P, Martin WF, Gutekunst K (2016) The Entner-Doudoroff pathway is an overlooked glycolytic route in cyanobacteria and plants. Proc Natl Acad Sci U S A 113 (19):5441–5446. https://doi.org/10.1073/pnas.1521916113

Costa KC, Lie TJ, Jacobs MA, Leigh JA (2013) H_2-independent growth of the hydrogenotrophic methanogen *Methanococcus maripaludis*. MBio 4(2). https://doi.org/10.1128/mBio.00062-13

Crofts AR, Rose SW, Burton RL, Desai AV, Kenis PJA, Dikanov SA (2017) The Q-cycle mechanism of the bc1 complex: a biologist's perspective on atomistic studies. J Phys Chem B 121(15):3701–3717. https://doi.org/10.1021/acs.jpcb.6b10524

Cunningham L, Pitt M, Williams HD (1997) The *cioAB* genes from *Pseudomonas aeruginosa* code for a novel cyanide-insensitive terminal oxidase related to the cytochrome *bd* quinol oxidases. Mol Microbiol 24:579–591

Daniel R, Danson M (1995) Did primitive microorganisms use nonhem iron proteins in place of NAD/P? J Mol Evol 40(6):559–563. https://doi.org/10.1007/BF00160501

Dunn AK (2018) Alternative oxidase activity reduces stress in *Vibrio fischeri* cells exposed to nitric oxide. J Bacteriol 200:e00797–e00717

Eck RV, Dayhoff MO (1966) Evolution of the structure of ferredoxin based on living relics of primitive amino acid sequences. Science 152(3720):363–366. https://doi.org/10.1126/science.152.3720.363

Ekici S, Pawlik G, Lohmeyer E, Koch HG, Daldal F (2012) Biogenesis of cbb_3-type cytochrome *c* oxidase in *Rhodobacter capsulatus*. Biochim Biophys Acta 1817:898–910

Friedrich CG, Bardischewsky F, Rother D, Quentmeier A, Fischer J (2005) Prokaryotic sulfur oxidation. Curr Opin Microbiol 8(3):253–259. https://doi.org/10.1016/j.mib.2005.04.005

Furdui C, Ragsdale SW (2000) The role of pyruvate ferredoxin oxidoreductase in pyruvate synthesis during autotrophic growth by the Wood-Ljungdahl pathway. J Biol Chem 275 (37):28494–28499. https://doi.org/10.1074/jbc.M003291200

Garcia-Horsman JA, Barquera B, Rumbley J, Ma J, Gennis RB (1994) The superfamily of heme-copper respiratory oxidases. J Bacteriol 176:5587–5600

Giuffrè A, Borisov VB, Arese M, Sarti P, Forte E (2014) Cytochrome *bd* oxidase and bacterial tolerance to oxidative and nitrosative stress. Biochim Biophys Acta 1837:1178–1187

Gunsalus RP, Park SJ (1994) Aerobic-anaerobic gene regulation in *Escherichia coli*: control by the ArcAB and Fnr regulons. Res Microbiol 145:437–450

Hall DO, Cammack R, Rao KK (1971) Role for ferredoxins in the origin of life and biological evolution. Nature 233(5315):136–138

Hirai T, Osamura T, Ishii M, Arai H (2016) Expression of multiple cbb_3 cytochrome *c* oxidase isoforms by combinations of multiple isosubunits in *Pseudomonas aeruginosa*. Proc Natl Acad Sci U S A 113:12815–12819

Ikeda T, Yamamoto M, Arai H, Ohmori D, Ishii M, Igarashi Y (2010) Enzymatic and electron paramagnetic resonance studies of anabolic pyruvate synthesis by pyruvate: ferredoxin oxidoreductase from *Hydrogenobacter thermophilus*. FEBS J 277:501–510. https://doi.org/10.1111/j.1742-4658.2009.07506.x

Jackson RJ, Elvers KT, Lee LJ, Gidley MD, Wainwright LM, Lightfoot J, Park SF, Poole RK (2007) Oxygen reactivity of both respiratory oxidases in *Campylobacter jejuni*: the *cydAB* genes encode a cyanide-resistant, low-affinity oxidase that is not of the cytochrome *bd* type. J Bacteriol 189:1604–1615

Jahn U, Huber H, Eisenreich W, Hugler M, Fuchs G (2007) Insights into the autotrophic CO2 fixation pathway of the archaeon *Ignicoccus hospitalis*: comprehensive analysis of the central carbon metabolism. J Bacteriol 189(11):4108–4119. https://doi.org/10.1128/JB.00047-07

Jünemann S (1997) Cytochrome *bd* terminal oxidase. Biochim Biophys Acta 1321:107–127
Kameya M, Arai H, Ishii M, Igarashi Y (2006) Purification and properties of glutamine synthetase from *Hydrogenobacter thermophilus* TK-6. J Biosci Bioeng 102(4):311–315
Kameya M, Ikeda T, Nakamura M, Arai H, Ishii M, Igarashi Y (2007) A novel ferredoxin-dependent glutamate synthase from the hydrogen-oxidizing chemoautotrophic bacterium *Hydrogenobacter thermophilus* TK-6. J Bacteriol 189(7):2805–2812
Kameya M, Kanbe H, Igarashi Y, Arai H, Ishii M (2017) Nitrate reductases in *Hydrogenobacter thermophilus* with evolutionarily ancient features: distinctive localization and electron transfer. Mol Microbiol 106(1):129–141. https://doi.org/10.1111/mmi.13756
Kawakami T, Kuroki M, Ishii M, Igarashi Y, Arai H (2010) Differential expression of multiple terminal oxidases for aerobic respiration in *Pseudomonas aeruginosa*. Environ Microbiol 12:1399–1412
Kuroki M, Igarashi Y, Ishii M, Arai H (2014) Fine-tuned regulation of the dissimilatory nitrite reductase gene by oxygen and nitric oxide in *Pseudomonas aeruginosa*. Environ Microbiol Rep 6:792–801
Kuypers MMM, Marchant HK, Kartal B (2018) The microbial nitrogen-cycling network. Nat Rev Microbiol 16(5):263–276. https://doi.org/10.1038/nrmicro.2018.9
Le Laz S, Kpebe A, Bauzan M, Lignon S, Rousset M, Brugna M (2016) Expression of terminal oxidases under nutrient-starved conditions in *Shewanella oneidensis*: detection of the A-type cytochrome *c* oxidase. Sci Rep 6:19726
Li F, Hinderberger J, Seedorf H, Zhang J, Buckel W, Thauer RK (2008) Coupled ferredoxin and crotonyl coenzyme A (CoA) reduction with NADH catalyzed by the butyryl-CoA dehydrogenase/Etf complex from *Clostridium kluyveri*. J Bacteriol 190(3):843–850. https://doi.org/10.1128/jb.01417-07
Lubner CE, Jennings DP, Mulder DW, Schut GJ, Zadvornyy OA, Hoben JP, Tokmina-Lukaszewska M, Berry L, Nguyen DM, Lipscomb GL, Bothner B, Jones AK, Miller A-F, King PW, Adams MWW, Peters JW (2017) Mechanistic insights into energy conservation by flavin-based electron bifurcation. Nat Chem Biol 13:655. https://doi.org/10.1038/nchembio.2348
Lyons JA, Aragao D, Slattery O, Pisliakov AV, Soulimane T, Caffrey M (2012) Structural insights into electron transfer in caa_3-type cytochrome oxidase. Nature 487:514–518
Mackenzie C, Eraso JM, Choudhary M, Roh JH, Zeng X, Bruscella P, Puskas A, Kaplan S (2007) Postgenomic adventures with *Rhodobacter sphaeroides*. Annu Rev Microbiol 61:283–307
Marco-Urrea E, Paul S, Khodaverdi V, Seifert J, von Bergen M, Kretzschmar U, Adrian L (2011) Identification and characterization of a Re-citrate synthase in *Dehalococcoides* strain CBDB1. J Bacteriol 193(19):5171–5178. https://doi.org/10.1128/jb.05120-11
Marcus RA, Sutin N (1985) Electron transfers in chemistry and biology. Biochim Biophys Acta (BBA) Rev Bioenerg 811(3):265–322. https://doi.org/10.1016/0304-4173(85)90014-X
Martinez-Espinosa RM, Marhuenda-Egea FC, Bonete MJ (2001) Assimilatory nitrate reductase from the haloarchaeon *Haloferax mediterranei*: purification and characterisation. FEMS Microbiol Lett 204(2):381–385
McGlynn SE, Chadwick GL, Kempes CP, Orphan VJ (2015) Single cell activity reveals direct electron transfer in methanotrophic consortia. Nature 526(7574):531–535. https://doi.org/10.1038/nature15512
Mitchell P (1976) Possible molecular mechanisms of the protonmotive function of cytochrome systems. J Theor Biol 62(2):327–367. https://doi.org/10.1016/0022-5193(76)90124-7
Miura A, Kameya M, Arai H, Ishii M, Igarashi Y (2008) A soluble NADH-dependent fumarate reductase in the reductive tricarboxylic acid cycle of *Hydrogenobacter thermophilus* TK-6. J Bacteriol 190(21):7170–7177. https://doi.org/10.1128/jb.00747-08
Miura H, Mogi T, Ano Y, Migita CT, Matsutani M, Yakushi T, Kita K, Matsushita K (2013) Cyanide-insensitive quinol oxidase (CIO) from *Gluconobacter oxydans* is a unique terminal oxidase subfamily of cytochrome *bd*. J Biochem 153:535–545

Mogi T, Ano Y, Nakatsuka T, Toyama H, Muroi A, Miyoshi H, Migita CT, Ui H, Shiomi K, Omura S, Kita K, Matsushita K (2009) Biochemical and spectroscopic properties of cyanide-insensitive quinol oxidase from *Gluconobacter oxydans*. J Biochem 146:263–271

Montoya L, Celis LB, Razo-Flores E, Alpuche-Solis AG (2012) Distribution of CO_2 fixation and acetate mineralization pathways in microorganisms from extremophilic anaerobic biotopes. Extremophiles 16(6):805–817. https://doi.org/10.1007/s00792-012-0487-3

Moore AL, Albury MS (2008) Further insights into the structure of the alternative oxidase: from plants to parasites. Biochem Soc Trans 36:1022–1026

Mouncey NJ, Kaplan S (1998) Oxygen regulation of the *ccoN* gene encoding a component of the cbb_3 oxidase in *Rhodobacter sphaeroides* $2.4.1^T$: involvement of the FnrL protein. J Bacteriol 180:2228–2231

Mukund S, Adams MW (1995) Glyceraldehyde-3-phosphate ferredoxin oxidoreductase, a novel tungsten-containing enzyme with a potential glycolytic role in the hyperthermophilic archaeon *Pyrococcus furiosus*. J Biol Chem 270(15):8389–8392. https://doi.org/10.1074/jbc.270.15.8389

Oelze J (2000) Respiratory protection of nitrogenase in *Azotobacter* species: is a widely held hypothesis unequivocally supported by experimental evidence? FEMS Microbiol Rev 24:321–333

Osamura T, Kawakami T, Kido R, Ishii M, Arai H (2017) Specific expression and function of the A-type cytochrome *c* oxidase under starvation conditions in *Pseudomonas aeruginosa*. PLoS One 12:e0177957

Otten MF, Stork DM, Reijnders WN, Westerhoff HV, Van Spanning RJ (2001) Regulation of expression of terminal oxidases in *Paracoccus denitrificans*. Eur J Biochem 268:2486–2497

Pereira MM, Santana M, Teixeira M (2001) A novel scenario for the evolution of haem-copper oxygen reductases. Biochim Biophys Acta 1505:185–208

Pereira MM, Sousa FL, Verissimo AF, Teixeira M (2008) Looking for the minimum common denominator in haem-copper oxygen reductases: towards a unified catalytic mechanism. Biochim Biophys Acta 1777:929–934

Peters JW, Beratan DN, Bothner B, Dyer RB, Harwood CS, Heiden ZM, Hille R, Jones AK, King PW, Lu Y, Lubner CE, Minteer SD, Mulder DW, Raugei S, Schut GJ, Seefeldt LC, Tokmina-Lukaszewska M, Zadvornyy OA, Zhang P, Adams MWW (2018) A new era for electron bifurcation. Curr Opin Chem Biol 47:32–38. https://doi.org/10.1016/j.cbpa.2018.07.026

Pire C, Martinez-Espinosa RM, Perez-Pomares F, Esclapez J, Bonete MJ (2014) Ferredoxin-dependent glutamate synthase: involvement in ammonium assimilation in *Haloferax mediterranei*. Extremophiles 18(1):147–159. https://doi.org/10.1007/s00792-013-0606-9

Poole RK, Hill S (1997) Respiratory protection of nitrogenase activity in *Azotobacter vinelandii*—roles of the terminal oxidases. Biosci Rep 17:303–317

Qian Z, Tianwei H, Mackey HR, van Loosdrecht MCM, Guanghao C (2019) Recent advances in dissimilatory sulfate reduction: from metabolic study to application. Water Res 150:162–181. https://doi.org/10.1016/j.watres.2018.11.018

Rathgeber C, Beatty JT, Yurkov V (2004) Aerobic phototrophic bacteria: new evidence for the diversity, ecological importance and applied potential of this previously overlooked group. Photosynth Res 81:113–128

Rauhamäki V, Wikström M (2014) The causes of reduced proton-pumping efficiency in type B and C respiratory heme-copper oxidases, and in some mutated variants of type A. Biochim Biophys Acta 1837:999–1003

Reher M, Gebhard S, Schonheit P (2007) Glyceraldehyde-3-phosphate ferredoxin oxidoreductase (GAPOR) and nonphosphorylating glyceraldehyde-3-phosphate dehydrogenase (GAPN), key enzymes of the respective modified Embden-Meyerhof pathways in the hyperthermophilic crenarchaeota *Pyrobaculum aerophilum* and *Aeropyrum pernix*. FEMS Microbiol Lett 273 (2):196–205. https://doi.org/10.1111/j.1574-6968.2007.00787.x

Safarian S, Rajendran C, Müller H, Preu J, Langer JD, Ovchinnikov S, Hirose T, Kusumoto T, Sakamoto J, Michel H (2016) Structure of a *bd* oxidase indicates similar mechanisms for membrane-integrated oxygen reductases. Science 352:583–586

Saha B, Borovskii G, Panda SK (2016) Alternative oxidase and plant stress tolerance. Plant Signal Behav 11:e1256530

Schut GJ, Adams MWW (2009) The iron-hydrogenase of *Thermotoga maritima* utilizes ferredoxin and NADH synergistically: a new perspective on anaerobic hydrogen production. J Bacteriol 191(13):4451–4457. https://doi.org/10.1128/jb.01582-08

Sekowska A, Kung HF, Danchin A (2000) Sulfur metabolism in *Escherichia coli* and related bacteria: facts and fiction. J Mol Microbiol Biotechnol 2(2):145–177

Shiba T, Kido Y, Sakamoto K, Inaoka DK, Tsuge C, Tatsumi R, Takahashi G, Balogun EO, Nara T, Aoki T et al (2013) Structure of the trypanosome cyanide-insensitive alternative oxidase. Proc Natl Acad Sci U S A 110:4580–4585

Shiro Y (2012) Structure and function of bacterial nitric oxide reductases: nitric oxide reductase, anaerobic enzymes. Biochim Biophys Acta 1817:1907–1913

Soulimane T, Buse G, Bourenkov GP, Bartunik HD, Huber R, Than ME (2000) Structure and mechanism of the aberrant ba_3-cytochrome *c* oxidase from *Thermus thermophilus*. EMBO J 19:1766–1776

Sousa FL, Alves RJ, Ribeiro MA, Pereira-Leal JB, Teixeira M, Pereira MM (2012) The superfamily of heme-copper oxygen reductases: types and evolutionary considerations. Biochim Biophys Acta 1817:629–637

Spaans SK, Weusthuis RA, van der Oost J, Kengen SW (2015) NADPH-generating systems in bacteria and archaea. Front Microbiol 6:742. https://doi.org/10.3389/fmicb.2015.00742

Stein LY, Klotz MG (2016) The nitrogen cycle. Curr Biol 26(3):R94–R98. https://doi.org/10.1016/j.cub.2015.12.021

Steuber J, Vohl G, Muras V, Toulouse C, Claußen B, Vorburger T, Fritz G (2015) The structure of Na^+-translocating of NADH:ubiquinone oxidoreductase of *Vibrio cholerae*: implications on coupling between electron transfer and Na^+ transport. Biol Chem 396:1015–1030

Stincone A, Prigione A, Cramer T, Wamelink MM, Campbell K, Cheung E, Olin-Sandoval V, Gruning NM, Kruger A, Tauqeer Alam M, Keller MA, Breitenbach M, Brindle KM, Rabinowitz JD, Ralser M (2015) The return of metabolism: biochemistry and physiology of the pentose phosphate pathway. Biol Rev Camb Philos Soc 90(3):927–963. https://doi.org/10.1111/brv.12140

Swingley WD, Sadekar S, Mastrian SD, Matthies HJ, Hao J, Ramos H, Acharya CR, Conrad AL, Taylor HL, Dejesa LC et al (2007) The complete genome sequence of *Roseobacter denitrificans* reveals a mixotrophic rather than photosynthetic metabolism. J Bacteriol 189:683–690

Tagawa K, Arnon DI (1962) Ferredoxins as electron carriers in photosynthesis and in the biological production and consumption of hydrogen gas. Nature 195:537–543. https://doi.org/10.1038/195537a0

Thauer RK, Jungermann K, Decker K (1977) Energy conservation in chemotrophic anaerobic bacteria. Bacteriol Rev 41(1):100–180

Valentine RC (1964) Bacterial ferredoxin. Bacteriol Rev 28(4):497–517

Wang R, Lin JQ, Liu XM, Pang X, Zhang CJ, Yang CL, Gao XY, Lin CM, Li YQ, Li Y, Lin JQ, Chen LX (2018) Sulfur oxidation in the acidophilic autotrophic *Acidithiobacillus* spp. Front Microbiol 9:3290. https://doi.org/10.3389/fmicb.2018.03290

Yamamoto M, Ikeda T, Arai H, Ishii M, Igarashi Y (2010) Carboxylation reaction catalyzed by 2-oxoglutarate:ferredoxin oxidoreductases from *Hydrogenobacter thermophilus*. Extremophiles 14:79–85. https://doi.org/10.1007/s00792-009-0289-4

Zafrilla B, Martinez-Espinosa RM, Bonete MJ, Butt JN, Richardson DJ, Gates AJ (2011) A haloarchaeal ferredoxin electron donor that plays an essential role in nitrate assimilation. Biochem Soc Trans 39(6):1844–1848. https://doi.org/10.1042/bst20110709

Chapter 3
Extracellular Electron Transfer in Bioelectrochemically Active Microorganisms

Takashi Fujikawa and Kengo Inoue

3.1 Introduction

Electrochemically active microorganisms capable of transferring electrons to/from electrodes play essential roles in bioelectrochemical systems, such as microbial fuel cells and microbial electrosynthesis (MES). Electrochemical and molecular biological studies have demonstrated the detailed mechanisms of extracellular electron transfer (EET) between microorganisms and electrodes. Extensive studies in the last two decades revealed that various microorganisms can transfer electrons to/from electrodes. Detailed mechanisms of electron transfer from microorganisms to electrodes have been intensively studied on two model microorganisms, *Geobacter sulfurreducens* and *Shewanella oneidensis*. These microorganisms are also capable of receiving electrons from electrodes, and the mechanisms of electron uptake have been also studied.

3.2 Extracellular Electron Transfer from Microorganisms to Electrodes

In the bioelectrochemical systems, such as microbial fuel cells, electrons are transferred from electrochemically active microorganisms to the electrodes (Fig. 3.1a). Electrons from cytoplasm are transferred across the cell membranes composed of lipid bilayers via proteins possessing redox-active cofactors, such as *c*-type cytochromes and iron-sulfur proteins and electrically conductive nanowires (Fig. 3.2).

T. Fujikawa · K. Inoue (✉)
Department of Biochemistry and Applied Biosciences, Faculty of Agriculture, University of Miyazaki, Miyazaki, Miyazaki, Japan
e-mail: kinoue@cc.miyazaki-u.ac.jp

M. Ishii, S. Wakai (eds.), *Electron-Based Bioscience and Biotechnology*,
https://doi.org/10.1007/978-981-15-4763-8_3

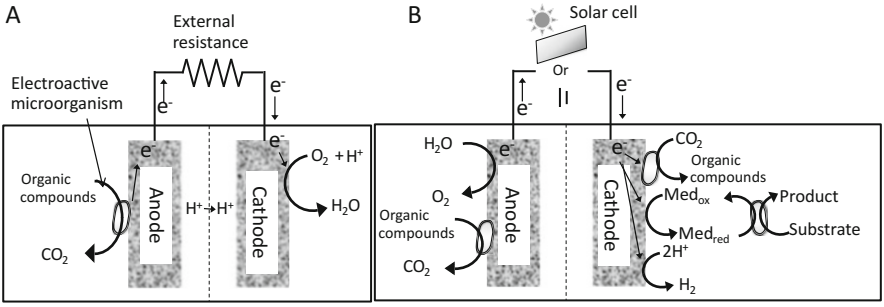

Fig. 3.1 Schematics of a microbial fuel cell (**a**) and a microbial electrosynthesis (microbial electrolysis cell) (**b**)

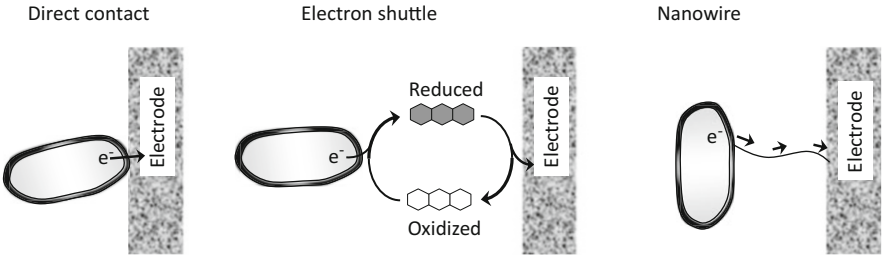

Fig. 3.2 Proposed mechanisms for electron transfer from electroactive microorganisms to the anode

Electron acceptors outside the cells are reduced by primary three different mechanisms, direct contact, electron conductive nanowires, and electron shuttles. The electron transfer mechanisms from the cell surface to the electrode mentioned here are not independently in typical cases but cooperatively, e.g., direct contact and nanowires for *G. sulfurreducens* and direct contact, nanowires, and electron shuttles for *S. oneidensis* (Fig. 3.3).

3.2.1 Direct Contact

In order to transfer electrons from inside the cell to an electrode outside the cell, the electrons must be passed through cell membranes which have insulator property. Electron carrier proteins, *c*-type cytochrome and/or iron-sulfur protein, localized near the cell membrane play essential roles for electron transfer from the cells to the outside in both well-studied microorganisms, *G. sulfurreducens* and *S. oneidensis* (Fig. 3.3). NADH produced in the process of respiration produces quinol by transferring electrons to quinone by NADH dehydrogenase. The electrons of NADH are transferred from inner membrane proteins to the redox-active proteins

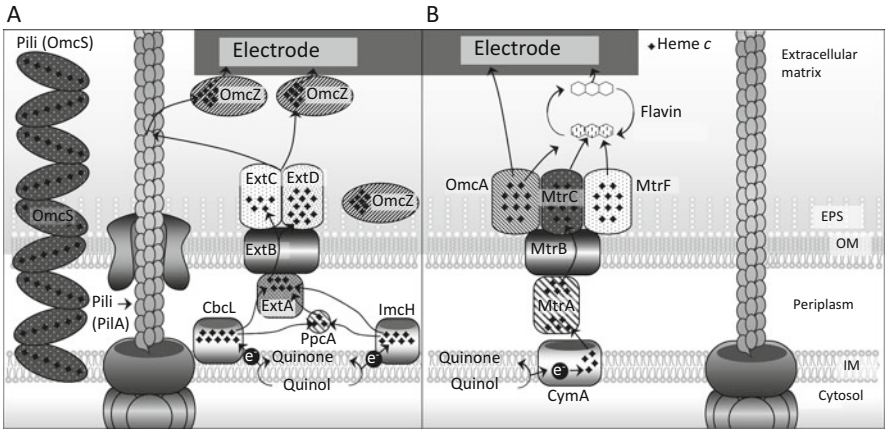

Fig. 3.3 Model for electron transfer from the inner membrane quinone pool to outside the cells in *Geobacter sulfurreducens* (**a**) and *Shewanella oneidensis* (**b**)

in periplasm, which subsequently transfer electrons to also redox-active outer membrane proteins.

In *G. sulfurreducens*, primary *c*-type cytochromes play essential roles in EET by direct contact (Fig. 3.3a). Inner membrane cytochromes, ImcH and CbcL, play important roles in transferring electrons to periplasm. EET via ImcH and CbcL is proposed to be in a redox potential-dependent manner. CbcL and ImcH are required for electron transfer to low (<-0.1 V [vs. SHE]) and high redox potential ($>+0.24$ V [vs. SHE]) electrodes, respectively (Levar et al. 2014; Zacharoff et al. 2016).

In the periplasm, triheme *c*-type cytochromes (most abundant and well-studied PpcA and its homologues PpcB, PpcC, PpcD, and PpcE) are thought to transfer electrons to other redox-active proteins in the outer membrane (Fig. 3.3a) (Lloyd et al. 2003). Among the well-studied outer membrane cytochromes, OmcB is an essential outer membrane cytochrome in the EET from the cells to ferric iron oxide, whereas the deletion of *omcB* gene showed no significant impact on current production (Leang et al. 2003). Electron conduits composed of ExtABCD (ExtA, a periplasmic *c*-type cytochrome; ExtB, an outer membrane integral protein with transmembrane domains; ExtC and ExtD, outer membrane lipoprotein *c*-type cytochromes) are proposed to be involved in electron transfer from periplasm to outer-surface or outer-surface redox-active proteins (Otero et al. 2018). Another essential protein for EET is an octaheme outer membrane cytochrome, OmcZ. OmcZ has a wide redox range (-420 to -60 mV [versus standard hydrogen electrode] for OmcZ) and specifically localized on the surface of the electrode (Inoue et al. 2010; Inoue et al. 2011). It has been also suggested that the wide redox range and multiple hemes contribute to the electron-storage capacity of the biofilms (Malvankar et al. 2012).

In *S. oneidensis*, also *c*-type cytochromes play important roles in EET (Fig. 3.3b). Electrons from intracellular quinol are transferred to *c*-type cytochrome CymA in the intracellular membrane (Myers and Myers 2000). In the periplasm, Fcc_3 (flavocytochrome c_3) and STC (small tetraheme cytochrome *c*) are thought to transfer electrons to the outer membrane complex composed of MtrA, MtrB, and MtrC, in the outer membrane (Ross et al. 2007; Fonseca et al. 2012; McMillan et al. 2013). MtrF, a homologue of MtrC and OmcA, is also responsible for electron transfer to the extracellular electron acceptor (Coursolle and Gralnick 2010). These proteins, except for MtrB (integral outer membrane β-barrel protein), are also mutiheme cytochromes. *omcA* gene-disrupted strain had less power generation capability in microbial fuel cells, and *mtrA*, *mtrB*, and *mtrC* gene-disrupted strains and *omcA* and *mtrC* double mutants almost lost power generation capabilities (Coursolle et al. 2010).

EET via direct contact by *S. loihica* (Newton et al. 2009), *Aeromonas hydrophilia* (Pham et al. 2003), *Rhodoferax ferrireducens* (Chaudhuri and Lovley 2003), and *Desulfobulbus propionicus* (Holmes et al. 2004) has been reported other than *G. sulfurreducens* and *S. oneidensis*.

3.2.2 *Electrically Conductive Nanowire*

G. sulfurreducens and *S. oneidensis* are known to produce electrically conductive nanowires. Microscopic and electrochemical analyses of pili produced by *G. sulfurreducens* using atomic force microscope equipped with a conductive tip revealed that the nanowire was electrically conductive (Reguera et al. 2005). Purified nanowire had temperature-dependent electrical conductivity similar to metals (Malvankar et al. 2011). *G. sulfurreducens* produces two kinds of electrically conductive nanowires composed of PilA and OmcS.

Deletion mutant of a proposed pilin domain protein, *pilA*, could not reduce insoluble Fe(III) oxide (Reguera et al. 2005), and, also, the *pilA* disruption showed severe inhibition of current production (Reguera et al. 2006). A recent biochemical study demonstrated that PilA was stabilized by electrostatic interaction with Spc (short pilin chaperone) encoded by the gene immediately downstream of *pilA* (Liu et al. 2019). Localization analysis by electron microscopy and immunogold labeling suggests that OmcS is localized along the nanowires (Leang et al. 2010). A recent study using cryoelectron microscopy of purified nanowire extracted from *G. sulfurreducens* cells revealed that the nanowires were composed of a *c*-type cytochrome OmcS (Filman et al. 2019; Wang et al. 2019). According to the three-dimensional structure, the nanowire had 46.7–47.5 Å filament repeat, and each subunit contained six hemes corresponding to the heme numbers of OmcS molecule.

S. oneidensis is also thought to produce electrically conductive nanowires (Gorby et al. 2006). The nanowires produced by the OmcA-disrupted mutant and the MtrC-disrupted mutant do not exhibit electrical conductivity, and these *c*-type cytochromes contribute to the electrical conductivity of the nanowire. A recent study

by electron cryotomography revealed that the nanowires were dynamic chains of interconnected outer membrane vesicles (Subramanian et al. 2018). *Synechocystis* and *Pelotomaculum thermopropionicum* also produced electrically conductive nanowires other than iron-reducing bacteria (Gorby et al. 2006).

3.2.3 Electron Shuttle

Electron shuttle is a soluble electron mediator, also called as mediator. The electron shuttles are reduced by receiving electrons from microorganisms and are oxidized by transferring electrons to an extracellular electron acceptor located far from the cells (Watanabe et al. 2009). Oxidized electron shuttles receive electrons again from the microorganism and reduce the electron acceptors. This process is repeated to transfer electrons between the microorganism and the electrode. There are known examples where natural substances, such as humic acid and sulfur, are used for iron reduction (Thygesen et al. 2009; Straub and Schink 2004). Some microorganisms can produce electron shuttles, such as flavin (*S. oneidensis* [Marsili et al. 2008] and other *Shewanella* species [Canstein et al. 2008]), riboflavin (*Geothrix fermentans* [Mehta-Kolte and Bond 2012]), phenazine (*Pseudomonas chlororaphis* [Hernandez et al. 2004], *P. aeruginosa* [Rabaey et al. 2005], *Pseudomonas* sp. [Pham et al. 2008]), quinone (*S. putrefaciens* [Newman and Kolter 2000], *Lactococcus lactis* [Freguia et al. 2009]), and melanin (*S. algae* [Turick et al. 2002]), by themselves. The advantage of electron transfer by the electronic shuttles is that they can transfer electrons to the electrode even if the electrode is physically distant.

3.3 Extracellular Electron Transfer from Electrodes to Microorganisms

In the microbial electrosynthesis (MES), also called electro-fermentation, electrons are transferred from cathodes to electrochemically active microorganisms (Fig. 3.1b). *G. metallireducens* and *G. sulfurreducens* were firstly reported to convert nitrate to nitrite and fumarate to succinate, respectively, by directly accepting electrons from cathodes (Gregory et al. 2004). The "microbial electron uptake" has been observed in various microorganisms, such as *Sporomusa ovata* (Nevin et al. 2010), *Sporomusa sphaeroides*, *Sporomusa silvacetica*, *Clostridium ljungdahlii*, *C. aceticum*, *Moorella thermoacetica* (also known as *C. thermoacetica*) (Nevin et al. 2011), *G. lovleyi* (Strycharz et al. 2008), *Anaeromyxobacter dehalogenans* (Strycharz et al. 2010), *Rhodopseudomonas palustris* (Bose et al. 2014), *Prosthecochloris aestaurii* (Ha et al. 2017), *Acidithiobacillus ferrooxidans* (Nakasono et al. 1997), and *Methanobacterium palustre* (Cheng et al. 2009),

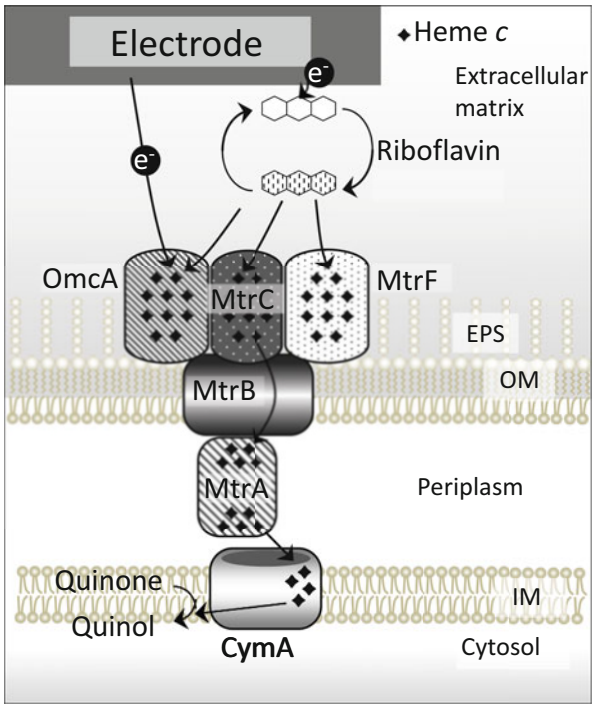

Fig. 3.4 Model for electron transfer from the cathode to *Shewanella oneidensis* cell

whereas very little is known about the molecular mechanisms of accepting electrons from electrodes in these microorganisms.

The mechanisms of the electron uptake from electrodes in *G. sulfurreducens* (Gregory et al. 2004; Dumas et al. 2008) and *S. oneidensis* (Ross et al. 2011) have been studied as well as EET from microorganisms to electrodes. In a *G. sulfurreducens* cell, PccH (GSU3274), a monoheme *c*-type cytochrome proposed to be localized at periplasm, plays an important role in electron uptake process (Strycharz et al. 2011). Deletion mutant of *pccH* did not accept electrons from electrodes, whereas the deletion of *c*-type cytochromes required for EET, such as OmcZ, OmcS, OmcB, and OmcE, did not show significant impact on electron uptake. Biochemical analysis demonstrated that PccH has unusually low redox potential (−24 mV versus standard hydrogen electrode) (Dantas et al. 2013). In *G. sulfurreducens*, the predicted electron pathway from electrodes to the cells is different from EET from cells to the electrodes. In contrast, in *S. oneidensis*, electrons from electrodes were proposed to be transferred via Mtr/CymA pathway by which electrons from cells are transferred to the electrodes (Ross et al. 2011; Okamoto et al. 2014) (Fig. 3.4). In *S. oneidensis*, MtrDEF was suggested to complement the function of MtrCAB significant partially, and riboflavin could be used as an electron shuttle as well as EET from microorganisms to the electrodes. There are only limited knowledge about the molecular mechanisms of microbial

electrosynthesis, and, thus, it requires further investigations for practical applications for producing various compounds.

References

Bose A, Gardel EJ, Vidoudez C, Parra EA, Girguis PR (2014) Electron uptake by iron-oxidizing phototrophic bacteria. Nat Commun 5:339

Canstein H, Ogawa J, Shimizu S, Lloyd JR (2008) Secretion of flavins by *Shewanella* species and their role in extracellular electron transfer. Appl Environ Microbiol 74:615–623

Chaudhuri SK, Lovley DR (2003) Electricity generation by direct oxidation of glucose in mediatorless microbial fuel cells. Nat Biotechnol 21:1229–1232

Cheng S, Xing D, Call DF, Logan BE (2009) Direct biological conversion of electrical current into methane by electromethanogenesis. Envrion Sci Technol 43:3953–3958

Coursolle D, Gralnick JA (2010) Modularity of the Mtr respiratory pathway of *Shewanella oneidensis* strain MR-1. Mol Microbiol 77:995–1008

Coursolle D, Baron DB, Bond DR, Gralnick JA (2010) The Mtr respiratory pathway is essential for reducing flavins and electrodes in *Shewanella oneidensis*. J Bacteriol 192:467–474

Dantas JM, Tomaz DM, Morgado L, Salgueiro CA (2013) Functional characterization of PccH, a key cytochrome for electron transfer from electrodes to the bacterium *Geobacter sulfurreducens*. FEBS Lett 587:2662–2668

Dumas C, Basseguy R, Bergel A (2008) Microbial electrocatalysis with *Geobacter sulfurreducens* biofilm on stainless steel cathodes. Electrochim Acta 53:2494–2500

Filman DJ, Marino SF, Ward JE, Yang L, Mester Z, Bullitt E, Lovley DR, Strauss M (2019) Cryo-EM reveals the structural basis of long-range electron transport in a cytochrome-based bacterial nanowire. Commun Biol 2:219

Fonseca MB, Paquete CM, Neto SE, Pacheco I, Soares CM, Louro RO (2012) Mind the gap: cytochrome interactions reveal electron pathways across the periplasm of *Shewanella oneidensis* MR-1. Biochem J 449:101–108

Freguia S, Masuda M, Tsujimura S, Kano K (2009) *Lactococcus lactis* catalyses electricity generation at microbial fuel cell anodes via excretion of a soluble quinone. Bioelectrochemistry 76:14–18

Gorby YA, Yanina S, McLean JS, Rosso KM, Moyles D, Dohnalkova A, Beveridge TJ, Chang IS, Kim BH, Kim KS, Culley DE, Reed SB, Romine MF, Saffarini DA, Hill EA, Shi L, Elias DA, Kennedy DW, Pinchuk G, Watanabe K, Ishii S, Logan B, Nealson KH, Fredrickson JK (2006) Electrically conductive bacterial nanowires produced by *Shewanella oneidensis* strain MR-1 and other microorganisms. Proc Natl Acad Sci U S A 30:11358–11363

Gregory KB, Bond DR, Lovley DR (2004) Graphite electrodes as electron donors for anaerobic respiration. Environ Microbiol 6:596–604

Ha PT, Lindemann SR, Shi L, Dohnalkova AC, Fredrickson JK, Madigan MT, Beyenal H (2017) Syntrophic anaerobic photosynthesis via direct interspecies electron transfer. Nat Commun 8:13924

Hernandez ME, Kappler A, Newman DK (2004) Phenazines and other redox-active antibiotics promote microbial mineral reduction. Appl Environ Microbiol 70:921–928

Holmes DE, Bond DR, Lovley DR (2004) Electron transfer by *Desulfobulbus propionicus* to Fe(III) and graphite electrodes. Appl Environ Microbiol 70:1234–1237

Inoue K, Qian X, Morgado L, Kim BC, Mester T, Izallalen M, Salgueiro CA, Lovley DR (2010) Purification and characterization of OmcZ, an outer-surface, octaheme *c*-type cytochrome essential for optimal current production by *Geobacter sulfurreducens*. Appl Environ Microbiol 76:3999–4007

Inoue K, Leang C, Franks AE, Woodard TL, Nevin KP, Lovley DR (2011) Specific localization of the *c*-type cytochrome OmcZ at the anode surface in current-producing biofilms of *Geobacter sulfurreducens*. Environ Microbiol Rep 3:211–217

Leang C, Coppi MV, Lovley DR (2003) OmcB, a *c*-type polyheme cytochrome, involved in Fe(III) reduction in *Geobacter sulfurreducens*. J Bacteriol 185:2096–2103

Leang C, Qian X, Mester T, Lovley DR (2010) Alignment of the *c*-type cytochrome OmcS along pili of *Geobacter sulfurreducens*. Appl Environ Microbiol 76:4080–4084

Levar CE, Chan CH, Mehta-Kolte MG, Bond DR (2014) An inner membrane cytochrome required only for reduction of high redox potential extracellular electron acceptors. MBio 5:e02034–e02014

Liu X, Zhan J, Jing X, Zhou S, Lovley DR (2019) A pilin chaperon required for the expression of electrically conductive *Geobacter sulfurreducens*. Environ Microbiol 21:2511–2522

Lloyd JR, Leang C, Myerson ALH, Coppi MV, Cuifo S, Methe B, Sandler SJ, Lovley DR (2003) Biochemical and genetic characterization of PpcA, a periplasmic *c*-type cytochrome in *Geobacter sulfurreducens*. Biochem J 369:153–161

Malvankar NS, Vargas M, Nevin KP, Franks AE, Leang C, Kim BC, Inoue K, Mester T, Covalla SF, Johnson JP, Rotello VM, Tuominen MT, Lovley DR (2011) Tunable metallic-like conductivity in microbial nanowire networks. Nat Nanotechnol 6:573–579

Malvankar NS, Mester T, Tuominen MT, Lovley DR (2012) Supercapacitors based on *c*-type cytochromes using conductive nanostructured networks of living bacteria. ChemPhysChem 13:463–468

Marsili E, Baron DB, Shikhare ID, Coursolle D, Gralnick JA, Bond DR (2008) *Shewanella* secretes flavins that mediate extracellular electron transfer. Proc Natl Acad Sci U S A 105:3968–3973

McMillan DGG, Marritt SJ, Firer-Sherwood MA, Shi L, Richardson DJ, Evans SD, Elliott SJ, Butt JN, Jeuken LJC (2013) Protein–protein interaction regulates the direction of catalysis and electron transfer in a redox enzyme complex. J Am Chem Soc 135:10550–10556

Mehta-Kolte MG, Bond DR (2012) *Geothrix fermentans* secretes two different redox-active compounds to utilize electron acceptors across a wide range of redox potentials. Appl Environ Microbiol 78:6987–6995

Myers JM, Myers CR (2000) Role of the tetraheme cytochrome CymA in anaerobic electron transport in cells of *Shewanella putrefaciens* MR-1 with normal levels of menaquinone. J Bacteriol 182:67–75

Nakasono S, Matsumoto N, Saiki H (1997) Electrochemical cultivation of *Thiobacillus ferrooxidans* by potential control. Bioelectrochem Bioenerg 43:61–66

Nevin KP, Woodard TL, Franks AE, Summers ZM, Lovley DR (2010) Microbial electrosynthesis: feeding microbes electricity to convert carbon dioxide and water to multicarbon extracellular organic compounds. MBio 1:e00103–e00110

Nevin KP, Hensley SA, Franks AE, Summers ZM, Ou J, Woodard TL, Snoeyebos-West OL, Lovley DR (2011) Electrosynthesis of organic compounds from carbon dioxide is catalyzed by a diversity of acetogenic microorganisms. Appl Envrion Microbiol 77:2882–2826

Newman DK, Kolter R (2000) A role for excreted quinones in extracellular electron transfer. Nature 405:94–97

Newton GJ, Mori S, Nakamura R, Hashimoto K, Watanabe K (2009) Analyses of current-generating mechanisms of *Shewanella loihica* PV-4 and *Shewanella oneidensis* MR-1 in microbial fuel cells. Appl Environ Microbiol 75:7674–7681

Okamoto A, Hashimoto K, Nelason KH (2014) Flavin redox bifurcation as a mechanism for controlling the direction of electron flow during extracellular electron transfer. Angew Chem Int Ed 53:10988–10991

Otero FJ, Chan CH, Bond DR (2018) Identification of different putative outer membrane electron conduits necessary for Fe(III) citrate, Fe(III) oxide, Mn(IV) oxide, or electrode reduction by *Geobacter sulfurreducens*. J Bacteriol 200:e00347–e00318

Pham CA, Jung SJ, Phung NT, Lee J, Chang IS, Kim BH, Yi H, Chun J (2003) A novel electrochemically active and Fe(III)-reducing bacterium phylogenetically related to *Aeromonas hydrophila*, isolated from a microbial fuel cell. FEMS Microbiol Lett 223:129–134

Pham TH, Boon N, Aelterman P, Clauwaert P, De Schamphelaire L, Vanhaecke L, De Maeyer K, Hofte M, Verstraete W, Rabaey K (2008) Metabolites produced by *Pseudomonas* sp. enable a Gram-positive bacterium to achieve extracellular electron transfer. Appl Microbiol Biotechnol 77:1119–1129

Rabaey K, Boon N, Hofte M, Verstraete W (2005) Microbial phenazine production enhances electron transfer in biofuel cells. Environ Sci Technol 39:3401–3408

Reguera G, McCarthy KD, Mehta T, Nicoll JS, Tuominen MT, Lovley DR (2005) Extracellular electron transfer via microbial nanowires. Nature 435:1098–1101

Reguera G, Nevin KP, Nicoll JS, Covalla SF, Woodard TL, Lovley DR (2006) Biofilm and nanowire production leads to increased current in *Geobacter sulfurreducens* fuel cells. Appl Environ Microbiol 72:7345–7348

Ross DE, Ruebush SS, Brantley SL, Hartshorne RS, Clarke TA, Richardson DJ, Tien M (2007) Characterization of protein-protein interactions involved in iron reduction by *Shewanella oneidensis* MR-1. Appl Environ Microbiol 73:5797–5808

Ross DE, Flynn JM, Baron DB, Gralnick JA, Bond DR (2011) Towards electrosynthesis in *Shewanella*: energetics of reversing the mtr pathway for reductive metabolism. PLoS One 6: e16649

Straub KL, Schink B (2004) Ferrihydrite-dependent growth of *Sulfurospirillum deleyianum* through electron transfer via sulfur cycling. Appl Environ Microbiol 70:5744–5749

Strycharz SM, Woodard TL, Johnson JP, Nevin KP, Sanford RA, Löffler FE, Lovley DR (2008) Graphite electrode as a sole electron donor for reductive dechlorination of tetrachlorethene by *Geobacter lovleyi*. Appl Environ Microbiol 74:5943–5947

Strycharz SM, Gannon SM, Boles AR, Franks AE, Nevin KP, Lovley DR (2010) Reductive dechlorination of 2-chlorophenol by *Anaeromyxobacter dehalogenans* with an electrode serving as the electron donor. Environ Microbiol Rep 2:289–294

Strycharz SM, Glaven RH, Coppi MV, Gannon SM, Perpetua LA, Liu A, Nevin KP, Lovley DR (2011) Gene expression and deletion analysis of mechanisms for electron transfer from electrodes to *Geobacter sulfurreducens*. Bioelectrochemistry 80:142–150

Subramanian P, Pirbadianb S, El-Naggar MY, Jensen GJ (2018) Ultrastructure of *Shewanella oneidensis* MR-1 nanowires revealed by electron cryotomography. Proc Natl Acad Sci U S A 115:E3246–E3255

Thygesen A, Poulsen FW, Min B, Angelidaki I, Thomsen AB (2009) The effect of different substrates and humic acid on power generation in microbial fuel cell operation. Bioresour Technol 100:1186–1191

Turick CE, Tisa LS, Caccavo F (2002) Melanin production and use as a soluble electron shuttle for Fe(III) oxide reduction and as a terminal electron acceptor by *Shewanella algae* BrY. Appl Environ Microbiol 68:2436–2444

Wang F, Gu Y, O'Brien JP, Yi SM, Yalcin SE, Srikanth V, Shen C, Vu D, Ing NL, Hochbaum AI, Egelman EH, Malvankar NS (2019) Structure of microbial nanowires reveals stacked hemes that transport electrons over micrometers. Cell 177:361–369

Watanabe K, Manefield M, Lee M, Kouzuma A (2009) Electron shuttles in biotechnology. Curr Biotechnol 20:633–641

Zacharoff L, Chan CH, Bond DR (2016) Reduction of low potential electron acceptors requires the CbcL inner membrane cytochrome of *Geobacter sulfurreducens*. Bioelectrochemistry 107:7–13

Chapter 4
Extracellular Electron Uptake Mechanisms in Sulfate-Reducing Bacteria

Xiao Deng and Akihiro Okamoto

4.1 Overall Introduction

The ubiquitous sulfate-reducing bacteria (SRB) participate in significant biogeological processes such as the cycling of sulfur (Jørgensen 1982; Berner and Raiswell 1983) and carbon and anaerobic oxidation of methane (AOM) (Boetius et al. 2000). Moreover, since hydrogen sulfide (H_2S), a metabolite of SRB, is a metal-corroding chemical, SRB induce anaerobic corrosion of metal infrastructure such as underground oil and gas pipelines. This results in significant economic losses amounting to 0.4% of the gross domestic product of an industrial nation (Koch et al. 2001; Beavers and Thompson 2006). SRB are one of the most ubiquitous bacteria in anaerobic environments, especially the marine environments that are abundant with sulfate (~28 mM in seawater) (Christensen 1984; Parkes et al. 1989; Muyzer and Stams 2008; Fichtel et al. 2012). These bacteria reduce sulfate as the electron acceptor to hydrogen sulfide, coupled with the oxidation of diverse organics, hydrocarbon (So and Young 1999), and hydrogen (H_2) as the electron donors. In addition to these soluble or gaseous energy sources, recent studies demonstrated that some SRB use solids as electron donor via extracellular electron uptake (EEU) processes (Deng et al. 2015, 2018; Beese-Vasbender et al. 2015; Deng and Okamoto 2018; Deng et al. 2020). Direct electron transport process from metal iron specimens into the cell interior was first proposed in two marine sedimentary SRB strains, *Desulfovibrio ferrophilus* strain IS5 and *Desulfobacterium corrodens* strain IS4.

X. Deng
CSIRO Land and Water, Floreat, WA, Australia

A. Okamoto (✉)
National Institute for Materials Science, Tsukuba, Ibaraki, Japan

Graduate School of Chemical Sciences and Engineering, Hokkaido University, Sapporo, Hokkaido, Japan
e-mail: okamoto.akihiro@nims.go.jp

M. Ishii, S. Wakai (eds.), *Electron-Based Bioscience and Biotechnology*,
https://doi.org/10.1007/978-981-15-4763-8_4

This was based on the observation of significantly faster anaerobic corrosion in the absence of organic electron donors and at rates higher than other conventional SRB strains which corrode iron by producing H_2S or depleting accumulated H_2 on the iron surface (Dinh et al. 2004). The direct EEU process from solids in SRB was shown by excluding the involvement of H_2 (generated as a result of proton reduction on the surface of a solid electron donor) as an electron mediator between the solids and SRB cells in whole-cell electrochemical measurements. It has also been proposed that EEU by SRB from solid electron donors is an important mechanism in mediating the interspecies electron transfer process from methane-oxidizing archaea to SRB in the AOM consortia (McGlynn et al. 2015; Wegener et al. 2015; Scheller et al. 2016) as well as the bacterial energy acquisition in energy-scarce subsurface environments (Deng et al. 2018). While the importance and ubiquity of EEU mechanism for the biogeological and biophysical processes and anaerobic iron corrosion have been suggested, the number of microbial species with experimental evidences is still limited.

The present chapter reviews the methodology and background physiochemistry for measuring and calculating the H_2-evolution overpotential of an electrode, bioelectrochemical analyses on electrodes poised at potentials in the potential window for avoiding H_2 evolution, and the temperature and electrode potential dependency of cell activity analyses for investigating whether H_2 is involved in the EEU process. Finally, the limitations of current studies are discussed and critical questions that need to be clarified in future studies are addressed.

4.2 Experimental Background and Methods to Characterize the EEU Process

Since the oxidation of iron [$Fe^0 \rightleftharpoons Fe^{2+} + 2e^-$; $E^0 = -0.44$ V versus standard hydrogen electrode (SHE)] can proceed with proton reduction ($2H^+ + 2e^- \rightleftharpoons H_2$, $E^0_{pH\ 7} = -0.413$ V), H_2 spontaneously forms on the surface of iron under neutral pH condition ($Fe^0 + 2H^+ \rightleftharpoons Fe^{2+} + H_2$, $\Delta G^0_{pH\ 7} = -5.2$ kJ/mol). Therefore, to confirm whether SRB conduct EEU from solids without using H_2 as an electron mediator, artificial electrodes with large overpotentials for H_2 evolution such as indium-tin doped oxide (ITO) and graphite electrodes have been used instead of iron for tracking EEU processes in three-electrode electrochemical reactors.

To determine the onset potential ($E_{on\text{-}set}$) of H_2 evolution for an electrode material under a specific experimental condition, one can apply linear sweep voltammetry (LSV), in which the electrode current is measured as scanning the electrode potential in the negative direction. Because the standard potential of H_2 evolution is $E = -0.059$ pH (V) at 298 K, the H_2 evolution can be assigned to the current that exhibits a shift of $E_{on\text{-}set}$, according to the pH of the electrolyte. A previous study determined that the $E_{on\text{-}set}$ for H_2 evolution on an ITO electrode in artificial seawater medium at neutral pH was approximately -0.9 V (Deng et al. 2015). Based on the

$E_{\text{on-set}}$, the potential window suitable for tracking EEU processes for a certain electrode material can be determined, in which the electrode serves as the sole electron donor providing sufficient energy for cell metabolism while inhibiting the production of H_2.

Results of LSV measurement also enable the calculation of the H_2 evolution current on the electrode at any potential by using the cathodic part of the Butler-Volmer equation as described in Eq. (4.1), provided the H_2 evolution current is small enough and the rate-limiting step is not shifted to the H^+ diffusion. The anodic part is omitted because oxidation reactions on the negatively poised electrode are negligible.

$$j_{H_2} = -j_0 \exp\left[-\frac{2a_c F\left(E - E_{eq}\right)}{RT}\right] \tag{4.1}$$

where j_{H_2} is the H_2-evolution current density on the electrode, j_0 is the exchange current, a_c is cathodic charge transfer coefficient, F is Faraday constant, E is electrode potential, E_{eq} is the equilibrium potential of H_2 evolution, R is the universal gas constant, and T is the temperature. a_c is first calculated based on two current values (j_1 and j_2), measured at different electrode potentials, E_1 and E_2, respectively, as described in the following equation:

$$a_c = -\frac{RT}{2F(E_1 - E_2)} \ln\left(\frac{j_1}{j_2}\right) \tag{4.2}$$

j_0 is then calculated by inserting j_1 and E_1 (or j_2 and E_2) into Eq. (4.1). With the calculated values of a_c and j_0, the j_{H_2} at any electrode potential E can be determined based on Eq. (4.1), unless H^+ diffusion limits the reaction rate. By this method, the j_{H_2} on an ITO electrode in artificial seawater electrolyte with a neutral pH at -0.4 V was found to be ~ -0.11 nA/cm^2. Chronoamperometry measurement which detects currents on an electrode poised at a constant potential showed that the SRB cells capable of EEU produced -0.2 to 20 μA/cm^2 currents (Deng et al. 2015, 2018; Beese-Vasbender et al. 2015; Deng and Okamoto 2018), which are 10^3 to 10^5-fold larger than the j_{H_2}, on electrodes poised at -0.4 V, strongly suggest in the EEU capabilities of SRB cells.

Furthermore, because Eq. (4.1) also describes the relationship between j and T, the theoretical value of H_2-evolution current density at temperature T_1, $j_{H_2,\text{theoretical},T_1}$, can be approximately calculated by using a_c and j_0 values obtained at a known temperature (different from T_1). If the calculated $j_{H_2,\text{theoretical},T_1}$ value is consistent with the measured value j_{H_2,T_1}, it can be considered that the observed current is caused by abiotic reactions (e.g., H_2 production). In contrast, if the $j_{H_2,\text{theoretical},T_1}$ deviates largely from j_{H_2,T_1}, it strongly suggests that the observed current is directly associated with microbial metabolic activities, because the cell activity is largely affected by temperature and can be severely hampered at a suboptimal temperature

only slightly different from the growth temperature. For example, when the reaction temperature decreases from 30 to 4 °C, in theory, the $j_{H_2,\text{theoretical},4°C}$ would be 95% of the $j_{H_2,30°C}$; however, the measured current at 4 °C with SRB cells was less than 20% of that at 30 °C, indicating that the current was attributable to the hampered metabolic activity of SRB cells at suboptimal temperature (Pietzsch et al. 1999) rather than to the inorganic H_2 formation.

Another electrochemical measurement method, differential pulse voltammetry (DPV), is used to examine whether H_2 is involved in the EEU process by microbes. In DPV, a small potential pulse (pulse height ΔE = 10–100 mV, pulse width P_w = ~50 ms level) is repetitively applied to the working electrode (with an interval time Δt = 0.5–5 s), while the potential of the working electrode is slightly changed for several mV after each pulse toward the negative (reduction) direction or the positive (oxidative) direction. Currents at timings right before (before faradic reaction, I_1) and near the end of the pulse (in the middle of faradic reaction; I_2) are measured. By recording the difference of I_1 and I_2 as ΔI, the charging current can be largely eliminated. Therefore, DPV detects the redox potential and relative amount of active species on the electrode surface with a high sensitivity (as low as 10^{-8} M). The DPV analysis of *D. ferrophilus* IS5 cells on the ITO electrode surface revealed that its OMCs had a redox potential of ~−0.46 V and a half width of ~130 mV (Deng et al. 2018). Because the redox potential of OMCs is much more positive compared to the H_2 evolution potential, the result indicates that OMCs solely mediate EEU in IS5 cells without the involvement with H_2. Additionally, the exclusion of H_2 in the EEU process of SRB was also achieved by observing the unchanged current by introducing H_2-metabolizing SRB (e.g., *Desulfobacterium vacuolatum* and *Desulfovibrio* sp. strain HS3) on the electrode surface (Beese-Vasbender et al. 2015; Deng et al. 2018).

4.3 EEU Pathways Across the Cellular Outer Membrane of SRB

Mechanisms of EEU in SRB have been studied using electrochemical, microbiological, and bioinformatic methods. Outer-membrane cytochromes (OMCs), biosynthesized iron sulfide nanoparticles (FeS NPs), and soluble redox mediators are proposed to mediate EEU in cells and solid surfaces (Fig. 4.1). These mechanisms are similar to those identified in iron-reducing bacteria (IRB) that export metabolically generated electrons to the extracellular solid electron acceptors.

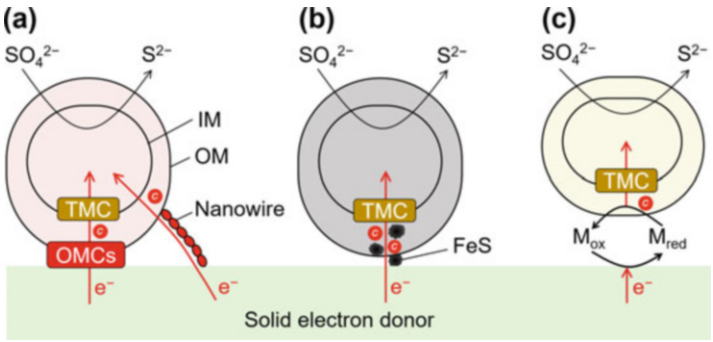

Fig. 4.1 Schematic illustration of identified mechanisms of extracellular electron uptake from solid electron donors coupled with sulfate reduction in sulfate-reducing bacteria (SRB). Electrons (e^-) were transferred across the outer membrane (OM) via (**a**) outer-membrane cytochromes (OMCs) and nanowire structure that is an extension of the OM, (**b**) electrically conductive iron sulfide nanoparticles (FeS NPs) biosynthesized on cell surface, and (**c**) diffusive redox mediators (M_{ox}/M_{red}). Periplasmic cytochromes (*c* in red circles) and/or periplasmic FeS NPs may facilitate the extracted electrons to be further transported to the cellular electron transport chain. *IM* inner membrane, *TMC* transmembrane complex

4.3.1 Outer-Membrane Cytochromes (OMCs) and Nanowires

OMCs are cytochrome proteins located on the cell outer membrane (OM) and were first identified in *Shewanella oneidensis* MR-1 (Myers and Myers 1992), an iron-reducing bacterium which respires oxide minerals (e.g., MnO_2 and Fe_2O_3) as electron acceptors when other soluble electron acceptors (e.g., oxygen) become scarce (Myers and Nealson 1988). The OMCs of *S. oneidensis* MR-1 consist of extracellularly localized decaheme cytochromes OmcA and MtrC, periplasmic decaheme MtrA, and an OM porin MtrB. The extracellular OmcA and MtrC interact with the periplasmic MtrA through MtrB (Myers and Myers 1992). These heme-porin complexes enable extracellular electron transport (EET) in *Shewanella* cells (Bretschger et al. 2007; Bucking et al. 2010; Jensen et al. 2010). Protein crystal structures (Clarke et al. 2011; Edwards et al. 2012, 2014, 2017), binding cofactors (Okamoto et al. 2013, 2014a; Hong and Pachter 2016; Tokunou et al. 2016), and electron transport mechanisms (Breuer et al. 2014) of OMCs have been studied extensively using *Shewanella* OMCs. Meanwhile, similar heme-porin complexes have been just recently identified in *D. ferrophilus* IS5 by gene and protein identification methods (Deng et al. 2018).

The IS5 genome harbors 26 genes encoding cytochromes with four or more heme-binding motifs [CX_nCH (n=2–5)], 7 of which are predicted to be localized in the OM region (Table 4.1). Furthermore, some of the protein products encoded by the potential OMCs gene clusters were detected on the isolated OM. The presence of OMCs in IS5 cells was confirmed by spectroscopic absorption measurement of the isolated OM fraction and was visualized by transmission electron microscopic (TEM) of cell cross-sections stained by a cytochrome-reactive diaminobenzidine

Table 4.1 Potential gene clusters encoding OMCs complex in the genome of *D. ferrophilus* IS5

Genes no.	Amino acids	Heme-binding motifs (most commonly CX_2CH)	Subcellular localization prediction
DFE_448	268	12	Periplasm
DFE_449	301	12	Periplasm
DFE_450	**340**	**6 (including one CX_5CH)**	**Extracellular**
DFE_451	343	N.A. (β-propeller protein)	Unknown
DFE_461	330	14	Periplasm
DFE_462	413	16	Periplasm
DFE_463	299	N.A. (β-propeller protein)	Unknown
DFE_464	**378**	**7 (including one CX_4CH)**	**Unknown but most likely extracellular**
DFE_465	386	7 (including one CX_3CH)	Periplasm

Bold characters indicate cytochromes with predicted extracellular localization

(DAB)-H_2O_2 method (McGlynn et al. 2015; Graham and Karnovsky 1966). Additionally, it was found that IS5 not only expressed OMCs on the cell surface but also the segmented nanowires with diameters ranging from 30 to 50 nm, which were most likely the extensions of OM and periplasmic space in a form of aligned OM vesicles (Fig. 4.1a) (Deng et al. 2018). Similar nanowire structures were also observed in *Shewanella* cells (Deng et al. 2018; Pirbadian et al. 2014; Subramanian et al. 2018). The capability of OMCs in mediating EEU was confirmed by IS5 cells upon controlling the expression of OMCs. The redox potential of IS5 OMCs was approximately −0.46 V (Deng et al. 2018), which is slightly more negative compared to that of the OMCs in *Shewanella* cells (−0.39 V) under EEU conditions. However, much needs to be explored about the IS5 OMCs, for instance, their protein crystal structure, potential binding cofactors, and whether they participate in mediation of the EET process.

The identified genes encoding OMCs in IS5 are widely found in the genomes of bacteria belonging to the phyla Aquificae, Thermodesulfobacteria, and Proteobacteria, which respire various sulfur compounds (e.g., thiosulfate, polysulfide, and sulfite) and primarily inhabit sedimentary environments (Deng et al. 2018). In contrast, the genes encoding OMCs in IRB strains, *Shewanella* and *Geobacter*, were found in the genomes of a few highly similar IRB strains living in oxic-anoxic water column and surface sediments. Because abundant minerals (e.g., iron-copper-sulfides) with adequately negative redox potentials can serve as potential electron donors for microbes, EEU mediated by OMCs may be potential energy acquisition strategy for a wide range of bacteria in these environments to surpass the competition for organic and gaseous electron donors (Deng and Okamoto 2017).

4.3.2 Conductive FeS Nanoparticle (NPs)-Mediated EEU

Electrically conductive NPs, such as palladium precipitated on the cell surface, were reported to function similarly to OMCs by mediating the transportation of

respiratory electrons to solid electron acceptors in some Gram-negative bacteria (Wu et al. 2011). The model of biosynthesized FeS NPs-mediated EEU in SRB was recently verified by a study using *Desulfovibrio vulgaris* Hildenborough, because many SRB like *D. vulgaris* lack a known EEU pathway, including OMCs and secretion of redox mediators (Heidelberg et al. 2004), but produce FeS.

D. vulgaris cells, cultivated in its growth medium supplemented with 2 mM Fe^{2+}, biosynthesized conductive FeS NPs (e.g., mackinawite) extracellularly, intracellularly, and on the cell surface. Electrochemical studies revealed that cells with biosynthesized FeS NPs became capable of direct EEU on the surface of −0.4 V-poised ITO electrodes, serving as the sole electron donor (Deng et al. 2020). By controlling the cell activity on the electrodes (e.g., by adding antibiotic, removing/re-supplementing sulfate or by maintaining a suboptimal growth temperature), it was revealed that the EEU of *D. vulgaris* was associated with its active cell metabolism. Notably, the electron uptake rate of FeS NPs-mediated EEU was approximately sevenfold faster in *D. vulgaris* than that mediated by OMCs in *D. ferrophilus* IS5, indicating that biosynthesized FeS NPs function as an efficient EEU conduit in SRB.

This finding significantly expands the ubiquity of EEU, which was previously considered to be a specific microbial process limited to those bacteria that possess OMCs, to a wider range of bacteria capable of self-synthesis of FeS NPs or have FeS NPs precipitated on the cell surface. FeS NPs are ubiquitously identified in nature, such as marine sediments, because they are predominantly produced by the ubiquitous SRB (Fortin et al. 1994; Donald and Southam 1999; Watson et al. 2000; Williams et al. 2005; Picard et al. 2016) and also in geological processes, e.g., the eruption of hydrothermal fluids and earthquakes (Findlay et al. 2019). These FeS NPs can be transported via water/ocean flow and precipitated on the cell surface of other bacteria. Based on the Pourbaix diagram, mackinawite and pyrrhotite that have been identified as EEU pathways in SRB are stable at conditions with pH $>$ 4, potentially more negative than −0.2 V, and a wide temperature range. The stable pH and potential ranges for mackinawite and pyrrhotite slightly shift to the acidic and reduced direction in accordance with elevated temperatures (Fig. 4.2) (Ning et al. 2015). This indicates that the EEU mechanism mediated by mackinawite and pyrrhotite can be exploited by a wide range of psychrophilic, mesophilic, and thermophilic bacteria for energy acquisition in slightly acidic, neutral, or alkaline reductive environments. In comparison, the semiconductive pyrite and greigite stay stable in lower pH even at strongly oxidative potentials. To further elucidate the distribution of FeS NPs-mediated EEU process, it would be important to explore whether the semiconductive greigite and pyrite can mediate EEU in SRB because they are also found in acidic environments with pH $<$ 4 (Sen and Johnson 1999; Meier et al. 2012; Sanchez-Andrea et al. 2013).

Given that SRB play a primary role in carbon mineralization in marine sedimentary environments (Jørgensen 1982; Berner and Raiswell 1983), the identified FeS NPs-mediated EEU brings novel insights into the biogeochemical cycles of carbon, iron, and sulfur. In addition, FeS NPs-mediated EEU may also provide a pathway for iron oxidation by SRB. A previous corrosion study has observed persistent corrosion of carbon steel by *D. vulgaris* after organic electrons depletion for up to 55 days

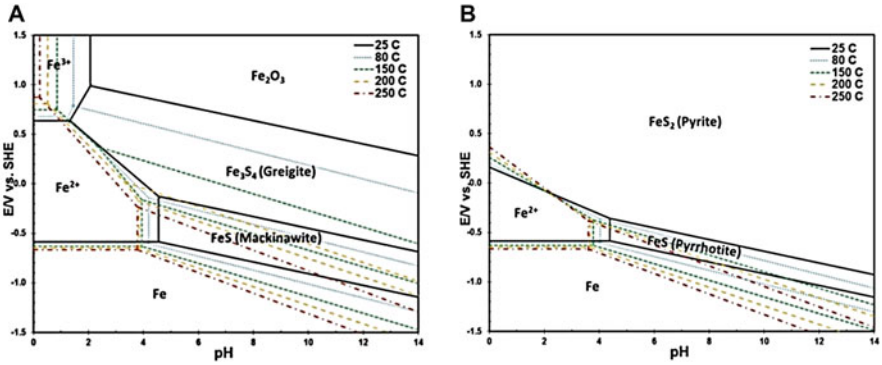

Fig. 4.2 Pourbaix diagrams for H_2S–H_2O–Fe system showing step changes in temperature up to 250 °C (T = 25–250 °C, $[H_2S]_{aq} = 9.4 \times 10^{-3}$ M, $[Fe^{2+}] = 10$ ppm, $[Fe^{3+}] = 10^{-6}$ M): (**a**) mackinawite/greigite and (**b**) mackinawite/greigite/pyrrhotite/pyrite. (Adapted from J. Ning *et al.*, Materials Science, 2015)

(Chen et al. 2015). Therefore, future identification of the mechanism underlying the synthesis of long, electrically conductive pathways via FeS NPs would contribute to the development of an effective strategy for inhibiting microbial iron corrosion.

4.3.3 Soluble Redox Electron Shuttles to Mediate EEU

Soluble redox mediators have been demonstrated to mediate the electron transportation process from cell interior to cell exterior in various microbes. So far, endogenous redox mediators, e.g., riboflavin (RF; $E^{\circ\prime} = -260$ mV), flavin mononucleotide (FMN; $E^{\circ\prime} = -205$ mV), and phenazine derivatives (e.g., phenazine-1-carboxylic acid, phenazine-1-carboxamide, and procyanin, with $E^{\circ\prime} = -275$, -150, and -32 mV, respectively), were identified to be secreted by *Geobacter sulfurreducens*, *S. oneidensis* MR-1, and *Pseudomonas aeruginosa* during cell growth (von Canstein et al. 2008; Marsili et al. 2008; Okamoto et al. 2014b). Meanwhile, exogenous redox mediators derived from the degradation of microbial and plant matter, such as humic acids (HA, $E^{\circ\prime} = -314$ to 430 mV) (Lovley et al. 1996; Jiang and Kappler 2008) artificial mediators [e.g., anthraquinone-2,6-disulfonate (2,6-AQDS; $E^{\circ\prime} = -186$ mV), and potassium ferricyanide ($E^{\circ\prime} = 436$ mV at pH 7)], were also identified (Nevin and Lovley 2000). The redox potentials of these membrane-permeable redox mediators are compatible to microbial cell metabolic processes, and some of these mediators, such as RF and FMN, can function as specific binding cofactors for OMCs (Okamoto et al. 2013, 2014b). Therefore, soluble mediators enable or accelerate electron transfer processes between cells and extracellular solids.

Although information about the capability of biosynthesizing and utilizing redox mediators remains very limited in SRB, it was reported that *Desulfotomaculum*

reducens MI-1, a Gram-positive SRB strain, secreted flavins during cell growth and used the flavins to facilitate the reduction of extracellular Fe^{3+} compounds (e.g., solid-phase hydrous ferric oxide). This suggested that this SRB strain may conduct EET mediated by flavins (Dalla Vecchia et al. 2014). Moreover, it was reported that the addition of redox mediators, RF and flavin adenine dinucleotide (FAD, $E^{\circ\prime} = -340$ mV), accelerated the corrosion of carbon steel and stainless steel by *D. vulgaris*, thereby suggesting that redox mediators may accelerate the EEU from metal iron in this SRB strain (Fig. 4.1c) (Li et al. 2015; Zhang et al. 2015). Further examination of the roles and mechanisms of redox mediators in the OMCs by SRB would contribute to our understanding of EEU mechanisms in SRB.

4.4 Microbial Physiology Coupled with EEU in SRB

4.4.1 Single Cell Activity Measurement for EEU Process

The surface-based cell activity analysis method, nanoscale secondary ion mass spectrometry (NanoSIMS), can be used to measure cell isotopic ratios (e.g., $^{13}C/C_{total}$ and $^{15}N/N_{total}$) at nanometer scale (Nana et al. 2018). It has been observed that when incubated on electrodes with isotopic C and nitrogen (N) sources (e.g., [1-^{13}C] acetate and $^{15}NH_4Cl$), the cells which obtain more energy from the electrode will assimilate more C and N, resulting in higher $^{13}C/C_{total}$ and $^{15}N/N_{total}$. NanoSIMS analysis has been commonly applied to analyze the distribution of cell activity on electrodes (Deng and Okamoto 2018; Saito et al. 2017).

NanoSIMS measurement of the cell activity of *D. ferrophilus* IS5 cells on electrodes at varied potentials (−0.2, −0.3, −0.4, and −0.5 V) demonstrated that cells, which conducted EEU at −0.4 and −0.5 V, obtained energy for C and N assimilation (Deng and Okamoto 2018). In contrast, cells at −0.2 and −0.3 V, which did not conduct EEU, had only $^{13}C/C_{total}$ and $^{15}N/N_{total}$ of natural abundances. Additionally, NanoSIMS measurement of cell activity at varied potentials also revealed the $E_{on\text{-}set}$ for EEU was consistent with the LSV measurement result. Therefore, NanoSIMS measurement of the potential dependency of cell activity could be applied to detect slow microbial EEU process and determine the $E_{on\text{-}set}$ of EEU process where the microbial signals are comparable to or smaller than the background signals.

4.4.2 Cell Growth of SRB During EEU

Electrochemical and NanoSIMS analyses on various SRB species with different EEU pathways, including *D. ferrophilus* IS5, *Desulfobacterium corrodens* IS4, and *D. vulgaris* Hildenborough, showed that their $E_{on\text{-}set}$ was similar and was

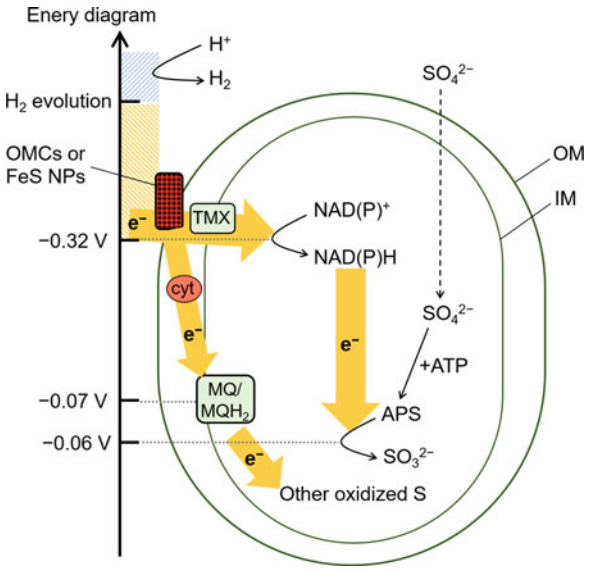

Fig. 4.3 Energy diagram of the extracellular electron uptake from extracellular solids via OMCs or FeS NPs in SRB. The onset potential for EEU is more negative than −0.3 V, which allows sufficient energy for generating nicotinamide adenine dinucleotide (phosphate) [NAD(P)H] and/or reduced menaquinone (MQH_2) which drives the reduction of oxidized sulfur (S) compounds (e.g., sulfate, SO_4^{2-}; sulfite, SO_3^{2-}) and intermediates, such as adenosine phosphosulfate (APS). If the solid has a redox potential negative enough for the proton (H^+) reduction, hydrogen (H_2) is formed on the electrode surface serving as an alternative electron donor for SRB. *cyt* periplasmic cytochrome, *OM* outer membrane, *IM* inner membrane, *TMX* transmembrane complex. Unit, V versus standard hydrogen electrode

approximately −0.3 V (Beese-Vasbender et al. 2015; Deng and Okamoto 2018). Therefore, EEU thermodynamically enables the generation of NAD(P)H ($E^{\circ\prime} = -0.32$ V) by reduction reactions and fuels cell growth (Fig. 4.3). However, in electrochemical studies using single-chamber three-electrode reactors equipped with −0.4 V-poised electrodes as the sole electron donor for incubating *D. ferrophilus* IS5 cells, cell activity was too slow to allow replication in a time span up to 66 days (Deng et al. Under review). The lack of cell growth on electrode surface in single-chamber reactors was also reported for the IRB strain *S. oneidensis* MR-1, which couples EEU with the reduction of oxygen or fumarate (Rowe et al. 2018). In contrast, some iron-oxidizing bacteria (IOB), e.g., *Acidithiobacillus ferrooxidans*, could grow in single-chamber reactors by coupling EEU with oxygen (O_2) reduction (Summers et al. 2013; Ishii et al. 2015). Therefore, although factors that differentiate SRB and IRB cells from IOB for growing on electrodes are unclear, EEU was proposed to supply limited energy for cell maintenance but not cell growth.

A recent study revealed factors specific to the electrochemical reactors that restricted cell growth on the electrodes by focusing on the generation of oxidative stress in the electrochemical reactors (Deng et al. Under review). By incubating IS5 cells in H-type reactors in which the counter electrode (CE) at which oxidation

reactions occur associated with EEU process is separated from cells using a proton-exchange membrane, the first evidence of the growth of *D. ferrophilus* IS5 cells on −0.4 V-poised electrodes was obtained by NanoSIMS analysis. Moreover, in addition to the exogenous oxidative stress, IS5 cell activity was also likely to be restricted by the endogenous oxidative stress produced by the reduction of trace amount of O_2 by the reduced cellular electron transport chain. Therefore, these results demonstrated that the EEU process is intrinsically coupled with the production of exogenous and endogenous oxidative stress and clarified that EEU is an important mechanism supporting cell growth under energy-limited conditions, rather than a mere support for cell maintenance.

However, it is possible that factors specific to the electrochemical systems that inhibit cell growth on the electrode surface. For example, the oxidizing species produced at the counter electrode or an unsuitable working electrode potential may supress cell acitity on the working electrode. These possibilities are currently under examination by Deng et al.

4.4.3 *Gene Expression of* D. ferrophilus *IS5 During EEU*

Transcriptome analysis of IS5 cells which generated currents on electrodes demonstrated upregulated expressions of genes encoding central energy metabolism, including ATP synthesis, sulfate-reducing pathway, and cell division and cell wall synthesis, compared to cells that generated lower currents or cells incubated without an electrode (Deng and Okamoto 2018). The analysis further revealed the significant upregulation of genes encoding OMCs but not those encoding periplasmic hydrogenases required for H_2 utilization in cells that produced higher currents. This in turn strongly suggested that OMCs are the pathway mediating the EEU process without the requirement of oxidizing H_2 as an electron mediator. Moreover, the upregulated levels of antioxidative genes were also observed in cells that produced higher current on an electrode poised at −0.5 V, compared to cells that produced lower currents at −0.4 V. This implied that cells that obtained more energy during EEU had to deal with more antioxidative stress, most likely originating endogenously from the reduction of trace O_2 in the system via the electron transport chain (Deng et al. Under review).

4.5 Future Perspective of EEU by SRB

4.5.1 *Exploration of New Genes for EEU Mechanism in SRB*

OMCs, FeS NPs, and redox mediators have been identified as different pathways mediating EEU in SRB. However, there is a possibility of the presence of new pathways. Therefore, the EEU potential should be explored in SRB living in various

environments. For example, a different EET pathway was recently identified in the Gram-positive bacterium *Listeria monocytogenes*, whereby a novel membrane-attached cytoplasmic NADH dehydrogenase mediated the transportation of respiratory electrons to membrane-localized quinone pool that was further transported to extracellular flavoprotein and/or flavin shuttles to reach extracellular electron acceptors (Light et al. 2018).

4.5.2 Proof of EEU Process in AOM and Iron Corrosion Processes

Although the capability of EEU from electrode has been identified in SRB (Dinh et al. 2004), electron extraction by cells from iron still remains unverified, largely due to the fact that H_2 spontaneously generates on the iron surface and serves as a potential electron donor. To exclusively identify EEU process in iron corrosion by SRB, approaches such as comparison of corrosion rates in wild-type, OMC-deficient, and hydrogenase-deficient strains would be useful. In addition, comparative gene expression analyses of OMCs and hydrogenases of SRB in the presence of iron and H_2 as the sole electron donor could provide insights into the corrosion mechanism.

EEU in SRB was also reported to be important for the activity of syntrophic consortia performing AOM. An interspecies electron transport model has been proposed for AOM consortia. This model states that SRB likely receive electrons directly from the methanotrophic archaea via OMCs and/or conductive pili structures (McGlynn et al. 2015; Wegener et al. 2015; Scheller et al. 2016) rather than using soluble intermediating compounds such as a methane-derived organic carbon compound (Moran et al. 2008). To directly prove this model, electrochemical analysis using archaeal and bacterial isolates that are put in separate anodic and cathodic chambers, respectively, would be required.

4.5.3 Electrical Incubation to Isolate Uncultivated SRB

It is estimated that more than 99.9% of subsurface microbes are uncultivated by conventional methods using soluble electron donors (Short 1997). Because minerals with sufficiently negative potentials, such as iron-copper-sulfides, and microbes potentially possessing an EEU pathway, are widespread in anoxic subsurface environments, electrical incubation methods using electrochemical reactors may enable the enrichment and isolation of novel uncultivated EEU-capable strains from these environments. Moreover, since EEU is not limited to cell-mineral interactions but also intercellular/interspecies interactions, EEU-capable microbes may also be found in non-mineral environments, such as animal guts. Gut microbial strains, such as *Desulfovibrio piger* and *Faecalibacterium prausnitzii*, have been reported to

conduct EET (Khan et al. 2012; de Campos Rodrigues and Rosenbaum Miriam 2014). Testing the capability and significance of EEU in these microbes related with host health may contribute to the development of new technologies for treating EEU-capable pathogens. Because previous studies suggested that different EEU-capable microbes may prefer different electrode potentials and electrode physical properties, using different electrode materials with different range of potential windows may enable the isolation of different EEU-capable microbes.

4.5.4 Proof of Ubiquity of EEU in Environments

Given that EEU-mediating pathways, including OMCs, FeS NPs, and redox mediators, are potentially widespread in sediment bacteria and electric current flow on the mineral surface of sediment hydrothermal vents has been reported (Nakamura et al. 2010), EEU likely plays important role in the energy acquisition by a wide range of bacteria in sediment environments. However, such a model describing EEU-supported subsurface biosphere would require identification of EEU-capable microbes in different sites and the comparison of cell metabolism in situ and ex situ. If EEU capability and the pathways can be identified in abundant microbial lineages, rigorous analysis of gene heritage in the phylogenetic tree would be possible and reveal the origin of EEU biomarker. If the biomarker is conserved vertically in numerous strains living in closely related habitat, it would signify the importance of EEU mediated by the biomarker in the environment. Furthermore, because hydrothermal vent systems like those on Earth are also present in extraterrestrial planets, such as on the icy surface of Europa (Gaidos et al. 1999; McCollom 1999; Chyba 2000; Zolotov and Shock 2003) and on ancient Mars (Michalski et al. 2017), identification of the capability of EEU via non-enzymatic pathways in SRB as well as other microbes with an ancient origin from minerals of hydrothermal vents would provide insights on the origin of life on Earth as well as possible life on extraterrestrial planets.

4.6 Conclusion

In this chapter, we introduced electrochemical methods and studies for identifying direct EEU process in SRB, the most ubiquitous and ancient bacteria on Earth (Shen and Buick 2004). The evolution of H_2 on the surface of solid electron donors has been a major obstacle in the research progress of the EEU mechanisms. By using stable electrodes with large overpotential for H_2 evolution and controlling the physicochemical parameters (e.g., temperature) during the EEU process, the possibility of H_2 involvement in EEU is finally excluded. So far, the identified EEU pathways in SRB include OMCs, FeS NPs, and possibly electron shuttles and can be ubiquitously found in subsurface environments. EEU might be an ancient energy conservation mechanism for supporting the subsurface ecosystems. These findings

contribute to our understanding of SRB physiology and have broad implications in other critical processes associated with SRB, such as anaerobic iron corrosion, AOM, and biogeochemical cycles of iron, sulfur, and carbon. In the future, we anticipate that new EEU pathways in SRB and the related electrosynthetic and biomedical applications will be established and an increasing number of microbes capable of EEU will be identified.

References

Beavers JA, Thompson NG (2006) External corrosion of pipelines in soil. In: Oil and gas pipelines. https://doi.org/10.1002/9781119019213.ch20

Beese-Vasbender PF, Nayak S, Erbe A, Stratmann M, Mayrhofer KJJ (2015) Electrochemical characterization of direct electron uptake in electrical microbially influenced corrosion of iron by the lithoautotrophic SRB Desulfopila corrodens strain IS4. Electrochim Acta 167:321–329

Berner RA, Raiswell R (1983) Burial of organic-carbon and pyrite sulfur in sediments over phanerozoic time—a new theory. Geochim Cosmochim Acta 47:855–862

Boetius A et al (2000) A marine microbial consortium apparently mediating anaerobic oxidation of methane. Nature 407:623–626

Bretschger O et al (2007) Current production and metal oxide reduction by Shewanella oneidensis MR-1 wild type and mutants. Appl Environ Microbiol 73:7003–7012

Breuer M, Rosso KM, Blumberger J (2014) Electron flow in multiheme bacterial cytochromes is a balancing act between heme electronic interaction and redox potentials. Proc Natl Acad Sci 111:611–616

Bucking C, Popp F, Kerzenmacher S, Gescher J (2010) Involvement and specificity of Shewanella oneidensis outer membrane cytochromes in the reduction of soluble and solid-phase terminal electron acceptors. FEMS Microbiol Lett 306:144–151

Chen YJ et al (2015) Long-term survival of Desulfovibrio vulgaris on carbon steel and associated pitting corrosion. Corros Sci 90:89–100

Christensen D (1984) Determination of substrates oxidized by sulfate reduction in intact cores of marine-sediments. Limnol Oceanogr 29:189–192

Chyba C (2000) Energy for microbial life on Europa (vol 403, p 381, 2000). Nature 406:368–368

Clarke TA et al (2011) Structure of a bacterial cell surface decaheme electron conduit. Proc Natl Acad Sci U S A 108:9384–9389

Dalla Vecchia E, Suvorova EI, Maillard J, Bernier-Latmani R (2014) Fe(III) reduction during pyruvate fermentation by Desulfotomaculum reducens strain MI-1. Geobiology 12:48–61

de Campos Rodrigues T, Rosenbaum Miriam A (2014) Microbial electroreduction: screening for new cathodic biocatalysts. ChemElectroChem 1:1916–1922

Deng X, Okamoto A (2017) Energy aquisition via electron uptake by the sulfate-reducing bacterium *Desulfovibrio ferrophilus* IS5. J Jpn Soc Extremophiles 16:67–75

Deng X, Okamoto A (2018) Electrode potential dependency of single-cell activity identifies the energetics of slow microbial electron uptake process. Front Microbiol 9:2744

Deng X, Nakamura R, Hashimoto K, Okamoto A (2015) Electron extraction from an extracellular electrode by Desulfovibrio ferrophilus strain IS5 without using hydrogen as an electron carrier. Electrochemistry 83:529–531

Deng X, Dohmae N, Nealson KH, Hashimoto K, Okamoto A (2018) Multi-heme cytochromes provide a pathway for survival in energy-limited environments. Sci Adv 4:eaao5682

Deng X, Dohmae N, Kaksonen AH, Okamoto A (2020) Biogenic iron sulfide nanoparticles to enable extracellular electron uptake in sulfate-reducing bacteria, Angewandte Chemie-International Edition. https://doi.org/10.1002/anie.201915196

Deng X, Saito J, Kaksonen A, Okamoto A (Under review) Enhancement of cell growth by uncoupling extracellular electron uptake and oxidative stress production in sediment sulfate-reducing bacterial

Dinh HT et al (2004) Iron corrosion by novel anaerobic microorganisms. Nature 427:829–832

Donald R, Southam G (1999) Low temperature anaerobic bacterial diagenesis of ferrous monosulfide to pyrite. Geochim Cosmochim Acta 63:2019–2023

Edwards MJ, Fredrickson JK, Zachara JM, Richardson DJ, Clarke TA (2012) Analysis of structural MtrC models based on homology with the crystal structure of MtrF. Biochem Soc Trans 40:1181–1185

Edwards MJ et al (2014) The X-ray crystal structure of Shewanella oneidensis OmcA reveals new insight at the microbe-mineral interface. FEBS Lett 588:1886–1890

Edwards MJ, Gates AJ, Butt J, Richardson DJ, Clarke TA (2017) Comparative structure-potentio-spectroscopy of the Shewanella outer membrane multiheme cytochromes. Curr Opin Electrochem 4:199–205

Fichtel K, Mathes F, Könneke M, Cypionka H, Engelen B (2012) Isolation of sulfate-reducing bacteria from sediments above the deep-subseafloor aquifer. Front Microbiol 3:65

Findlay AJ et al (2019) Iron and sulfide nanoparticle formation and transport in nascent hydrothermal vent plumes. Nat Commun 10:1597

Fortin D, Southam G, Beveridge TJ (1994) Nickel sulfide, iron-nickel sulfide and iron sulfide precipitation by a newly isolated desulfotomaculum species and its relation to nickel resistance. FEMS Microbiol Ecol 14:121–132

Gaidos EJ, Nealson KH, Kirschvink JL (1999) Biogeochemistry—life in ice-covered oceans. Science 284:1631–1633

Graham RC, Karnovsky MJ (1966) The early stages of absorption of injected horseradish peroxidase in the proximal tubules of mouse kidney: ultrastructural cytochemistry by a new technique. J Histochem Cytochem 14:291–302

Heidelberg JF et al (2004) The genome sequence of the anaerobic, sulfate-reducing bacterium Desulfovibrio vulgaris Hildenborough. Nat Biotechnol 22:554–559

Hong G, Pachter R (2016) Bound flavin–cytochrome model of extracellular electron transfer in Shewanella oneidensis: analysis by free energy molecular dynamics simulations. J Phys Chem B 120:5617–5624

Ishii T, Kawaichi S, Nakagawa H, Hashimoto K, Nakamura R (2015) From chemolithoautotrophs to electrolithoautotrophs: CO2 fixation by Fe(II)-oxidizing bacteria coupled with direct uptake of electrons from solid electron sources. Front Microbiol 6:994

Jensen HM et al (2010) Engineering of a synthetic electron conduit in living cells. Proc Natl Acad Sci U S A 107:19213–19218

Jiang J, Kappler A (2008) Kinetics of microbial and chemical reduction of humic substances: implications for electron shuttling. Environ Sci Technol 42:3563–3569

Jørgensen BB (1982) Mineralization of organic matter in the sea bed—the role of sulphate reduction. Nature 296:643–645

Khan MT et al (2012) The gut anaerobe Faecalibacterium prausnitzii uses an extracellular electron shuttle to grow at oxic–anoxic interphases. ISME J 6:1578–1585

Koch GH, Brongers MPH, Thompson NG, Virmani YP, Payer JH (2001) Corrosion cost and preventive strategies in the United States. NACE International, Dublin

Li HB et al (2015) Extracellular electron transfer is a bottleneck in the microbiologically influenced corrosion of C1018 carbon steel by the biofilm of sulfate-reducing bacterium Desulfovibrio vulgaris. PLoS One 10:e0136183

Light SH et al (2018) A flavin-based extracellular electron transfer mechanism in diverse Gram-positive bacteria. Nature 562:140

Lovley DR, Coates JD, BluntHarris EL, Phillips EJP, Woodward JC (1996) Humic substances as electron acceptors for microbial respiration. Nature 382:445–448

Marsili E et al (2008) Shewanella Secretes flavins that mediate extracellular electron transfer. Proc Natl Acad Sci U S A 105:3968–3973

McCollom TM (1999) Methanogenesis as a potential source of chemical energy for primary biomass production by autotrophic organisms in hydrothermal systems on Europa. J Geophys Res Planets 104:30729–30742
McGlynn SE, Chadwick GL, Kempes CP, Orphan VJ (2015) Single cell activity reveals direct electron transfer in methanotrophic consortia. Nature 526:531–535
Meier J, Piva A, Fortin D (2012) Enrichment of sulfate-reducing bacteria and resulting mineral formation in media mimicking pore water metal ion concentrations and pH conditions of acidic pit lakes. FEMS Microbiol Ecol 79:69–84
Michalski JR, Dobrea EZN, Niles PB, Cuadros J (2017) Ancient hydrothermal seafloor deposits in Eridania basin on Mars. Nat Commun 8:15978
Moran JJ et al (2008) Methyl sulfides as intermediates in the anaerobic oxidation of methane. Environ Microbiol 10:162–173
Muyzer G, Stams AJM (2008) The ecology and biotechnology of sulphate-reducing bacteria. Nat Rev Microbiol 6:441–454
Myers CR, Myers JM (1992) Localization of cytochromes to the outer-membrane of anaerobically grown Shewanella-Putrefaciens Mr-1. J Bacteriol 174:3429–3438
Myers CR, Nealson KH (1988) Bacterial manganese reduction and growth with manganese oxide as the sole electron-acceptor. Science 240:1319–1321
Nakamura R et al (2010) Electrical current generation across a Black Smoker Chimney. Angew Chem Int Ed 49:7692–7694
Nana GYG et al (2018) Division-based, growth rate diversity in bacteria. Front Microbiol 9:849
Nevin KP, Lovley DR (2000) Potential for nonenzymatic reduction of Fe(III) via electron shuttling in subsurface sediments. Environ Sci Technol 34:2472–2478
Ning J, Zheng Y, Brown B, Young D, Nesic S (2015) Construction and verification of Pourbaix diagrams for hydrogen sulfide corrosion of mild steel. In: NACE—International corrosion conference series 2015
Okamoto A, Hashimoto K, Nealson KH, Nakamura R (2013) Rate enhancement of bacterial extracellular electron transport involves bound flavin semiquinones. Proc Natl Acad Sci U S A 110:7856–7861
Okamoto A et al (2014a) Cell-secreted flavins bound to membrane cytochromes dictate electron transfer reactions to surfaces with diverse charge and pH. Sci Rep 4:5628
Okamoto A et al (2014b) Uptake of self-secreted flavins as bound cofactors for extracellular electron transfer in Geobacter species. Energy Environ Sci 7:1357–1361
Parkes RJ, Gibson GR, Muellerharvey I, Buckingham WJ, Herbert RA (1989) Determination of the substrates for sulfate-reducing bacteria within marine and estuarine sediments with different rates of sulfate reduction. J Gen Microbiol 135:175–187
Picard A, Gartman A, Girguis PR (2016) What do we really know about the role of microorganisms in iron sulfide mineral formation? Front Earth Sci 4:68
Pietzsch K, Hard BC, Babel W (1999) A Desulfovibrio sp capable of growing by reducing U(VI). J Basic Microbiol 39:365–372
Pirbadian S et al (2014) Shewanella oneidensis MR-1 nanowires are outer membrane and periplasmic extensions of the extracellular electron transport components. Proc Natl Acad Sci U S A 111:12883–12888
Rowe AR et al (2018) Tracking electron uptake from a cathode into Shewanella cells: implications for energy acquisition from solid-substrate electron donors. mBio 9:e02203-17
Saito J, Hashimoto K, Okamoto A (2017) Nanoscale secondary ion mass spectrometry analysis of individual bacterial cells reveals feedback from extracellular electron transport to upstream reactions. Electrochemistry 85:444–446
Sanchez-Andrea I, Stams AJM, Amils R, Sanz JL (2013) Enrichment and isolation of acidophilic sulfate-reducing bacteria from Tinto River sediments. Environ Microbiol Rep 5:672–678
Scheller S, Yu H, Chadwick GL, McGlynn SE, Orphan VJ (2016) Artificial electron acceptors decouple archaeal methane oxidation from sulfate reduction. Science 351:703–707

Sen AM, Johnson B (1999) Acidophilic sulphate-reducing bacteria: candidates for bioremediation of acid mine drainage. In: Biohydrometallurgy and the environment toward the mining of the 21st century, pt A, vol 9, pp 709–718

Shen YN, Buick R (2004) The antiquity of microbial sulfate reduction. Earth Sci Rev 64:243–272

Short JM (1997) Recombinant approaches for accessing biodiversity. Nat Biotechnol 15:1322–1323

So CM, Young LY (1999) Isolation and characterization of a sulfate-reducing bacterium that anaerobically degrades alkanes. Appl Environ Microbiol 65:2969

Subramanian P, Pirbadian S, El-Naggar MY, Jensen GJ (2018) Ultrastructure of Shewanella oneidensis MR-1 nanowires revealed by electron cryotomography. Proc Natl Acad Sci U S A 115:E3246–E3255

Summers ZM, Gralnick JA, Bond DR (2013) Cultivation of an obligate Fe(II)-oxidizing lithoautotrophic bacterium using electrodes. mBio 4:e00420-12

Tokunou Y, Hashimoto K, Okamoto A (2016) Acceleration of extracellular electron transfer by alternative redox-active molecules to riboflavin for outer-membrane cytochrome c of Shewanella oneidensis MR-1. J Phys Chem C 120:16168–16173

von Canstein H, Ogawa J, Shimizu S, Lloyd JR (2008) Secretion of flavins by Shewanella species and their role in extracellular electron transfer. Appl Environ Microbiol 74:615–623

Watson JHP et al (2000) Structural and magnetic studies on heavy-metal-adsorbing iron sulphide nanoparticles produced by sulphate-reducing bacteria. J Magn Magn Mater 214:13–30

Wegener G, Krukenberg V, Riedel D, Tegetmeyer HE, Boetius A (2015) Intercellular wiring enables electron transfer between methanotrophic archaea and bacteria. Nature 526:587–590

Williams KH et al (2005) Geophysical imaging of stimulated microbial biomineralization. Environ Sci Technol 39:7592–7600

Wu XE et al (2011) A role for microbial palladium nanoparticles in extracellular electron transfer. Angew Chem Int Ed 50:427–430

Zhang PY, Xu DK, Li YC, Yang K, Gu TY (2015) Electron mediators accelerate the microbiologically influenced corrosion of 304 stainless steel by the Desulfovibrio vulgaris biofilm. Bioelectrochemistry 101:14–21

Zolotov MY, Shock EL (2003) Energy for biologic sulfate reduction in a hydrothermally formed ocean on Europa. J Geophys Res Planets 108:5022

Chapter 5
Conversion of Electrical Energy into Life Energy

Norio Matsumoto

5.1 Introduction

Most living organisms acquire energy by "respiration." Respiration is a redox reaction using an electron acceptor and an electron donor. Since the respiratory mechanism of microorganisms is highly diverse, various electron acceptors and donors can be used in the process. Surprisingly, certain microorganisms can respire using redox materials generated by electrochemical reactions, which use electrical energy. This phenomenon can be regarded as a conversion from electrical energy to life energy. In this chapter, we introduce the principle of "electrochemical cultivation" (cultivation of microorganisms using electrochemical energy) and demonstrate the scope of producing useful compounds using the same.

5.2 Viewing Respiration from the Electrochemical Perspective

Respiration, which is common in most living organisms, is the process of acquiring energy necessary for life processes in the form of chemical potential by redox reaction between an electron donor and an electron acceptor. Animals, plants, fungi, and microorganisms that live in an aerobic environment acquire energy by respiration using organic compounds as an electron donor and oxygen as an electron acceptor. On the other hand, since most microorganisms have diverse respiratory mechanisms, some respire using reduced metal ions instead of organic compounds as electron donors. For example, the iron-oxidizing bacterium performs respiration

N. Matsumoto (✉)
Central Research Institute of Electric Power Industry, Abiko, Chiba, Japan
e-mail: norio@criepi.denken.or.jp

M. Ishii, S. Wakai (eds.), *Electron-Based Bioscience and Biotechnology*,
https://doi.org/10.1007/978-981-15-4763-8_5

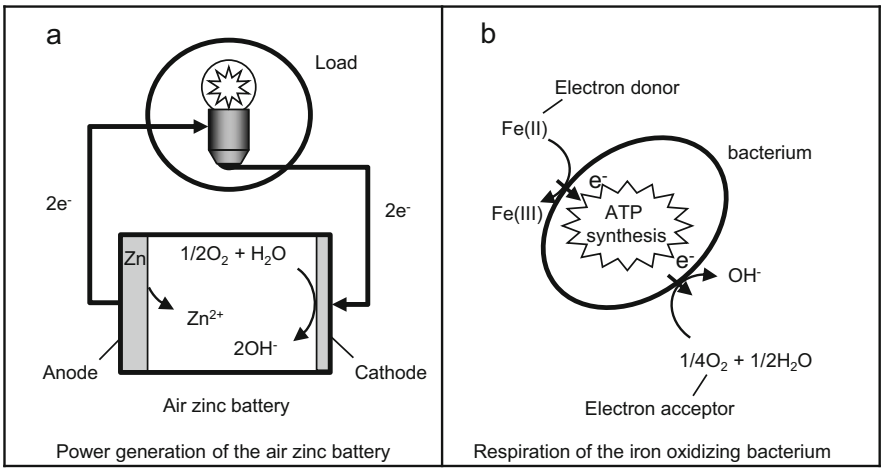

Fig. 5.1 Comparison of battery power generation (**a**) and microbial respiration (**b**)

using a Fe(II) ion as an electron donor and oxygen as an electron acceptor. In terms of electrochemical expression, iron-oxidizing bacteria obtain energy using the potential difference between the following two reactions (Dean 1999).

$$\mathrm{Fe(II)} \rightarrow \mathrm{Fe(III)} + \mathrm{e}^- \qquad +0.771\ \mathrm{V} \tag{5.1}$$

$$1/4\mathrm{O_2} + \mathrm{H}^+ + \mathrm{e}^- \rightarrow 1/2\mathrm{H_2O} \qquad +1.229\ \mathrm{V} \tag{5.2}$$

This is comparable to microorganisms obtaining energy from a "battery" formed in nature. To demonstrate, a comparison of the reaction of a typical zinc-air battery and the respiration of iron-oxidizing bacteria is shown below.

Figure 5.1a shows a schematic diagram of a typical zinc-air battery. When this battery is connected to a load, such as a light bulb, an oxidation reaction of zinc occurs at the negative electrode, and electrons flow to the load. On the other hand, the reaction at the positive electrode shows reduction of oxygen to water by the received electrons. In this way, a pair of oxidation and reduction reactions occur inside the battery, and energy is consumed in the process of moving electrons.

Figure 5.1b shows the respiratory process of iron-oxidizing bacteria. Comparing these two reactions, it can be seen that "negative electrode/electron donor," "positive electrode/electron acceptor," and "load/microorganism" are comparable.

Considering that the basis of respiration is an oxidation-reduction reaction, we arrive at the idea that it is possible to cultivate iron-oxidizing bacteria using electrical energy instead of the chemical potential of a substance, similar to turning on a light bulb using power supply connected to an outlet. Based on this idea, we can conduct electrochemical cultivation of microorganisms.

In the following sections, the principle of electrochemical cultivation of iron-oxidizing bacteria will be explained, and the concept of potential control necessary to realize electrochemical cultivation and the equipment required will be introduced.

5.3 Principle of the Electrochemical Cultivation

In this section, the principle of electrochemical cultivation will be explained using high-density cultivation of iron-oxidizing bacteria as an example, one of the most suitable organisms for application of this method.

Iron-oxidizing bacteria are chemical autotrophic microorganisms that inhabit hot springs and mines and are used in industries as well. For example, they are used in "bacterial leaching" to extract and recover useful metals in mines. As described above, this microorganism respires using Fe(II) ions as an electron donor and oxygen as an electron acceptor. Therefore, when culturing this microorganism, it is sufficient to aerate the medium containing Fe(II) ions. However, since the energy obtained from the redox couple of Fe(II)-oxygen is very poor, when all the Fe (II) ions are consumed, the final cell density is at most 10^8 cells/mL. This is about 1/100th the density of a culture of *Escherichia coli* that respires using glucose, which is a high energy density material. The idea of increasing concentration of Fe(II) ions in the culture medium might be proposed in order to achieve high-density culture of iron-oxidizing bacteria. However, a high concentration of dissolved Fe(II) ions in a culture solution inhibits growth; hence, it is difficult to carry out high-density cultivation of iron-oxidizing bacteria in a medium with high concentration of dissolved Fe(II).

Fe(III) ions generated by respiration of iron-oxidizing bacteria can be easily reduced to Fe(II) ions by applying a negative potential to the electrode immersed in the culture medium. The regenerated Fe(II) ions are then used for respiration by iron-oxidizing bacteria and help in the growth of microorganisms. By repeating this, it is possible to maintain a semi-permanent supply of Fe(II) ions that the microorganism uses as an electron donor, while maintaining a low ion concentration that does not inhibit the growth of the microorganism. As a result, it will eventually be possible to obtain a dense microbial suspension that cannot be achieved by conventional cultivation methods (Fig. 5.2).

According to our experiments, electrochemical cultivation led to a 50–100-fold increase in cell density of iron-oxidizing bacteria compared to cultivation without electrochemical method (Fig. 5.3) (Matsumoto et al. 1999). As shown in the figure, the ideal logarithmic growth could be maintained for 4 days in the electrochemical

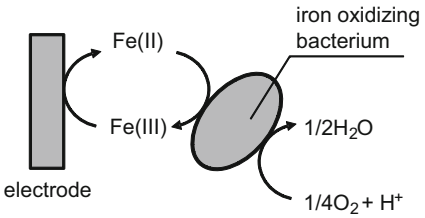

Fig. 5.2 Principle of electrochemical cultivation of an iron-oxidizing bacterium. Since Fe(II) ions are regenerated at the electrode in the electrochemical cultivation, the growth of microorganisms continues semi-permanently

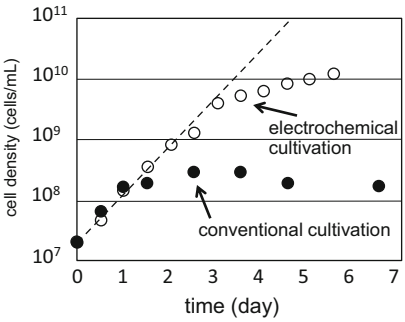

Fig. 5.3 Effect of electrochemical cultivation on the growth of iron-oxidizing bacteria

cultivation by electrochemical regeneration of the Fe(II) ions that is necessary for the respiration of iron reducing bacteria. The microbial growth curve deviated from logarithmic growth in the latter half of the electrochemical cultivation as the rate of Fe(II) consumption by iron-oxidizing bacteria exceeded the rate of Fe(II) production on the electrode, and the growth became electrode reaction rate dependent. Application of electrochemical cultivation to iron-oxidizing bacteria is advantageous as it promotes high-density culture of iron-oxidizing bacteria, which is difficult to achieve with conventional methods, and also allows the required Fe(II) ions to be recycled electrochemically. Furthermore, production of "organic matter" using "electrical energy" is an interesting feature of electrochemical cultivation.

5.4 Importance of Potential Control in the Electrochemical Cultivation

In order to convert Fe(III) in the culture solution to Fe(II), a negative potential is applied to the electrode inserted in the culture medium to initiate an electrochemical reduction. At this point, it is necessary to consider the potential of the electrode that causes the desired reaction. The reason is that besides Fe(II) ions, other redox materials are present, which can initiate a reduction reaction in the culture medium. An undesired reaction in the culture medium may lead to energy loss and may produce substances toxic to microorganisms. Figure 5.4 shows a schematic diagram of a reduction reaction that can occur in a culture medium of iron-oxidizing bacteria. A reduction reaction from Fe(III) to Fe(II) occurs when a reduction potential is applied to the electrode inserted into the cultivation medium. When a further negative potential is applied to the electrode, depending on the material of the electrode, hydrogen peroxide is generated by the reduction of dissolved oxygen. Subsequently, the electrode develops a reduction potential, leading to metallic iron precipitation and hydrogen gas generation by electrolysis of water. If such unintended reactions occur, energy required for Fe(II) production will be wasted.

Hydrogen peroxide production should especially be avoided since it has an inhibitory effect on the growth of microorganisms. In order to avoid these

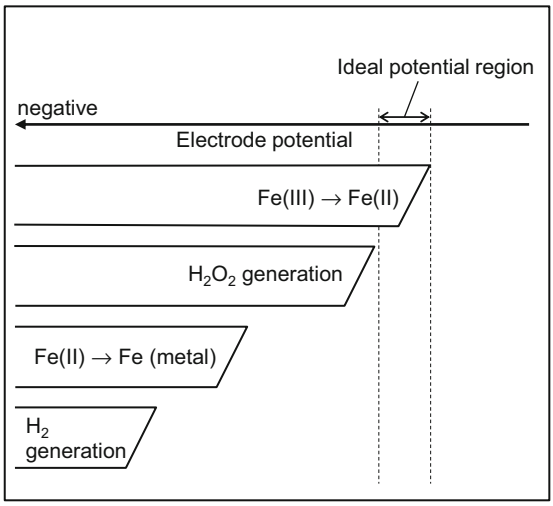

Fig. 5.4 Relationship between electrode potential and occurring reduction reaction in the medium of iron-oxidizing bacteria

unintended reactions and to enable the reduction of Fe(III) to Fe(II), it is necessary to accurately control the electrode potential in the cultivation medium. In the next section, the configuration of an electrochemical cultivation system using a three-electrode potential control method is described.

5.5 Configuration of the Electrochemical Cultivation System

The basic configuration of an apparatus for electrochemical cultivation is shown in Fig. 5.5. The cultivation bath consists of two tanks separated by an ion exchange membrane, and electrodes are set in each tank. One of these tanks is used as a cultivation unit, and the other is used as a counter unit filled with an electrolyte. A cultivation medium containing a redox material is poured into the cultivation unit. The electrode in the cultivation unit is called a working electrode, and the electrode in the counter unit is called a counter electrode. The electrode installed in each tank should be of a material inert toward redox reactions. In general, noble metals like platinum or a carbon plate are preferred for these electrodes.

Application of potential difference between the electrodes installed in each unit can cause a redox reaction in the working electrode set in the cultivation unit. However, such a method cannot control the reaction occurring at the working electrode accurately. Therefore, in order to control the redox potential of the working electrode, a third electrode called a “reference electrode” is installed in its vicinity.

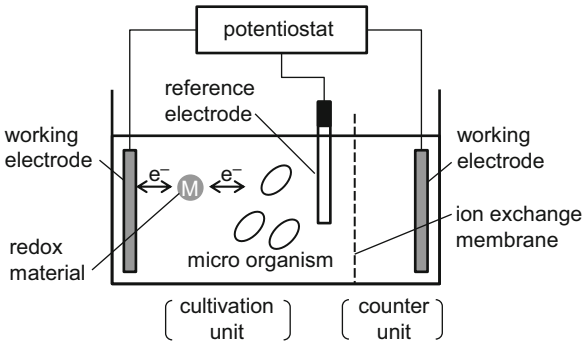

Fig. 5.5 Schematic drawing for the electrochemical cultivation system

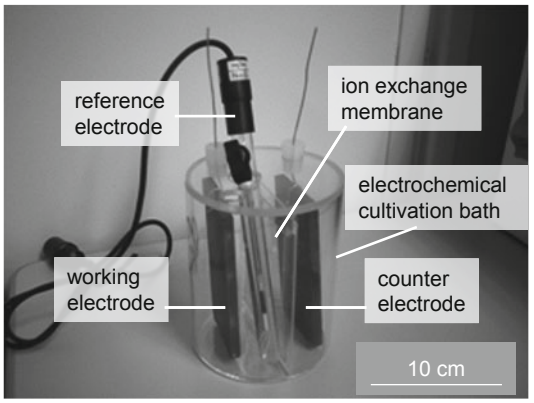

Fig. 5.6 Image of typical electrochemical cultivation bath

Thus, the potential is controlled by connecting three electrodes: working electrode, counter electrode, and reference electrode, to a potentiostat. The electrochemical cultivation device can be designed in various shapes according to the characteristics of the microorganism. The most basic shape of electrochemical cultivation device is shown in Fig. 5.6. In this device, the body is made of glass with 75 mm diameter, 90 mm height, and an ion exchange membrane (Nafion® N-117) is attached to the center with water-resistant glue. A pair of carbon plates (70 mm × 35 mm, 5 mm thickness) is used as the working electrode and the counter electrode, and an Ag/AgCl electrode (DKK-TOA Corp.) is used as the reference electrode.

While the abovementioned device is used for microbial suspensions, it has also been used for electrochemical cultivation on agar plates, a common microbial culture method. We created a flat plate electrochemical cultivation device by placing a working electrode, a counter electrode, and a reference electrode on the bottom of a petri dish and layering agar containing an electrode redox material on it (Fig. 5.7). It has been confirmed that when the potential control is performed in this setup, the redox potential of the agar located on the working electrode can be controlled. The advantage of plate electrochemical cultivation is that a colony of microorganisms that grow under specific electrochemically controlled conditions can be cultured and isolated.

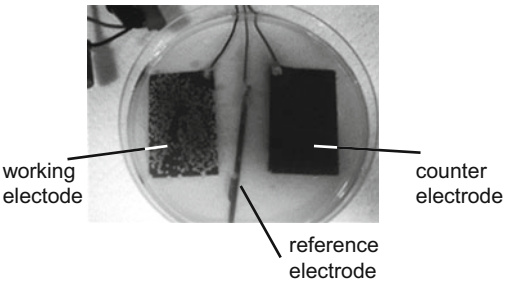

Fig. 5.7 Example of electrochemical cultivation for the flat plate agar

5.6 Application of Electrochemical Cultivation

Electrochemical cultivation can also be applied to microorganisms that live in an anaerobic environment. This section introduces an example of electrochemical cultivation application to the screening of previously uncultured anaerobic microorganisms in soil environments.

Many of the anaerobic microorganisms found in the soil environment are known to be difficult to cultivate using ordinary culture methods. Since some of these microorganisms may have useful functions, such as drug production capacity, a culture method capable of cultivating them is desired. It has been reported in recent years that redox organic materials containing quinone groups, such as humic substances (Fig. 5.8a) found in soil, may exchange electrons with environmental microorganisms and participate in their respiration (Lovley et al. 1996). If such elaborate electron exchange occurring in the soil environment can be reproduced, the possibility of cultivating previously uncultured microorganisms will greatly increase. To study the same, we performed electrochemical cultivation of quinone-reducing bacteria that can grow using anthraquinone disulfonate (AQDS) as an electron acceptor (Fig. 5.8b).

Application of electrochemical cultivation to quinone-reducing bacteria generates an oxidized quinone that is the electron donor for the bacteria on the working electrode. Therefore, it is necessary to control the potential of the working electrode at which quinone oxidation reaction occurs. Moreover, it is necessary to place the whole cultivation bath in an anaerobic atmosphere. Although the direction of reaction occurring at the working electrode of anaerobic electrochemical cultivation is opposite to that of the aerobic one, the same apparatus can be used.

We obtained soil samples that demonstrated reduction of AQDS and may contain previously uncultured quinone-reducing bacteria. These soil samples were suspended in a medium containing AQDS in the cultivation unit of the electrochemical cultivation bath. The potential of the working electrode was set at +0.1 V (vs. Ag/AgCl); AQDS was oxidized at this potential, and the cultivation was carried out for 5 days in an anaerobic atmosphere containing hydrogen gas. We succeeded in cultivating the quinone-reducing bacteria group at a high density of 4×10^8 cells/mL, which was about seven times higher than that observed with the normal cultivation (Fig. 5.9). The bacteria further formed colonies on the agar plate,

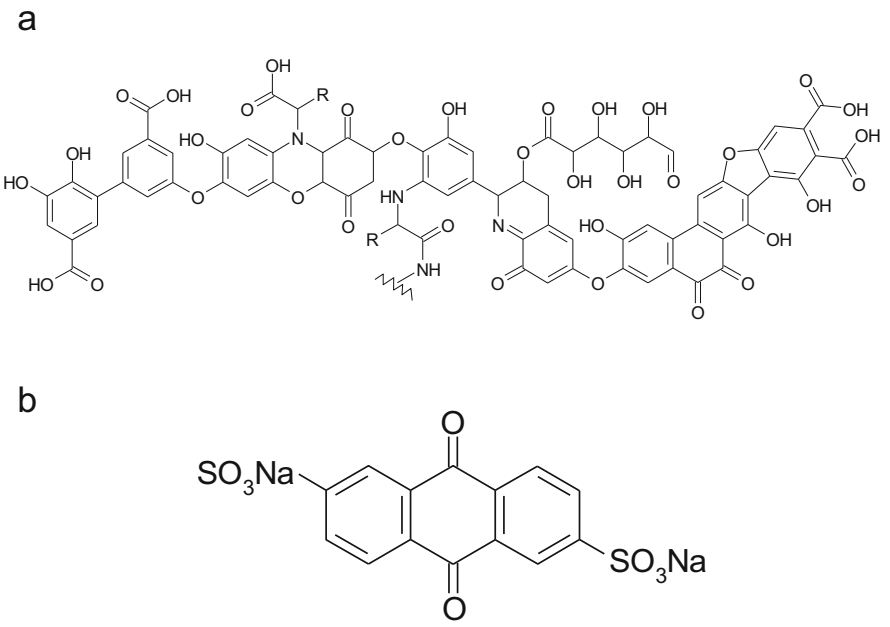

Fig. 5.8 Model structure of humic substances, redox substances in soil (**a**) and molecular formula for oxidized form of anthraquinone disulfonate disodium (**b**)

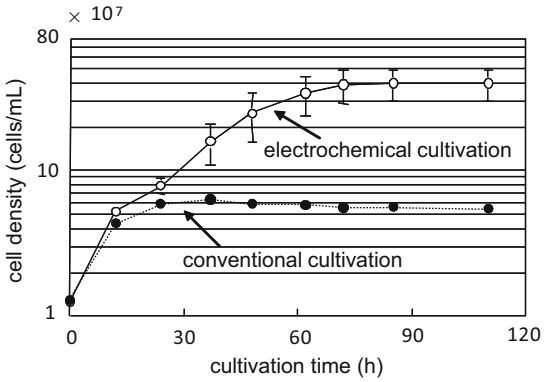

Fig. 5.9 Result for electrochemical cultivation of quinone-reducing bacteria

resulting in the isolation of two types of quinone-reducing bacterium. One was presumed to be closely related to the genus *Desulfitobacter*, which contains many absolute anaerobic microorganisms, and the other was presumed to be closely related to the genus *Enterobacter*, which contains facultative anaerobic microorganisms (Matsumoto et al. 2006). Although the bacteria isolated did not have any

distinctive property, we expect that this increases the possibility of discovering unknown functional microorganisms by applying the electrochemical cultivation method using AQDS to other environmental samples.

5.7 Possibility of Substance Production Using Electrochemical Cultivation

As described above, iron-oxidizing bacteria are autotrophic microorganisms that do not require any organic compounds for growth and fix CO_2 as a carbon source. When iron-oxidizing bacteria are regarded as one of the organic products, the electrochemical cultivation of iron-oxidizing bacteria can be said to be a system that produces organic compounds using "electric energy." If the ability to produce pharmaceutical or chemical compounds can be imparted to iron-oxidizing bacteria by genetic engineering, electrochemical cultivation will be a system that enables the production of compounds using electric energy. The growth environment of iron-oxidizing bacteria has a low pH; hence, it is necessary to overcome this barrier to produce substances in such an environment. On the other hand, as shown in the application examples, focusing on previously uncultured microorganisms such as quinone-reducing bacteria and screening microorganisms that produce useful materials by electrochemical cultivation holds promise. We hope that electrochemical cultivation will be established as a new method for culturing microorganisms.

References

Dean JA (ed) (1999) Lange's handbook of chemistry, 15th edn. McGraw-Hill, New York, pp 8.124–8.137

Lovley DR, Coates JD, Blunt-Harris EL et al (1996) Humic substances as electron acceptors for microbial respiration. Nature 382:445–448

Matsumoto N, Nakasono S, Ohmura N et al (1999) Extension of logarithmic growth of *Thiobacillus ferrooxidans* by potential controlled electrochemical reduction of Fe(III). Biotechnol Bioeng 64:716–721

Matsumoto N, Hirano S, Ohmura N (2006) Electrochemical control of microorganisms (Part 9) Electrochemical cultivation of bacteria using a quinone compound, CRIEPI report V05031 (in Japanese)

Part II
Electron Based Biotechnology

Chapter 6
Electrochemical Interactions Between Microorganisms and Conductive Particles

Souichiro Kato

6.1 Introduction

Electrochemically active microorganisms have an ability to acquire energy through transferring electrons to or from extracellular solid materials. The ability is specifically termed as extracellular electron transfer (EET). Since its discovery, various types of microbial electrochemical systems (MESs), in which electrochemically active microorganisms function as biocatalysts, have been developed (Logan and Rabaey 2012; Kato 2015). Microbial fuel cells (MFC) and microbial electrosynthesis cells are the representatives of MESs, in which microbial cells interact with artificial, macroscopic electrodes. Considering natural environments where electrochemically active microorganisms are originally present, they would interact with naturally occurring conductive materials such as iron minerals. It is well-known that considerably large parts of iron minerals are present in the form of nano-sized particles in environments (Hochella et al. 2008). Hence, knowledge on the electrochemical interaction between microbial cells and small conductive particles is crucial for understanding the ecophysiology of electrochemically active microorganisms. Furthermore, such electrochemical interaction between calls and particles has led to development of new biotechnologies. In this chapter, recent progresses in the following three research topics are introduced from the viewpoints of both basic study and biotechnological application: facilitated long-range electron transfer in artificial conductive biofilm, electric syntrophy (interspecies electron transfer via conductive particles), and microbial photo-electrosynthesis with semiconductive nano-particles.

S. Kato (✉)
Bioproduction Research Institute, National Institute of Advanced Industrial Science and Technology, Sapporo, Japan
e-mail: s.katou@aist.go.jp

M. Ishii, S. Wakai (eds.), *Electron-Based Bioscience and Biotechnology*,
https://doi.org/10.1007/978-981-15-4763-8_6

6.2 Facilitated Long-Range Electron Transfer in Artificial Conductive Biofilm

Electrochemically active microorganisms perform EET via various mechanisms (Torres et al. 2010). The first mechanism is the direct electron transfer mediated by redox proteins such as *c*-type cytochromes (*c*-Cyts) located on cell surfaces. Microorganisms using this mechanism need to adhere to solid conductive materials, resulting in the limitation in number of microbial cells that participate in EET processes. If the cells away from the electrode can also participate in EET processes, the efficiency of the MESs can be improved. The second mechanism is EET via self-secreted, naturally occurring and/or artificially supplied electron mediators (Watanabe 2008). In this mechanism, microbial cells are able to perform EET without direct contact to solid surfaces. However, their EET efficiencies are generally limited by the diffusion of mediator compounds (Torres et al. 2010). The third mechanism is EET via conductive biofilm. *Geobacter sulfurreducens* is well-known to produce such conductive biofilm on both anodic and cathodic electrodes, in which conductive pili and secreted extracellular *c*-Cyts contribute its conductivity (Reguera 2018). EET based on conductive biofilm is the most efficient among the three mechanisms, since a large number of microbial cells in thick biofilm are able to interact with distant electrodes. However, the ability to produce conductive biofilms is limited to only some species in the genus *Geobacter* (Rotaru et al. 2015; Kato 2017).

Recent studies demonstrated that microbial EET reactions can be facilitated by formation of "artificial conductive biofilm" that consists of composites of electrochemically active microbial cells and conductive nano- and/or micro-particles. This concept was first proposed by Nakamura et al. (2009). They demonstrated that an anodic current-generating bacterium, *Shewanella loihica*, has the ability to self-organize an electrically conductive network using nano-particles of semiconductive iron oxides (hematite, α-Fe_2O_3), which largely increased the current generation capability. Photo-electrochemical and molecular genetic approaches revealed that electron hopping between outer-membrane *c*-Cyts of *Shewanella* and hematite particles is crucial for construction of the conductive network (Okamoto et al. 2012). The same research group showed that supplementation of various (semi) conductive particles including magnetite (Fe_3O_4) and biogenic iron sulfides can induce formation of artificial conductive biofilm by *Shewanella* spp. and also *Geobacter* spp. (Kato et al. 2010, 2013; Nakamura et al. 2010). Considering that (semi)conductive iron oxide and iron sulfide minerals are abundantly present in natural environments (Weber et al. 2006), long-range electron transfer mediated by iron minerals is considered to largely contribute to the functioning of microbial communities in various environments.

So far many research groups have attempted to improve the efficiency of MESs using induction of artificial conductive biofilm by supplementation with conductive nano-and micro-particles. Yu et al. largely improved a performance of MFC with pure-culture of *Shewanella oneidensis* by forming conductive biofilm with

micro-sized graphite particles (Yu et al. 2011). Improvements of anodic current generation have been achieved by supplementation with diverse conductive materials, including magnetite (Peng et al. 2013), iron sulfides (Jiang et al. 2014), antimony-doped tin oxide (Zhang et al. 2015), gold (Chen et al. 2018), and also biologically reduced graphene oxides (Yong et al. 2014; Yoshida et al. 2016). Furthermore, this approach is also effective for enhancement of cathodic reactions. For example, artificial conductive biofilm composed of microbial cells and biologically reduced graphene oxides exhibited improved reduction of oxygen (Zhuang et al. 2012) and fumarate (Yong et al. 2014) in MFC bio-cathodes. Induction of artificial conductive biofilm is expected as a promising approach for improvement of diverse MESs, since it can promote microbial electrochemical reactions relatively easily, inexpensively, and environmentally friendly compared to other approaches such as genetic modification of microorganisms and supplementation with artificial mediator compounds.

6.3 Electric Syntrophy: Interspecies Electron Transfer via Conductive Particles

Some important microbial metabolic processes, in particular those proceed under anoxic conditions, are achieved by cooperation of multiple microbial species through energy/electron exchanges, which is specifically termed as syntrophy. Small chemicals such as organics, nitrogen and sulfur compounds, and formate/H_2 usually function as the energy/electron careers. In addition, recent studies demonstrated that interspecies energy/electron exchange is also mediated by electric currents flowing through conductive materials, which is specifically termed as electric syntrophy or direct interspecies electron transfer (Kouzuma et al. 2015; Lovley 2017). Electric syntrophy requires "electrical wires" that connect cells of two different electrochemically active microorganisms. Summers et al. demonstrated that conductive pili produced by microorganisms themselves work as electrical wires that connect metabolisms of *Geobacter metallireducens* (oxidation of ethanol) and *G. sulfurreducens* (reduction of fumarate) (Summers et al. 2010). Furthermore, Kato et al. demonstrated that nano-particles of conductive iron minerals such as magnetite can also facilitate electric syntrophy, using model microbial consortium consisting of two electrochemically active bacteria, namely, *G. sulfurreducens* and *Thiobacillus denitrificans* (Kato et al. 2012a).

Since electric syntrophy can enhance known microbial syntrophic processes and potentially can design new syntrophic processes, it has received considerable attention for their application to biotechnologies. Enhancement of methane fermentation processes, which has been already utilized for energy-saving waste(water) treatments, has been most intensively investigated. Since methanogenic archaea produce methane only from limited substrates (acetate, methanol, and H_2/CO_2), methane production from organic waste(water) requires the cooperation of multiple microbial

species. Syntrophic interaction of organic acid-oxidizing bacteria and methanogenic archaea is regarded as the rate-limiting step of methanogenic processes (Kato and Watanabe 2010). This syntrophic reaction is generally mediated by interspecies electron transfer with formate/H_2 as the electron career. In contrast, it was demonstrated that electric current flowing through conductive materials can facilitate syntrophic methanogenesis. Morita et al. proposed for the first time that electric syntrophy via conductive biofilm produced by *Geobacter* spp. could facilitate methanogenesis in an anaerobic digester (Morita et al. 2011). Similarly, Kato et al. showed that supplementation with conductive iron oxide particles induces electric syntrophy and enhances methanogenesis in microbial communities derived from rice paddy soil (Kato et al. 2012b). Recent studies using a pure and defined co-cultures of *Geobacter* spp. and methanogens in the order *Methanosarcinales* revealed that conductive pili and outer-membrane and/or extracellular *c*-Cyts play pivotal roles in the direct interspecies electron transfer and conductive nano-particles can compensate for (at least part of) their functions and further facilitate electric syntrophy processes (Rotaru et al. 2014a, b; Ueki et al. 2018; Holmes et al. 2019). It has been reported that methanogenesis via electric syntrophy can be facilitated by diverse range of conductive materials, including iron oxides (Cruz Viggi et al. 2014; Yamada et al. 2015), iron sulfides (Kato and Igarashi 2019), graphite (Chen et al. 2014a), and carbon nanomaterials (Lin et al. 2017; Tian et al. 2017). In particular, finding that inexpensive carbon materials such as activated carbon (Liu et al. 2012; Rotaru et al. 2014b) and biochar (Chen et al. 2014b) facilitate methanogenesis would make it possible to drastically reduce the cost in application to wastewater treatment. Improvement of efficiency and stability of methane fermentation of actual wastewater has been demonstrated by experiments using laboratory scale bioreactors (Barua and Dhar 2017; Baek et al. 2016; Dang et al. 2016; Zhao et al. 2016, and reviewed in Martins et al. 2018). Further investigation on microbial physiology and development of low-cost materials with high biocompatibility will proceed applicational use of electric syntrophy for wastewater treatment.

In addition to methanogenesis, several microbial processes, including reductive dichlorination (Aulenta et al. 2013) and anaerobic methane oxidation (McGlynn et al. 2015), are known to be driven by electric syntrophy, which suggests that stimulation of microbial syntrophy has the potential to be applied to various biotechnologies. For example, it has been reported that supplementation with conductive iron oxides into contaminated soil or a bioreactor containing chlorinated aromatic compounds facilitates reductive dechlorination of trichloroethene or 2,4-dichloronitrobenzene, respectively (Aulenta et al. 2013; Wang et al. 2017). Also, Cruz Viggi et al. showed that biodegradation of petroleum hydrocarbons in sediments can be stimulated by introduction of cm-long graphite rods into contaminated sediment to electrically connect the anaerobic sediment and the overlying O_2-containing surface water (Cruz Viggi et al. 2015).

6.4 Microbial Photo-electrosynthesis with Semiconductive Nano-particles

Microbial electrosynthesis is a biotechnology in which electrochemically active microorganisms convert CO_2 into valuable organics with the aid of high-energy electrons supplied from cathodic electrodes (Igarashi and Kato 2017; Prévoteau et al. 2019). Although microbial electrosynthesis has attracted much attention in recent years, such systems require a large number of macroscopic electrode assemblies, which will be limitations when considering widespread commercialization (Sasaki et al. 2018). As a new biotechnology that can solve this issue, "microbial photo-electrosynthesis" was proposed (Sakimoto et al. 2016a). They demonstrated that a non-photosynthetic bacterium (an acetogen *Moorella thermoacetica*) converts CO_2 into acetate using photo-excited high-energy electrons in the conduction band of semiconductive CdS nano-particles that formed by the microorganism itself. Although cysteine was used as a sacrificial electron source in this research, the same research group then achieved production of acetate using water as an electron source by combining the CdS-*M. thermoacetica* system with TiO_2 nano-particles carrying Mn(II) phthalocyanine catalysts (Sakimoto et al. 2016b). Although these studies are still at the stage of the proof of concept with small scale reactors, it has been estimated that this approach, namely, microbial photosynthesis using semiconductor materials and non-photosynthetic microorganisms, has a potential to exceed the energy conversion efficiency of CO_2 fixation by general photosynthetic organisms (Liu et al. 2016).

6.5 Concluding Remarks

In this chapter, several types of electrochemical interactions between microorganisms and conductive particles are introduced from both basic and applied perspectives. Further understanding of this type of interaction will help to elucidate the unknown ecophysiology of electrochemically active microorganisms. Furthermore, most of the technologies introduced here are currently in the early stage of development. Further research on reactor engineering, enlargement of reactor systems, and improvement of long-term durability will achieve the new and efficient MESs.

References

Aulenta F, Rossetti S, Amalfitano S, Majone M, Tandoi V (2013) Conductive magnetite nanoparticles accelerate the microbial reductive dechlorination of trichloroethene by promoting interspecies electron transfer processes. ChemSusChem 6:433–436

Baek G, Kim J, Lee C (2016) A long-term study on the effect of magnetite supplementation in continuous methane fermentation of dairy effluent—enhancement in process performance and stability. Bioresour Technol 222:344–354

Barua S, Dhar BR (2017) Advances towards understanding and engineering direct interspecies electron transfer in anaerobic digestion. Bioresour Technol 244:698–707

Chen S, Rotaru AE, Liu F, Philips J, Woodard TL, Nevin KP, Lovley DR (2014a) Carbon cloth stimulates direct interspecies electron transfer in syntrophic co-cultures. Bioresour Technol 173:82–86

Chen S, Rotaru AE, Shrestha PM, Malvankar NS, Liu F, Fan W, Nevin KP, Lovley DR (2014b) Promoting interspecies electron transfer with biochar. Sci Rep 4:5019

Chen M, Zhou X, Liu X, Zeng RJ, Zhang F, Ye J, Zhou S (2018) Facilitated extracellular electron transfer of *Geobacter sulfurreducens* biofilm with in situ formed gold nanoparticles. Biosens Bioelectron 108:20–26

Cruz Viggi C, Rossetti S, Fazi S, Paiano P, Majone M, Aulenta F (2014) Magnetite particles triggering a faster and more robust syntrophic pathway of methanogenic propionate degradation. Environ Sci Technol 48:7536–7543

Cruz Viggi C, Presta E, Bellagamba M, Kaciulis S, Balijepalli SK, Zanaroli G, Petrangeli Papini M, Rossetti S, Aulenta F (2015) The "Oil-Spill Snorkel": an innovative bioelectrochemical approach to accelerate hydrocarbons biodegradation in marine sediments. Front Microbiol 6:881

Dang Y, Holmes DE, Zhao Z, Woodard TL, Zhang Y, Sun D, Wang LY, Nevin KP, Lovley DR (2016) Enhancing methane fermentation of complex organic waste with carbon-based conductive materials. Bioresour Technol 220:516–522

Hochella MF Jr, Lower SK, Maurice PA, Penn RL, Sahai N, Sparks DL, Twining BS (2008) Nanominerals, mineral nanoparticles, and Earth systems. Science 319:1631–1635

Holmes DE, Ueki T, Tang HY, Zhou J, Smith JA, Chaput G, Lovley DR (2019) A membrane-bound cytochrome enables *Methanosarcina acetivorans* to conserve energy from extracellular electron transfer. MBio 10:e00789-19

Igarashi K, Kato S (2017) Extracellular electron transfer in acetogenic bacteria and its application for conversion of carbon dioxide into organic compounds. Appl Microbiol Biotechnol 101:6301–6307

Jiang X, Hu J, Lieber AM, Jackan CS, Biffinger JC, Fitzgerald LA, Ringeisen BR, Lieber CM (2014) Nanoparticle facilitated extracellular electron transfer in microbial fuel cells. Nano Lett 14:6737–6742

Kato S (2015) Biotechnological aspects of microbial extracellular electron transfer. Microbes Environ 30:133–139

Kato S (2017) Influence of anode potentials on current generation and extracellular electron transfer paths of *Geobacter* species. Int J Mol Sci 18:E108

Kato S, Igarashi K (2019) Enhancement of methanogenesis by electric syntrophy with biogenic iron-sulfide minerals. Microbiology 8:e00647

Kato S, Watanabe K (2010) Ecological and evolutionary interactions in syntrophic methanogenic consortia. Microbes Environ 25:145–151

Kato S, Nakamura R, Kai F, Watanabe K, Hashimoto K (2010) Respiratory interactions of soil bacteria with (semi)conductive iron-oxide minerals. Environ Microbiol 12:3114–3123

Kato S, Hashimoto K, Watanabe K (2012a) Microbial interspecies electron transfer via electric currents through conductive minerals. Proc Natl Acad Sci U S A 109:10042–10046

Kato S, Hashimoto K, Watanabe K (2012b) Methanogenesis facilitated by electric syntrophy via (semi)conductive iron-oxide minerals. Environ. Microbiol. 14:1646–1654

Kato S, Hashimoto K, Watanabe K (2013) Iron-oxide minerals affect extracellular electron-transfer paths of *Geobacter* spp. Microbes Environ 28:141–148

Kouzuma A, Kato S, Watanabe K (2015) Microbial interspecies interactions: recent findings in syntrophic consortia. Front Microbiol 6:477

Lin R, Cheng J, Zhang J, Zhou J, Cen K, Murphy JD (2017) Boosting biomethane yield and production rate with graphene: The potential of direct interspecies electron transfer in anaerobic digestion. Bioresour Technol 239:345–352

Liu F, Rotaru AE, Shrestha PM, Malvankar NS, Nevin KP, Lovley DR (2012) Promoting direct interspecies electron transfer with activated carbon. Energy Environ Sci 5:8982–8989

Liu C, Colón BC, Ziesack M, Silver PA, Nocera DG (2016) Water splitting-biosynthetic system with CO2 reduction efficiencies exceeding photosynthesis. Science 352:1210–1213

Logan BE, Rabaey K (2012) Conversion of wastes into bioelectricity and chemicals by using microbial electrochemical technologies. Science 337:686–690

Lovley DR (2017) Syntrophy goes electric: Direct interspecies electron transfer. Annu Rev Microbiol 71:643–664

Martins G, Salvador AF, Pereira L, Alves MM (2018) Methane production and conductive materials: a critical review. Environ Sci Technol 52:10241–10253

McGlynn SE, Chadwick GL, Kempes CP, Orphan VJ (2015) Single cell activity reveals direct electron transfer in methanotrophic consortia. Nature 526:531–535

Morita M, Malvankar NS, Franks AE, Summers ZM, Giloteaux L, Rotaru AE, Rotaru C, Lovley DR (2011) Potential for direct interspecies electron transfer in methanogenic wastewater digester aggregates. MBio 2:e00159-11

Nakamura R, Kai F, Okamoto A, Newton GJ, Hashimoto K (2009) Self-constructed electrically conductive bacterial networks. Angew Chem Int Ed 48:508–511

Nakamura R, Okamoto A, Tajima N, Newton GJ, Kai F, Takashima T, Hashimoto K (2010) Biological iron-monosulfide production for efficient electricity harvesting from a deep-sea metal-reducing bacterium. ChemBioChem 11:643–645

Okamoto A, Hashimoto K, Nakamura R (2012) Long-range electron conduction of *Shewanella* biofilms mediated by outer membrane *c*-type cytochromes. Bioelectrochemistry 85:61–65

Peng X, Yu H, Ai L, Li N, Wang X (2013) Time behavior and capacitance analysis of nano-Fe_3O_4 added microbial fuel cells. Bioresour Technol 144:689–692

Prévoteau A, Carvajal-Arroyo JM, Ganigué R, Rabaey K (2019) Microbial electrosynthesis from CO_2: forever a promise? Curr Opin Biotechnol 62:48–57

Reguera G (2018) Microbial nanowires and electroactive biofilms. FEMS Microbiol Ecol 94:086

Rotaru AE, Shrestha PM, Liu F, Shrestha M, Shrestha D, Embree M, Zengler K, Wardman C, Nevin KP, Lovley DR (2014a) A new model for electron flow during anaerobic digestion: direct interspecies electron transfer to *Methanosaeta* for the reduction of carbon dioxide to methane. Energy Environ Sci 7:408–415

Rotaru AE, Shrestha PM, Liu F, Markovaite B, Chen S, Nevin KP, Lovley DR (2014b) Direct interspecies electron transfer between *Geobacter metallireducens* and *Methanosarcina barkeri*. Appl Environ Microbiol 80:4599–4605

Rotaru AE, Woodard TL, Nevin KP, Lovley DR (2015) Link between capacity for current production and syntrophic growth in *Geobacter* species. Front Microbiol 6:744

Sakimoto KK, Wong AB, Yang P (2016a) Self-photosensitization of nonphotosynthetic bacteria for solar-to-chemical production. Science 351:74–77

Sakimoto KK, Zhang SJ, Yang P (2016b) Cysteine-cystine photoregeneration for oxygenic photosynthesis of acetic acid from CO_2 by a tandem inorganic-biological hybrid system. Nano Lett 16:5883–5887

Sasaki K, Sasaki D, Kamiya K, Nakanishi S, Kondo A, Kato S (2018) Electrochemical biotechnologies minimizing the required electrode assemblies. Curr Opin Biotechnol 50:182–188

Summers ZM, Fogarty HE, Leang C, Franks AE, Malvankar NS, Lovley DR (2010) Direct exchange of electrons within aggregates of an evolved syntrophic coculture of anaerobic bacteria. Science 330:1413–1415

Tian T, Qiao S, Li X, Zhang M, Zhou J (2017) Nano-graphene induced positive effects on methanogenesis in anaerobic digestion. Bioresour Technol 224:41–47

Torres CI, Marcus AK, Lee HS, Parameswaran P, Krajmalnik-Brown R, Rittmann BE (2010) A kinetic perspective on extracellular electron transfer by anode-respiring bacteria. FEMS Microbiol Rev 34:3–17

Ueki T, Nevin KP, Rotaru AE, Wang LY, Ward JE, Woodard TL, Lovley DR (2018) *Geobacter* strains expressing poorly conductive pili reveal constraints on direct interspecies electron transfer mechanisms. MBio 9:e01273-18

Wang C, Ye L, Jin J, Chen H, Xu X, Zhu L (2017) Magnetite nanoparticles enhance the performance of a combined bioelectrode-UASB reactor for reductive transformation of 2,4-dichloronitrobenzene. Sci Rep 7:10319

Watanabe K (2008) Recent developments in microbial fuel cell technologies for sustainable bioenergy. J Biosci Bioeng 106:528–536

Weber KA, Achenbach LA, Coates JD (2006) Microorganisms pumping iron: anaerobic microbial iron oxidation and reduction. Nat Rev Microbiol 4:752–764

Yamada C, Kato S, Ueno Y, Ishii M, Igarashi Y (2015) Conductive iron oxides accelerate thermophilic methanogenesis from acetate and propionate. J Biosci Bioeng 119:678–682

Yong YC, Yu YY, Zhang X, Song H (2014) Highly active bidirectional electron transfer by a self-assembled electroactive reduced-graphene-oxide-hybridized biofilm. Angew Chem Int Ed 53:4480–4483

Yoshida N, Miyata Y, Doi K, Goto Y, Nagao Y, Tero R, Hiraishi A (2016) Graphene oxide-dependent growth and self-aggregation into a hydrogel complex of exoelectrogenic bacteria. Sci Rep 6:21867

Yu YY, Chen HL, Yong YC, Kim DH, Song H (2011) Conductive artificial biofilm dramatically enhances bioelectricity production in *Shewanella*-inoculated microbial fuel cells. Chem Commun 47:12825–12827

Zhang X, Liu H, Wang J, Ren G, Xie B, Liu H, Zhu Y, Jiang L (2015) Facilitated extracellular electron transfer of *Shewanella loihica* PV-4 by antimony-doped tin oxide nanoparticles as active microelectrodes. Nanoscale 7:18763–18769

Zhao Z, Zhang Y, Holmes DE, Dang Y, Woodard TL, Nevin KP, Lovley DR (2016) Potential enhancement of direct interspecies electron transfer for syntrophic metabolism of propionate and butyrate with biochar in up-flow anaerobic sludge blanket reactors. Bioresour Technol 209:148–156

Zhuang L, Yuan Y, Yang G, Zhou S (2012) In situ formation of graphene/biofilm composites for enhanced oxygen reduction in biocathode microbial fuel cells. Electrochem Commun 21:69–72

Chapter 7
Bioelectrochemical and Reversible Interconversion in the Proton/Hydrogen and Carbon Dioxide/Formate Redox Systems and Its Significance in Future Energy Systems

Yuki Kitazumi and Kenji Kano

7.1 Introduction

Energy is an integral part of human activities. The industrialization and growing population in the world require increasing amounts of energy. To a great extent, major economies of the present-day world rely on fossil fuels. Increasing consumption of fossil fuels is not environmentally friendly, since fossil fuels release greenhouse gases and other pollutants as major contributors to planet warming (European Commission 2003). These global energy problems could be solved by sourcing environmentally clean, cheap, and sustainable energy systems. The introduction of hydrogen (H_2) is considered as the universal vector for conveying renewable forms of energy and as an ultimate ideal sustainable non-pollutant fuel (Rand 2011; Ren et al. 2017; Sahaym and Norton 2008). The proposal to use H_2 as both an energy vector and an ultimate fuel has become known as hydrogen economy or hydrogen energy system in the present day (Fig. 7.1), though the term "hydrogen economy" was first used by J. O'Mara Bockris in 1970 at General Motors Technical Center (Abe et al. 2019). On the other hand, electrical energy is the most important, versatile, and useful of the secondary energy sources and can be obtained and stored by electrochemical reactions in suitable electrochemical devices. Fuel cells that convert the primary energy source, H_2, to the secondary one, electricity, to generate water (H_2O) are key technologies for a hydrogen economy. H_2 can be produced from H_2O as a huge storeroom of H_2, although a lot of electric energy is required in splitting H_2O into H_2 and oxygen (O_2) by electrolysis at conventional electrodes. In any event, electrochemistry, a truly interfacing science, plays vital and important role to construct environmentally clean, cheap, and sustainable energy systems.

Y. Kitazumi · K. Kano (✉)
Division of Applied Life Science, Graduate School of Agriculture, Kyoto University, Kyoto, Japan
e-mail: kitazumi.yuki.7u@kyoto-u.ac.jp; kano.kenji.5z@kyoto-u.ac.jp

M. Ishii, S. Wakai (eds.), *Electron-Based Bioscience and Biotechnology*,
https://doi.org/10.1007/978-981-15-4763-8_7

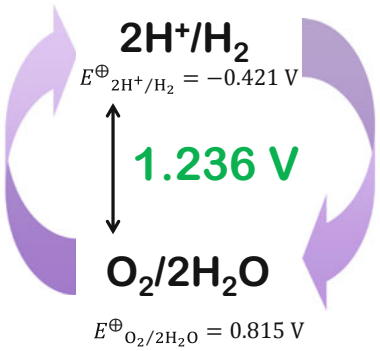

Fig. 7.1 Schematic of the hydrogen economy, in which two redox couples: $2H^+/H_2$ and $O_2/2H_2O$ play important roles. The difference in the biological standard redox potentials ($E^{\oplus}$) of the two couples is 1.236 V at 1×10^5 Pa and 25 °C. $E^{\oplus}$ is referred to the standard hydrogen electrode (SHE)

Future well-being of the planet Earth may lie in the hands of electrochemists (Rand 2011).

However, the electrochemical interconversions between proton (H^+) and H_2 and between O_2 and H_2O usually have large energy losses in kinetics at conventional electrodes. Such energy loss is often called overpotential in the field of electrochemistry. It is very important to minimize the energy loss during the interconversion of energy sources to realize ideal and sustainable energy systems. In order to decrease the overpotentials of the H_2 oxidation and the O_2 reduction in H_2/O_2 fuel cells, devices have to rely on the requirement of catalysts, usually novel metals such as platinum (Pt). Because of availability and economic issue in the use of Pt, extensive researches have been done during the last few decades to decrease or replace Pt in fuel cells. H_2O splitting into H_2 and O_2 also requires catalysts.

One of the strategies to decrease the overpotential of the interconversion is utilization of redox enzymes as electrode catalysts. Hydrogenase (H_2ase) catalyzes the reversible redox reactions of H^+/H_2, while multicopper oxidase (MCO) catalyzes a 4-electron redox reaction of O_2 without producing any intermediate. Photosynthetic organisms or thylakoid membranes can catalyze photochemical splitting of H_2O.

On one level, H_2 shows poor properties in storage and transportation issues. Alternative and attractive fuels in this sense may be some liquid or ionic solutes with high water solubility that can be completely burned in their oxidation. One of the possible fuels is formate ($HCOO^-$) (Asefa et al. 2019). However, it is very important to construct a technology to re-reduce its oxidized product, carbon dioxide (CO_2), in order to prevent an increase in the greenhouse gas. Unfortunately, the redox interconversion of the $CO_2/HCOO^-$ couple has extremely high kinetic barrier at conventional electrodes, and then large overpotentials are required. Energetic researches have been devoted to find and synthesize effective catalysts for the interconversion of the redox couple (Chaplin and Wragg 2003; Enthaler et al. 2010; Gunasekar et al. 2016; Asefa et al. 2019; Grubel et al. 2020). The platinum group elements show relatively high catalytic activity (Enthaler et al. 2010; Gunasekar et al. 2016; Grubel et al. 2020). However, the selectivity and activity in such metal-based catalytic reactions are not acceptable for ideal and sustainable energy systems. The

development of effective catalysts for the interconversion reaction is an attractive subject. From biochemical viewpoints, it is well-known that methylotrophic bacteria express a variety of redox enzymes involved in the C1 metabolism (Kletzin and Adams 1996; Rotaru et al. 2014; Shi et al. 2015). Molybdenum (Mo) or tungsten (W)-containing formate dehydrogenase (FDH) catalyzes the reversible interconversion of the $CO_2/HCOO^-$ redox couple under mild conditions (Reda et al. 2008; Bassegoda et al. 2014; Maia et al. 2016; Yu et al. 2017). Electrochemical properties of FDHs have been actively investigated (Reda et al. 2008; Bassegoda et al. 2014; Sakai et al. 2015, 2017; Jang et al. 2018; Jayathilake et al. 2019).

Significant advantageous properties of biological redox catalysts (or redox enzymes) compared with metal-based catalysts are (1) extremely high catalytic activity, (2) low reorganization energy, (3) high specificity, (4) high identicalness and uniformity (thanks to biological expression), and (5) enormous chemical versatility. These factors are very convenient from the viewpoint of their application. In addition, the redox potential of the electrochemically communicating site of redox enzymes can be definitely defined, which leads to more rigorous discussion on current-potential curves of catalytic waves. However, redox enzymes have huge size and are fragile. The size matter causes characteristic features in direct communication of enzymes with electrodes. In general, the non-catalytic direct redox signal density of redox enzymes is too low to be detected since the surface concentration of such enzymes with huge sizes is quite low, and therefore the enzymatically amplified catalytic redox signal is actually detectable. The orientation of redox enzymes is a key factor determining the distance between the electrode surface and the redox site located near the surface of the enzyme of a large size, since the standard interfacial electron transfer rate constant (k°) decreases exponentially with the distance (d) between the electrode surface and the redox site of the enzyme, as given by the following equation (Bard and Faulkner 2001):

$$k^\circ = k^\circ_{\max} \exp(-\beta d) \tag{7.1}$$

where $k^\circ_{\max}$ is the standard rate constant at the closest approach, and β is the decay coefficient. Therefore, it is very important to control the orientation of redox enzymes on electrodes by tuning the nanostructure and the surface property of mesoporous electrodes as scaffolds for the enzymes.

In this chapter, several applications of bioelectrocatalytic reactions of H_2ase and FDH will be introduced. The adsorption of these enzymes on suitably tuned mesoporous electrodes realizes bioelectrocatalytic reversible conversion of H_2 and HCOOH. MCO-modified electrodes and thylakoid membrane-modified electrodes realize a 4-electron reduction of O_2 and photobioelectrochemical splitting of H_2O, respectively. H_2/O_2 and $HCOO^-/O_2$ biofuel cells are constructed by the combination of suitable bioelectrodes. Photosynthetic energy conversion is also realized by the combination of these enzyme-modified electrodes.

7.2 H_2/O_2 Biofuel Cells

Biofuel cells (rightly, biological fuel cells) are bioelectrochemical devices that convert the reaction energy in the oxidation of several biological fuels with O_2 into the electrical energy with the aid of redox enzymes as electrode catalysts (Barton et al. 2004; Cracknell et al. 2008; Meredith and Minteer 2012; Mazurenko et al. 2017a, b; Mano and de Poulpiquet 2018). The concept of the biofuel cell was first introduced by Yahiro et al. (1964). Generally, biofuel cells consist of a two-electrode setup with the aid of corresponding redox enzymes (Fig. 7.2); fuels are oxidized at the bioanode, and electrons flow through the external electric circular to the biocathode, at which oxidants, usually O_2, are reduced (to H_2O). Some proton-exchange membrane is often employed to separate two compartments while accelerating H^+ transfer, although it is not essential thanks to the substrate specificity of redox enzymes. The first H_2/O_2 biofuel cell was reported in 2001 (Tsujimura et al. 2001a), though whole bacterial cells *Desulfovibrio vulgaris* (Hildenborough) were used as electrode catalysts. In the recent past, O_2-tolerant or O_2-sensitive H_2ases are frequently utilized as electrode catalysts in biocathodes of H_2/O_2 biofuel cells (Vincent et al. 2007; Armstrong and Hirst 2011; Lojou 2011; Mazurenko et al. 2017a, b).

H_2ases catalyze H_2 oxidation and also frequently inverse H^+ reduction. They are classified into [Ni–Fe]-, [Fe–Fe]-, and [Fe]-H_2ases according to the active site component (Vincent et al. 2007; Armstrong and Hirst 2011). The native electron acceptors of H_2ases can be replaced with several artificial redox compounds (in the oxidized form). Some redox compounds reduced by the H_2ase reaction are re-oxidized at electrodes. In this way, the enzymatic reaction can be coupled with the electrode reaction through the artificial redox compound called mediator. This reaction system is referred to as mediated electron transfer (MET)-type bioelectrocatalysis (Fig. 7.3, upper) and is applicable to most other redox enzymes.

Suitably tuned electrodes can play as electron donors for H_2ases; the enzyme reaction is directly coupled with the electrode reaction without any mediator. The reaction system is referred to as direct electron transfer (DET)-type bioelectrocatalysis (Fig. 7.3, lower). Enzymes capable of the DET-type reactions

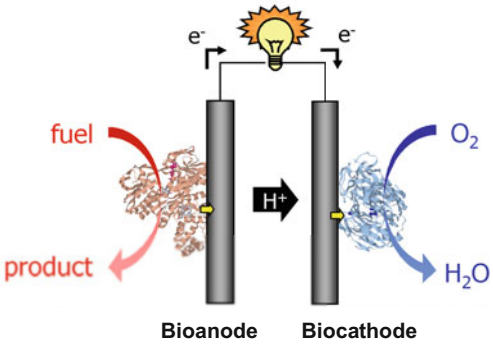

Fig. 7.2 Schematic of biofuel cells

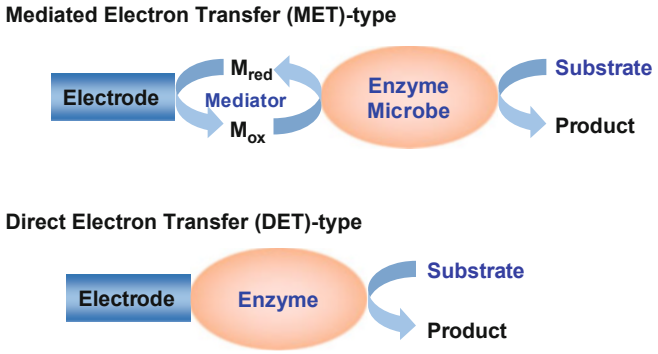

Fig. 7.3 Schematic of mediated electron transfer (MET) and direct electron transfer (DET)-type bioelectrocatalyses

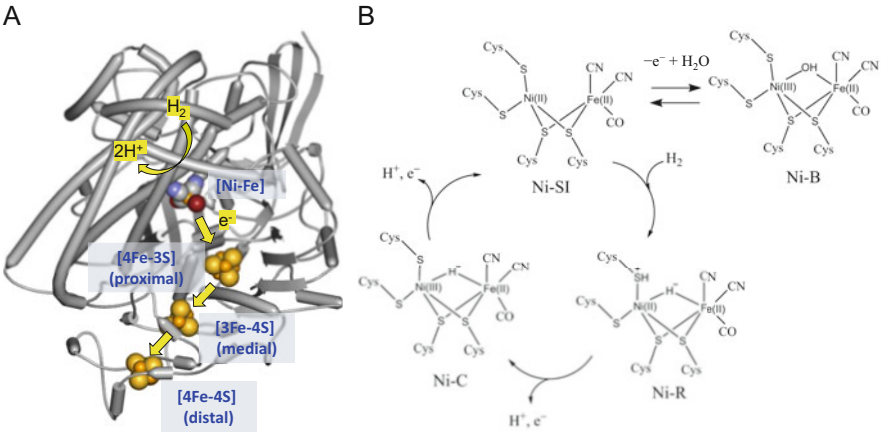

Fig. 7.4 (**a**) Structure of a [Ni–Fe]-H_2ase. The structural data were taken from PDB 5XLE. The pathway of the electron transfer is indicated by yellow arrow lines. (**b**) The structural change in the catalytic cycle and the oxidative inactivation to the Ni-B state (Mazurenko et al. 2017b)

are small in number. Standard and O_2-sensitive [Ni–Fe] H_2ase from *Desulfovibrio vulgaris* Miyazaki F (*Dv*MF) is composed of large and small subunits. The large subunit contains [Ni–Fe] cluster as the catalytic center for the $2H^+/H_2$ conversion, while the small subunit contains three iron-sulfur (FeS) clusters called proximal, medial, and distal in turn from the [Ni–Fe] cluster (Fig. 7.4). In the DET-type communication, the distal FeS cluster plays as the electrode-active redox center (Lojou 2011). [Ni–Fe]-H_2ases from *Dv*MF, *Escherichia coli* (*Ec*), *Allochromatium vinosum* (*Av*), *Ralstonia eutropha* (*Re*), and *Ralstonia metallidurans* (*Rm*) have been frequently used as bioanode catalysts for the H_2 oxidation (Mazurenko et al. 2017b), since the formal potential of the distal FeS cluster of these H_2ases is rather negative. This characteristic is important to minimize the overpotential of the H_2 oxidation.

Thermostable and O_2-tolerant H_2ase from *Hydrogenovibrio marinus* (*Hm*) (Yoon et al. 2011) is also useful, though its formal potential is slightly positive compared with those of the abovementioned H_2ases (So et al. 2016).

MCO catalyzes a 4-electron reduction of O_2 into H_2O without generation of intermediate species. The native electron donors of MCOs can be replaced with artificial redox compounds (reduced form) or even with electrodes. Therefore, MCO can play as an electrode catalysis in the 4-electron reduction of O_2 in both MET- and DET-type bioelectrocatalyses (Mano and de Poulpiquet 2018). MCOs contain four copper (Cu) atoms classified into a type 1 Cu site (T1) and a type 2–3 Cu (T2/3) cluster. O_2 is reduced at the T2/3 Cu cluster, while electrons are accepted at the T1 Cu site from reduced mediators in the MET-reaction or from electrodes in the DET-reaction (Fig. 7.5). Bilirubin oxidase (BOD) from the fungus *Myrothecium verrucaria* (*Mv*) has been frequently utilized as a bioelectrocatalysis, since *Mv* BOD works even at neutral pH (Tsujimura et al. 2004) (in contrast, optimum pH values of most MCOs are located in slightly acidic region), and the formal potential of the T1 Cu site is rather positive (Tsujimura et al. 2005; Christenson et al. 2006; Kamitaka et al. 2007). Thermostable BOD from the bacterium *Bacillus pumilus* (*Bp*) is also utilized (de Poulpiquet et al. 2014).

Electrochemical coupling of an H_2ase-based bioanode and an MCO-based biocathode yields an H_2/O_2 biofuel cell. The power density of fuel cells is the product of the current density and the cell voltage. In order to increase the limiting current density, mesoporous materials such as Ketjen black, carbon nanotubes, carbon nanofibers, and gold nanoparticles are often utilized, since the ratio of the electrochemically active surface area against the projected area increases, as the major reason in the MET-type reaction.

On the other hand, such mesoporous structures work as scaffolds suitable for the DET-type reaction and improve the heterogeneous electron transfer kinetics. Probability of the enzyme orientations suitable for the DET-reactions increases in the mesoporous structures with sizes close to that of the enzyme (Sugimoto et al. 2016, 2017; Kitazumi et al. 2020). This is the curvature effect of the mesoporous structure in the DET-type reaction. The microporous structure also improves the heterogeneous electron transfer kinetics between enzymes and the electrode because of an increase in the electric field at the edge of the microstructures due to the expansion of the electric diffuse double layer (Kitazumi et al. 2013, 2020).

On the other hand, in order to increase the open-circuit voltage (OCV) and to decrease the overpotential in H_2/O_2 biofuel cells, it is important to utilize an H_2ase with a negative formal potential for the distal FeS and an MCO with a positive formal potential for the T1 Cu site. Fast kinetics in the electroenzymatic reaction is also important to decrease the operational overpotential. The curvature effect and the electric double layer effect of nanostructured materials are very important to improve the performance of the DET-type bioelectrocatalysis. In the case of the MET-type reaction, some energy loss (some gap in the formal potentials of a mediator and an enzyme, $E_M^{\circ\prime}$ and $E_E^{\circ\prime}$) is required to create the standard driving force ($-\Delta_r G^\circ$) in the electron transfer from a substrate-reduced enzyme to an oxidized mediator for the

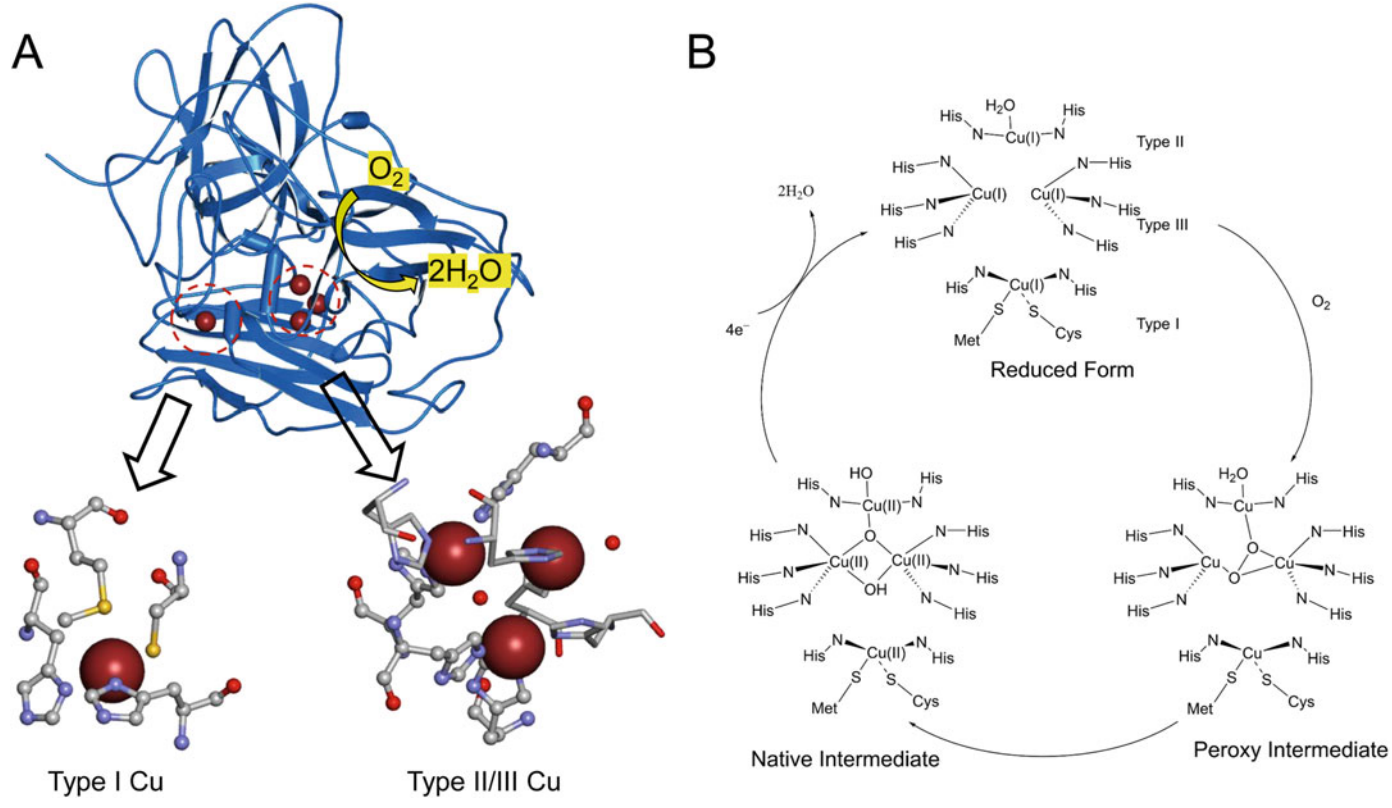

Fig. 7.5 (**a**) Structure of BOD. The structural data were taken from PDB 3ABG. (**b**) The catalytic cycle of a 4-electron reduction of O_2 at the T2/3 Cu site (Mazurenko et al. 2017b)

substrate oxidation (and vice versa), in which $\Delta_r G^\circ$ is the standard Gibbs energy of the reaction and is given by:

$$\Delta_r G^\circ = -nF\left(E_M^{\circ\prime} - E_E^{\circ\prime}\right), \tag{7.2}$$

where n and F are the total number of electrons in the electron transfer and the Faraday constant, respectively. The requirement of the situation in which $E_M^{\circ\prime} > E_E^{\circ\prime}$ for the substrate oxidation is attributable to the fact that the self-exchange electron transfer rate constant (k_{self}) of artificial mediators is usually very small (or the reorganization energy (λ) is usually very large for artificial mediators that easily change the structure during the redox reaction), as given by the following equations (Marcus and Sutin 1985):

$$k \cong \sqrt{k_{self,D} k_{self,A} \exp\left(-\frac{\Delta_r G^\circ}{RT}\right)}, \tag{7.3}$$

and

$$RT \ln \frac{k_{self}}{Z} = -\Delta^\ddagger G_{self}^\circ = -\frac{\lambda}{4}, \tag{7.4}$$

where $k_{self,\ D}$ and $k_{self,\ A}$ are k_{self} of the electron donor and acceptor, respectively. R and T are the gas constant and the absolute temperature, respectively. Z is a coefficient of the absolute kinetics, and $\Delta^\ddagger G_{self}^\circ$ is the standard Gibbs energy of the activation. In this sense, the DET-type bioelectrocatalysis is preferred to the MET-type one in theory to minimize the overpotential.

Since the saturated concentrations of H_2 and O_2 in aqueous solutions are very low, the catalytic current becomes controlled by the diffusion of the gaseous substrates soon after electrolysis under quiescent conditions. Gas bubbling is often utilized to convect the electrolyte solutions and supply such gaseous substrates. More suitable method to minimize or avoid the concentration polarization near bioelectrodes is utilization of gas diffusion bioelectrodes under quiescent conditions (Fig. 7.6). A review article details several setups of the systems (So et al. 2017). In order to bring out better performance of gas diffusion bioelectrodes, the control of the hydrophobicity for the gas diffusion and the hydrophilicity for the enzymatic reaction is very important. Some redox enzymes utilize gaseous substrates not in solvated state but in gas phase. Typical examples are Mo- or W-complexed molybdopterin FDHs (Zhong et al. 2015) and probably most of H_2ases. Therefore, the three-boundary phase in gas diffusion bioelectrodes provides a situation very suitable for the DET-type bioelectrocatalyses of gaseous substrates and drastically increases the catalytic current density.

Unfortunately, H_2ases have one drawback in electrochemical application; most of H_2ases including O_2-tolerant ones are non-catalytically oxidized and inactivated into the Ni-B state (Fig. 7.4) at high potentials of electrodes and solutions even in the

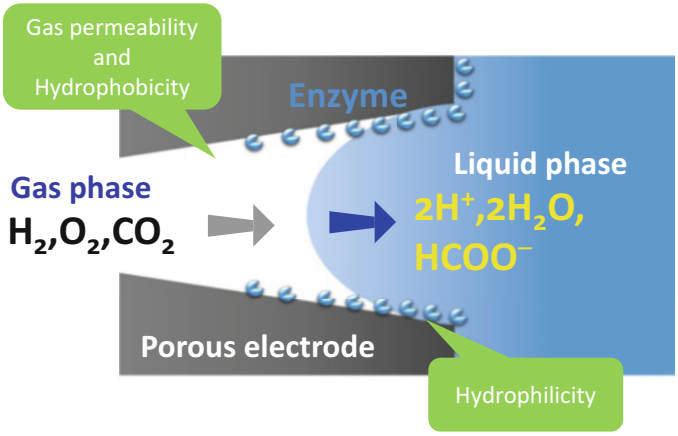

Fig. 7.6 Schematic of gas diffusion electrodes

absence of O_2. Although the oxidative inactivation is reversible, the characteristic restricts the performance of H_2/O_2 biofuel cells especially at decreased operational potentials, at which the electrode potential of the H_2ase-bioanode would become sufficiently positive. Several attempts have been reported in order to overcome this issue. In the MET-type configuration, hydrogels based on viologen entities were used to immobilize *Dv*MF H_2ase and mediate the electron transfer from the enzyme to the electrode (Plumeré et al. 2014). The enzymatically reduced redox gels on the electrode were auto-oxidized with dissolved O_2 on the side of the electrolyte solution, but the partially oxidized gels were immediately reduced by the MET-type enzymatic reaction, and then the solution potential in the gels remained rather negative, resulting in the protection of the O_2-sensitive H_2ase in the gels from the oxidative inactivation by O_2. Because of the MET-type reaction system, direct oxidative inactivation of H_2ase on the bioanode is also minimized. In the DET-type configuration, it was found that a gas diffusion electrode system was effective to protect the oxidative inhibition of H_2ase even at high electrode potentials (So et al. 2017). Since the oxidative inactivation at electrodes can be considered as an electrochemical competitive inhibition of H_2ase (So et al. 2014a, b) (Fig. 7.4), the inhibition was minimized by the catalytic cycle predominantly proceeding at increased concentrations of gaseous H_2 at the three-boundary phase biointerface.

The performance of H_2/O_2 biofuel cells is well summarized in the literature (Mazurenko et al. 2017b). The OCV values of most of the H_2/O_2 biofuel cells in the literature are approximately 1 V, and some DET-type electroenzymatic devices give OCVs of 1.12–1.14 V (Monsalve et al. 2015; So et al. 2016; Xia et al. 2016). These OCV values are very close to the standard electromotive force of 1.23 V for the 1 atm-H_2/O_2 fuel cell at 25 °C and OCVs of Pt-based polymer electrolyte H_2/O_2 fuel cells (about 1 V) at 80 °C. This means that the overpotentials in both of the

bioanode and biocathode are very small. The maximum power density of the H_2/O_2 biofuel cells reported to date is 6.1 mW cm^{-2} at 25 °C under 1 atm-H_2/air conditions (Xia et al. 2016) and 8.4 mW cm^{-2} at 40 °C under 1 atm-H_2/O_2 conditions (So et al. 2016) both under quiescent conditions. These values are the world record at present as H_2/O_2 biofuel cells.

7.3 Construction of Photobioelectrochemical H_2O Splitting System

Water splitting ($2H_2O \rightarrow 2H_2 + O_2$) would be one of the important technological breakthroughs to construct a hydrogen economy. Electrolysis of H_2O at conventional electrodes results in large overpotential (and then large energy loss), though water splitting of seawater (or sodium chloride solution) is industrially used to provide sodium hydroxide and chlorine. Photochemical water splitting is still under development. The photosynthesis of photosynthetic organisms occurs in the thylakoid membrane in the chloroplast. The photosynthesis converts CO_2 in the atmosphere to organic substances by excited electrons generated by photobiochemical splitting of H_2O as a sacrificial reagent (Barber 2009); in water splitting in the photosynthesis, the exited electrons are shunted, not to H^+, but to the electron transport chain in photosystem II (PSII). When the excited electrons are extracted to an electrode, the photosynthetic charge separation system may be regarded as a photo-driven bioanode. In order to construct photo-driven bioanodes, several artificial electron acceptors have been utilized for chloroplasts (Haehnel and Hochheimer 1979; Okano et al. 1984), photosystem I (PSI) (Hill et al. 1985), PSII (Lemieux et al. 2001), photosynthetic microorganisms (Martens and Hall 1994; Torimura et al. 2001; Tsujimura et al. 2001b), and thylakoid membranes (Mimcault and Carpentier 1989; Carpentier et al. 1989; Hasan et al. 2014).

Characteristics required as mediators to be used in photo-driven bioanodes are low barrier in electrode kinetics, high stability, suitable solubility, and low redox potential (to minimize the overpotential). In addition, ideal mediators should have large O_2 tolerance (because O_2 evolution occurs at the bioanode with the PSII function) and have high permeability of biomembranes when whole cells or organisms are used. By considering these factors and a linear-free energy relationship in the electron transfer from thylakoid membranes to mediators (Kano 2019), our group proposed to use 1,2-naphthoquinone (NQ) or hexaammineruthenium (III) ($[Ru(NH_3)_6]^{3+}$) as a mediator of photo-driven bioanodes based on thylakoid membranes from spinach (Takeuchi et al. 2018; Adachi et al. 2019). The thylakoid membranes were embedded within water-spread multi-walled carbon nanotubes (MWCNTs) that were mounted on a light-permeable indium tin oxide (ITO) electrode (Fig. 7.7). MWCNTs are stabilized with each other by π–π staking after drying. ITO electrodes were spattered to form a thin gold (Au) film with a thickness of 4 nm before

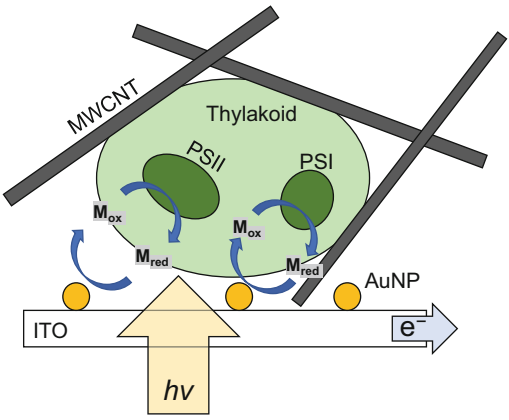

Fig. 7.7 Schematic of a thylakoid membrane/MWCNT-mounted Au/ITO electrode as a photo-driven bioanode

MWCNT-mounting in order to improve the electrode kinetics of the mediator. The thin Au film was acceptably light permeable. The photocurrent densities were 0.1 mA cm^{-2} with NQ (Takeuchi et al. 2018) and 0.18 mA cm^{-2} with $[Ru(NH_3)_6]^{3+}$ (Adachi et al. 2019) at a light flux density of 1.5 mmol m^{-2} s^{-1}. The latter value of the photo current density is the world record at present as a photo-driven bioanode to realize photobioelectrochemical H_2O splitting.

Electrochemical coupling of the photo-driven bioanode with a DET-type MCO-based biocathode yielded a bioelectrochemical photocell (called bio-solar cell) (Adachi et al. 2019). The cell exhibited an OCV of 0.61 V and a maximum power of 50 μW cm^{-2}, the best performance in the world. Ideally, in this bio-solar cell, O_2 is reduced to H_2O at the biocathode and is regenerated at the photo-driven bioanode with PSII from H_2O. This is a typical and ideal example of an electrochemical device to underpin a hydrogen economy in Fig. 7.1, though further trial to decrease the overpotential of the photobioelectrochemical H_2O splitting is required in the future.

7.4 Bioelectrochemical Hydrogen Economy and Its Expansion to C1 Society

As mentioned in Sect. 7.2, most H_2ases catalyze both H_2 oxidation and H^+ reduction. The broken line in Fig. 7.8 shows a typical steady-state catalytic wave of bidirectional DET-type bioelectrocatalysis in the case of a system with a low kinetic barrier in the interfacial electron transfer between an enzyme and an electrode (Armstrong and Hirst 2011). The oxidized and reduced substrates are reversibly interconverted, indicating that the system does not have any overpotential in the interconversion. Such reversible redox reactions are almost impossible to be realized with metal-based catalysts and are only realized by biocatalysts in electrochemistry.

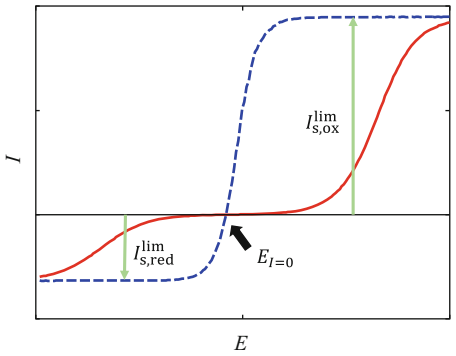

Fig. 7.8 Conceptional steady-state catalytic waves in bidirectional DET-type bioelectrocatalysis under quiescent conditions with rather large (broken line) and small (solid line) values of the standard interfacial electron transfer rate constant (k°)

Similar sigmoidal waves of bidirectional DET-type bioelectrocatalysis were observed with W-containing FDH from *Methylobacterium extorquens* (*Me*) AM1 for two redox couples of CO_2/$HCOO^-$ and NAD^+/NADH (Sakai et al. 2017; Reda et al. 2008; Bassegoda et al. 2014) and ferredoxin-$NADP^+$ reductase (FNR) from *Chlamydomonas reinhardtii* for a redox couple of $NADP^+$/NADPH (Siritanaratkul et al. 2017; Wan et al. 2018).

The FDH from *Me*AM1 is a heterodimeric soluble enzyme in the family of molybdopterin enzyme; W-containing subunit contains a tungstopterin cofactor as the catalytic center for the CO_2/$HCOO^-$ interconversion and FeS clusters, while diaphorase subunit contains a non-covalently bound flavin mononucleotide (FMN) as the catalytic center for the NAD^+/NADH interconversion and FeS clusters (Fig. 7.9). The FNR is a monomeric flavoenzyme with a molecular mass of 45 kDa having flavin adenine dinucleotide (FAD) as a sole redox cofactor.

The appearance of the steady-state wave indicates that any concentration polarization does not occur at the electrode surface and that the current is controlled by the electroenzymatic process. At positive potentials, the steady-state current reaches a limiting value ($I^{lim}_{s,ox}$) for the oxidation of a reduced substrate (H_2 in the case of H_2ase) as given by:

$$I^{lim}_{s,ox} = n_S F A k_{c,ox} \Gamma_E, \tag{7.5}$$

where n_S is the number of electrons of the substrate, A is the surface area of the electrode, $k_{c,\,ox}$ is the catalytic constant of the substrate oxidation by the enzyme, and Γ_E is the surface concentration of the enzyme. At negative potentials, the steady-state current reaches a limiting value ($I^{lim}_{s,red}$) for the reduction of an oxidized substrate (H^+ in the case of H_2ase) as given by:

$$I^{lim}_{s,red} = n_S F A k_{c,red} \Gamma_E, \tag{7.6}$$

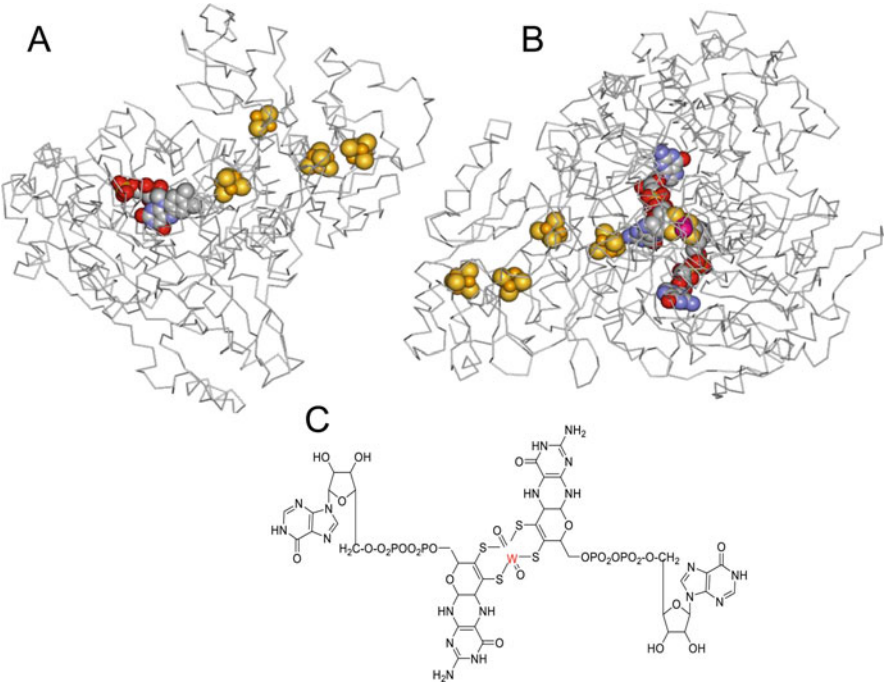

Fig. 7.9 Tentative structures of (**a**) diaphorase subunit and (**b**) molybdopterin subunit. (**c**) The structure of W-centered molybdopterin (Moco). The structural data for diaphorase and molybdopterin subunits were taken from PDB 5XF9 (NAD^+-reducing H_2ase) and PDB 1H0H (formate dehydrogenase from *Desulfovibrio gigas*), respectively

where $k_{c,red}$ is the catalytic constant of the substrate reduction. The ratio $I_{s,ox}^{lim}/I_{s,red}^{lim}(=k_{c,ox}/k_{c,red})$ does not necessarily correspond to the equilibrium potential of the substrate ($E_{S,\ eq}$):

$$E_{S,eq} = E_S^{\circ\prime} + \frac{n_S F}{RT} \ln \frac{c_{ox}}{c_{red}}, \tag{7.7}$$

where $E_S^{\circ\prime}$ is the formal potential of the substrate, and c_{ox} and c_{red} are the bulk concentrations of the oxidized and reduced substrates, respectively. The reason is that the process is not an elementary reaction, and therefore low of mass action does not hold. Fortunately, the potential at which the steady-state sigmoidal wave crosses the potential axis of zero current (called zero current potential, $E_{I\ =\ 0}$) is identical with $E_{S,eq}$.

With a high kinetic barrier in the electron transfer between an enzyme and an electrode, steady-state waves show two sigmoidal parts, as shown by a solid line in Fig. 7.8. In such cases, one could not get the information on $E_{S,eq}$. The shifted values of the wave in the direction of the potential axis correspond to the overpotentials caused by the kinetic processes. When the catalytic constants are sufficiently large,

some concentration polarization will occur, and the current depends on time. Under such conditions, rotating disk electrode methods are required to get steady-state currents. When the limiting current is controlled by the diffusion of substrate, the reductive and oxidative limiting currents reflect c_{ox} and c_{red}, respectively, as in the case of non-catalytic conventional electrochemical measurements.

Even for the MET-type bioelectrocatalysis, bidirectional mono-sigmoidal waves were observed under logically tuned conditions for the $2H^+/H_2$ redox couple with *Desulfovibrio vulgaris* cells (Tatsumi et al. 1999) and the $CO_2/HCOO^-$ redox couple with W-containing FDH (Sakai et al. 2015).

The essential requirement for such a two-way DET-reaction is that $E_S^{\circ\prime}$ and the formal potential of the electrochemically active site in enzymes ($E_E^{\circ\prime}$) are close with each other in order to minimize the kinetic barrier of uphill intramolecular electron transfer of one of the bidirectional reactions in the enzymes, as evidenced by Eqs. (7.2) and (7.3), where $E_M^{\circ\prime}$ in Eq. (7.2) is replaced with $E_S^{\circ\prime}$. In the case of the MET reaction, it is very important to adjust the pH value to satisfy the condition in which $E_M^{\circ\prime} \cong E_E^{\circ\prime}$ (Tatsumi et al. 1999; Sakai et al. 2015).

The other requirement for fast electron transfer of the uphill reactions ($\Delta_r G^\circ > 0$) is that k_{self} in Eq. (7.3) should be very large, that is, λ in Eq. (7.4) should be very small. Peptide matrix frequently plays an important role to minimize the geometric change. Therefore, the uphill electron transfer is often observed in the intramolecular electron transfers in redox proteins in some instances. (Such situation of small value of λ in redox proteins also affects $E_E^{\circ\prime}$. For example, although Cu^+ prefers a tetrahedral coordination and the ligand of Cu^{2+} arranges in a square planar configuration, the ligands and the conformations of type I copper of blue copper proteins (e.g., of MCO) remain almost unchanged during the redox reaction, and they considerably deviate from those preferred by Cu^{2+}, leading to a destabilization of the oxidized state and then a rise in the formal potential to get strong oxidation activity.)

In the case of FDH, the formal potentials of tungstopterin, FeSs, and FMN seem to be located close with each other and also close with those of the redox couples of $CO_2/HCOO^-$ and $NAD(P)^+/NAD(P)H$. Molybdopterin enzymes frequently show the catalytic activity toward bidirectional redox reactions of biologically important redox couples with negative formal potentials such as the carboxylate/aldehyde redox couple (Reda et al. 2008; Bassegoda et al. 2014; Sakai et al. 2015; Huber et al. 1995; Siritanaratkul et al. 2017; Wan et al. 2018). Therefore, bioelectrocatalytic reactions with molybdopterin enzymes as well as H_2ases will attract lots of attention in the near future.

As mentioned above, H_2 is an attractive energy source in the sustainable society. Although H_2 has many excellent properties as fuel, H_2 has critical problems in its storage and transportation issues because of its gaseous properties. Liquid fuels or highly water-soluble ionic solutes are easy to store and transport. One of the possible candidates as fuels is $HCOO^-$ (Enthaler et al. 2010; Asefa et al. 2019) as described in Introduction. Since the formal potential of $CO_2/HCOO^-$ and H^+/H_2 is very close

with each other, the interconversion between the two redox couples is very useful to underpin the sustainable society:

$$CO_2 + H_2 \rightleftarrows HCOO^- + H^+ \tag{7.8}$$

Several attempts have been tried (Enthaler et al. 2010; Asefa et al. 2019). We have realized the reversible interconversion without overpotentials by using the bidirectional catalytic reactions of H_2ase from *Dv*MF and FDH from *Me*AM1 (Adachi et al. 2018). Such biotechnology would facilitate the storage and the transportation of the primary energy sources.

In addition, FDH from *Me*AM1 realizes the reversible interconversion between CO_2/$HCOO^-$ and NAD(P)$^+$/NAD(P)H couples:

$$CO_2 + NAD(P)H \rightleftarrows HCOO^- + NAD(P)^+ \tag{7.9}$$

On the other hand, NAD$^+$-reducing H_2ase (from *Hydrogenophilus thermoluteolus*) realizes the reversible interconversion between $2H^+$/H_2 and NAD(P)$^+$/NAD(P)H couples:

$$2H^+ + NAD(P)H \rightleftarrows H_2 + NAD(P)^+ + H^+ \tag{7.10}$$

The structure of the NAD$^+$-reducing H_2ase has been solved (Shomura et al. 2017) and is considered to be similar to that of the FDH from *Me*AM1.

7.5 Conclusion

Bioelectrochemical coupling of H_2ase and FDH reactions with the electrode reaction realizes electrochemically reversible redox reactions of the two redox couples, $2H^+$/H_2 and CO_2/$HCOO^-$, respectively. The redox couples are also reversibly interconverted with each other by using corresponding enzymes. NAD$^+$-reducing H_2ase, FDH, and FNR are also utilized as electrocatalysts for an electrochemically reversible redox reaction of the biologically most important redox couple, NAD(P)$^+$/NAD(P)H. Bioelectrocatalytic reactions based on MCO and thylakoid membrane realize the 4-electron reduction of O_2 and the photobioelectrochemical H_2O splitting, respectively, with small overpotentials. These bioelectrochemical and biochemical reactions can construct a hydrogen/C1 economy as an expansion of the hydrogen economy (Fig. 7.10).

In addition, the NAD(P)$^+$/NAD(P)H redox couple can be reversibly linked to the redox couples $2H^+$/H_2 and CO_2/$HCOO^-$ by NAD$^+$-reducing H_2ase and FDH, respectively. The reversible NAD(P)$^+$/NAD(P)H redox couple is also linked to a huge variety of biological redox reactions by NAD(P)-dependent dehydrogenases. This linkage is very useful in (electro)enzymatic organic synthesis and

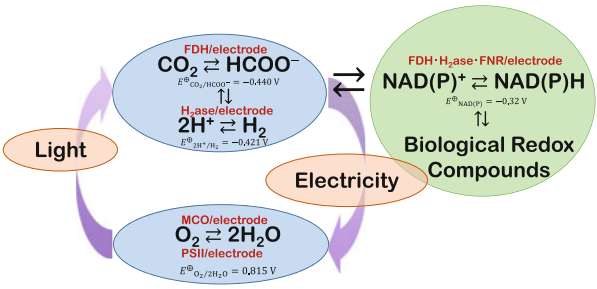

Fig. 7.10 Schematic of a bioelectrochemical/biochemical hydrogen/C1 economy. $E^{\oplus}$ is the biological standard redox potential vs. SHE

bioelectrochemical sensing. The proposed hydrogen/C1 economy is indeed an environmentally clean, cheap, and sustainable energy system.

References

Abe JO, Popoola API, Ajenifuja E, Popoola OM (2019) Hydrogen energy, economy and storage: review and recommendation. Int J Hydrog Energy 44:15072–15086

Adachi T, Kitazumi Y, Shirai O, Kano K (2018) Construction of a bioelectrochemical formate generating system from carbon dioxide and dihydrogen. Electrochem Commun 97:78–76

Adachi T, Kataoka K, Kitazumi Y, Shirai O, Kenji Kano K (2019) A bio-solar cell with thylakoid membranes and bilirubin oxidase. Chem Lett 48:686–689

Armstrong FA, Hirst J (2011) Reversibility and efficiency in electrocatalytic energy conversion and lessons from enzymes. Proc Natl Acad Sci U S A 108:14049–14054

Asefa T, Koh K, Yoon CW (2019) CO_2-mediated H_2 storage-release with nanostructured catalysis: recent progress, challenges, and perspectives. Adv Energy Mater 9:1901158

Barber J (2009) Photosynthetic energy conversion: natural and artificial. Chem Soc Rev 38:185–196

Bard AJ, Faulkner LR (2001) Electrochemical methods fundamentals and applications, 2nd edn. Wiley, New York, pp 130–132, Section 3.6.4

Barton SC, Gallaway J, Atanassov P (2004) Enzymatic biofuel cells for implantable and microscale devices. Chem Rev 104:4867–4886

Bassegoda A, Madden C, Wakerley DW, Reisner E, Hirst J (2014) Reversible interconversion of CO_2 and formate by a molybdenum-containing formate dehydrogenase. J Am Chem Soc 136:15473–15476

Carpentier R, Lemieux S, Mimeault M, Purcell M, Goetze DC (1989) A photoelectrochemical cell using immobilized photosynthetic membranes. J Electroanal Chem 276:391–401

Chaplin RPS, Wragg AA (2003) Effects of process conditions and electrode material on reaction pathways for carbon dioxide electroreduction with particular reference to formate formation. J Appl Electrochem 33:1107–1123

Christenson A, Shleev S, Mano N, Heller A, Gorton L (2006) Redox potentials of the blue active sites of bilirubin oxidases. Biochim Biophys Acta Bioenerg 1757:1634–1641

Cracknell JA, Vincent KA, Armstrong FA (2008) Enzymes as working or inspirational electrocatalysts for fuel cells and electrolysis. Chem Rev 108:2439–2461

de Poulpiquet A, Ciaccafava A, Gadiou R, Gounel S, Giudici-Orticoni MT, Mano N, Lojou E (2014) Design of a H_2/O_2 biofuel cell based on thermostable enzymes. Electrochem Commun 42:72–74

Enthaler S, von Langermann J, Schmidt T (2010) Carbon dioxide and formic acid—the couple for environmental-friendly hydrogen storage? Energy Environ Sci 3:1207–1217

European Commission (2003) Hydrogen energy and fuel cells: a vision of our future. Office for Official Publications of the European Communities, Luxembourg

Grubel K, Jeong H, Yoon CW, Autrey T (2020) Challenges and opportunities for using formate to store, transport, and use hydrogen. J Energy Chem 41:216–224

Gunasekar GH, Park K, Jung K-D, Yoon S (2016) Recent developments in the catalytic hydrogenation of CO_2 to formic acid/formate using heterogeneous catalysts. Inorg Chem Front 3:882–895

Haehnel W, Hochheimer HJ (1979) On the current generated by a galvanic cell driven by photosynthetic electron transport. Bioelectrochem Bioenerg 6:563–574

Hasan K, Dilgin Y, Emek SC, Tavahodi M, Akerlund HE, Albertsson P, Gorton L (2014) Photoelectrochemical communication between thylakoid membranes and gold electrodes through different quinone derivatives. ChemElectroChem 1:131–139

Hill HAO, Walton NJ, Whitford D (1985) The coupling of heterogeneous electron transfer to photosystem-1. J Electroanal Chem 187:109–119

Huber C, Skopan H, Feicht R, White H, Simon H (1995) Pterin cofactor, substrate specificity, and observations on the kinetics of the reversible tungsten-containing aldehyde oxidoreductase from *Clostridium thermoaceticum*. Arch Microbiol 164:110–118

Jang J, Jeon BW, Kim YH (2018) Bioelectrochemical conversion of CO_2 to value added product formate using engineered *Methylobacterium extorquens*. Sci Rep 8:7211

Jayathilake BS, Bhattachrya S, Vaidehi N, Narayanan SR (2019) Efficient and selective electrochemically driven enzyme-catalyzed reduction of carbon dioxide to formate using formate dehydrogenase and an artificial cofactor. Acc Chem Res 52:676–685

Kamitaka Y, Tsujimura S, Kataoka K, Sakurai T, Ikeda T, Kano K (2007) Effects of axial ligand mutation of the type I copper site in bilirubin oxidase on direct electron transfer-type bioelectrocatalytic reduction of dioxygen. J Electroanal Chem 601:119–124

Kano K (2019) Fundamentals and applications of redox enzyme-functionalized electrode reactions. Electrochemistry 87:301–311

Kitazumi Y, Shirai O, Yamamoto M, Kano K (2013) Numerical simulation on diffuse double layer around microporous electrodes based on Poisson-Boltzmann equation. Electrochim Acta 112:171–175

Kitazumi Y, Shirai O, Kano K (2020) Significance of nanostructures of an electrode surface in direct electron transfer-type bioelectrocatalysis of redox enzymes, Chap. 7. In: Lakhveer Singh L, Mahapatra DM, Liu H (eds) ACS symposium series 1342 "Novel catalyst materials for bioelectrochemical systems: fundamentals and applications". American Chemical Society, Washington, DC, pp 147–163

Kletzin A, Adams MWW (1996) Tungsten in biological systems. FEMS Microbiol Rev 18:5–63

Lemieux S, Carpentier R, Allen H, Hill O, Walton NJ, Whitford D (2001) Properties of a photosystem II preparation in a photochemical cell. J Electroanal Chem 496:109–119

Lojou E (2011) Hydrogenases as catalysts for fuel cells: strategies for efficient immobilization at electrode interfaces. Electrochim Acta 56:10385–10397

Maia LB, Fonseca L, Moura I, Moura JJG (2016) Reduction of carbon dioxide by a molybdenum-containing formate dehydrogenase: a kinetic and mechanistic study. J Am Chem Soc 138:8834–8846

Mano N, de Poulpiquet A (2018) O_2 reduction in enzymatic biofuel cells. Chem Rev 118:2392–2468

Marcus RA, Sutin N (1985) Electron transfers in chemistry and biology. Biochim Biophys Acta 811:265–322

Martens N, Hall EAH (1994) Diaminodurene as a mediator of a photocurrent using intact cells of cyanobacteria. Photochem Photobiol 59:91–98

Mazurenko I, de Poulpiquet A, Lojou E (2017a) Recent developments in high surface area bioelectrodes for enzymatic fuel cells. Curr Opin Electrochem 5:74–84

Mazurenko I, Wang X, de Poulpiquet A, Lojou E (2017b) H_2/O_2 enzymatic fuel cells: from proof-of-concept to powerful devices. Sustain Energy Fuels 1:1475–1501

Meredith MT, Minteer SD (2012) Biofuel cells; enhanced enzymatic bioelectrocatalysis. Annu Rev Anal Chem 5:157–179

Mimcault M, Carpentier R (1989) Kinetics of photocurrent induction by a thylakoid containing electrochemical cell. J Electroanal Chem 276:145–158

Monsalve K, Mazurenko I, Lalaoui N, Le Goff A, Holzinger M, Infossi P, Nitsche S, Lojou JY, Giudici-Orticoni MT, Cosnier S, Logou E (2015) A H_2/O_2 enzymatic fuel cell as a sustainable power for a wireless device. Electrochem Commun 60:216–220

Okano M, Iida T, Shinohara H, Kobayashi H (1984) Water photolysis by a photoelectrochemical cell using an immobilized chloroplasts-methyl viologen system. Agric Biol Chem 48:1977–1983

Plumeré N, Rüdiger O, Oughli A, Williams R, Vivekananthan J, Pöller S, Lubitz W, Shuhmann W (2014) A redox hydrogel protects hydrogenase from high-potential deactivation and oxygen damage. Nat Chem 6:822–827

Rand DAJ (2011) A journey on the electrochemical road to sustainability. J Solid State Electrochem 15:1579–1622

Reda T, Plugge CM, Abram NJ, Hirst J (2008) Reversible interconversion of carbon dioxide and formate by an electroactive enzyme. Proc Natl Acad Sci U S A 105:10654–10658

Ren JW, Musyoka NM, Langmi HW, Mathe M, Liao SL (2017) Current research trends and perspectives on materials-based hydrogen storage solution: a critical review. Int J Hydrog Energy 42:289–311

Rotaru A-E, Shrestha PM, Liu F, Shrestha M, Shrestha D, Embree M, Zengler K, Wardman C, Nevin KP, Lovley DR (2014) A new model for electron flow during anaerobic digestion: direct interspecies electron transfer to *Methanosaeta* for the reduction of carbon dioxide to methane. Energy Environ Sci 7:408–415

Sahaym U, Norton MG (2008) Advances in the application of nanotechnology in enabling a 'hydrogen economy'. J Mater Sci 43:5395–5429

Sakai K, Hsieh BC, Maruyama A, Kitazumi Y, Shirai O, Kano K (2015) Interconversion between formate and hydrogen carbonate by tungsten-containing formate dehydrogenase-catalyzed mediated bioelectrocatalysis. Sens Biosens Res 5:90–96

Sakai K, Sugimoto Y, Kitazumi Y, Shirai O, Takagi K, Kano K (2017) Direct electron transfer-type bioelectrocatalytic interconversion of carbon dioxide/formate and NAD^+/NADH redox couples with tungsten-containing formate dehydrogenase. Electrochim Acta 228:537–544

Shi J, Jiang Y, Jiang Z, Wang X, Wang X, Zhang S, Han P, Yang C (2015) Enzymatic conversion of carbon dioxide. Chem Soc Rev 44:5981–6000

Shomura Y, Taketa M, Nakashima H, Tai H, Nakagawa H, Ikeda Y, Ishii M, Igarashi Y, Nishihara H, Yoon KS, Ogo S, Hirota S, Higuch Y (2017) Structural basis of the redox switches in the NAD^+-reducing soluble [NiFe]-hydrogenase. Science 357:928–938

Siritanaratkul B, Megarity CF, Roberts TG, Samuels TOM, Winkler M, Warner JH, Happe T, Armstrong FA (2017) Transfer of photosynthetic $NADP^+$/NADPH recycling activity to a porous metal oxide for highly specific, electrochemically-driven organic synthesis. Chem Sci 8:4579–4586

So K, Kitazumi Y, Shirai O, Kurita K, Nishihara H, Higuchi Y, Kano K (2014a) Gas-diffusion and direct electron transfer-type bioanode for hydrogen oxidation with oxygen-tolerant [NiFe]-hydrogenase as an electrocatalyst. Chem Lett 43:1575–1577

So K, Kitazumi Y, Shirai O, Kurita K, Nishihara H, Higuchi Y, Kano K (2014b) Kinetic analysis of inactivation and enzyme reaction of oxygen-tolerant [NiFe]-Hydrogenase at direct electron transfer-type bioanode. Bull Chem Soc Jpn 87:1177–1185

So K, Kitazumi Y, Shirai O, Nishikawa K, Higuchi Y, Kano K (2016) Direct electron transfer-type dual gas diffusion H_2/O_2 biofuel cells. J Mater Chem A 4:8742–8749

So K, Sakai K, Kano K (2017) Gas diffusion bioelectrodes. Curr Opin Electrochem 5:173–182

Sugimoto Y, Takeuchi R, Kitazumi Y, Shirai O, Kano K (2016) Significance of mesoporous electrodes for noncatalytic faradaic process of randomly oriented redox proteins. J Phys Chem C 120:26270–26277

Sugimoto Y, Kitazumi Y, Shirai O, Kano K (2017) Effects of mesoporous structures on direct electron transfer-type bioelectrocatalysis: facts and simulation on a three-dimensional model of random orientation of enzymes. Electrochemistry 85:82–87

Takeuchi R, Suzuki A, Sakai K, Kitazumi Y, Shirai O, Kano K (2018) Construction of photo-driven bioanodes using thylakoid membranes and multi-walled carbon nanotubes. Bioelectrochemistry 122:158–163

Tatsumi H, Takagi K, Fujita M, Kano K, Ikeda T (1999) Electrochemical study of reversible hydrogenase reaction of *Desulfovibrio vulgaris* cells with methyl viologen as an electron carrier. Anal Chem 71:1753–1759

Torimura M, Miki A, Wadano A, Kano K, Ikeda T (2001) Electrochemical investigation of *Cyanobacteria Synechococcus* sp. PCC7942-catalyzed photoreduction of exogenous quinones and photoelectrochemical oxidation of water. J Electroanal Chem 496:21–28

Tsujimura S, Fujita F, Tatsumi H, Kano K, Ikeda T (2001a) Bioelectrocatalysis-based dihydrogen/dioxygen fuel cell operating at physiological pH. Phys Chem Chem Phys 3:1331–1335

Tsujimura S, Wadano A, Kano K, Ikeda T (2001b) Photosynthetic bioelectrochemical cell utilizing cyanobacteria and water-generating oxidase. Enzyme Microb Technol 29:225–231

Tsujimura S, Nakagawa T, Kano K, Ikeda T (2004) Kinetic study of direct bioelectrocatalysis of dioxygen reduction with bilirubin oxidase at carbon electrodes. Electrochemistry 72:437–439

Tsujimura S, Kuriyama A, Fujieda N, Kano K, Ikeda T (2005) Mediated spectroelectrochemical titration of proteins for redox potential measurements by a separator-less one-compartment bulk electrolysis method. Anal Biochem 337:325–331

Vincent KA, Parkin A, Armstrong FA (2007) Investigating and exploiting the electrocatalytic properties of hydrogenases. Chem Rev 107:4366–4413

Wan L, Megarity CF, Siritanaratkul B, Armstrong FA (2018) A hydrogen fuel cell for rapid, enzyme-catalysed organic synthesis with continuous monitoring. Chem Commun 54:972–975

Xia HQ, So K, Kitazumi Y, Shirai Y, Nishikawa K, Higuchi Y, Kano K (2016) Dual gas-diffusion membrane- and mediatorless dihydrogen/air-breathing biofuel cell operating at room temperature. J Power Sources 335:105–112

Yahiro AT, Lee SM, Kimble DO (1964) Bioelectrochemistry: I. Enzyme utilizing bio-fuel cell studies. Biochim Biophys Acta 88:375–383

Yoon KS, Fukuda K, Fujisawa K, Nishihara H (2011) Purification and characterization of a highly thermostable, oxygen-resistant, respiratory [FeNi]-hydrogenase from marine, aerobic, hydrogen-oxidizing bacterium *Hydrogenovibrio marinus*. Int J Hydrog Energy 36:7081–7088

Yu X, Niks D, Mulchandani A, Hille R (2017) Efficient reduction of CO_2 by the molybdenum-containing formate dehydrogenase from *Cupriavidus necator* (*Ralstonia eutropha*). J Biol Chem 292:16872–16879

Zhong H, Fujii K, Nakano Y, Jin FM (2015) Effect of CO_2 bubbling into aqueous solutions used for electrochemical reduction of CO_2 for energy conversion and storage. J Phys Chem 119:55–61

Chapter 8
Application of Enzymatic Reactions Involving Electron Transfer and Energy Supply for the Production of Useful Chemicals

Jun Ogawa, Michiki Takeuchi, Akinori Ando, Ryotaro Hara, Makoto Hibi, and Shigenobu Kishino

8.1 Introduction

It has long been said that the introduction of bioprocesses that utilize biological reactions in chemical production processes is effective in preserving petroleum resources and in keeping environmental harmony. While usefulness has been found for a variety of compounds and corresponding bioprocesses have been designed, there is a need for the discovery of novel tools beyond the existing framework in biological reactions.

Microorganisms exhibiting various metabolisms are excellent targets for this purpose, and a number of studies have been conducted on microbial enzymes with the aim of developing them as industrial catalysts. As a result, many microbial enzymes were developed; however, most of them actually used in industrially at present are enzymes using water as a substrate (mainly, hydrolases such as lipase, esterase, protease, acylase, amidase). Microbial enzymes such as hydantoinase, carbamylase, lactonase, nitrile hydratase, and phosphatase have been put to practical use in the production of optically active compounds and commodity chemicals. Since these enzymes have excellent activity and stability and easy to control, they are considered to be useful as catalysts for chemical industry. However, these

J. Ogawa (✉) · A. Ando · S. Kishino
Division of Applied Life Sciences, Graduate School of Agriculture, Kyoto University, Sakyo-ku, Kyoto, Japan
e-mail: ogawa.jun.8a@kyoto-u.ac.jp

M. Takeuchi · R. Hara
Laboratory of Industrial Microbiology, Graduate School of Agriculture, Kyoto University, Sakyo-ku, Kyoto, Japan

M. Hibi
Biotechnology Research Center and Department of Biotechnology, Toyama Prefectural University, Imizu, Toyama, Japan

M. Ishii, S. Wakai (eds.), *Electron-Based Bioscience and Biotechnology*,
https://doi.org/10.1007/978-981-15-4763-8_8

enzymatic reactions alone will not be sufficient to handle a variety of chemical reactions such as redox reactions and condensation reactions.

In recent years, efforts have been made to apply microbial enzymes to bioprocesses with attractive reactions such as reduction (for carbonyl groups, olefins, etc.), hydroxylation reactions, carbon-carbon bond-forming reactions, and transfer reactions (reactions that require energy such as ATP). Here, we will look at the progress of such novel enzyme tool developments in the reactions of generating hydroxyl groups as examples and also discuss the use of multiple enzyme systems to diversify the bioprocess application.

8.2 Trends of Microbial Enzyme Development

Bioprocess development related to the production of optically active alcohols as chiral building blocks is a good example to understand the trends of microbial enzyme development. In the early days, asymmetric hydrolysis of racemic esters by lipases and esterases was the mainstream. Recently, processes for synthesizing chiral compounds utilizing reductase have appeared. At present, aiming at the development of next-generation enzyme catalysts, the target enzymatic reactions were expanded to oxidation reactions (oxygenases), hydration reactions, and carbon-carbon bond-forming reactions for simultaneous chiral control (Fig. 8.1).

From the viewpoint of enzyme system, target reactions have been changing from single-enzyme system for kinetic resolution by hydrolase to dynamic optical resolution with racemase, reductase system including coenzyme regeneration system, oxygenase system requiring electron transfer accessary, and complex condensation enzyme systems requiring high energy.

8.3 Key Tools for Enzymatic Chiral Hydroxyl Group Formation

When whole microbial cells, such as baker's yeast, are used as the catalyst for the asymmetric reduction of carbonyl compounds, two enzyme systems might be mainly involved in the production reaction. One is the enzyme catalyzing the asymmetric reduction of prochiral carbonyl compounds to chiral alcohols, i.e., carbonyl reductases. The other is a cofactor regeneration system, which supplies NADH or NADPH through the oxidation of the energy source, such as carbohydrates and alcohols. Generally, carbonyl reductases require NADH or NADPH as a cofactor for the reduction reactions, so a sufficient supply of cofactor in the same microbial cells is required for efficient production reactions (Fig. 8.1a).

Cytochrome P450 monooxygenases act as hydroxylases on the inactive carbon-hydrogen bonds of alkanes, fatty acids, terpenes, and steroids and are expected to be

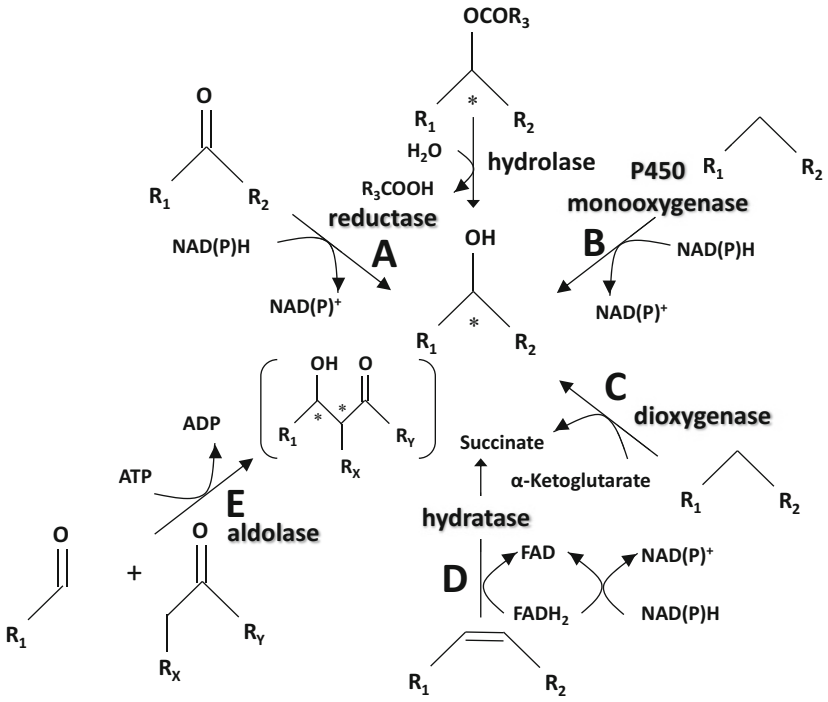

Fig. 8.1 Enzymatic reactions involving electron transfer and energy supply for the production of chiral alcohols: (**a**) reductase-catalyzing reaction, (**b**) cytochrome P450 monooxygenase-catalyzing reaction, (**c**) Fe(II)/α-ketoglutarate-dependent dioxygenase-catalyzing reaction, and (**d**) hydratase-catalyzing reaction, (**e**) aldolase-catalyzing reaction

potential catalysts for fine chemical synthesis. However, the need for electron-donating cofactor NADPH is one of the main barriers prohibiting the practical use of cytochrome P450 monooxygenases. In this chapter, the example of cytochrome P450 BM-3 from *Bacillus megaterium* for the asymmetric hydroxylation of propylbenzene and 3-chlorostyrene supported by coupling with NADPH regeneration system is described (Fig. 8.1b).

Fe(II)/α-ketoglutarate-dependent dioxygenases (Fe/αKG-DOs) also act as hydroxylases on the inactive carbon-hydrogen bonds. Fe/αKG-DOs are expected as novel hydroxylases acting on hydrophilic substrates in contrast with cytochrome P450 monooxygenases that prefer hydrophobic substrates. However, it needs α-ketoglutarate (αKG) as a co-substrate. We established a hydroxylation system using recombinant *Escherichia coli* expressing Fe/αKG-DOs and providing αKG via modified central metabolic pathway. Many Fe/αKG-DOs which are applicable for the hydroxylation system are introduced in this chapter (Fig. 8.1c).

We recently found novel fatty acid hydratase with regioselectivity to carbon-carbon double bonds and stereoselectivity in hydroxyl group introduction. The hydratase needs FAD and NADH as a cofactor and an activator, respectively. The

use of this enzyme for chiral hydroxylated fatty acid synthesis coupled with NADH-providing system from glucose via glycolytic pathway of *E. coli* is also described in this chapter (Fig. 8.1d).

We tried to develop energy-requiring bioprocesses using ATP or phosphorylated high-energy substrates. In this method, two features of baker's yeast serve as driving force: (1) the excellent ATP regeneration system and (2) baker's yeast cell treated by organic solvent (toluene or acetone) temporarily accumulate fructose 1,6-diphosphate (FDP) out of a cell under existence of glucose and phosphate. In order to construct a microbial platform for an energy-requiring bioprocess, we established an efficient enzymatic process in which 2′-deoxyribonucleosides are synthesized from glucose, acetaldehyde, and a nucleobase via carbon-carbon bond formation by aldol condensation reaction requiring a high-energy substrate provided by the yeast's glycolytic pathway as an energy-generating system (Fig. 8.1e).

8.4 Microbial Bioreduction System for Chiral Alcohol Production

A novel bioreduction system, in which *E. coli* transformant cells coexpressing an NAD(P)H-dependent carbonyl reductase gene and that of glucose dehydrogenase (GDH) (Kataoka et al. 1992a, 1998) as a cofactor regenerator are used as a catalyst, has been developed for asymmetric reduction of prochiral carbonyl compounds to the corresponding chiral alcohols (Fig. 8.2). The production of optically active 4-chloro-3-hydroxybutanoate esters (CHBEs) is a typical successful example of this bioreduction system.

An aldehyde reductase (AR1) of *Sporobolomyces salmonicolor* (Kataoka et al. 1992b) and a carbonyl reductase (S1) of *Candida magnoliae* (Wada et al. 1998) were found to catalyze NADPH-dependent stereospecific reduction of 4-chloro-3-oxobutanoate esters (COBE) to (*R*)- and (*S*)-CHBE, respectively. These yeast enzymes have been successfully applied to the *E. coli* coexpression system for the practical production (Kataoka et al. 1999; Kizaki et al. 2001). 300–350 g/L (*R*)- or

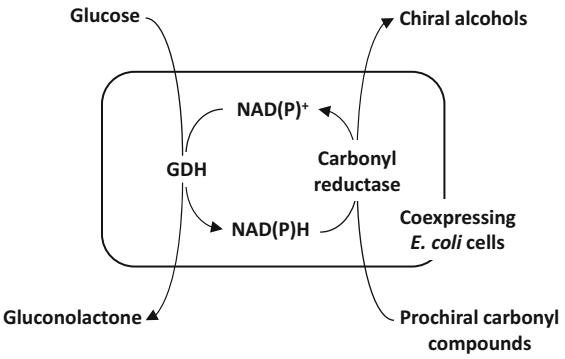

Fig. 8.2 Bioreduction system for the production of chiral alcohols by an *E. coli* transformant co-expressing carbonyl reductase and glucose dehydrogenase (GDH) genes

(*S*)-CHBE of high optical purity (92–100% *e.e.*) was stoichiometrically obtained on incubation of the transformant cells in a reaction mixture containing COBE, glucose, and a catalytic amount of NADPH. Very high turnover numbers of $NADP^+$ (13,500 and 35,000 mol CHBE/mol, respectively) were reported.

This bioreduction system is applicable to the production of many other useful chiral alcohols, by replacing the carbonyl reductase gene for other appropriate enzyme genes for carbonyl reduction. A good library of microbial carbonyl reductases with different substrate- and stereospecificities (i.e., aldehyde reductase isozyme (AR2) from *Sporobolomyces salmonicolor*, carbonyl reductases (S4, R, etc.) from *Candida magnoliae*, conjugated polyketone reductases from *Candida parapsilosis* and *Mucor ambiguus*, menadione reductase from *Candida macedoniensis*, levodione reductase from *Corynebacterium aquaticum*, 1-amino-2-propanol dehydrogenase from *Rhodococcus erythropolis*, secondary alcohol dehydrogenase from *Nocardia fusca*, etc.) has been made. The expression of the genes encoding these enzymes with the GDH gene in *E. coli* cells has been shown to be practically useful for many chiral alcohol production processes (Kita et al. 1999a, b; Wada et al. 1999a, b; Yasohara et al. 1999, 2000, 2001; Xie et al. 1999; Yoshizumi et al. 2001).

8.5 Regio- and Stereoselective Hydroxylation by Cytochrome P450

Some cytochrome P450s exhibit high regio- and stereoselective monooxygenation activity. Therefore, cytochrome P450s are expected to be potential catalysts for fine chemical synthesis. Cytochrome P450 BM-3 wild type (WT) and a mutant F87G showed high activities toward propylbenzene and 3-chlorostyrene with considerable stereoselectivity (Li et al. 2001). Furthermore, reaction analysis using cytochrome P450 BM-3 mutants revealed that the stereoselectivity is under the control of the residue size at position 87 of this enzyme (Li et al. 2001).

We reported oxidation of propylbenzene and 3-chlorostyrene by WT with high turnover (479 nmol 1-phenyl-1-propanol/min/nmol P450 and 300 nmol 3-chlorostyrene oxide/min/nmol P450). Furthermore, the residue size at position 87 of P450 BM-3 was found to play critical roles in determining stereoselectivity in oxidation of propylbenzene and 3-chlorostyrene. Replacement of Phe87 with Val, Ala, and Gly resulted in decreases in optical purity of produced (*R*)-(+)-1-phenyl-1-propanol from 90.0% to 37.4%, 26.0%, and −15.6% *e.e.*, respectively, and in increases in those of produced (*R*)-(+)-3-chlorostyrene oxide from −61.0% to −38.0%, 67.0%, and 94.6% *e.e.*, respectively (Li et al. 2001). WT and a mutant with replacement of Phe87 with Gly (F87G) were applied to asymmetric hydroxylation coupled with NADPH regeneration system using GDH (Fig. 8.3). These results indicated the high potential of cytochrome P450 BM-3 and its mutants for preparation of useful chiral compounds.

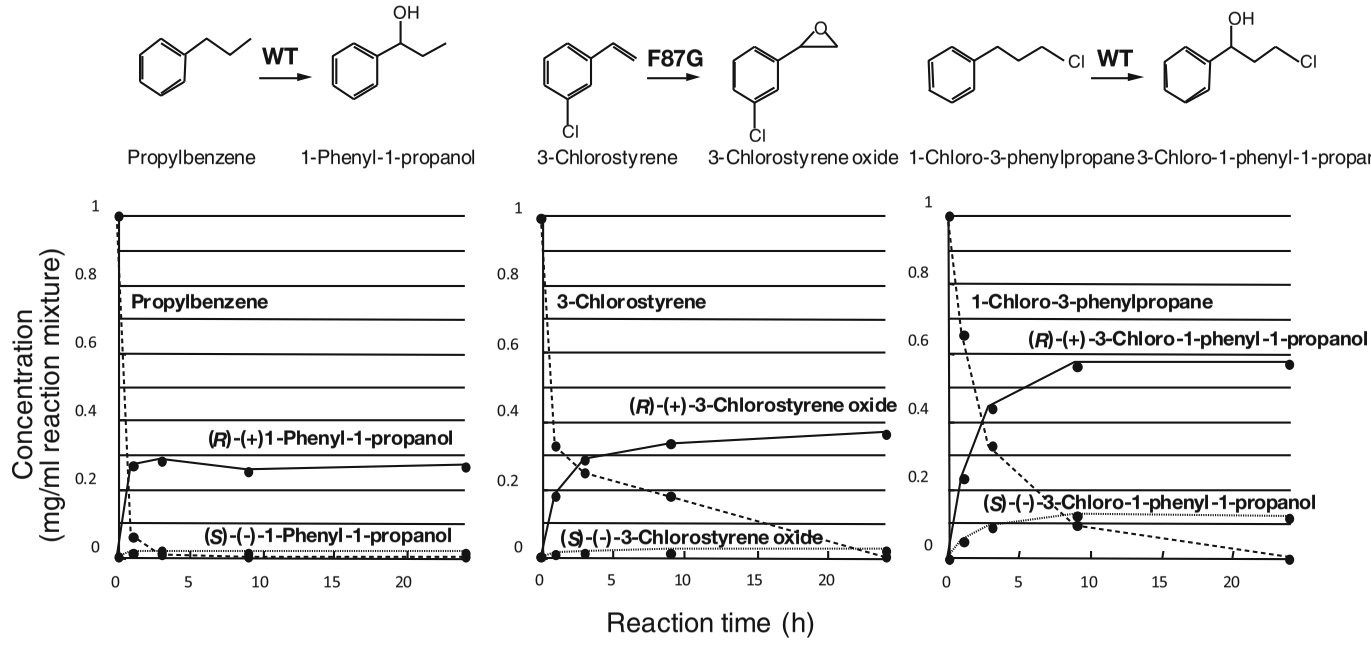

Yield (%)	28.6
Optical purity of (*R*)-product (% *e.e.*)	90.0
Activity (nmol/min/nmol P450)	0.429

Yield (%)	36.5
Optical purity of (*R*)-product (% *e.e.*)	90.6
Activity (nmol/min/nmol P450)	3.10

Yield (%)	68.9
Optical purity of (*R*)-product (% *e.e.*)	65.3
Activity (nmol/min/nmol P450)	1.65

Fig. 8.3 Regio- and stereoselective transformation of propylbenzene, 3-chlorostyrene, and 1-chloro-3-phenylpropane by cytochrome P450 BM-3 WT and a mutant F87G

8.6 Regio- and Stereoselective Hydroxylation by Fe(II)/α-Ketoglutarate-Dependent Dioxygenases

Recently, we identified several novel types of Fe/αKG-DOs that catalyze the hydroxylation of free aliphatic amino acids. Some hydroxyl aliphatic amino acids have several chiral carbons and may be important as precursors and chiral auxiliaries in the chemical synthesis of other compounds (Palomo et al. 1990; Blaskovich et al. 1998). In this section, we describe these novel Fe/αKG-DOs and reviewed the homology of their catalytic characteristics and process development toward their industrial applications.

8.6.1 L-Isoleucine 4-Hydroxylase

Recently, we reported a novel metabolic pathway for L-isoleucine via (2*S*,3*R*,4*S*)-4-hydroxyisoleucine (HIL) and (2*S*,3*R*)-2-amino-3-methyl-4-ketopentanoic acid (AMKP) in *Bacillus thuringiensis* 2e2 (Kodera et al. 2009; Ogawa et al. 2011). HIL synthesis was found to be catalyzed stereoselectively by a novel Fe/αKG-DO, L-isoleucine 4-hydroxylase (IDO) (Fig. 8.4a). This metabolic pathway functions as an effective bypass pathway that compensates for the incomplete TCA cycle in *Bacillus* species (Perlman et al. 1977).

Moreover, IDO stereoselectively hydroxylates several aliphatic L-amino acids as well as L-isoleucine (Hibi et al. 2011). It converts L-leucine and L-norvaline into (2*S*)-4-hydroxyleucine and (2*S*,4*S*)-4-hydroxynorvaline, respectively. When L-norleucine is used as the substrate, single diastereomers of (2*S*)-4-hydroxynorleucine and (2*S*)-5-hydroxynorleucine are produced together at a ratio of 10:1. Interestingly, when IDO reacts with L-alloisoleucine, it does not produce a C4-hydroxylated product but rather a C3-hydroxylated form of L-alloisoleucine.

8.6.2 Fe/αKG-DOs Closely Homologous with L-Isoleucine 4-Hydroxylase

IDO is a member of the Pfam family PF10014 (the former DUF 2257) of uncharacterized conserved bacterial proteins. By in silico screening of PF10014 member enzymes, five function-unknown Fe/αKG-DOs were found to have amino acid sequence homology with IDO: AVI of *Agrobacterium vitis* S4, BPE of *Bordetella petrii* DSM 12804, GOX of *Gluconobacter oxydans* 621H, MFL of *Methylobacillus flagellatus* KT, and HilB of *Pantoea ananatis* AJ13355. According to the results of substrate specificity analysis, all of these Fe/αKG-DOs have the sulfoxidation activity of L-methionine in common. Of these, AVI, BPE, GOX, and MFL convert L-leucine into (2*S*)-4-hydroxyleucine as well as IDO, but they do not

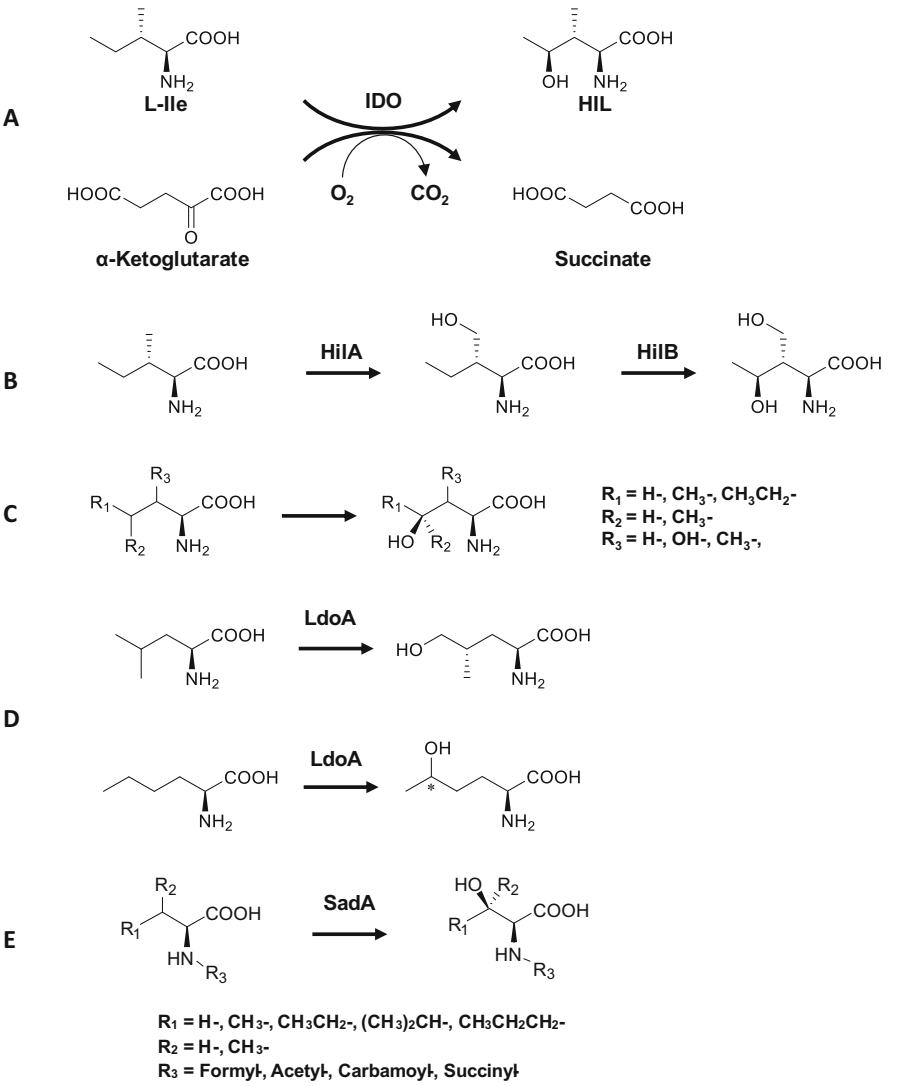

Fig. 8.4 Reactions of L-amino acids oxygenation by Fe/αKG-DOs. (**a**) L-isoleucine hydroxylation by IDO, (**b**) cascade hydroxylation reactions of L-isoleucine catalyzed by HilA and HilB, (**c**) regio- and stereoselective hydroxylation of aliphatic L-amino acids catalyzed by IDO and its homologues, (**d**) regio- and stereoselective hydroxylation of L-leucine catalyzed by LdoA, and (**e**) regio- and stereoselective hydroxylation of *N*-substituted aliphatic L-amino acids catalyzed by SadA

react with L-isoleucine. As for AVI and BPE, they additionally have unique terminal C4-hydroxylation activity toward L-threonine and produced the corresponding diol. Although HilB was shown to catalyze C4-hydroxylation of L-isoleucine and L-leucine, the primary role of HilB was recently elucidated in *P. ananatis* AJ13355.

There is another gene-encoded Fe/αKG-DO, HilA, next to HilB gene in the genome of the microorganism. HilA has no amino acid sequence homology with IDO and has the specific ability to terminally hydroxylate the methyl group of L-isoleucine and L-valine, to produce (2*S*,3*S*)-4′-hydroxyisoleucine and (2*S*)-4-hydroxyvaline. Because HilB also has C4-hydroxylation activity of (2*S*,3*S*)-4′-hydroxyisoleucine, a novel metabolic pathway converting L-isoleucine into (2*S*,3*S*,4*S*)-4,4′-dihydroxyisoleucine is carried out by HilA and HilB in *P. ananatis* AJ13355 (Fig. 8.4b). Thus, some IDO-like Fe/αKG-DOs categorized as PF10014 are highly regioselective hydroxylases acting on the C4-position of aliphatic L-amino acid substrates (Fig. 8.4c).

8.6.3 *L-Leucine 5-Hydroxylase*

L-Leucine 5-hydroxylase (LdoA) found in *Nostoc punctiforme* PCC 73102 is a unique type of Fe/αKG-DO (Hibi et al. 2012a). LdoA has no amino acid sequence homology with and shows distinct regioselectivity in hydroxylation when compared to, the IDO-like Fe/αKG-DOs and HilA. LdoA catalyzes regio- and stereoselective C5-hydroxylation of L-leucine and L-norleucine into (2*S*,4*S*)-5-hydroxyleucine and (2*S*)-5-hydroxynorleucine, respectively (Fig. 8.4d). (2*S*,4*S*)-5-Hydroxyleucine is an intermediate in the conversion pathway of L-leucine into (2*S*,4*S*)-4-methylproline, which is known to be a common component of nostopeptolides and nostocyclopeptides produced by several *Nostoc* species (Becker et al. 2004; Hoffmann et al. 2003; Jokela et al. 2010). LdoA is the enzyme responsible for this conversion pathway in *N. punctiforme* PCC 73102 (Luesch et al. 2003). Nostopeptolide A1 and A3 produced by *Nostoc* sp. Lukešová 30/93 were found to be weak inhibitors of the expression and production of proinflammatory mediators in response to TNF treatment in human lung microvascular cells (Pflüger et al. 2013). Thus, (2*S*,4*S*)-4-methylproline biosynthetic enzymes like LdoA could be integral for the industrial production of these bioactive peptides.

8.6.4 N-*Succinyl L-Leucine 3-Hydroxylase*

As another unique type of Fe/αKG-DO, *N*-succinyl L-leucine 3-hydroxylase (SadA) was found in *Burkholderia ambifaria* AMMD (Hibi et al. 2012b). SadA has no amino acid sequence homology with and shows distinct regioselectivity in hydroxylation, when compared to the IDO-like Fe/αKG-DOs, HilA, and LdoA. SadA has catalytic activity toward several *N*-substituted L-amino acids, such as *N*-succinyl, *N*-acetyl, *N*-formyl, and *N*-carbamoyl ones (Fig. 8.4e). Among them, *N*-succinyl L-leucine is the best substrate for SadA, and it is converted into *N*-succinyl L-threo-β-hydroxyleucine with over 99% diastereoselectivity. Similarly, SadA catalyzes stereoselective C3-hydroxylation of several *N*-succinyl L-amino acids, such as

N-succinyl L-valine, *N*-succinyl L-2-aminobutyrate, *N*-succinyl L-isoleucine, and *N*-succinyl L-leucine into corresponding *N*-succinyl β-hydroxy L-amino acids, such as *N*-succinyl L-β-hydroxyvaline, *N*-succinyl L-threonine, (2*S*,3*R*)-*N*-succinyl L-β-hydroxyisoleucine, and *N*-succinyl L-threo-β-hydroxyleucine. L-threo-β-hydroxyleucine is a promising target material for preparation of cyclic depsipeptides that possess useful physiological activities (Tymiak et al. 1989; Taniguchi et al. 2003).

Using a combination of SadA and LasA, which is an *N*-succinyl L-amino acid desuccinylase also found in *B. ambifaria* AMMD, *N*-succinyl L-leucine was successfully converted into L-threo-β-hydroxyleucine with 93% of molar yield and over 99% of diastereomeric excess (Hibi et al. 2015). Consequently, this new biocatalytic production system has advantages in optical purity and reaction efficiency for application in the industrial mass production of several useful β-hydroxy α-amino acids.

8.6.5 *Catalytic Properties of the Aliphatic Amino Acid Hydroxylases*

Most of these enzymes, except for HilA, are confirmed to have sulfoxidation activity as well as hydroxylation activity, and in these reactions, the side chains of L-methionine and L-leucine, respectively, are common substrate structures. The hydroxylation reaction is more effective than the sulfoxidation reaction in all cases, and the hydroxylation of L-isoleucine with IDO is the most efficient among the reactions of these Fe/αKG-DOs. Additionally, preference for weak acidic and low-temperature conditions is common to the hydroxylation reactions of these Fe/αKG-DOs. For example, the highest activities were observed at pH 6.0 and 30 °C for IDO (Kodera et al. 2009), at pH 5.0 and 20 °C for LdoA (Hibi et al. 2012a), and at pH 6.5 and 30 °C for SadA (Hibi et al. 2012b).

8.6.6 *Practical Use of Fe(II)/α-Ketoglutarate-Dependent Dioxygenases Coupled with Co-substrate Generation System*

(2*S*,3*R*,4*S*)-4-hydroxyisoleucine (HIL), which was originally found in the seeds of fenugreek, the annual herb *Trigonella foenum-graceum* (Fowden et al. 1973), is a promising compound for drug and functional food development because of its anti-diabetes and anti-obesity activity. We have recently developed an efficient production system for HIL using a genetically manipulated *E. coli* 2Δ strain heterologously expressing IDO (Smirnov et al. 2010). Because the *E. coli* 2Δ strain lacks the activities of αKG dehydrogenase, isocitrate lyase, and isocitrate dehydrogenase

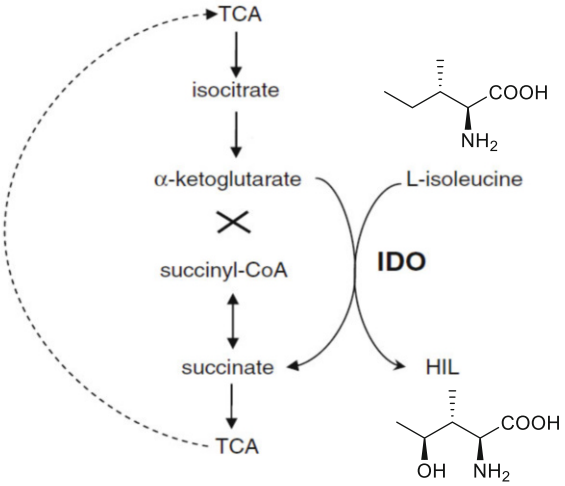

Fig. 8.5 Modified TCA cycle in the *E. coli* 2Δ strain resulting from the simultaneous oxidation of L-isoleucine and αKG

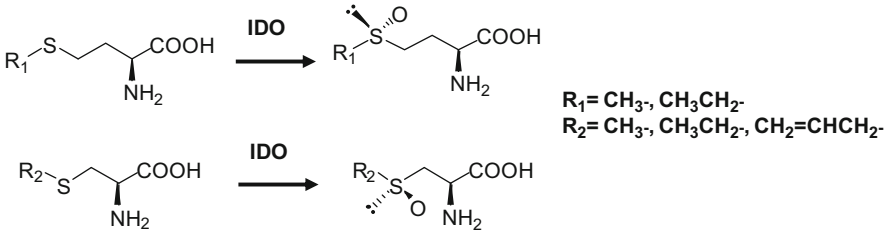

Fig. 8.6 Asymmetric sulfoxidation of sulfur-containing L-amino acids catalyzed by IDO

kinase/phosphatase, it could not grow in a minimal medium due to the blockage of TCA during succinate synthesis. The IDO activity in the 2Δ strain was able to "shunt" destroyed TCA, thereby coupling L-isoleucine hydroxylation and cell growth (Fig. 8.5). Using this strain, we performed the direct biotransformation of L-isoleucine into HIL with 82% yield and over 99% optical purity. This system could easily be applied to the production of other IDO-producible hydroxy amino acids described above.

Furthermore, IDO was found to catalyze asymmetric sulfoxidation of L-methionine, L-ethionine, *S*-methyl-L-cysteine, *S*-ethyl-L-cysteine, and *S*-allyl-L-cysteine into corresponding (*S*)-configured sulfoxides such as L-methionine (*S*)-sulfoxide, L-ethionine (*S*)-sulfoxide, (+)-methiin, (+)-ethiin, and (+)-alliin (Fig. 8.6) (Hibi et al. 2013). (+)-Methiin and (+)-alliin are promising materials for use in functional foods or drugs since they have antibiotic, antioxidant, anti-inflammatory, antidiabetic, anti-Alzheimer's, and anti-cholesterolemic effects. By using the dried

cell powder of IDO-expressing *E. coli* as a biocatalyst, preparative scale productions of these chiral sulfoxides with high enantiomeric purity could easily be accomplished via bioconversion, allowing further development of their industrial applications.

8.7 Regio- and Stereoselective Hydration of Unsaturated Fatty Acids by Fatty Acid Hydratase

Fatty acid saturation metabolism, the so-called biohydrogenation, is considered to be a detoxifying metabolism of gut bacteria to transform toxic-free polyunsaturated fatty acids to less toxic-free saturated fatty acids. We revealed the complex metabolic pathway of the biohydrogenation in lactic acid bacteria in detail (Kishino et al. 2013). The enzyme system of biohydrogenation was found to consist of four enzymes. The concerned action of these enzymes, i.e., hydratase, dehydrogenase, isomerase, and enone reductase, accomplishes the saturation of a carbon-carbon double bond and generated unique polyunsaturated fatty acid molecular species such as hydroxy fatty acids, oxo fatty acids, and conjugated fatty acids as intermediates. Chiral hydroxy fatty acids were efficiently produced by the hydratase under the optimized conditions.

8.7.1 Linoleic Acid Δ9 Hydratase

Linoleic acid Δ9 hydratase which is involved in linoleic acid saturation metabolism of *Lactobacillus plantarum* AKU 1009a was cloned as his-tagged recombinant enzyme, purified with affinity column, and characterized (Takeuchi et al. 2015). The enzyme required FAD as a cofactor for its activity, and the activity was enhanced by NADH. The maximum activities for hydration of linoleic acid and for dehydration of 10-hydroxy-*cis*-12-octadecenoic acid (HYA) were observed at 37 °C, pH 5.5, with 0.5 M NaCl. C16 and C18 free fatty acids with *cis*-9 double bond served as substrates for hydration with C10 regiospecificity and (*S*) stereospecificity (Fig. 8.7). 10-Hydroxy fatty acids served as substrates for dehydration reactions. The apparent K_m value for linoleic acid was estimated to be 92 μM with its k_{cat} values at 2.6×10^{-2} s^{-1}, and Hill factor was 3.3. The apparent K_m value for HYA was estimated to be 98 μM with its k_{cat} values at 1.2×10^{-3} s^{-1}.

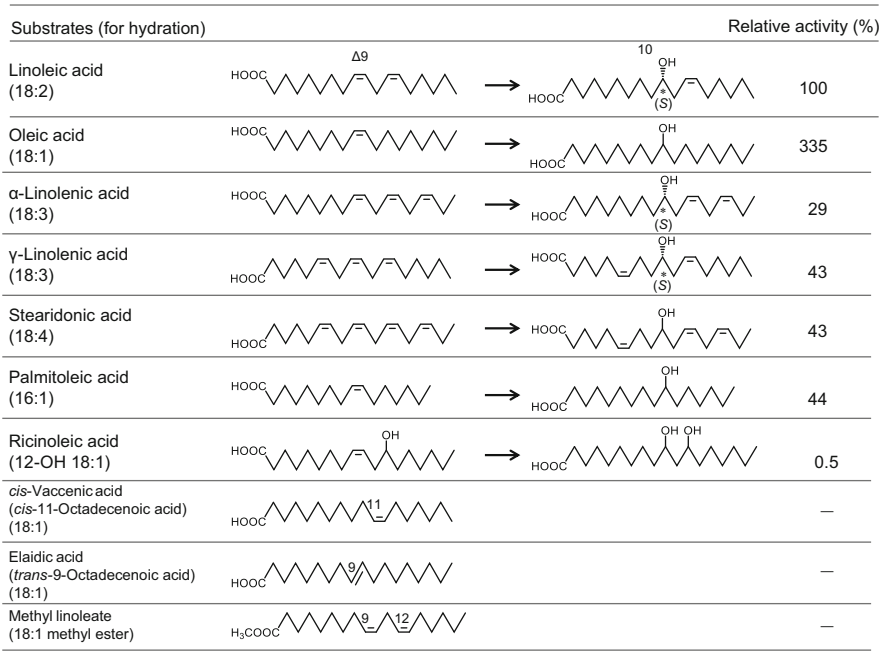

Fig. 8.7 Substrate specificity of hydration reaction catalyzed by linoleic acid Δ9 hydratase

8.7.2 Efficient Enzymatic Production of Hydroxy Fatty Acids by Linoleic Acid Δ9 Hydratase

E. coli overexpressing linoleic acid Δ9 hydratase from *Lactobacillus plantarum* AKU 1009a was applied to produce hydroxy fatty acids with industrial potentials (Takeuchi et al. 2015). 280 g/L of linoleic acid (1 M) was converted into 10-hydroxy-*cis*-12-octadecenoic acid with high conversion rate, 98% (mol/mol), by the cells of the recombinant *E. coli* with the presence of FAD (0.1 mM) and NADH (5 mM). Lowering the reaction temperature reduced the solubility of the products and resulted in the high yield by controlling the reaction equilibrium. Oleic acid, α-linolenic acid, γ-linolenic acid, stearidonic acid, *cis*-9-hexadecenoic acid, and 12-hydroxy-*cis*-9-octadecenoic acid were also converted into corresponding 10-hydroxy fatty acids with conversion rates of 98%, 96%, 95%, 93%, 98%, and 99% (mol/mol) to 280 g/L of each substrate, respectively. Although the hydratase required NADH for its maximal activity, the recombinant *E. coli* well catalyzed the reaction with glucose instead of NADH, suggested that the *E. coli* cells supplied NADH via glucose metabolism. 10-Hydroxy-*cis*-12-octadecenoic acid was produced with high accumulation (289 g/L) and high yield (97 mol%) in the reaction mixture containing glucose instead of NADH.

8.8 Construction of Microbial Platform for an Energy-Requiring Bioprocess

When developing an efficient bioprocess, it is important to consider how to supply the cofactor that accelerates the enzymatic reaction. One good example is enzymatic carbonyl reduction for chiral alcohol synthesis with the cofactor (NAD(P)H) regeneration system. We tried to extend this concept to energy-requiring bioprocesses using ATP or phosphorylated high-energy substrates (Fig. 8.1e). In this method, two features of baker's yeast serve as driving force: (1) the excellent ATP regeneration system and (2) baker's yeast cell treated by organic solvent (toluene or acetone) temporarily accumulate fructose 1,6-diphosphate (FDP) out of a cell under existence of glucose and phosphate (Tochikura et al. 1967; Tochikura 1978; Horinouchi et al. 2006a). We tried to provide the convenient recipe for the establishment of energy-requiring bioprocess. If energy regeneration by yeast can be introduced into the aldol condensation process as the supplier of energy or high-energy substrates, it can expand the industrial applications. Therefore, this application of microbial glycolysis is a promising strategy to establish a variety of energy-requiring bioprocesses for a sustainable green society.

8.8.1 Practical 2′-Deoxyribonucleoside Production Involving a Carbon-Carbon Bond-Forming Reaction with High-Energy Substrates

As an example of a microbial platform for an energy-requiring bioprocess, we established a process that efficiently and enzymatically synthesizes 2′-deoxyribonucleoside from glucose, acetaldehyde, and a nucleobase. This method consists of the coupling reactions of the reversible nucleoside degradation pathway catalyzed by deoxyriboaldolase (DERA), phosphopentomutase (PPMase), and nucleoside phosphorylase (NPase) (Fig. 8.8) (Horinouchi et al. 2003, 2006a, b, c; Ogawa et al. 2003) and energy generation through the yeast glycolytic pathway. In this method, DERA reaction is used to generate a deoxyribose skeleton, and D-glyceraldehyde 3-phosphate, which is a substrate for this reaction together with acetaldehyde, is provided from glucose via FDP through baker's yeast glycolysis. High concentration of acetaldehyde was added to the reaction mixture to direct this process consisting of many equilibrium reactions such as PPMase and NPase reactions to the synthesis of 2′-deoxyribonucleosides. For this purpose, acetaldehyde-tolerant enzymes were screened and applied to the reaction.

Using *E. coli* that co-express DERA and PPMase, commercial NPase, and acetone-dried yeast in a one-pot reaction system, an efficient process for 2′-deoxyribonucleoside production was established (Fig. 8.8). In the one-pot reaction that performed glycolysis, aldol condensation, phosphoryl transfer, and base addition all at once, ATP required for the synthesis of phosphorylated intermediates was

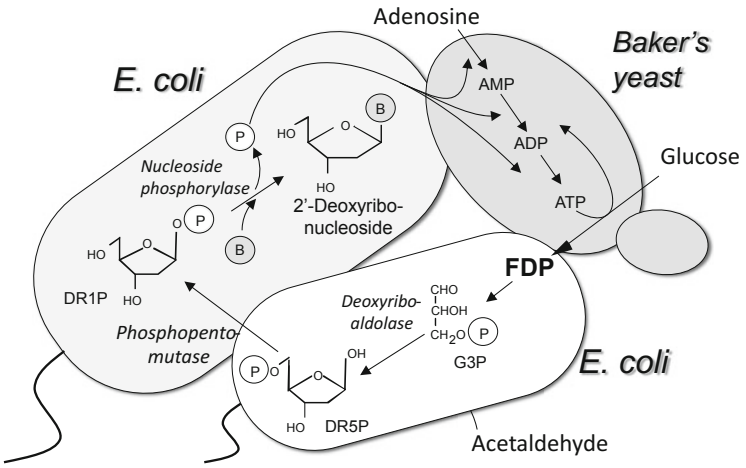

Fig. 8.8 One-pot enzymatic synthesis of 2′-deoxyribonucleoside from glucose, acetaldehyde, and nucleobase

obtained through glycolysis by adding a catalytic amount of adenosine. In addition, to reuse the by-produced phosphoric acid, which shifts the reaction equilibrium toward the decomposition side, for ATP regeneration, made possible to control the concentration of phosphoric acid in low in the reaction system to avoid 2′-deoxyribonucleoside phosphorolysis, then achieved high accumulation of 2′-deoxyribonucleoside.

2′-Deoxyribonucleoside was produced with efficient energy transfer under phosphate-limiting reaction conditions. Keeping the nucleobase concentration low and the mixture at a low reaction temperature increased the yield of 2′-deoxyribonucleoside relative to the amount of added nucleobase, indicating that energy was efficiently generated from glucose via the yeast glycolytic pathway under these reaction conditions. Using a one-pot reaction in which small amounts of adenine, adenosine, and acetone-dried yeast were fed into the reaction, 75 mM of 2′-deoxyinosine, the deaminated product of 2′-deoxyadenosine, was produced from glucose (600 mM), acetaldehyde (250 mM), adenine (70 mM), and adenosine (20 mM) with a high yield relative to the total base moiety input (83%). Moreover, a variety of natural 2′-deoxyribonucleosides were further synthesized by introducing a base-exchange reaction into the process (Horinouchi et al. 2012).

8.9 Conclusion

Bioprocess utilizing enzyme functions for chemical industry is becoming increasingly diversified. For example, the target on which an enzyme acts is expanding from natural products, mainly plant biomass, to synthetic compounds. In addition, the

types of enzymes used have been diversified, and there is also a tendency to utilize them in a complex manner. To cope with these situations, the expansion of the enzyme library and the development of platform technologies such as host cells and reaction environments that can maximize the function of the enzyme will be important.

To expand the enzyme library, it will be necessary to use various methodologies such as traditional microbial enzyme screening, modern artificial evolution, and artificial enzyme design depending on the situation. In addition, as the technologies for controlling complex enzyme reaction systems, as in the case of *E. coli* expressing a coenzyme regeneration system useful for the reductase, a novel host cell with general-purpose functions such as ATP supply and electron transport, will bring a breakthrough. Considering the future, the expansion of enzyme libraries along with the development of platform technologies, based on the standpoint of the ultimate use of energy, such as hydrocarbon, hydrogen, electricity, and solar energy, seems to be important.

The functions of microbial enzymes are diverse. It is interesting how industrial use focusing on these functions will be developed in the future.

Acknowledgments This work was supported in part by the Japanese Ministry of Education, Science, Sports and Culture Grants-in-aid KAKENHI 23248014 and 22658027 (to J.O.) and 30432347 and 21780070 (to M.H.), the Bio-Oriented Technology Research Advancement Institution of Japan (to J.O.), and NEDO Innovation Commercialization Venture Support Project (in collaboration with NITTO PHARMA and J.O.).

References

Becker JE, Moore RE, Moore BS (2004) Cloning, sequencing, and biochemical characterization of the nostocyclopeptide biosynthetic gene cluster: molecular basis for imine macrocyclization. Gene 325:35–42

Blaskovich MA, Evindar G, Rose NGW, Wilkinson S, Luo Y, Lajoie GA (1998) Stereoselective synthesis of *threo* and *erythro* β-hydroxy and β-disubstituted-β-hydroxy α-amino acids. J Org Chem 63:3631–3646

Fowden L, Pratt HM, Smith A (1973) 4-Hydroxyisoleucine from seed of *Trigonella foenum-graecum*. Phytochemistry 12:1707–1711

Hibi M, Kawashima T, Kodera T, Smirnov SV, Sokolov PM, Sugiyama M, Shimizu S, Yokozeki K, Ogawa J (2011) Characterization of *Bacillus thuringiensis* L-isoleucine dioxygenase for production of useful amino acids. Appl Environ Microbiol 77:6926–6930

Hibi M, Kawashima T, Sokolov PM, Smirnov SV, Kodera T, Sugiyama M, Shimizu S, Yokozeki K, Ogawa J (2012a) L-Leucine 5-hydroxylase of *Nostoc punctiforme* is a novel type of Fe(II)/α-ketoglutarate-dependent dioxygenase that is useful as a biocatalyst. Appl Microbiol Biotechnol 97:2467–2472

Hibi M, Kawashima T, Kasahara T, Sokolov PM, Smirnov SV, Kodera T, Sugiyama M, Shimizu S, Yokozeki K, Ogawa J (2012b) A novel Fe(II)/α-ketoglutarate-dependent dioxygenase from *Burkholderia ambifaria* has β-hydroxylating activity of *N*-succinyl L-leucine. Lett Appl Microbiol 55:414–441

Hibi M, Kawashima T, Yajima H, Smirnov SV, Kodera T, Sugiyama M, Shimizu S, Yokozeki K, Ogawa J (2013) Enzymatic synthesis of chiral amino acid sulfoxides by Fe(II)/α-ketoglutarate-dependent dioxygenase. Tetrahedron Asymmetry 24:990–994

Hibi M, Kasahara T, Kawashima T, Yajima H, Kozono S, Smirnov SV, Kodera T, Sugiyama M, Shimizu S, Yokozeki K, Ogawa J (2015) Multi-enzymatic synthesis of optically pure β-hydroxy α-amino acids. Adv Synth Catal 357:767–774

Hoffmann D, Hevel JM, Moore RE, Moore BS (2003) Sequence analysis and biochemical characterization of the nostopeptolide A biosynthetic gene cluster from *Nostoc* sp. GSV224. Gene 311:171–180

Horinouchi N, Ogawa J, Sakai T, Kawano T, Matsumoto S, Sasaki M, Mikami Y, Shimizu S (2003) Construction of deoxyriboaldolase-expressing *Escherichia coli* and its application to 2-deoxyribose 5-phosphate synthesis from glucose and acetaldehyde for 2-′-deoxyribonucleoside production. Appl Environ Microbiol 69:3791–3797

Horinouchi N, Ogawa J, Kawano T, Sakai T, Saito K, Matsumoto S, Sasaki M, Mikami Y, Shimizu S (2006a) Efficient production of 2-deoxyribose 5-phosphate from glucose and acetaldehyde by coupling reaction of the alcoholic fermentation system of baker's yeast and deoxyriboaldolase-expressing *Escherichia coli*. Biosci Biotechnol Biochem 70:1371–1378

Horinouchi N, Ogawa J, Kawano T, Sakai T, Saito K, Matsumoto S, Sasaki M, Mikami Y, Shimizu S (2006b) Biochemical retrosynthesis of 2′-deoxyribonucleosides from glucose, acetaldehyde and a nucleobase. Appl Microbiol Biotechnol 71:615–621

Horinouchi N, Ogawa J, Kawano T, Sakai T, Saito K, Matsumoto S, Sasaki M, Mikami Y, Shimizu S (2006c) One-pot microbial synthesis of 2′-deoxyribonucleoside from glucose, acetaldehyde, and a nucleobase. Biotechnol Lett 28:877–881

Horinouchi N, Sakai T, Kawano T, Matsumoto S, Sasaki M, Hibi M, Shima J, Shimizu S, Ogawa J (2012) Construction of microbial platform for an energy-requiring bioprocess: practical 2-′-deoxyribonucleoside production involving a C-C coupling reaction with high energy substrates. Microb Cell Factories 11:82

Jokela J, Herfindal L, Wahlsten M, Permi P, Selheim F, Vasconcelos V, Doskeland SO, Sivonen K (2010) A novel cyanobacterial nostocyclopeptide is a potent antitoxin against microcystins. ChemBioChem 11:1594–1599

Kataoka M, Nomura Y, Shimizu S, Yamada H (1992a) Enzymes involved in the NADPH regeneration system coupled with asymmetric reduction of carbonyl compounds in microorganisms. Biosci Biotechnol Biochem 56:820–821

Kataoka M, Sakai H, Morikawa T, Katoh M, Miyoshi T, Shimizu S, Yamada H (1992b) Characterization of aldehyde reductase of *Sporobolomyces salmonicolor*. Biochim Biophys Acta 1122:57–62

Kataoka M, Rohani LPS, Wada M, Kita K, Yanase H, Urabe I, Shimizu S (1998) *Escherichia coli* transformant expressing the glucose dehydrogenase gene from *Bacillus megaterium* as a cofactor regenerator in a chiral alcohol producing system. Biosci Biotechnol Biochem 62:167–169

Kataoka M, Yamamoto K, Kawabata H, Wada M, Kita K, Yanase H, Shimizu S (1999) Stereoselective reduction of ethyl 4-chloro-3-oxobutanoate by *Escherichia coli* transformant cells co-expressing the aldehyde reductase and glucose dehydrogenase genes. Appl Microbiol Biotechnol 51:486–490

Kishino S, Takeuchi M, Park SB, Hirata A, Kitamura N, Kunisawa J, Kiyono H, Iwamoto R, Isobe Y, Arita M, Arai H, Ueda K, Shima J, Takahashi S, Yokozeki K, Shimizu S, Ogawa J (2013) Polyunsaturated fatty acid saturation by gut lactic acid bacteria affecting host lipid composition. Proc Natl Acad Sci U S A 110:17808–17813

Kita K, Nakase K, Yanase H, Kataoka M, Shimizu S (1999a) Purification and characterization of new aldehyde reductase from *Sporobolomyces salmonicolor* AKU4429. J Mol Catal B Enzymatic 6:305–313

Kita K, Kataoka M, Shimizu S (1999b) Diversity of 4-chloroacetoacetate ethyl ester-reducing enzymes in yeasts and their application to chiral alcohol synthesis. J Biosci Bioeng 88:591–598

Kizaki N, Yasohara Y, Hasegawa J, Wada M, Kataoka M, Shimizu S (2001) Synthesis of optically pure ethyl (*S*)-4-chloro-3-hydroxybutanoate by *Escherichia coli* transformant cells coexpressing the carbonyl reductase and glucose dehydrogenase genes. Appl Microbiol Biotechnol 55:590–595

Kodera T, Smirnov SV, Samsonova NN, Kozlov YI, Koyama R, Hibi M, Ogawa J, Yokozeki K, Shimizu S (2009) A novel L-isoleucine hydroxylating enzyme, L-isoleucine dioxygenase from *Bacillus thuringiensis*, produces (2*S*,3*R*,4*S*)-4-hydroxyisoleucine. Biochem Biophys Res Commun 390:506–510

Li QS, Ogawa J, Schmid RD, Shimizu S (2001) Residue size at position 87 of cytochrome P450 BM-3 determines its stereoselectivity in propylbenzene and 3-chlorostyrene oxidation. FEBS Lett 508:249–252

Luesch H, Hoffmann D, Hevel JM, Becker JE, Golakoti T, Moore RE (2003) Biosynthesis of 4-methylproline in cyanobacteria: cloning of *nosE* and *nosF* genes and biochemical characterization of the encoded dehydrogenase and reductase activities. J Org Chem 68:83–91

Ogawa J, Saito K, Sakai T, Horinouchi N, Kawano T, Matsumoto S, Sasaki M, Mikami Y, Shimizu S (2003) Microbial production of 2-deoxyribose 5-phosphate from acetaldehyde and triosephosphate for the synthesis of 2′-deoxyribonucleosides. Biosci Biotechnol Biochem 67:933–936

Ogawa J, Kodera T, Smirnov SV, Hibi M, Samsonova NN, Koyama R, Yamanaka H, Mano J, Kawashima T, Yokozeki K, Shimizu S (2011) A novel L-isoleucine metabolism in *Bacillus thuringiensis* generating (2*S*,3*R*,4*S*)-4-hydroxyisoleucine, a potential insulinotropic and anti-obesity amino acid. Appl Microbiol Biotechnol 89:1929–1938

Palomo C, Arrieta A, Cossio FP, Aizpurua JM, Mielgo A, Aurrekoetxea N (1990) Highly stereoselective synthesis of α-hydroxy β-amino acids through β-lactams: application to the synthesis of the taxol and bestatin side chains and related systems. Tetrahedron Lett 31:6429–6432

Perlman D, Perlman KL, Bodanszky M (1977) Microbial production of vitamin B_{12} antimetabolites. II. 2-amino-4-keto-3-methylpentanoic acids from *Bacillus cereus* 439. Bioorg Chem 6:263–271

Pflüger M, Kapuscik A, Lucas R, Koppensteiner A, Katzlinger M, Jokela J, Eger A, Jacobi N, Wiesner C, Hofmann E, Önder K, Kopecky J, Schütt W, Hundsberger H (2013) A combined impedance and AlfaLISA-based approach to identify anti-inflammatory and barrier-protective compounds in human endothelium. J Biomol Screen 18:67–74

Smirnov SV, Kodera T, Samsonova NN, Kotlyarova VA, Rushkevich NY, Kivero AD, Sokolov PM, Hibi M, Ogawa J, Shimizu S (2010) Metabolic engineering of *Escherichia coli* to produce (2*S*,3*R*,4*S*)-4-hydroxyisoleucine. Appl Microbiol Biotechnol 88:719–726

Takeuchi M, Kishino S, Hirata A, Park SB, Kitamura N, Ogawa J (2015) Characterization of the linoleic acid Δ9 hydratase catalyzing the first step of polyunsaturated fatty acid saturation metabolism in *Lactobacillus plantarum* AKU 1009a. J Biosci Bioeng 119:636–641

Taniguchi M, Suzumura KI, Nagai K, Kawasaki T, Saito T, Takasaki J, Suzuki KI, Fujita S, Tsukamoto SI (2003) Structure of YM-254890, a novel $G_{q/11}$ inhibitor from *Chromobacterium* sp. QS3666. Tetrahedron 59:4533–4538

Tochikura T (1978) Production of nucleotide-related substance by yeast and utilization of fermentation energy to biosynthetic process. Hakko Kogaku Kaishi (in Japanese) 56:508–526

Tochikura T, Kuwahara M, Yagi S, Okamoto H, Tominaga Y, Kano T, Ogata K (1967) Fermentation and metabolism of nucleic acid-related compounds in yeast. J Ferment Technol 45:511–529

Tymiak AA, McCormick TJ, Unger SE (1989) Structure determination of lysobactin, a macrocyclic peptide lactone antibiotic. J Org Chem 54:1149–1157

Wada M, Kataoka M, Kawabata H, Yasohara Y, Kizaki N, Hasegawa J, Shimizu S (1998) Purification and characterization of NADPH-dependent carbonyl reductase, involved in stereoselective reduction of ethyl 4-chloro-3-oxobutanoate, from *Candida magnoliae*. Biosci Biotechnol Biochem 62:280–285

Wada M, Kawabata H, Kataoka M, Yasohara Y, Kizaki N, Hasegawa J, Shimizu S (1999a) Purification and characterization of an aldehyde reductase from *Candida magnoliae*. J Mol Catal B Enzymatic 6:333–339

Wada M, Yoshizumi A, Nakamori S, Shimizu S (1999b) Purification and characterization of monovalent cation-activated Levodione reductase from *Corynebacterium aquaticum* M-13. Appl Environ Microbiol 65:4399–4403

Xie SX, Ogawa J, Shimizu S (1999) NAD^+-dependent (*S*)-specific secondary alcohol dehydrogenase involved in stereoinversion of 3-pentyn-2-ol catalyzed by *Nocardia fusca* AKU 2123. Biosci Biotechnol Biochem 63:1721–1729

Yasohara Y, Kizaki N, Hasegawa J, Takahashi S, Wada M, Kataoka M, Shimizu S (1999) Synthesis of optically active ethyl 4-chloro-3-hydroxybutanoate by microbial reduction. Appl Microbiol Biotechnol 51:847–851

Yasohara Y, Kizaki N, Hasegawa J, Wada M, Kataoka M, Shimizu S (2000) Molecular cloning and overexpression of the gene encoding an NADPH-dependent carbonyl reductase from *Candida magnoliae*, involve in stereoselective reduction of ethyl 4-chloro-3-oxobutanoate. Biosci Biotechnol Biochem 64:1430–1436

Yasohara Y, Kizaki N, Hasegawa J, Wada M, Kataoka M, Shimizu S (2001) Stereoselective reduction of alkyl 3-oxobutanoate by carbonyl reductase from *Candida magnoliae*. Tetrahedron Asymmetry 12:1713–1718

Yoshizumi A, Wada M, Takagi H, Shimizu S, Nakamori S (2001) Cloning, sequence analysis, and expression in *Escherichia coli* of the gene encoding monovalent cation-activated Levodione reductase from *Corynebacterium aquaticum* M-13. Biosci Biotechnol Biochem 65:830–836

Chapter 9
Fatty Acid Production from Xylose by Xylose-Assimilating Thraustochytrid and Cellular NADPH/NADP$^+$ Balance

Masahiro Hayashi, Ayako Matsuda, and Aya Nagaoka

9.1 Introduction

Biofuel utilization has been developed internationally to prevent global warming (Hoekman et al. 2012; Bahadar and Bilal 2013; Sawangkeaw and Ngamprasertsith 2013; Majidian et al. 2018). However, the use of sugarcane or corn as a raw material for biofuel competes with their use as foodstuff. Therefore, saccharified lignocellulosic plant biomass, which is not used as foodstuff, is expected to be a raw material for biofuel production. Because saccharified lignocellulosic biomass contains hexoses (such as glucose), pentoses (such as xylose), lignin, and pectin, pentoses and hexoses have to be utilized as a carbon source for biofuel (Jeffries et al. 2007; Young et al. 2010; Bideaux et al. 2015; Hohenschuh et al. 2015; Sharma et al. 2018). For the effective utilization of a pentose in saccharified lignocellulosic biomass, genetically modified microorganisms that can produce ethanol or fatty acids from pentoses were developed (Desai and Rao 2009; Ji et al. 2010; Tamakawa et al. 2014; Wasylenko and Stephanopoulos 2015; Gonçalves et al. 2014).

M. Hayashi (✉) · A. Matsuda
Department of Marine Biology and Environmental Sciences, Faculty of Agriculture, University of Miyazaki, Miyazaki, Japan
e-mail: hayash-m@cc.miyazaki-u.ac.jp

A. Nagaoka
Department of Marine Biology and Environmental Sciences, Faculty of Agriculture, University of Miyazaki, Miyazaki, Japan

Present Address: Hayashikane Sangyo Co. Ltd., Shimonoseki, Yamaguchi, Japan

M. Ishii, S. Wakai (eds.), *Electron-Based Bioscience and Biotechnology*,
https://doi.org/10.1007/978-981-15-4763-8_9

9.2 Microbial Production of Fatty Acids by Thraustochytrids as Biofuels

9.2.1 Thraustochytrids

Thraustochytrids are marine unicellular protists distributed in marine and brackish waters worldwide (Kimura and Naganuma 2001; Raghukumar 2002; Honda et al. 1998). They accumulate a remarkable amount of fatty acids, such as docosahexaenoic (DHA) and palmitic acid, in the droplets of cells (Nagano et al. 2009; Gupta et al. 2012; Raghukumar 2008; Ratledge 2004). Moreover they also accumulate carotenoids such as astaxanthin and squalene (Hong 2013; Aasen et al. 2016; Kaya et al. 2014; Nakazawa et al. 2012; Aki 2003). Because thraustochytrids are heterotrophic oleaginous microorganisms, they consume a large amount of carbon in the form of glucose, glycerol, or acetate, for growth and fatty acid synthesis. However, carbon sources much cheaper than glucose are required for the production of biofuels by thraustochytrids (Tajima et al. 2018; Iwasaka et al. 2013; Gupta et al. 2013a; Scott et al. 2011; Song et al. 2015). Although the use of saccharified lignocellulosic plant biomass as a carbon source for microorganisms was investigated recently, this material contains a significant amount of pentose, such as xylose. Because thraustochytrids are not able to assimilate xylose, novel xylose-assimilating thraustochytrids were isolated for the use of saccharified lignocellulosic plant biomass as a carbon source (Merkx-Jacques et al. 2018). In this chapter, isolation of novel xylose-assimilating thraustochytrids, elucidation of their xylose assimilation ability and its enhancement by xylose adaptation of the isolate, and importance of redox balance ($NADPH/NADP^+$) for xylose utilization and fatty acid synthesis by thraustochytrids are addressed.

9.2.2 Isolation and Characterization of Xylose-Assimilating Thraustochytrids

Thraustochytrids were isolated from seawater, sea sand, dead leaves from mangroves, or sea grasses from a coastal area in Japan. After the concentration of thraustochytrid cells using a pine-pollen method, xylose-assimilating thraustochytrids were isolated on agar plates containing xylose as the sole carbon source (Gupta et al. 2013b; Taoka et al. 2008). The isolate mh1912 was selected on the basis of their growth on and consumption of xylose as the sole carbon source in the medium. However, the growth and carbon source consumption of the isolate were much lower than those observed on glucose. A phylogenetic analysis based on the sequences of the 18S rRNA gene showed that the isolate (mh1912) belonged to the genus *Aurantiochytrium* (Honda and Yokoyama 2007; Yokoyama et al. 2007).

9.2.3 *Adaptation of Thraustochytrids to Xylose Assimilation*

To activate the xylose metabolism in cells, the xylose-assimilating thraustochytrids, mh1912 was cultivated in medium containing xylose as the sole carbon source for >3 years (Fig. 9.1). After the adaptation of isolate to xylose, their growth and xylose consumption were greatly increased. The enzymatic activities of xylose isomerase (0.035–0.073 units/mg protein) and xylulokinase (0.050–0.280 units/mg protein) were increased in the cells of adapted mh1912 compared with its non-adapted counterparts. Conversely, xylose reductase activity was not detected in adapted cells, and xylitol dehydrogenase activity was not different between adapted and non-adapted cells. These results suggested that the xylose-assimilating thraustochytrid isolate mh1912 metabolized xylose via the xylose isomerase pathway using xylulose-5-phosphate as a substrate for the pentose phosphate pathway. Moreover, metabolomics analysis of adapted and non-adapted cells of strain mh1912 also showed that xylose metabolism was activated in the former. Xylose and xylulose were not detected in the adapted cells of strain mh1912; in contrast, they accumulated in the non-adapted cells. These results suggested that incorporated xylose in the adapted cells of mh1912 was rapidly metabolized via the pentose phosphate pathway. In the non-adapted cells of mh1912, xylose and xylulose accumulated because of the low xylose metabolism activity.

The non-adapted mh1912 cells contained 18.8% lipids in dry cells. In contrast, this amount increased to 47.6% in the adapted isolate. *Aurantiochytrium* synthesize fatty acids via the fatty acid synthase (FAS) and polyketide synthase-like polyunsaturated fatty acid synthase (PUFA synthase) pathways. It seems that xylose adaptation observed in strain mh1912 afforded citrate as a substrate for both energy metabolism via the TCA cycle and fatty acid synthesis via FAS and PUFA.

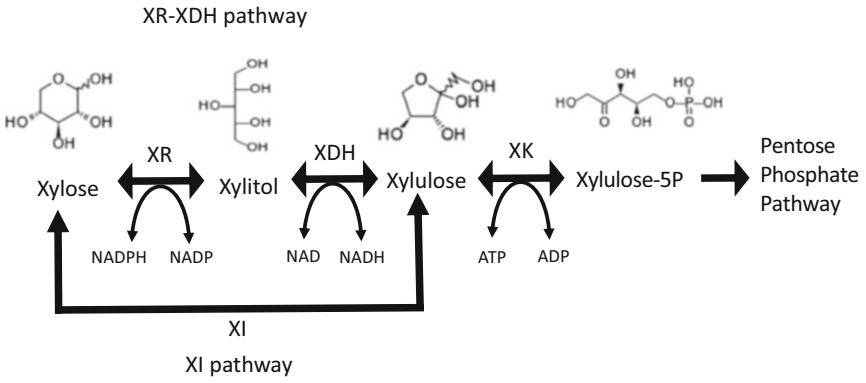

Fig. 9.1 Metabolic pathway of xylose. Although enzymatic activity of XR was not detected in *Aurantiochytrium* sp. mh1912, those of XI and XK were increased by xylose adaptation in the cells. *XR* xylose reductase, *XDH* xylitol dehydrogenase, *XK* xylulokinase, *XI* xylose isomerase

Although NADPH was an essential coenzyme for fatty acid synthesis, metabolomics analysis showed that the level of NADPH was increased in adapted cells compared with non-adapted cells. It was shown that generation cycle of NADPH from $NADP^+$ (pentose phosphate pathway, malic enzymes, isocitrate dehydrogenase, etc.), which was activated by xylose adaptation, richly supplied NADPH for the fatty acid synthesis pathway in the xylose-adapted mh1912 cells. In the non-adapted cells, as NADPH was not generated actively, the NADPH/$NADP^+$ ratio was much lower than that observed in the adapted cells. It was clearly shown that the redox balance in the cells, such as the NADPH/$NADP^+$ ratio, greatly affected fatty acid synthesis in thraustochytrids (Fig. 9.2).

9.2.4 Carbon/Nitrogen Balance Affects Lipid Synthesis in Thraustochytrids

Nitrogen deficiency caused lipid accumulation in the cells of many microalgae and microorganisms (Fei et al. 2006; Kakizono et al. 1992; Piorreck et al. 1984). The xylose-adapted strain mh1912 was also cultivated in medium containing 3% xylose and 1% (C/N ratio = 9.7), 0.5% (C/N ratio = 19.5), and 0.25% (C/N ratio = 38.9) yeast extract as a nitrogen source. The cells cultivated in the medium containing 1% yeast extract exhibited faster growth and xylose consumption. The total cellular lipid content increased as the concentration of nitrogen source in the medium decreased. The total lipid content of the cells grown in the medium containing 1% yeast extract was 47.6%. However, it increased to 72.2% as a result of the decrease (to 0.25%) in the nitrogen source. Moreover, regarding the fatty acid profile of the cells, the decrease in the nitrogen source caused an increase in palmitic acid and a decrease in DHA (Fig. 9.3).

The metabolomics analysis showed that, although xylose or xylulose were not detected in the nitrogen-sufficient cells, these compounds were accumulated in the nitrogen-deficient cells. In contrast, metabolites of the TCA cycle, such as succinate, fumarate, and malate, were enriched in the nitrogen-sufficient cells. These results suggest that the carbon source supply was adequate for energy metabolism and protein synthesis to support the growth of nitrogen-sufficient cells. Moreover, the carbon source accumulated as a storage of energy in nitrogen-deficient cells. In fact, the nitrogen-deficient cells contained high levels of NADPH, which is an essential coenzyme for fatty acid synthesis, and a higher NADPH/$NADP^+$ ratio than the nitrogen-sufficient cells. It was shown that generation cycle of NADPH from $NADP^+$, which was activated by nitrogen deficiency, supplied NADPH at high levels for the fatty acid synthesis pathway in the nitrogen-deficient cells. In the

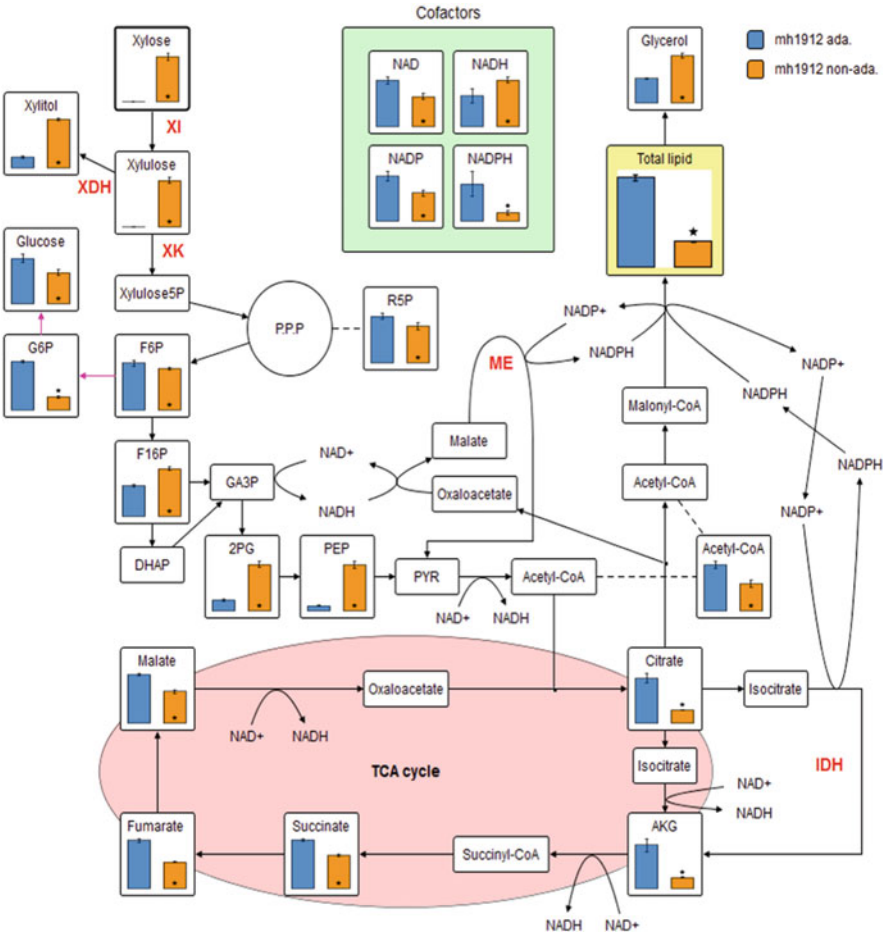

Fig. 9.2 Effects of xylose adaptation on the metabolite contents of xylose-assimilating thraustochytrid. Black bars show the metabolites in xylose-adapted mh1912 cells. White bars show the metabolites in xylose not-adapted mh1912cells. Abbreviations: *Xylulose5P* xylulose-5-phosphate, *G6P* glucose-6-phosphate, *F6P* fructose-6-phosphate, *F16P* fructose-1,6-bisphosphate, *R5P* ribose-5-phosphate, *GA3P* glyceraldehyde-3-phosphate, *DHAP* dihydroxyacetone phosphate, *2PG* 2-phosphoglycerate, *PEP* phosphoenolpyruvate, *PYR* pyruvate, *AKG* α-ketoglutarate, *XR* xylose reductase, *XDH* xylitol dehydrogenase, *XK* xylulokinase, *XI* xylose isomerase

nitrogen-sufficient cells, as NADPH was not actively generated, the NADPH/$NADP^+$ ratio was much lower than that observed in nitrogen-deficient cells. It was clearly shown that redox balance, such as the NADPH/$NADP^+$ ratio, greatly affects fatty acid synthesis in thraustochytrids.

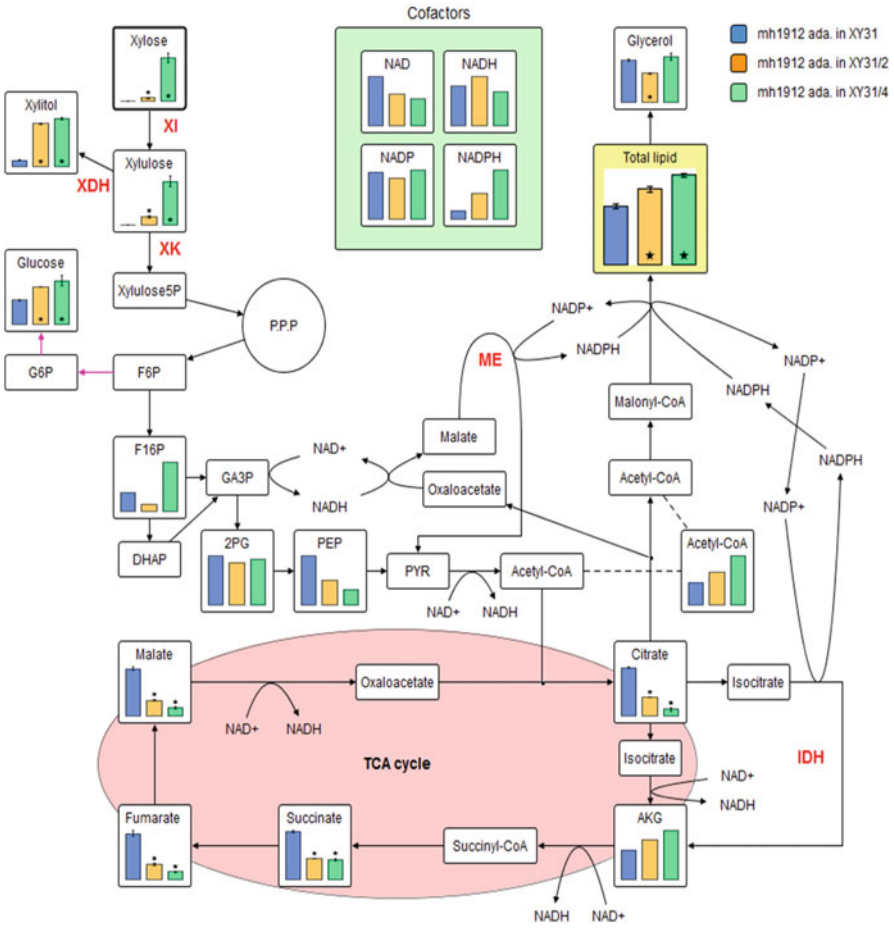

Fig. 9.3 Effects of nitrogen deficiency on the metabolite contents of xylose-assimilating thraustochytrid. Black bars show the metabolites in nitrogen-deficient mh1912 cells. White bars show the metabolites in nitrogen-sufficient mh1912cells. Abbreviations: *Xylulose5P* xylulose-5-phosphate, *G6P* glucose-6-phosphate, *F6P* fructose-6-phosphate, *F16P* fructose-1,6-bisphosphate, *GA3P* glyceraldehyde-3-phosphate, *DHAP* dihydroxyacetone phosphate, *2PG* 2-phosphoglycerate, *PEP* phosphoenolpyruvate, *PYR* pyruvate, *AKG* α-ketoglutarate, *XR* xylose reductase, *XDH* xylitol dehydrogenase, *XK* xylulokinase, *XI* xylose isomerase

References

Aasen IM, Ertesvåg H, Heggeset TMB, Liu B, Brautaset T, Vadstein O et al (2016) Thraustochytrids as production organisms for docosahexaenoic acid (DHA), squalene, and carotenoids. Appl Microbiol Biotechnol 100:4309–4321

Aki T (2003) Thraustochytrid as a potential source of carotenoids. JAOCS 80:789–794

Bahadar A, Bilal KM (2013) Progress in energy from microalgae: a review. Renew Sust Energ Rev 27:128–148

Bideaux C, Montheard J, Cameleyre X, Molina-Jouve C, Alfenore S (2015) Metabolic flux analysis model for optimizing xylose conversion into ethanol by the natural C5-fermenting yeast *Candida shehatae*. Appl Microbiol Biotechnol 100:1489–1499

Desai TA, Rao CV (2009) Regulation of arabinose and xylose metabolism in *Escherichia coli*. Appl Environ Microbiol 76:1524–1532

Fei S, Shaohong W, Xi W, Tianwei T (2006) Effect of nitrogen limitation on the ergosterol production by fed-batch culture of *Saccharomyces cerevisiae*. J Biotechnol 122:285–292

Gonçalves DL, Matsushika A, de Sales BB, Goshima T, Bon EPS, Stambuk BU (2014) Xylose and xylose/glucose co-fermentation by recombinant *Saccharomyces cerevisiae* strains expressing individual hexose transporters. Enzym Microb Technol 63:13–20

Gupta A, Barrow CJ, Puri M (2012) Omega-3 biotechnology: thraustochytrids as a novel source of omega-3 oils. Biotechnol Adv 30:1733–1745

Gupta A, Singh D, Barrow CJ, Puri M (2013a) Exploring potential use of Australian thraustochytrids for the bioconversion of glycerol to omega-3 and carotenoids production. Biochem Eng J 78:11–17

Gupta A, Wilkens S, Adcock JL, Puri M, Barrow CJ (2013b) Pollen baiting facilitates the isolation of marine thraustochytrids with potential in omega-3 and biodiesel production. J Ind Microbiol Biotechnol 40:1231–1240

Hoekman SK, Broch A, Robbins C, Ceniceros E, Natarajan M (2012) Review of biodiesel composition, properties, and specifications. Renew Sust Energ Rev 16:143–169

Hohenschuh W, Hector R, Murthy GS (2015) A dynamic flux balance model and bottleneck identification of glucose, xylose, xylulose co-fermentation in *Saccharomyces cerevisiae*. Bioresour Technol 188:153–160

Honda D, Yokoyama R (2007) Taxonomic rearrangement of the genus *Schizochytrium* sensu lato based on morphology, chemotaxonomic characteristics, and 18S rRNA gene phylogeny (Thraustochytriaceae, Labyrinthulomycetes): emendation for *Schizochytrium* and erection of *Aurantiochytrium* and *Oblongichytrium* gen. nov. Mycoscience 48:199–211

Honda D, Yokochi Y, Nakahara T, Erata M, Higashihara T (1998) *Schizochytrium limacinum* sp. nor., a new thraustochytrid from a mangrove area in the west Pacific Ocean. Mycol Res 102:439–448

Hong W-K (2013) Characterization of a squalene synthase from the thraustochytrid microalga *Aurantiochytrium* sp. KRS101. J Microbiol Biotechnol 23:759–765

Iwasaka H, Aki T, Adachi H, Watanabe K, Kawamoto S, Ono K (2013) Utilization of waste syrup for production of polyunsaturated fatty acids and xanthophylls by *Aurantiochytrium*. J Oleo Sci 62:729–736

Jeffries TW, Grigoriev IV, Grimwood J, Laplaza JM, Aerts A, Salamov A et al (2007) Genome sequence of the lignocellulose-bioconverting and xylose-fermenting yeast *Pichia stipitis*. Nat Biotechnol 25:319–326

Ji X-J, Nie Z-K, Huang H, Ren L-J, Peng C, Ouyang P-K (2010) Elimination of carbon catabolite repression in *Klebsiella oxytoca* for efficient 2, 3-butanediol production from glucose–xylose mixtures. Appl Microbiol Biotechnol 89:1119–1125

Kakizono T, Kobayashi M, Nagai S (1992) Effect of carbon/nitrogen ratio on encystment accompanied with astaxanthin formation in a green alga, *Haematococcus pluvialis*. J Ferm Bioeng 74:403–405

Kaya K, Nakazawa A, Matsuura H, Honda D, Inouye I, Watanabe MM (2014) Thraustochytrid *Aurantiochytrium* sp. 18W-13a accumulates high amounts of squalene. Biosci Biotechnol Biochem 75:2246–2248

Kimura H, Naganuma T (2001) Thraustochytrids: a neglected agent of the marine microbial food chain. Aquat Ecosyst Health Manag 4:13–18

Majidian P, Tabatabaei M, Zeinolabedini M, Naghshbandi MP, Chisti Y (2018) Metabolic engineering of microorganisms for biofuel production. Renew Sust Energ Rev 82:3863–3885

Merkx-Jacques A, Rasmussen H, Muise DM, Benjamin JJR, Kottwitz H, Tanner K et al (2018) Engineering xylose metabolism in thraustochytrid T18. Biotechnol Biofuels 11:248–265

Nagano N, Taoka Y, Honda D, Hayashi M (2009) Optimization of culture conditions for growth and docosahexaenoic acid production by a marine thraustochytrid, *Aurantiochytrium limacinum* mh0186. J Oleo Sci 58:623–628

Nakazawa A, Matsuura H, Kose R, Kato S, Honda D, Inouye I et al (2012) Optimization of culture conditions of the thraustochytrid *Aurantiochytrium* sp. strain 18W-13a for squalene production. Bioresour Technol 109:287–291

Piorreck M, Baasch K-H, Pohl P (1984) Biomass production, total protein, chlorophylls, lipids and fatty acids of freshwater green and blue-green algae under different nitrogen regimes. Phytochemistry 23:207–216

Raghukumar S (2002) Ecology of the marine protists, the Labyrinthulomycetes (Thraustochytrids and Labyrintulids). Eur J Protistol 38:127–145

Raghukumar S (2008) Thraustochytrid marine protists: production of PUFAs and other emerging technologies. Mar Biotechnol 10:631–640

Ratledge C (2004) Fatty acid biosynthesis in microorganisms being used for single cell oil production. Biochimie 86:807–815

Sawangkeaw R, Ngamprasertsith S (2013) A review of lipid-based biomasses as feedstocks for biofuels production. Renew Sust Energ Rev 25:97–108

Scott SD, Armenta RE, Berryman KT, Norman AW (2011) Use of raw glycerol to produce oil rich in polyunsaturated fatty acids by a thraustochytrid. Enzym Microb Technol 48:267–272

Sharma NK, Behera S, Arora R, Kumar S, Sani RK (2018) Xylose transport in yeast for lignocellulosic ethanol production: current status. J Biosci Bioeng 125:259–267

Song X, Zang X, Zhang X (2015) Production of high docosahexaenoic acid by *Schizochytrium* sp. using low-cost raw materials from food industry. J Oleo Sci 64:197–204

Tajima T, Tomita K, Miyahara H, Watanabe K, Aki T, Okamura Y et al (2018) Efficient conversion of mannitol derived from brown seaweed to fructose for fermentation with a thraustochytrid. J Biosci Bioeng 125:180–184

Tamakawa H, Tomita Y, Yokoyama A, Konoeda Y, Ikushima S, Yoshida S (2014) Metabolomic and transcriptomic analysis for rate-limiting metabolic steps in xylose utilization by recombinant *Candida utilis*. Biosci Biotechnol Biochem 77:1441–1448

Taoka Y, Nagano N, Okita Y, Izumida H, Sugimoto S, Hayashi M (2008) Effect of addition of Tween 80 and potassium dihydrogenphosphate to basal medium on the isolation of marine eukaryotes, thraustochytrids. J Biosci Bioeng 105:562–565

Wasylenko TM, Stephanopoulos G (2015) Metabolomic and ^{13}C-metabolic flux analysis of a xylose-consuming *Saccharomyces cerevisiae* strain expressing xylose isomerase. Biotechnol Bioeng 112:470–483

Yokoyama R, Salleh B, Honda D (2007) Taxonomic rearrangement of the genus *Ulkenia* sensu lato based on morphology, chemotaxonomical characteristics, and 18S rRNA gene phylogeny (Thraustochytriaceae, Labyrinthulomycetes): emendation for *Ulkenia* and erection of *Botryochytrium*, *Parietichytrium*, and *Sicyoidochytrium* gen. nov. Mycoscience 48:329–341

Young E, Lee S-M, Alper H (2010) Optimizing pentose utilization in yeast: the need for novel tools and approaches. Biotechnol Biofuels 3:24

Chapter 10
Control of Microbial Metabolism by Electrochemical Cultivation Method

Shin-ichi Hirano

10.1 Introduction

Microbial metabolism, involving energy gain processes such as respiration, fermentation, and photosynthesis, is based on electron flow from an electron donor to an acceptor, including a lot of oxidation/reduction reactions. From this viewpoint, microbial processes resemble an electric circuit producing energy from electron flow between the anode and cathode (Fig. 10.1). Although various microbial metabolic pathways have been used for industrial chemical production, the yield and selectivity of products are limited by the metabolic limitation of balanced redox reactions. Since an imbalance between oxidation and reduction reactions would stop cell growth and metabolism, microbes often concomitantly produce energy-rich products (hydrogen, methane, ethanol, and butanol) to balance the redox reactions in a cell. Therefore, manipulation of electron flow in redox reactions during microbial metabolism and redox balance can control microbial metabolic processes, overcoming the limitations by balancing the reactions.

In the recent few decades, considering global warming and energy security, microbial technologies are being promoted for producing commodity chemicals and fuels from biomass to diverge from the existing fossil resource-dependent strategies. In order to establish this technology, increased efficiency of microbial metabolism in the production process has become an important research goal. Parameters affecting the efficiency of microbial processes, such as chemical component of medium, pH, temperature, oxidation/reduction potential (ORP), oxygen supply, and hydraulic retention time, in the continuous system have been investigated. However, controlled microbial metabolism for producing a targeted product still remains challenging. Recently, attention has been focused on

S.-i. Hirano (✉)
Central Research Institute of Electric Power Industry, Abiko, Chiba, Japan
e-mail: s-hirano@criepi.denken.or.jp

M. Ishii, S. Wakai (eds.), *Electron-Based Bioscience and Biotechnology*,
https://doi.org/10.1007/978-981-15-4763-8_10

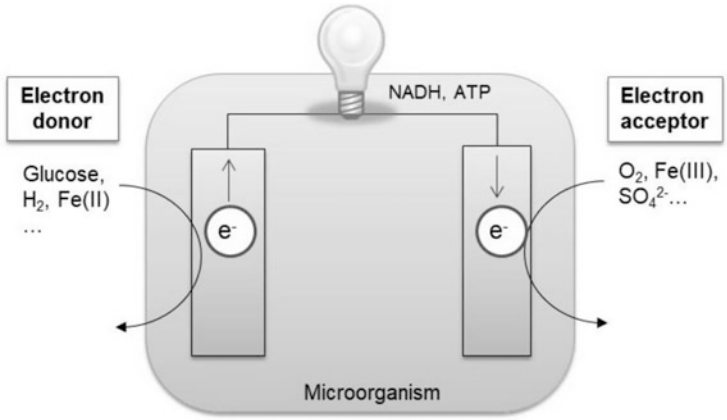

Fig. 10.1 Microbial life is based on electron flow from an electron donor to an acceptor

bioelectrochemical systems (BES) to electrochemically control the redox reactions in microbial metabolism by utilizing the interaction between a microbial cell and electrochemically regulated electrode (Harnisch and Schröder 2010; Wang and Ren 2013). As described in Chap. 5 by Matsumoto, we have constructed a BES to promote microbial growth of several metal-respiring bacteria, such as iron-oxidizing bacteria (*Acidithiobacillus*), by electrochemical reproduction of oxidized/reduced metal ions and continuous supply of metal ions as electron donor/acceptor. Furthermore, we have expanded the application of BES to microbial material-producing processes, such as fermentation, by a single pure culture and mixed consortium, and thereby increase the efficiency of production of a specifically targeted chemical based on the control of microbial metabolism. In this chapter, we will outline the metabolic control of microbial reactions using BES, with the help of a few recent examples.

10.2 Concept and Basics of BES Application in Microbial Processes

The electrochemical cultivation method is performed using a bioelectrochemical reactor (BER) composed of two culture vessels separated by an ion-exchange membrane and a three-electrode system including an anode, a reference electrode, and a cathode, as shown in Chap. 5. This BES apparatus may also be used to control the metabolism of microorganisms. Control of microbial metabolism by BES can be roughly divided into two concepts: (1) A culture method based on electron transfer between an electrode with reduction potential and a microorganism (Fig. 10.2a, b). In this concept, the electrode supplies electrons to the microorganism as a reducing equivalent or extracts electrons from the microorganism as an electron acceptor.

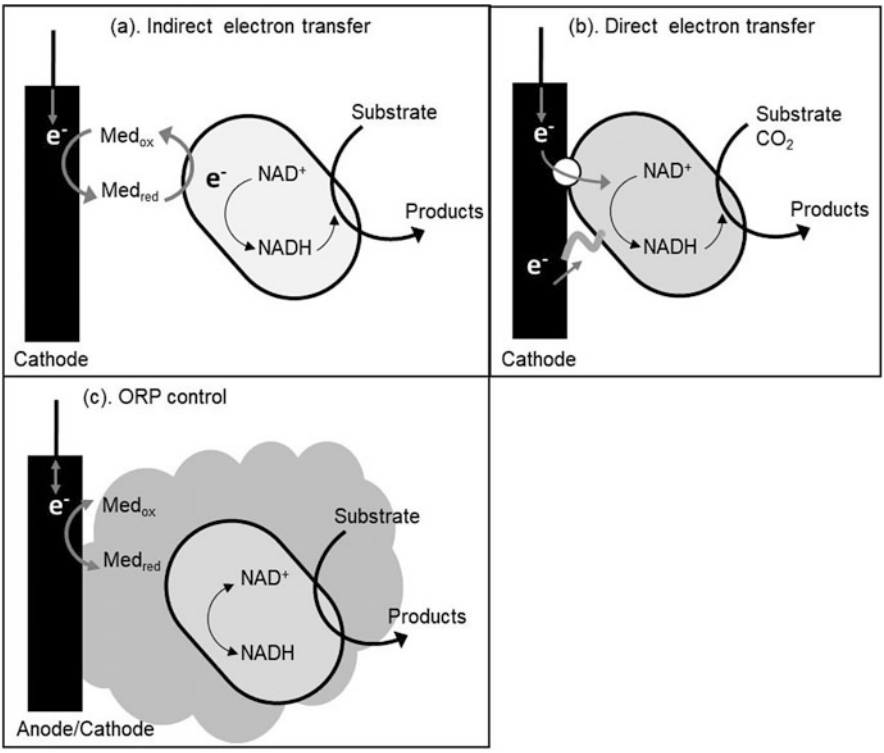

Fig. 10.2 Concept of control of metabolism by BES. (**a**, **b**) Supply of electrons from electrode to microbial cells; only electroactive microbes with electroactive enzymes or nanowires can directly gain electron from electrode. (**c**) Regulation of ORP by controlling the balance of redox pair of the electron mediator on the electrode

Only specific microbes (a part of acetogens, methanogen, iron-reducing bacteria, and sulfate-reducing bacteria) have the ability to interact with the electrode using membrane-bound redox proteins (Gregory et al. 2004; Cheng et al. 2009; Nevin et al. 2011). Thus, for the application of BES to most microbes, artificial soluble redox-active molecules (anthraquinones, neutral red, methylene blue, methylviologen, etc.), as electron mediators, are added to the cultivation medium to support electron transfer between the microbe and electrode. (2) An electrochemical culture method using electrodes for regulating the oxidation/reduction potential (ORP) of medium for suitable conditions of the targeted microorganism (Fig. 10.2c). Extracellular ORP is known to be an important parameter controlling microbial metabolism. Extracellular ORP has been suggested to affect the intracellular ORP through NADH/NAD^+ balance (Liu et al. 2013). ORP, in a certain environment, is determined by the ratio of oxidant to reductant of all redox substances contained in the environment. Although improvement of yield by chemical control of ORP via the added oxidizing or reducing agents has been known (Du et al. 2006; Li et al. 2010; Zhu et al. 2014), retention of a constant ORP by chemical oxidant/reductant is

difficult, since the consumption of substrate and production of metabolite might cause the ORP to fluctuate in the medium during cultivation. Therefore, BES could be a feasible way to regulate ORP for controlling microbial metabolism.

A method of supplying or extracting electrons by the electrode from microbial cells is expected to control microbial metabolism and improve the productivity of a specific metabolite by overcoming the balanced redox pair in the microbial process, such as fermentation, thereby producing biochemicals or biofuels. Application of BES in fermentation has been designated as electro-fermentation (EF) (Schievano et al. 2016). When CO_2 is used as a substrate, instead of an organic substrate, the supplied electrons are used for CO_2 reduction and conversion via microbial metabolism. This process is designated as microbial electrosynthesis (MES) and has attracted much attention recently considering it to possibly be a sustainable carbon-free material production method using electricity from natural energy, such as solar power and wind power. In both EF and MES, electron supply and electrochemical ORP regulation are used to optimize the redox balance in microbial metabolism and increase the production of target products. Technologies related to the above two concepts of BES are separately summarized hereafter, using examples of both EF and MES.

10.3 Application of BES in Controlling Microbial Metabolism

10.3.1 Metabolic Control by Electron Supply from Cathode to Microbial Cells

Electron transfer reactions between electrodes and microorganisms have a long history in the field of MFC research, and many studies have been conducted on the extracellular electron transfer mechanism of microorganisms (Logan 2009). Moreover, microorganisms capable of extracellular electron transfer, using extracellular electron mediators (methylviologen, neutral red, etc.) have already been reported previously. MFC-related studies aim to generate larger electric currents by capturing electrons from organic substances and delivering them to the electrode via microorganisms capable of extracellular electron transfer. In recent years, however, by focusing on the redox abilities of such microorganisms, it has been proposed to control their metabolism by supplying electrons to the cells from the electrodes (Rabaey and Rozendal 2010). Intracellular metabolism is closely associated with oxidation and reduction. Fermentation requires the production of by-products for recycling the electronic carriers such as NADH and NADPH in order to continue metabolism. In respiration, the supply of electron acceptors is essential. By supplying the reducing power (electron donor and electron itself) or oxidative power (electron acceptor) required by microorganisms from outside, fermentation and respiration processes may be controlled and product yield increased. Examples of

application of BES in fermentation or respiration for the production of biochemicals/biofuels, including our current ones, have already been reported. Some representative examples are presented in this chapter.

10.3.1.1 Enhancement of Butanol Production by *Clostridium acetobutylicum* by Supplying Electrons to BER

Butanol produced from biomass through acetone-butanol-ethanol (ABE) fermentation by solventogenic clostridial strains has attracted much attention as a biofuel. However, industrial production of bio-based butanol is still limited due to low yield of butanol. Moreover, acetate, butyrate, acetone, and ethanol are simultaneously produced with butanol in ABE fermentation. In the metabolic pathways of ABE fermentation, NADH generated by glycolysis is essential as a reducing equivalent for the production of ethanol and butanol. Therefore, increasing the availability of NADH can enhance the production of butanol. Electron mediator, such as methylviologen (MV), is used to alter metabolite patterns in ABE fermentation. It has been reported to enhance butanol yield by 9.4% and reduce acetone and hydrogen production (Rao and Mutharasan 1986). It is considered to interact and transfer electrons during metabolic reactions in *C. acetobutylicum* and change the $NADH/NAD^+$ level and metabolic flux for butanol production. Therefore, metabolic control and electron flow have become an important research topic for efficient butanol production. To further increase butanol production, BES has been applied to the butanol production of *Clostridium* strain by supplying electrons from the cathode to cells, via electron mediator for increasing the available NADH. Kim and Kim reported a 26% increase in product yield and simultaneous reduction of by-product concentrations with the cultivation of *Clostridium acetobutylicum* in BER (Kim and Kim 1988). We also attempted to apply BES for the incubation of *Clostridium acetobutylicum* cells at a stationary phase, since *C. acetobutylicum* switches its metabolism from acid-producing to solvent-producing in the stationary phase (Hirano et al. 2012). *C. acetobutylicum* cells were filled in BER with a three-electrode potentiostat system and MV as an electron mediator. First, a constant reduction potential was applied to the working electrode at −0.7 V (Ag/AgCl) during cultivation; however, constant electrolysis at −0.7 V inhibited glucose consumption. By decreasing electrolysis time for 10 min and three times during 72-h incubation, the inhibition of glucose consumption could be avoided and a threefold increase of butanol production established (Fig. 10.3). To understand the changes in metabolic flow due to electron supply, we compared the metabolome between cultivated cells in BER and that without electrolysis. In BER at −0.7 V, NADH in a cell was largely increased and so were other metabolites (butanol, ethanol, and lactate) consuming NADH for their production. In the BER experiment, 0.18 mmol electrons (calculated from electric current during electrolysis) were supplied. If all these electrons got engaged in NAD reduction and butanol production, a maximum of 0.09 mmol of butanol would be electrochemically generated (butyryl-CoA + 2NADH = butanol + $2NAD^+$). However, we obtained much more

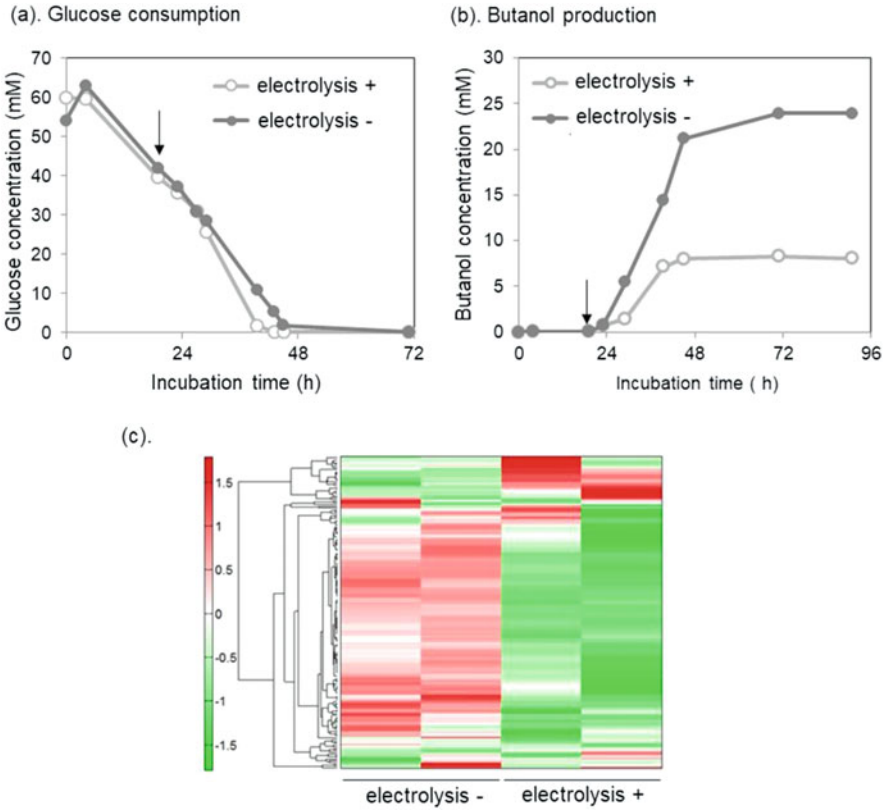

Fig. 10.3 Effect of cathodic electron supply to *Clostridium acetobutylicum* on butanol production. (**a**, **b**) Cathodic potential (−0.8 V) was applied on the working electrode in BER with *C. acetobutylicum* at the time indicated by arrow (in the figures) for 10 min. Glucose consumption and butanol production were compared between culture sample with electrolysis in BER (*closed circle*) and control without electrolysis (*open circle*). (**c**) Metabolomic profiles in cells with and without electrolysis during cultivation by CE-TOFMS; 179 metabolites were detected. Metabolites with levels higher than the average are shown in shades of red and those with lower levels are shown in shades of green

amount of butanol (about 30 times) in BER compared to that generated electrochemically. Clearly, the NADH generated by electron supply from the working electrode alone cannot account for the high butanol production in BER. In contrast, since accumulation of acetate, hydrogen, and anabolic components (such as amino acids and nucleotides) were decreased at −0.7 V in BER, the low electron supply was considered to induce a change of metabolic flow by suppressing by-product formation and anabolic processes related to cell construction and activating solvent production using carbon and NADH required in anabolism. NADH/NAD^+ redox responsive repressor (Rex) for solventogenic shift has already been reported in *Clostridium* (Wietzke and Bahl 2012); unbalanced NADH/NAD^+ resulting from

low electron supply might promote butanol production through Rex regulatory system. To estimate the effectiveness of BES in butanol production by *C. acetobutylicum*, energy efficiency was calculated. Combustion energy of butanol, increased by electrolysis ($W_{butanol}$), was compared to the electrical energy calculated from electric current and voltage during electrolysis (W_{in}). $W_{butanol}/W_{input}$ was determined as 71 in this experiment, the value indicating a small electrical input to induce a much larger energy production in BER. This study proved that electron supply from an electrode to microbial cells in BES can modify the metabolic flow in the fermentative microbe and increase the yield of a target product.

10.3.2 Improvement of Methane Fermentation Process by ORP Control in BER

ORP is an important parameter for controlling microbial processes (both growth and metabolism). BES can maintain ORP of a medium at a constant value by electrochemically oxidizing or reducing electron mediators (electroactive substances) included in the medium. Therefore, an electron mediator and electric current are required to adjust the extracellular ORP. Electrochemical regulation of ORP is important not only to avoid the addition of strong oxidizing and reducing agents that may be potentially cytotoxic but also to maintain higher- or lower-redox potential environments that are difficult to set otherwise with the addition of oxidizing and reducing agents. There are reports about the metabolic control of microbial consortium, as well as of single pure culture, by electrochemical ORP regulation. The current section introduces the application of BES in the regulation of ORP and control of metabolic activity of microbial consortium, including different types of syntrophic microbes.

Anaerobic digestion is an important microbial process from the perspective of both organic waste treatment and energy production. The anaerobic digestion process is composed of mainly three steps: hydrolysis of substrate, degradation of hydrolysis products to H_2/CO_2 or acetate, and generation of methane from H_2/CO_2 or acetate by methanogens (Fig. 10.4).

Our group aimed to efficiently recover methane from organic wastes by controlling the microbial community involved in anaerobic digestion in BER (Sasaki et al. 2010). BER has a carbon electrode for controlling the ORP by oxidizing or reducing anthraquinone 2,6-disulfonate (electron mediator) in medium (Fig. 10.5a). The anaerobic digestion in BER was continuously operated at 55 °C using dog food slurry (DFS) as an artificial garbage substrate. ORP of the medium was −0.47 V in BER without electrolysis (non-BER). Applied potentials of −0.6 V or less in BER enabled the stable processing of organic substances and generation of methane at three times higher organic loading rate (31.8 gCODcr/L/day) than in a conventional reactor or non-BER (Fig. 10.5b). In BER, at −0.6 V, only small electric currents (approximately 200 μA) flow during the experiment, having no relation with the

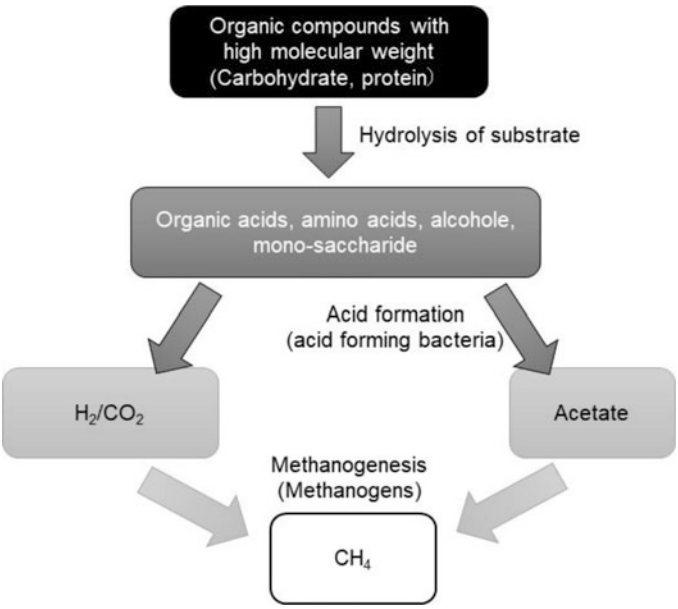

Fig. 10.4 Anaerobic digestion process includes three major reactions: hydrolysis, acid formation, and methanogenesis. Each reaction step is dependent on different microbial groups

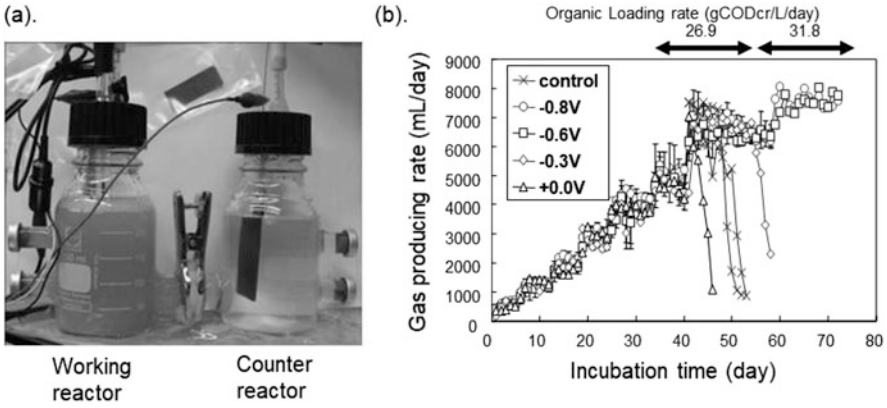

Fig. 10.5 Application of BES to anaerobic digestion process of artificial garbage sludge. (**a**) H-type BER. The working reactor, with a working electrode and reference electrode, is separated from the counter reactor, with a counter electrode, by an ion-exchange membrane. Microbial consortium and substrate for anaerobic digestion are incubated in the working reactor. (**b**) Four different redox potentials (+0, −0.3, −0.6, −0.8 V) were applied to the working electrode, and cultivation performed with semi-batch style, increasing the organic loading rate (OLR). Control experiment without electrolysis was performed similarly

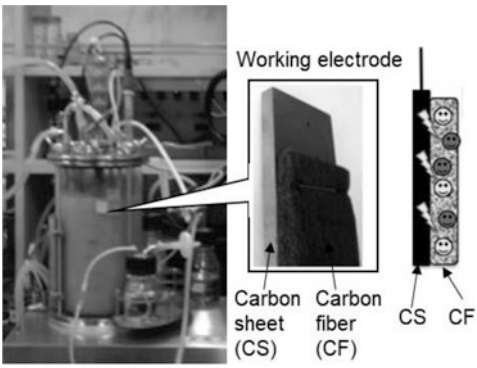

Fig. 10.6 Scale-up of BER for anaerobic digestion in 4-L reactor. To sustain electroactive microbes near the working electrode, a conductive carbon fiber textile was attached to the working electrode (*carbon sheet*)

organic loading rate. Therefore, electric currents detected in BER were considered to be used for maintaining the redox potential, and not for supplying electrons as reducing equivalents for microbes. Microbial community analysis revealed a much higher abundance of the hydrogenotrophic methanogen *Methanothermobacter thermautotrophicus* and acetoclastic methanogen *Methanoculleus thermophilicus* presented on the working electrode at −0.6 and −0.8 V than in non-BER or at another anodic potential. Maintaining redox potential of −0.6 V or less around a carbon electrode was indicated to activate methanogens contributing to methane formation and stabilize the whole process at a high organic loading rate. The increased production of methane (106 kJ/L/day at 19.6 gCODcr/L/day (OLR), 161 kJ/L/day at 31.8 gCODcr/L/day (OLR)) with respect to the input energy as electric current (87 J/L/day in BER at −0.8 V) was sufficiently large in terms of combustion energy, thus indicating it as an energetically effective process.

To extend the application of BES to industrial anaerobic digestion, the latter was investigated in BER using substrates like sewage sludge and agricultural cellulosic waste and similarly applied cathodic potential stabilized process and increased methane production (Sasaki et al. 2013; Hirano and Matsumoto 2018). Moreover, a scale-up of anaerobic digestion in BER with 4 L volume (Fig. 10.6) was constructed, and the effect of ORP regulation on methane fermentation at high OLR was verified. Further studies on reactor design (electrodes, ion-exchange membrane, etc.) would still be required for scale-up and application of BES in anaerobic digestion for industrial purposes.

In order to understand the mechanism of improvement of methane fermentation by ORP control in BER, influence of different potentials on the hydrogenotrophic methanogen *Methanothermobacter thermautotrophicus*, which predominated in BER with DFS, was investigated using BER without the addition of any oxidizing or reducing agent (Hirano et al. 2013). Experiments with BES revealed methane production and *M. thermautotrophicus* growth to be increased 1.6- and 3.5-times at −0.8 V, compared to that in the control experiment without electrolysis or at anodic potential, respectively. As described above, growth and activity of methanogen can be controlled by regulating the ORP of the medium, resulting in stabilization of the anaerobic digestion process at high OLR.

10.4 Conversion of CO_2 into C1 or Long-Chain Chemicals due to Electron Supply to Autotrophs

Since CO_2 emitted from industrial activities is considered to be a factor (a greenhouse gas) causing climate change, its reduction is an important issue. Therefore, the development of a CO_2 conversion technology for producing value-added chemicals has attracted considerable attention recently. Reduction capacity is essential for the useful conversion of CO_2 into some chemical. There has been a growing interest in developing non-photosynthetic routes for the conversion of CO_2 to fuels and chemicals, since efficiency of a photosynthetic process is low (Prévoteau et al. 2019). CO_2 conversion by supply of electricity as a reducing agent, derived from recent renewable energies such as solar power or wind power, has the potential to replace a production process derived from fossil resources. In contrast to photosynthesis using sunlight, these processes are designated as microbial electrosynthesis.

10.4.1 Direct Electron Supply to Methanogens and Acetogens

In electrosynthesis, electrons are directly supplied to microorganisms via the electrode, although the electrode is not a natural electron donor for the microorganisms. Therefore, this technique is not applicable to all microorganisms, and its applicability has been proven in groups of hydrogen-assimilating microorganisms, namely, methanogens and acetogens, till date. Direct electron supply to microbes and conversion of CO_2 were first reported in the methanogen *Methanobacterium palustre*. *M. palustre* formed biofilm on a working electrode poised at a reductive potential and showed methane-producing activity from CO_2 proportional to that obtained with electric current. Since *M. palustre* can use electric current for methane production instead of H_2, the process was named as electromethanogenesis (Cheng et al. 2009). Subsequently, Nevin et al. reported the current-dependent synthesis of organic acids (acetic acid, 2-oxobutyric acid, and formic acid) in the acetogen *Sporomusa ovata* on the cathode poised at -0.4 V in the absence of hydrogen (Nevin et al. 2010). Analysis of metabolites in the culture confirmed the stable production of acetate and oxobutyrate, which correlated with electric current during the experiment. The ratio of electrons converted to organic acids to the total input electrons was as high as $86 \pm 21\%$ at the maximum. Combining the electrochemical and microbial reactions, CO_2 content may be reduced by applying a much lower potential compared to that in the direct electroreduction of CO_2. Electrochemical production of acetate by *S. ovata* has also been reported for several other acetogens (Nevin et al. 2011). Furthermore, microbial conversion of CO_2 to long-chain organic compounds using electricity had already been suggested (Rabaey and Rozendal 2010; Batlle-Vilanova et al. 2017).

10.4.2 Electron Supply to Iron-Oxidizing Bacteria via Iron Ion

Another approach for CO_2 conversion by electrolysis is to transfer an electron to the metabolic process of genetically modified iron-oxidizing bacteria *Acidithiobacillus ferrooxidans*. *A. ferrooxidans* derives its metabolic energy from the oxidation of Fe^{2+} and fixes CO_2. The Fe^{3+} ions generated by *A. ferrooxidans* metabolism can be reduced to Fe^{2+} by electrochemical reaction on the cathode of BER. The Fe^{3+}/Fe^{2+} couple acts as an electron mediator from the electrode to *A. ferrooxidans* cells. Indeed, Matsumoto et al. had reported electron supply from the electrode through Fe redox couple to promote the growth of *A. ferrooxidans* (Matsumoto et al. 1999). Kerman et al. had developed isobutyric acid (IBA)-producing *A. ferrooxidans*, genetically modified with heterologous 2-keto decarboxylase from *Lactococcus lactis* (Kernan et al. 2016). By supplying electrons to the genetically modified *A. ferrooxidans* via Fe^{2+}/Fe^{3+} couple in a continuous culture system, IBA was produced at 0.063 mg/L/h and efficiency in terms of Gibbs free energy was 0.33% (Guan et al. 2017).

In direct electron-supplying approaches, scale-up of the processes may be difficult, since the reaction area remains limited to only the electrode surface. Therefore, indirect approaches with soluble redox mediators may be preferred for electron supply to microbes in large-scale reactors. However, indirect approaches described in this chapter showed low productivity, and thus considerable effort regarding reactor configuration and metabolic engineering to increase productivity will be essential in future.

10.4.3 Combination of Electrochemical CO_2 Reduction and Microbial Process

Electron supply to autotrophs, directly or via electron mediator, is a novel approach for microbial CO_2 conversion, as described above. Another approach of electron supply for microbial CO_2 conversion has been developed, in which electrons are used for CO_2 reduction on the cathode and for production of formate. Although electrochemical reduction of CO_2 is thermodynamically possible and has a history of more than 100 years of research (Taheri et al. 2015), the product is limited to the C1 compound (carbon monoxide, formate). Combination of electrochemical CO_2 reduction and microbial process has been investigated for the production of long-chain carbon chemicals. Li et al. had reported a technique for converting CO_2 into higher alcohol (isobutanol) by the recombinant *Ralstonia eutropha* H16, which can grow from electrochemically produced formate (Li et al. 2012). While this report provided a clear proof of concept, its further application is limited due to inadequate genetic tools for metabolic engineering in *R. eutropha*. Therefore, our group employed a reductive glycine pathway (RGP) in the common industrial microbe *Escherichia coli* (Tashiro et al. 2018). RGP is the most efficient route for formate assimilation.

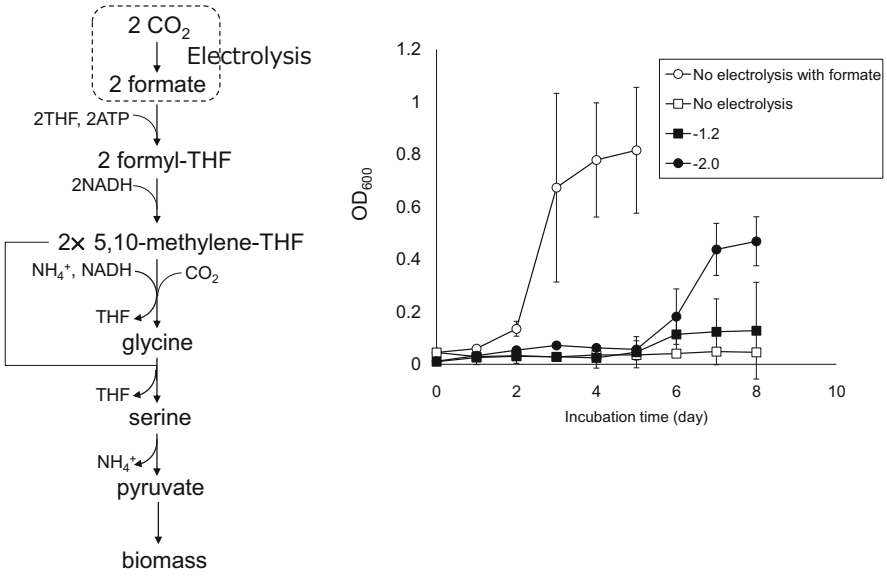

Fig. 10.7 Combination of electrochemical CO_2 reduction and microbial reaction. (**a**) CO_2 is first reduced to formate on cathodic electrode. Then, formate is assimilated through RGP in gene modified *E. coli*. (**b**) The RGP strain was cultivated in BER (250 mL volume) with the potential of the working electrode at −2.0 V (closed circle), −1.2 V (closed square). No electrolysis with formate (open circle), or without formate (open square) were performed as controls

It requires one CO_2, two formate, three NAD(P)H, and two ATP molecules for one molecule of pyruvate in central metabolism (Fig. 10.7a), whereas the CB cycle requires five NADPH and seven ATP molecules for one molecule of pyruvate. Although wild-type *E. coli* is heterotrophic, recombinant *E. coli* can use CO_2 and electricity in BER equipped with indium sheet as a working electrode (Fig. 10.7b). This system has incredible potential for biochemical production, since various biosynthetic pathways have been constructed in *E. coli* to produce valuable chemicals from central metabolites. However, further investigation would still be required to replace the chemical production based on fossil sources, since formate generation (10 mM/day) and cell growth ($OD_{660} = 0.47$ for 8 days) are low owing to possible growth inhibition by the electrochemical formation of reactive oxygen species (e.g., H_2O_2).

10.5 Conclusion

Till date, metabolic engineering by genetic recombination (addition or deletion of genes for metabolic pathways) has produced many microorganisms useful in improving bioprocesses. However, genetic recombination may not always provide

the desired effect due to restriction of redox balance. Therefore, metabolic control by BES, described in this chapter, could be useful for improving and expanding the application of various microbial processes in biofuel and biochemical production, treatment of wastes, and CO_2 conversion. Using the electricity obtained from natural energy sources (solar and wind energies), EF and MES may become CO_2-free or CO_2-negative chemical producing processes, replacing those based on fossil resources. BES is gaining increasing attention for this future prospect. Most of the studies in this field are still in a proof-of-concept stage, and there are many problems and challenges regarding productivity, conversion rate, electron yield, and scale-up. This field is expected to develop with multifaceted and integrated approaches including electrochemistry, microbiology, and material engineering.

References

Batlle-Vilanova P et al (2017) Microbial electrosynthesis of butyrate from carbon dioxide: production and extraction. Bioelectrochemistry 117:57–64

Cheng S, Xing D, Call DF, Logan BE (2009) Direct biological conversion of electrical current into methane by electromethanogenesis. Environ Sci Technol 43(10):3953–3958

Du C et al (2006) Use of oxidoreduction potential as an indicator to regulate 1,3-propanediol fermentation by *Klebsiella pneumoniae*. Appl Microbiol Biotechnol 69(5):554–563

Gregory KB, Bond DR, Lovley DR (2004) Graphite electrodes as electron donors for anaerobic respiration. Environ Microbiol 6(6):596–604

Guan J et al (2017) Development of reactor configurations for an electrofuels platform utilizing genetically modified iron oxidizing bacteria for the reduction of CO_2 to biochemicals. J Biotechnol 245:21–27

Harnisch F, Schröder U (2010) From MFC to MXC: chemical and biological cathodes and their potential for microbial bioelectrochemical systems. Chem Soc Rev 39(11):4433–4448

Hirano SI, Matsumoto N (2018) Analysis of a bio-electrochemical reactor containing carbon fiber textiles for the anaerobic digestion of tomato plant residues. Bioresour Technol 249:809–817

Hirano S, Matsumoto N, Ohmura N (2012) Development of novel biorefining technology with electrolysis (part III)—enhancement of butanol production by supply of reducing power. CRIEPI report V11047

Hirano S et al (2013) Electrochemical control of redox potential affects methanogenesis of the hydrogenotrophic methanogen *Methanothermobacter thermautotrophicus*. Lett Appl Microbiol 56(5):315–321

Kernan T et al (2016) Engineering the iron-oxidizing chemolithoautotroph *Acidithiobacillus ferrooxidans* for biochemical production. Biotechnol Bioeng 113(1):189–197

Kim TS, Kim BH (1988) Electron flow shift in *Clostridium acetobutylicum* fermentation by electrochemically introduced reducing equivalent. Biotechnol Lett 10:123–128

Li J et al (2010) Effect of redox potential regulation on succinic acid production by *Actinobacillus succinogenes*. Bioprocess Biosyst Eng 33(8):911–920

Li H et al (2012) Integrated electromicrobial conversion of CO_2 to higher alcohols. Science 335 (6076):1596

Liu CG, Xue C, Lin YH, Bai FW (2013) Redox potential control and applications in microaerobic and anaerobic fermentations. Biotechnol Adv 31(2):257–265

Logan BE (2009) Exoelectrogenic bacteria that power microbial fuel cells. Nat Rev Microbiol 7 (5):375–381

Matsumoto N, Nakasono S, Ohmura N, Saiki H (1999) Extension of logarithmic growth of *Thiobacillus ferrooxidans* by potential controlled electrochemical reduction of Fe(III). Biotechnol Bioeng 64(6):716–721

Nevin KP, Woodard TL, Franks AE, Summers ZM, Lovley DR (2010) Microbial electrosynthesis: feeding microbes electricity to convert carbon dioxide and water to multicarbon extracellular organic compounds. mBio 1(2):e00103-10

Nevin KP et al (2011) Electrosynthesis of organic compounds from carbon dioxide is catalyzed by a diversity of acetogenic microorganisms. Appl Environ Microbiol 77(9):2882–2886

Prévoteau A, Carvajal-Arroyo JM, Ganigué R, Rabaey K (2019) Microbial electrosynthesis from CO_2: forever a promise? Curr Opin Biotechnol 62:48–57

Rabaey K, Rozendal RA (2010) Microbial electrosynthesis-revisiting the electrical route for microbial production. Nat Rev Microbiol 8(10):706–716

Rao G, Mutharasan R (1986) Alcohol production by *Clostridium acetobutylicum* induced by methyl viologen. Biotechnol Lett 8:893–896

Sasaki K et al (2010) Bioelectrochemical system stabilizes methane fermentation from garbage slurry. Bioresour Technol 101:3415–3422

Sasaki D et al (2013) Operation of a cylindrical bioelectrochemical reactor containing carbon fiber fabric for efficient methane fermentation from thickened sewage sludge. Bioresour Technol 129:366–373

Schievano A et al (2016) Electro-fermentation—merging electrochemistry with fermentation in industrial applications. Trends Biotechnol 34(11):866–878

Taheri A et al (2015) An iron electrocatalyst for selective reduction of CO_2 to formate in water: including thermochemical insights. ACS Catal 5(12):7140–7151

Tashiro Y et al (2018) Electrical-biological hybrid system for CO_2 reduction. Metab Eng 47:211–218

Wang H, Ren ZJ (2013) A comprehensive review of microbial electrochemical systems as a platform technology. Biotechnol Adv 31(8):1796–1807

Wietzke M, Bahl H (2012) The redox-sensing protein Rex, a transcriptional regulator of solventogenesis in *Clostridium acetobutylicum*. Appl Microbiol Biotechnol 96(3):749–761

Zhu Y et al (2014) Metabolic changes in *Klebsiella oxytoca* in response to low oxidoreduction potential, as revealed by comparative proteomic profiling integrated with flux balance analysis. Appl Environ Microbiol 80(9):2833–2841

Part III
Electron Based Biocorrosion

Chapter 11
Microbiologically Influenced Corrosion

Satoshi Wakai

11.1 Introduction

Corrosion of metal materials proceeds by coupling of ionization at the anode and an electron donation reaction at the cathode. For example, corrosion of metallic iron is coupled with an anode reaction, $Fe^0 \rightarrow Fe^{2+} + 2e^-$, to a cathodic reaction of oxygen reduction, $1/2O_2 + 2H^+ + 2e^- \rightarrow H_2O$, under aerobic conditions, or a cathodic reaction of proton reduction, $2H^+ + 2e^- \rightarrow H_2$, under acidic or anaerobic conditions. The anodic reactions under oxygen and oxygen-free conditions are the same, although the latter is considerably slower than that under acidic conditions. Therefore, the corrosion reaction should be considerably slow under anaerobic conditions at room temperature, but a phenomenon has been observed that drastically accelerates this process by the involvement of microorganisms. Little is known about the cathode reaction by microorganisms; however, it is certain that this is an electrochemical phenomenon that couples the redox reactions of the anode and cathode.

The corrosion of metal materials caused by microorganisms has been long known and referred to as MIC. MIC is defined as the direct or indirect corrosion of metal materials by activity or presence of microorganisms. The commonly accepted cost associated with metal corrosion is $276 billion annually in the United States (https://www.corrosioncost.com/), and this phenomenon is known to have generated significant economic losses. However, the proportion of MIC in the total corrosion cannot be estimated due to the ambiguous definition as described above.

Similar results have been obtained following the latest calculation of data in Japan (Shinohara 2019). According to a trial calculation in the 2015 financial year, 5.3 trillion yen is 1.02% of gross national profit (GNP). This value is based on the Hoar

S. Wakai (✉)
Institute for Extra-cutting-edge Science and Technology Avant-garde Research (X-star), Japan Agency for Marine-Earth Science and Technology (JAMSTEC), Yokosuka, Japan
e-mail: wakais@jamstec.go.jp

M. Ishii, S. Wakai (eds.), *Electron-Based Bioscience and Biotechnology*,
https://doi.org/10.1007/978-981-15-4763-8_11

method (Hoar 1971). The Uhlig method (Uhlig 1950) is another calculation method, and according to this, the annual corrosion cost is approximately 3.9 trillion yen. This method is mainly calculated based on initial costs, whereas the Hoar method includes maintenance cost in addition to initial cost. In 1974, the ratio of Hoar against Uhlig (Hoar/Uhlig ratio) is 0.45, but in 2015, it has risen to 1.35. Namely, the proportion of maintenance cost in modern society is higher than that during high economic growth periods due to the high costs associated with maintaining old infrastructure. There are concerns that the future society will have even greater costs, such as maintenance and renewal of existing infrastructure. To establish a sustainable society by maintaining a healthy infrastructure, we have to prevent economic loss due to massive anticorrosion treatments and sudden accidents, environmental pollution due to corrosion or leakage accidents in energy-related facilities, chemical factories, etc. Therefore, the social significance of correctly understanding MIC has great implications.

MIC is merely one category of the metal corrosion. Behavior of metal corrosion is governed by the physicochemical parameters of the environment it is used in. Chemical parameters include chloride ion concentration and pH, and physical parameters include temperature and external force. Therefore, although life span prediction of a metal material is estimated based on physicochemical parameters, sometimes corrosion proceeds more rapidly than estimated. Although corrosion at such an unexpected rate is due to change in the physicochemical parameters of the environment and construction failure, when the cause cannot be identified by various inspections, it is presumed to be MIC. Such estimation by method process of elimination is due to the lack of accurate diagnostic techniques for MIC.

As mentioned above, despite MIC being a long known phenomenon, its criterion is based on a process of elimination and empirical rules. Dependence of such an ambiguous diagnostic method incurs a great amount of time and labor, an increase in corrosion due to a delay in diagnosis, and occurrence of a secondary accident, e.g., leakage of oil and chemical accidents. In this chapter, I will discuss why this situation persists, describe a brief history of MIC research, and propose a way forward for future endeavors based on the latest information.

11.2 History of MIC Research

There were three turning points in MIC research to date. The first is the proposal of the cathodic depolarization theory, the second is the discovery of novel corrosive microorganisms, and the third is the breakthrough in genetic analysis technology.

11.2.1 Cathodic Depolarization Theory

Among the academic papers accessible in my survey, the oldest papers that correlate corrosion with microorganisms appear to be in 1910 (Gaines 1910). Prior to that, in 1891, Garrett seemed to have considered biological effects based on the accelerated corrosion of lead by water-containing nitrogen compounds (Garett 1891). Despite the fact that the relationship between microorganisms and metal corrosion has known for more than 100 years, little is known about the mechanisms of MIC, indicating the complexity of it. Decades have passed with the only recognition stating that corrosion involving microorganisms occurs; the cathodic depolarization theory was then proposed in 1934 (von Wolzogen Kühr and van der Vlugt 1934). This is the first turning point in the study of MIC in relation to sulfate-reducing bacteria (SRB), which has attracted some attention.

In 1931, hydrogen-consuming SRB was reported (Stephenson and Stickland 1931), followed by von Wolzogen Kühr and van der Vlugt (1934) who proposed the cathodic depolarization theory as a metal corrosion mechanism by hydrogen-consuming SRB. In an anaerobic and neutral environment, the corrosion reaction of metallic irons is slow. It is caused by a slow rate of electron loss at the cathode, and the metallic iron achieves a polarization state. Conversely, according to the cathodic depolarization theory, hydrogen-consuming bacteria quickly remove hydrogen generated on the cathode surface. This leads to the loss of electrons, returning to the depolarized state, and promoting corrosion.

Since the cathodic depolarization theory was proposed, many researchers have spent a lot of research time to verify this theory. Currently, many researchers and engineers have recognized SRB as causative microorganisms. In addition, when faced with the accelerated corrosions that cannot be explained by physicochemical parameters, the first suspicion is MIC by SRB. However, there are many cases where reproduction of corrosion cannot be confirmed using a laboratory scale test, even if an attempt is made to reproduce the corrosion using SRB cultured from the corrosive environment. Why has the cathodic depolarization theory been accepted for a long time? SRB can be divided into hydrogen-consuming chemotrophs and organotrophs based on its metabolic mode, both of which produce hydrogen sulfide through a sulfate reduction reaction. Accumulation of high concentrations of hydrogen sulfide causes chemically induced corrosion, and a highly visible black-colored iron sulfide corrosion product is easily formed with a small amount of iron and hydrogen sulfide. For example, Fig. 11.1 shows cultures of hydrogen-consuming chemotrophic and organotrophic SRBs and iron-corrosive methanogen after cultivation of metallic iron. However, the amounts of corroded iron present in SRB vials are almost the same when compared with abiotic controls and are approximately ten-fold less than those in the iron-corrosive methanogen.

Although the cathodic depolarization theory is still widely believed, I do not think it is explained by hydrogen-utilizing ability based on the structure of hydrogenase and results of corrosion tests using hydrogen-utilizing microorganisms as reported by Mori et al. (2010). Unfortunately, in a recently published review article, it has

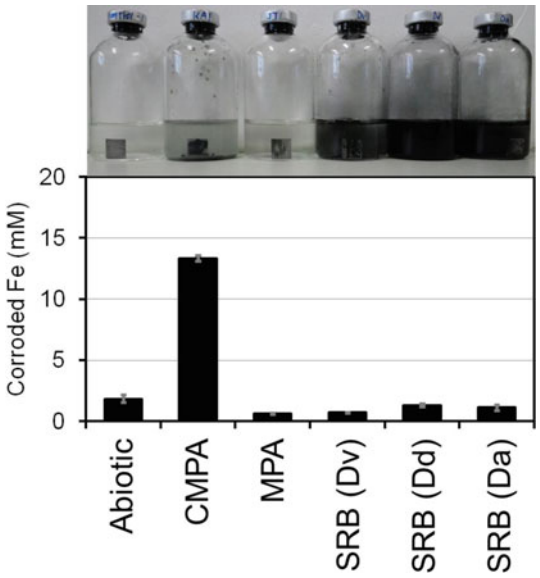

Fig. 11.1 Confliction between color alteration of cultures and corrosion ability. Picture represents culture bottles after cultivation. Bottom graph represents the concentrations of corroded Fe in the culture of abiotic and various microorganisms: Abiotic, abiotic control; CMPA, iron-corrosive methanogen *M. maripaludis* KA1; MPA, non-corrosive methanogen *M. maripaludis* JJ^T; SRB (Dv), hydrogen-consuming SRB *Desulfovibrio vulgaris* NBRC104121; SRB (Dd), hydrogen-consuming SRB *Desulfovibrio dechloracetivorans* NBRC105816; and SRB (Da), hydrogen-nonconsuming heterotrophic SRB *Desulfopila aestuarii* JCM14042

been reported that the reaction of consuming hydrogen from the metal surface promotes hydrogen regeneration and induces corrosion. There is structural issue of hydrogenase, and the active center for catalytic reactions is positioned deep inside the enzyme (Volbeda et al. 1996; Peters et al. 1998; Shima et al. 2008). Furthermore, [H] or H_2 bound to the metal surface cannot coordinate to this active center (Fig. 11.2). Namely, hydrogen-consuming hydrogenase can use only free molecular hydrogen as a substrate. As reported by Mori et al. (2010), almost all hydrogen-consuming bacteria and archaea isolated from natural environments did not show accelerated corrosion. They isolated hydrogen-consuming acetogens, SRB, and methanogens, and then conducted corrosion tests. As a result, only one strain of methanogens showed accelerated corrosion, whereas others showed similar levels of corrosion compared with those of the abiotic control. Notably, corrosion-accelerating ability is the unique to corrosive microorganisms and hydrogen-consuming abilities do not directly correlate to corrosion ability.

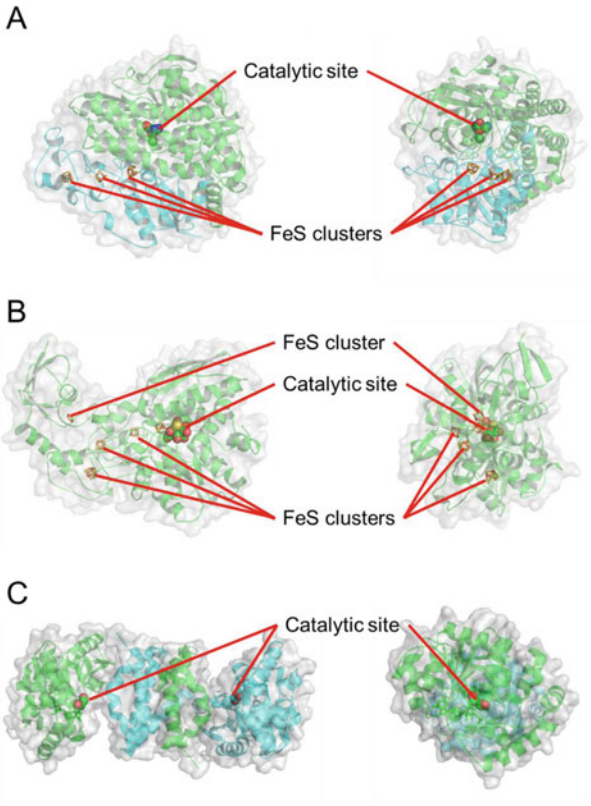

Fig. 11.2 Structure and active site of hydrogenases. (**a**) [NiFe]-hydrogenase from *Desulfovibrio gigas* (PDB ID: 2FRV), which has a Ni–Fe cluster as catalytic site and a [3Fe–4S] cluster and two [4Fe–4S] cluster as FeS cluster. (**b**) [FeFe]-hydrogenase from *Clostridium pasteurianum* (PDB ID: 1FEH), which has a H-cluster as catalytic site and three [4Fe–4S] cluster and a [2Fe–2S] cluster as FeS cluster; and (**c**) [Fe]-hydrogenase from *Methanocaldococcus jannaschii* (PDB ID: 3DAG), which has an iron center as catalytic site

11.2.2 Novel Iron-Corrosive Anaerobes

If cathodic depolarization by hydrogen-consuming bacteria does not hold, it is necessary to consider what reaction promotes electron flow at the cathode. Therefore, the next turning point was a paper on novel corrosive microorganisms (Dinh et al. 2004). Although, in this paper causative biomolecules were not identified, a new model was proposed in which microbial cells directly utilize electrons in metallic iron in a cathodic reaction. Furthermore, they reported on both corrosive SRB and corrosive methanogens. This direct electron uptake model brings controversy in MIC research.

The biggest factor that led to the proposal of a new corrosion model may be the use of metallic iron as a sole energy source for microbial cultivation. The success of this cultivation method indicates that in addition to indirect models such as sulfide and acid production, corrosion is promoted by using metallic iron directly as an energy source, namely, some microorganisms may be able to corrode directly. Since the proposal of the cathodic depolarization theory, many researchers and engineers have focused on the presence of SRB in the corrosive environment, and commercial

kits for easily cultivating SRB have been used, making it easy to qualitatively and quantitatively determine its existence. However, although many engineers and researcher focus on the existence of SRB in this way, they often face problems such as corrosion not being reproducible as the laboratory scale experiment. There are some problems in conventional methods using such commercial kits and using easy-to-use media. For example, it is incorrect to construct an experimental system in which a corrosion test is conducted using a nutrient-rich medium for cultivation, even though abundant nutrients do not exist in the actual environment. Such tests verify only indirect effects of microbial metabolites, and it cannot evaluate the direct corrosion ability of microorganisms. These experimental results are not sensible to explain the phenomenon in the natural environment where the nutrient concentration is quite low. In addition, use of commercial kits for cultivation of SRB does not evaluate the corrosiveness of exhibiting microorganisms, since more than 99% of microorganisms in the natural environment cannot be cultured, and it is also impractical to count only the number of cultivable SRB. Of course, monitoring of SRB in an environment where corrosion is an issue is meaningful as information for environmental assessment.

The percentage of MIC caused by microorganisms that use metallic iron, as an energy source, compared to the total MIC is still unclear, but the concept of a direct corrosion mechanism has changed the overall range of corrosive microorganisms considerably. In fact, after 2004, various types of novel corrosive microorganisms have been reported.

11.2.3 Next-Generation Sequencing (NGS)

With the development of culture technology, novel corrosive microorganisms have been reported. However, in the actual environment, microbial communities consisting of various microorganisms are formed. As an analysis method of microbial communities, approximately 30 years ago, a clone library method was used. However, this method requires a lot of time and effort (Wakai 2016). Alternatively, approximately 20 years ago, denaturing gradient gel electrophoresis (DGGE) analysis method (Muyzer et al. 1993), which was excellent for comparative analysis compared with the clone library method, became popular and used in many environmental microbiology studies. Thereafter, next-generation sequencing (NGS) analysis was developed, which made it possible to comprehensively clarify the microbial community in the environment and to simultaneously compare and analyze multiple samples (Voelkerding et al. 2009). The arrival of NGS technology is the third turning point in the development of MIC research.

When MIC is suspected, culture-dependent methods have been used as verification tools for a long time. In particular, the colonies of general bacteria and SRB are formed on the nutrient-rich agar medium and are counted. In addition, based on the report that some microorganisms would positively affect corrosion, quantitative PCR method has recently been used to measure the copy numbers of target genes

from SRB, sulfur-oxidizing bacteria, iron-oxidizing bacteria, iron-reducing bacteria, etc. However, the quantitative PCR technique has high detection accuracy, and the presence of unknown corrosive bacteria is completely neglected. Therefore, NGS analysis has been most recently applied to several samples from corrosion environments, where MIC is suspected, and corrosion induction has been found in complex microbial systems.

The development of next-generation sequencers resulted in a drastic improvement of gene analysis technology, has made it possible to comprehensively analyze the genetic information of microorganisms in the environment (especially genes related to classification indices), and have been used in the research field of environmental microbiology including MIC research (Ducey and Hunt 2013; Fierer et al. 2012; Vigneron et al. 2016). Alternatively, it is a concern that the publications of some reports have misinterpreted results and improper experimental design. The microbial community analysis was conducted only after corrosion, and the corrosion was identified as MIC based on the detection of some microorganisms such as SRB and iron-oxidizing bacteria. Such speculation based on the detection of specific microorganisms can be accomplished using conventional PCR detection method. NGS technology is a comparative analysis technology, and it has no meaning unless there is an appropriate comparison target. For example, it is necessary to compare among corroded and non-corroded samples and samples before and after corrosion. As the most unique case analyzed thus far, in a microbial community, half of which was the total occupied by SRB, the accelerated corrosion was not observed. However, when one acetogen *Acetobacterium* sp. was coexisting with SRB, the corrosion was induced (Wakai et al. 2015). As it has been reported that coexistence of SRB promotes the corrosion of iron-corrosive methanogens (Ito et al. 2011), the acetogens may be key corrosive agent in this instance, and SRB may enhance only the corrosion by the acetogens. Thus, an exhaustive analysis, such as NGS, may be required for unknown phenomena rather than a limited analysis method with high specificity.

11.3 Related Microorganisms to MIC

Microorganisms involving in MIC are described in detail in Chap. 13 and will be briefly introduced here. One of the most careful microorganisms at the field level by many researchers and engineers would be SRB. This is due to many studies on MIC having targeted SRB as described above, and their existence can be easily seen by a black corrosion product and hydrogen sulfide odor on site. In fact, generation of hydrogen sulfide, a corrosive gas, is one of the by-products and is a good way to monitor the behavior of SRB and the consequent generation of hydrogen sulfide. However, as described above, novel types of corrosive microorganisms having direct corrosion ability have been reported, and we have to pay the attention to the risk of unknown corrosive microorganisms. SRB and methanogens that can induce corrosion without abundant nutrients due to direct electron transfer. In direct

corrosion type of SRB, it has been reported that multi-heme protein in the outer membrane contribute to electron transfer, and genes encoding for those are also identified (Deng et al. 2018). Similarly, iron-corrosive methanogens have been also reported (Uchiyama et al. 2010; Mori et al. 2010), and novel type of extracellular hydrogenase related to corrosion ability is identified (Tsurumaru et al. 2018). Conventionally, detection of SRB and methanogen has been conducted by amplification of *dsr* and *mcr* genes, respectively. However, all SRB and methanogens have these genes; iron-corrosive type strains of SRB and methanogens could not be identified by conventional methods. Identifications of causative genes for induction of accelerated corrosion improved reliability of diagnosis method for MIC. Moreover, it has been reported that corrosion by iron-corrosive methanogens is further accelerated in the presence of SRB (Ito et al. 2011). SRB used in this experiment has no corrosive ability in a modified artificial seawater medium supplied with metallic iron, but when it coexists with the iron-corrosive methanogen, it enhances the corrosion by iron-corrosive methanogen (details are given in Chap. 14). Perhaps some of the corrosion that had been estimated to be caused by SRB includes systems where iron-corrosive methanogens are the actual causative bacteria and SRBs play the role of enhancers.

SRB is also related to the problem of souring in oil production wells, and SRB-derived sulfides are considered to affect souring of crude oil and corrosion of piping. To suppress souring, nitrate may be added as an oxidizing agent, but another unexpected corrosion has sometime occurred. To examine the influence of nitrate addition on secondary corrosion, the corrosion ability by nitrate-reducing bacteria has been researched. Iino et al. (2015) isolated iron-corrosive nitrate-reducing bacteria from petroleum facilities in Japan (Iino et al. 2015). It suggests that the addition of nitrate to oil-related facilities may increase the risk of corrosion by iron-corrosive nitrate-reducing bacteria. Notably, this iron-corrosive nitrate-reducing bacteria does not possess hydrogen-consuming ability, it is possible to consider the corrosive ability regardless of authenticity of the cathodic depolarization theory.

Since the corrosion by direct electron transfer mechanism has been reported, various corrosive microorganisms have been reported. Of these, iron-corrosive acetogen and neutrophilic iron-oxidizing bacteria probably possess direct electron transfer mechanism as corrosion property (Kato et al. 2015; McBeth et al. 2011). In addition, we found corrosion behavior by iodide-oxidizing bacteria, although it is an indirect corrosion by metabolites (Wakai et al. 2014). In an iodine recovery facility at a water-soluble gas field in Japan, an injection pipeline was drastically corroded. After enrichment of iodide-oxidizing bacteria in the corrosion products of the deteriorated pipe and lab-based cultures using brine water supplied with carbon steel and diluted nutrient, some strains of iodide-oxidizing bacteria were isolated and corrosion tests was conducted. Notably, isolated strains were separated to two types, one that can corrode metallic iron and carbon steel, but not stainless steel, and the other can corrode all three metal materials. These iodide-oxidizing bacteria can produce molecular iodine by oxidizing iodide ion, and the molecular iodine, which is a strong oxidant, can corrode metallic iron and carbon steel. Since the corrosion of stainless steel (SUS316) required approximately 3 mM molecular iodine, stainless

steel-corroding-type iodide-oxidizing bacteria may produce and accumulate molecular iodine since only 1 mM iodide ion was supplied (unpublished). Finally, the corrosion at this iodine recovery facility was judged to be typical SRB corrosion (Lim et al. 2011), due to the corrosion decreasing by switching the sulfuric acid used for pH adjustment to hydrochloric acid. These results suggest that there are various possibilities for corrosion in natural environments.

Many other reviews mention the correlations of sulfur-oxidizing, iron-oxidizing, iron-reducing, manganese-oxidizing bacteria, etc. (Procópio 2020; Skovhus et al. 2017; Vigneron et al. 2018), although there are no experiments using well-defined isolated strains. However, it is concerning that there may be a significant number of other microorganisms that induce corrosion by unknown mechanisms. For example, in recent years, the corrosion of stainless steel in a freshwater environment has been occasionally been observed. However, results of a microbial community analysis show that corrosive microorganisms were not detected and consisted of large amounts of general bacteria. I think that some of the bacteria considered as general bacteria may become corrosive depending on conditions, and I collectively refer to these microorganism groups as opportunistic corrosive bacteria (Fig. 11.3).

11.4 MIC Is an Infectious Disease of Metal Material

The term "opportunistic" was used above as an author's term, and the MIC problem should be addressed as a microbial infectious disease of metal materials (Fig. 11.4) (Wakai 2019). In human infectious diseases, almost all causative microorganisms are well characterized. Medical doctors are familiar with infectious microorganisms and know how symptoms of the infection present themselves. Once causative microorganisms are discovered, diagnostic techniques are developed, the cause can be quickly identified, and a correct treatment method can be administered. In addition, preventive medicine has been developed to eliminate the cause.

Alternatively, in MIC, these measures have not yet been developed. In particular, an overview of causative microorganism has not yet been elucidated. As a result, diagnostic techniques are still undeveloped, and the cause cannot be identified quickly nor can appropriate treatment be selected. If a quick diagnosis is not possible, the environment will continue to be affected by corrosion during that time. Even if a simple and quick diagnosis is made, if the diagnosis is not appropriate, corrosion cannot be suppressed, and after the replacement of base material, the same corrosion will reappear.

It is necessary to urgently establish a diagnostic technique, although currently the overview and mechanism of causative microorganisms are unknown, and genes and biological molecules for detection of those cannot be determined. Since microorganisms are clearly involved in microbial corrosion, the risk of MIC can be eliminated by sterilization. However, it is near impossible in the environment where many metal materials are used. Coating of metal materials is one of the effective anticorrosion treatments, although maintaining the soundness of coating is the

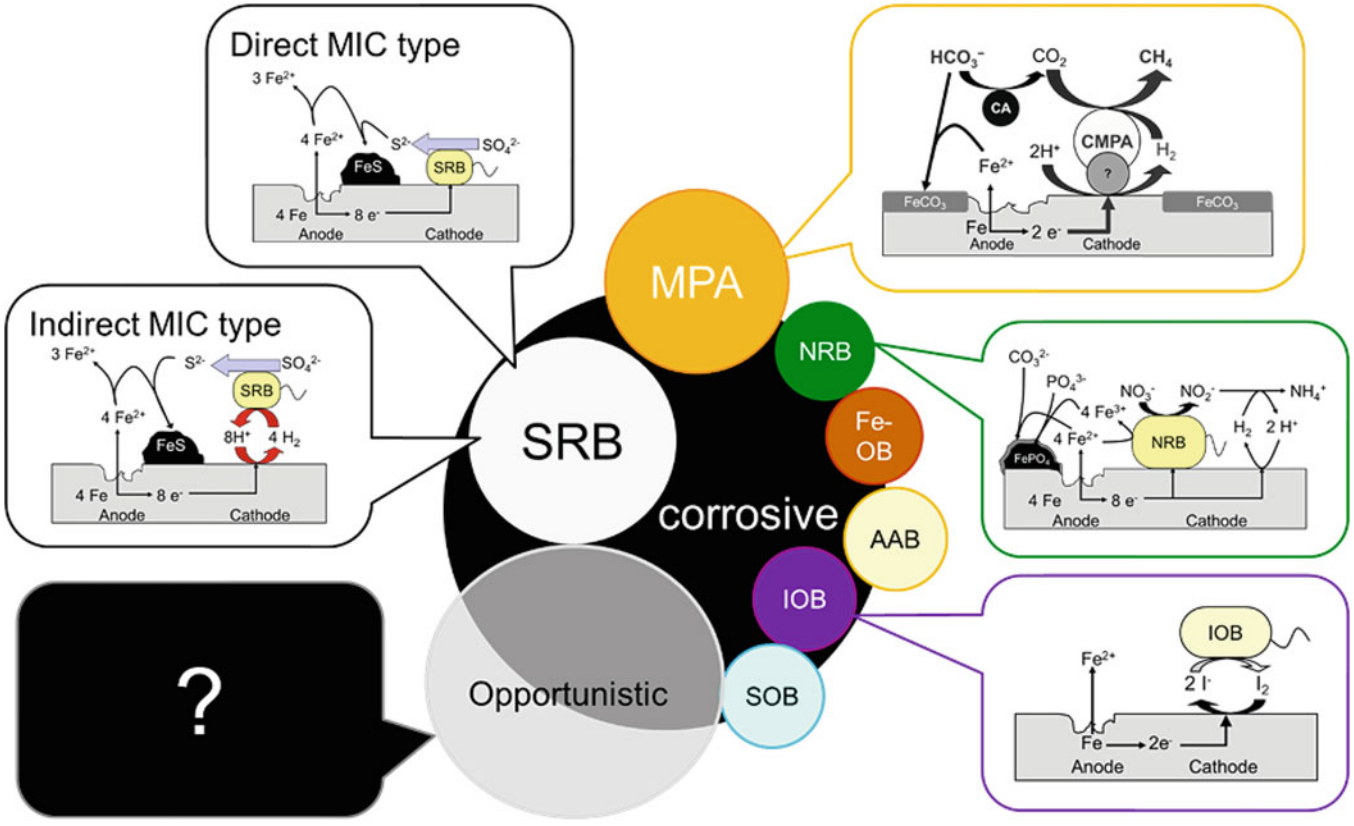

Fig. 11.3 Corrosive microorganisms and proposed corrosion mechanism. SRB divided into two types: one is direct MIC, which corrodes by directly using electrons from metal, and another is indirect MIC, which chemically corrode by producing hydrogen sulfide. MPA divided into iron-corrosive (CMPA) and non-corrosive. Similarly, nitrate-reducing bacteria (NRB), iron-oxidizing bacteria (Fe-OB), and acetic acid bacteria (AAB) are clearly divided into iron-corrosive and non-corrosive types. Iodide-oxidizing bacteria (IOB) chemically corrode by producing molecular iodine. Some sulfur-oxidizing bacteria (SOB) can accelerate iron dissolution, however, little is known. Opportunistic means general bacteria, which corrode by unknown mechanism

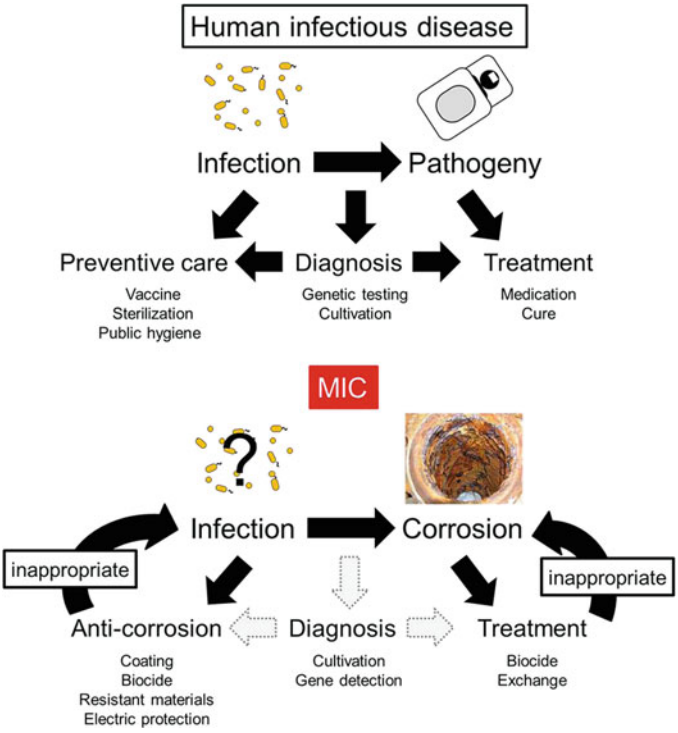

Fig. 11.4 Analogy of MIC against human infectious disease. In human infectious disease, pathogenic microorganisms are well-known, and then preventive care, diagnosis, and treatment are appropriately conducted. In contrast, MIC overview of corrosive microorganisms is unknown, and then anticorrosion, diagnosis, and treatment are undeveloped. Inappropriate anticorrosion and treatment cause considerable cost and reappearance of corrosion

most important issue, and deterioration may promote the progression of localized corrosion. To construct a sustainable society based on the maintenance of infrastructure, we must seriously address the microbial corrosion problem.

11.5 Concluding Remarks

In this chapter, I touched on the brief history of MIC research, outlined the latest corrosive microorganisms, and described the problems surrounding MIC research. In particular, I noted that the cathode depolarization theory cannot be applied to all hydrogen-consuming microorganisms, and various types of corrosive microorganisms have been reported in recent years. In addition, since MIC relates to considerable economic loss and potential environmental pollution, MIC must be diagnosed quickly and accurately, and proper treatment efforts to prevent it are necessary.

However, there are many remaining issues such as understanding the overview and mechanism of corrosive microorganisms. Most recently, the field of electromicrobiology research has become popular, and we can share understandings of the reaction of microorganisms receiving electrons from solid metals and extracellular electron transfer. This chapter is closed with the hope that the promotion and sharing of understanding will contribute to the development of research in this field.

References

Deng X, Dohmae N, Nealson KH, Hashimoto K, Okamoto A (2018) Multi-heme cytochromes provide a pathway for survival in energy-limited environments. Sci Adv 4:eaao5682

Dinh HT, Kuever J, Mußmann M, Hassel AW, Stratmann M, Widdel F (2004) Iron corrosion by novel anaerobic microorganisms. Nature 427:829–832

Ducey TF, Hunt PG (2013) Microbial community analysis of swine wastewater anaerobic lagoons by next-generation DNA sequencing. Anaerobe 21:50–57

Fierer N, Lauber CL, Ramirez KS, Zaneveld J, Bradford MA, Knight R (2012) Comparative metagenomic, phylogenetic and physiological analyses of soil microbial communities across nitrogen gradients. ISME J 6:1007–1017

Gaines RH (1910) Bacterial Activity as a Corrosive Influence in the Soil. Ind Eng Chem 2:128–130

Garett JH (1891) The action of water on lead. H.K. Lewis, London

Hoar TP (1971) Report of the committee on corrosion and protection. Department of Trade and Industry, London

Iino T, Ito K, Wakai S, Tsurumaru H, Ohkuma M, Harayama S (2015) Iron corrosion induced by non-hydrogenotrophic nitrate-reducing Prolixibacter sp. MIC1-1. Appl Environ Microbiol 81:1839–1846

Ito K, Wakai S, Tsurumaru H, Iino T, Mori K, Uchiyama T, Miki O, Harayama S (2011) Iron corrosion by methane producing archaea (MPA) and sulfate reducing bacteria (SRB) utilizing metallic iron as an electron donor. Zairyo-to-Kankyo 60:402–410. (in Japanese), Corr Eng 60:336–345

Kato S, Yumoto I, Kamagata Y (2015) Isolation of acetogenic bacteria that induce biocorrosion by utilizing metallic iron as the sole electron donor. Appl Environ Microbiol 81:67–73

Lim CP, Zhao D, Takase Y, Miyanaga K, Watanabe T, Tomoe Y, Tanji Y (2011) Increased bioclogging and corrosion risk by sulfate addition during iodine recovery at a natural gas production plant. Appl Microbiol Biotechnol 89:825–834

McBeth JM, Little BJ, Ray RI, Farrar KM, Emerson D (2011) Neutrophilic iron-oxidizing "Zetaproteobacteria" and mild steel corrosion in nearshore marine environments. Appl Environ Microbiol 77:1405–1412

Mori K, Tsurumaru H, Harayama S (2010) Iron corrosion activity of anaerobic hydrogen-consuming microorganisms isolated from oil facilities. J Biosci Bioeng 110:426–430

Muyzer G, deWaal EC, Uitterlinden AG (1993) Profiling of complex microbial populations by denaturing gradient gel electrophoresis analysis of polymerase chain reaction-amplified genes coding for 16S rRNA. Appl Environ Microbiol 59:695–700

Peters JW, Lanzilotta WN, Lemon BJ, Seefeldt LC (1998) X-ray crystal structure of the Fe-only hydrogenase (CpI) from Clostridium pasteurianum to 1.8 angstrom resolution. Science 282:1853–1858

Procópio L (2020) The era of 'omics' technologies in the study of microbiologically influenced corrosion. Biotechnol Lett 42:341–356

Shima S, Pilak O, Vogt S, Schick M, Stagni MS, Meyer-Klaucke W, Warkentin E, Thauer RK, Ermler U (2008) The crystal structure of [Fe]-hydrogenase reveals the geometry of the active site. Science 321:572–575

Shinohara T (2019) Corrosion cost survey in Japan in FY 2015. In: Proceedings of NACE-EAPA, paper no. EAPA19NOV-14049, Yokohama, 11−14 Nov 2019

Skovhus TL, Eckert RB, Rodrigues E (2017) Management and control of microbiologically influenced corrosion (MIC) in the oil and gas industry—overview and a North Sea case study. J Biotechnol 256:31–45

Stephenson M, Stickland LH (1931) Hydrogenase: the reduction of sulphate to sulphide by molecular hydrogen. Biochem J 25:215–220

Tsurumaru H, Ito N, Mori K, Wakai S, Uchiyama T, Iino T, Hosoyama A, Ataku H, Nishijima K, Mise M, Shimizu A, Harada T, Horikawa H, Ichikawa N, Sekigawa T, Jinno K, Tanikawa S, Yamazaki J, Sasaki K, Yamazaki S, Fujita N, Harayama S (2018) An extracellular [NiFe] hydrogenase mediating iron corrosion is encoded in a genetically unstable genomic island in Methanococcus maripaludis. Sci Rep 8:15149

Uchiyama T, Ito K, Mori K, Tsurumaru H, Harayama S (2010) Iron-corroding methanogen isolated from a crude-oil storage tank. Appl Environ Microbiol 76:1783–1788

Uhlig HH (1950) Cost of corrosion to United States. Corrosion 6(1):29–33

Vigneron A, Alsop EB, Chambers B, Lomans BP, Head IM, Tsesmetzis N (2016) Complementary microorganisms in highly corrosive biofilms from an offshore oil production facility. Appl Environ Microbiol 82:2545–2554

Vigneron A, Head IM, Tsesmetzis N (2018) Damage to offshore production facilities by corrosive microbial biofilms. Appl Microbiol Biotechnol 102:2525–2533

Voelkerding KV, Dames SA, Durtschi JD (2009) Next-generation sequencing: from basic research to diagnostics. Clin Chem 55:641–658

Volbeda A, Garcin E, Piras C, De Lacey AL, Fernandez VM, Hatchikian EC, Frey M, Fontecilla-Camps JC (1996) Structure of the [Nife] hydrogenase active site: evidence for biologically uncommon Fe ligands. J Am Chem Soc 118:12989–12996

von Wolzogen Kühr CAH, van der Vlugt LS (1934) The graphitization of cast iron as an electrochemical process in anaerobic soil. Water 18:147–165

Wakai S (2016) Gene analysis for the evaluation of the effect of environmental factors. In: Kanematsu H, Barry DM (eds) Corrosion control and surface control: environmentally friendly approaches. Springer, Japan, pp 169–184

Wakai S (2019) Biochemical and thermodynamic analyses of energy conversion in extremophiles. Biosci Biotechnol Biochem 83:49–64

Wakai S, Ito K, Iino T, Tomoe Y, Mori K, Harayama S (2014) Corrosion of iron by iodide-oxidizing bacteria isolated from brine in an iodine production facility. Microb Ecol 68:519–527

Wakai S, Fujii S, Masanari M, Miyanaga K, Tanji Y, Sambongi Y (2015) Corrosion test using bottom water from oil-storage tank and microbial community analysis by next generation sequencer. Zairyo-to-Kankyo 64:540–544. (in Japanese), Corr Eng 64:460–465

Chapter 12
Electrochemistry on Corrosion Engineering

Nobumitsu Hirai

12.1 Corrosion Reaction of Base Metals

The corrosion of based metals, such as iron, copper, zinc, and so on, generally can be explained by "electrochemical local cell mechanism." Figure 12.1 shows the schematic illustration of voltaic cell.

The negative and positive electrodes of voltaic are zinc and copper plates, respectively. On the negative electrode, anodic dissolution of metallic zinc is performed:

$$Zn \rightarrow Zn^{2+} + 2e^{-} \tag{12.1}$$

On the positive electrode, hydrogen generation reaction is performed:

$$2H^{+} + 2e^{-} \rightarrow H_2 \tag{12.2}$$

And the overall reaction is as follows:

$$Zn + 2H^{+} \rightarrow Zn^{2+} + H_2 \tag{12.3}$$

Gibbs free energy of this overall reaction is negative so that this reaction proceeds spontaneously with taking the electric energy through the external load. When the zinc and copper plates are connected directly and are dipped into the solution, the same reactions, the anodic dissolution of metallic zinc on the zinc plate and the hydrogen generation on the copper one, are performed without taking the energy, as shown in Fig. 12.2. When only the zinc plate is dipped into the solution, the same

N. Hirai (✉)
National Institute of Technology, Suzuka College, Suzuka, Mie, Japan
e-mail: hirai@chemsuzuka-ct.ac.jp

M. Ishii, S. Wakai (eds.), *Electron-Based Bioscience and Biotechnology*,
https://doi.org/10.1007/978-981-15-4763-8_12

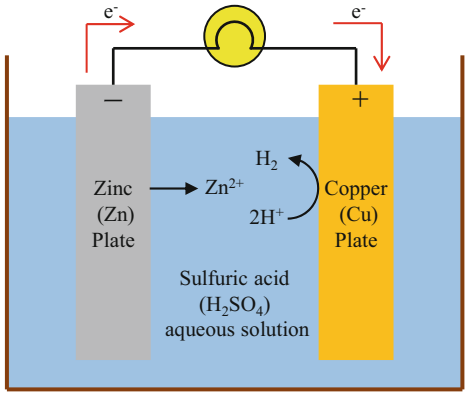

Fig. 12.1 Schematic illustration of voltaic cell

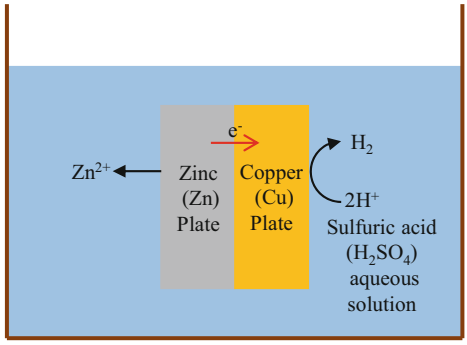

Fig. 12.2 Schematic illustration of the zinc and copper plates connected each other, which are dipped into the sulfuric acid aqueous solution

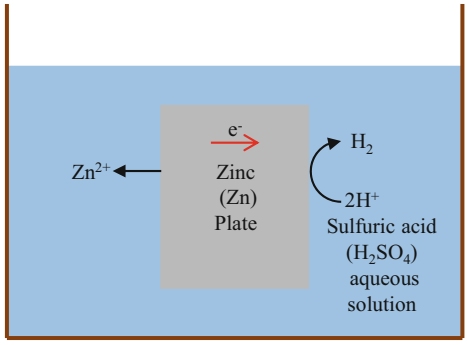

Fig. 12.3 Schematic illustration of the zinc plate, which is dipped into the sulfuric acid aqueous solution

reactions, both the anodic dissolution of metallic zinc and the hydrogen generation on the zinc one, are performed without taking the energy, as shown in Fig. 12.3. This is one example of the zinc corrosion.

Next, let's consider the corrosion of base metal. Base metal (M) dissolves into aqueous solution as follows:

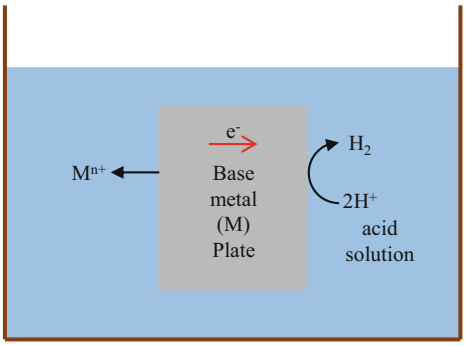

Fig. 12.4 Schematic illustration of the typical corrosion of base metal in acid aqueous solution

$$M \rightarrow M^{n+} + ne^- \tag{12.4}$$

The electrons are produced by this anodic reaction, but the reaction stops soon if there are no cathodic reactions. Continuous dissolution of base metal occurs only when there are some cathodic reactions. Hydrogen generation is one of the most typical cathodic reactions in acid aqueous solution:

$$2H^+ + 2e^- \rightarrow H_2 \tag{12.5}$$

And the overall reaction is as follows:

$$2M + (2n)H^+ \rightarrow 2M^{n+} + nH_2 \tag{12.6}$$

Figure 12.4 shows the schematic illustration of the typical corrosion of base metal in acid aqueous solution. Generally, the surface of the base metal is not uniform. For example, there are grain boundaries, where elemental segregations are observed, on the surface. There might be scratches on the surface. Adhesion of precipitates, stains, microorganisms, biofilms, and so on is uneven on the surface. Therefore, both the place which is easy to dissolve and the one where the hydrogen generation is likely to occur exist on one plate of base metal. It can be considered to be similar to the state in which the positive and negative electrodes of the battery were short-circuited. This reaction mechanism is called electrochemical local cell mechanism. The part where the anodic reaction, that is, the dissolution of base metal, occurs is called a local anode, and the part where the cathodic reaction occurs is called a local cathode.

The cathodic reaction on the local cathode is not only hydrogen generation. When the oxygen is dissolved in the aqueous solution, oxygen reduction reaction might occur as the cathodic reaction:

$$O_2 + 2H_2O + 4e^- \rightarrow 4OH^- \tag{12.7}$$

The contribution of dissolved oxygen can be almost ignored in acid aqueous solution: however, oxygen reduction reaction is the main cathode reaction in neutral

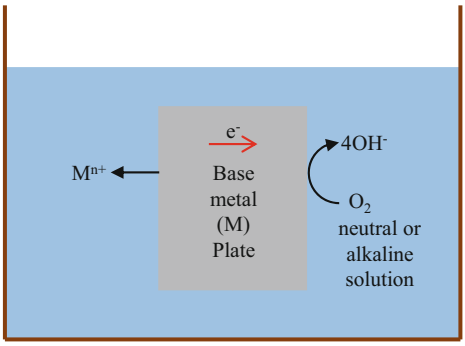

Fig. 12.5 Schematic illustration of the typical corrosion of base metal in neutral or alkaline aqueous solution

or alkaline aqueous solution since the concentration of hydrogen ions is low. In that case, the overall reaction is as follows:

$$4\mathrm{M} + n\mathrm{O_2} + (2n)\mathrm{H_2O} \rightarrow 4\mathrm{M}^{n+} + (4n)\mathrm{OH}^- \tag{12.8}$$

Figure 12.5 shows the schematic illustration of the typical corrosion of base metal in neutral or alkaline aqueous solution. It is noteworthy that the dissolved base metal might form rust especially in neutral or alkaline aqueous solution. For example, iron rust formed in alkaline solution consists of mainly FeOOH with small amount of Fe_2O_3 and Fe_3O_4.

As mentioned above, the main cathodic reaction in acid solution is hydrogen generation, and that in neutral or alkaline solution is c when a sufficient amount of oxygen is dissolved in the solution. However, when there are little oxygen near the plate of base metal in neutral or alkaline solution, the other cathodic reactions might affect the corrosion of base metal.

12.2 Corrosion Current and Corrosion Potential

As mentioned above, the corrosion of base metal is accompanied by cathode reduction, such as hydrogen generation, oxygen reduction, etc. It is noteworthy that the corrosion rate (corrosion current) of base metal must be the same as the cathodic reduction rate (reduction current). Therefore, it is very important what the main cathodic reaction is. Figure 12.6 shows local anodic and cathodic polarization curves of base metal in acid solution.

The limiting process of the corrosion of base metal is the charge transfer one. And the limiting process of hydrogen generation is also the charge transfer one because of sufficient amounts of hydrogen ions in acid solution. Therefore, the corrosion rate as well as the rate of hydrogen generation increases exponentially with the potential. At corrosion potential (E_{corr}), the corrosion rate (corrosion current, I_{corr}) of base metal is

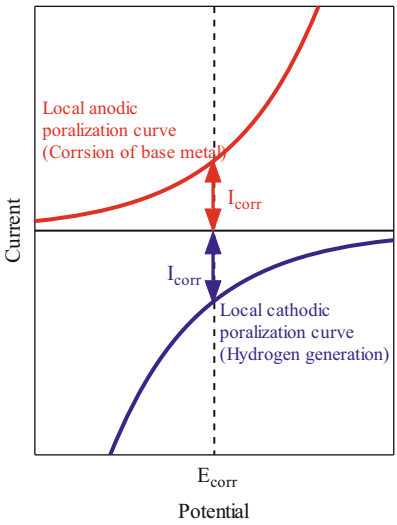

Fig. 12.6 Local anodic and cathodic polarization curves of base metal in acid solution

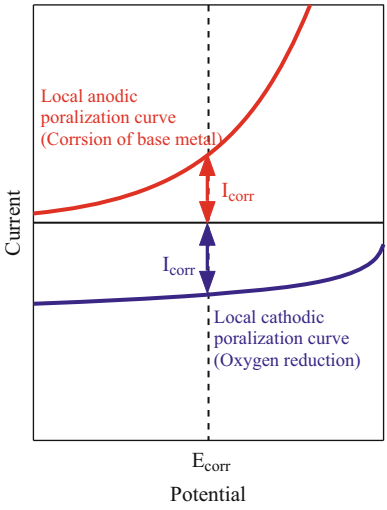

Fig. 12.7 Local anodic and cathodic polarization curves of base metal in neutral or alkaline solution

the same as the hydrogen generation rate (reduction current, I_{corr}) as shown in Fig. 12.6.

Figure 12.7 shows local anodic and cathodic polarization curves of base metal in neutral or alkaline solution. The limiting process of the corrosion of base metal in neutral or alkaline solution is also the charge transfer one; however, the limiting process of oxygen reduction is generally the mass transport one. Therefore, the corrosion rate increases exponentially with the potential, but the oxygen reduction rate is almost constant with potential and is roughly proportional to the concentration of dissolved oxygen in the solution. At corrosion potential (E_{corr}), the corrosion rate

(corrosion current, I_{corr}) of base metal is the same as the oxygen reduction rate (reduction current, I_{corr}) so that the corrosion rate is roughly proportional to the concentration of dissolved oxygen in the solution.

Here, corrosion current and corrosion potential are explained when hydrogen generation or oxygen reduction is the main cathodic reaction. When the other cathodic reactions might affect the corrosion, the limiting process of the cathodic reactions, as well as Gibbs free energies of the overall reactions, which must be negative for spontaneous proceeding of the corrosion, should be taken in account.

12.3 Equilibria and Kinetics of Corrosion

As mentioned above, an iron plate generally dissolves in acid solution but normally forms rust in neutral or alkaline solution. Thus, the corrosion behavior is affected by pH. The corrosion behavior is affected also by potential. Potential-pH diagrams, called Pourbaix diagrams, which are obtained based on the equilibria between metal, metal ions, and oxides, are often very useful in considering the corrosion of metal. These diagrams can be derived from the reference book Pourbaix (1966) or calculated from Nernst equations.

These diagrams are sometimes very effective in understanding metal corrosion, but not necessarily just enough. For example, iron dissolves rapidly in diluted nitric acid aqueous solution, but the dissolution rate in concentrated nitric acid aqueous solution is very low. The corrosion of iron pre-immersed in chromate or nitrite aqueous solution is very slow. The corrosion speed of base metal covered with native oxide layer is often far from that without native oxide layer by surface polishing. These phenomena cannot be explained by potential-pH diagrams. The passivity (passive state) refers to a state of metal corroding in an extremely slow state despite the metal should be corroded from the viewpoint of ionization tendency of metals. Generally, the passivity is caused by the formation of very dense layers with a thickness of 1–10 nm consisting of oxides and/or hydroxides formed on the surface of metals. The corrosion resistance of base metals depends strongly on passivation formation process. And the passivity usually suppresses general corrosion, but sometimes doesn't suppress local corrosion. Microbiologically influenced corrosion is mainly a local corrosion so that the passivity on the metal surface should be taken in account.

12.4 Intergranular Corrosion and Crevice Corrosion

As mentioned above, microbiologically influenced corrosion is mainly a local corrosion. In order to distinguish the microbiologically influenced corrosion and the others, the knowledge of local corrosion is meaningful. There are various types

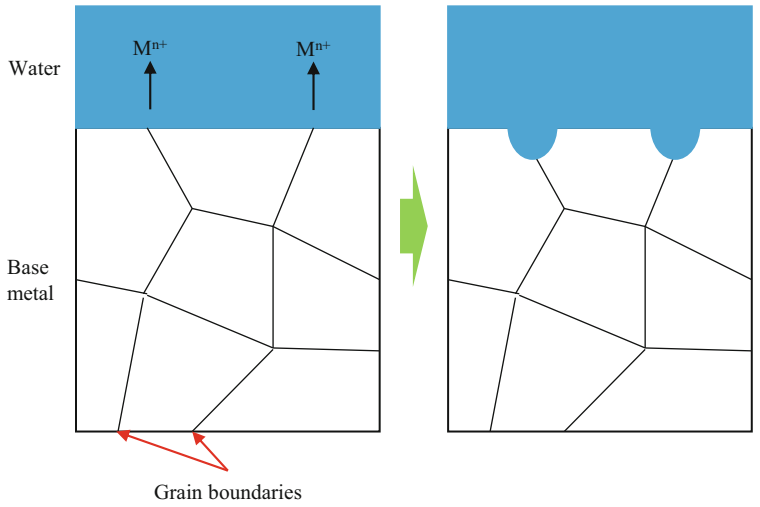

Fig. 12.8 Cross-sectional schematic illustrations near the interface between water and base metal with grain boundaries before and after intergranular corrosion

of local corrosion. In this section, intergranular corrosion (Armijo 1968) and crevice corrosion (Rosenfeld and Marshakov 1964) are introduced.

Microbiologically influenced corrosion sometimes occurs at the grain boundaries; the knowledge of intergranular corrosion is indispensable. Intergranular corrosion is a phenomenon in which the grain boundaries of metal crystal and their surroundings are preferentially corroded. Figure 12.8 shows cross-sectional schematic illustrations near the interface between water and base metal with grain boundaries before and after intergranular corrosion. Some of the stainless steel sometimes corrode severely only at the grain boundaries under a certain heat pre-treatment. It is called sensitizing heat treatment that heat treatment is carried out under a certain condition that causes sensitivity to intergranular corrosion. The condition of sensitizing heat treatment strongly depends on the materials. For example, the condition of sensitizing heat treatments of austenite stainless steel and ferrite stainless steel are totally different each other.

Crevice corrosion is one of wet corrosion phenomena and is a local corrosion that occurs at crevice. Figure 12.9 shows cross-sectional schematic illustrations near the interface between water and base metal with crevice before and after crevice corrosion. The component of the solution at crevice might be very different from that of the bulk solution so that the severe corrosion might occur by the electrochemical local cell mechanism. The crevice corrosion can be suppressed by preventing stagnant of the aqueous solution at crevice. One of the main components of biofilms is water, and the water might stagnate in biofilm so that the effect of crevice corrosion should be considered.

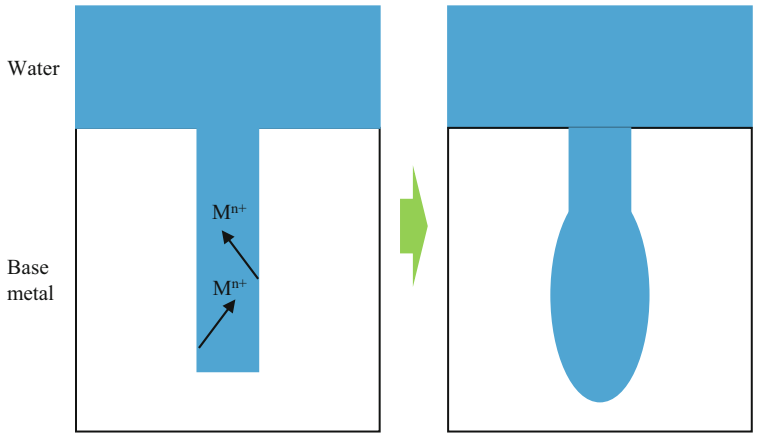

Fig. 12.9 Cross-sectional schematic illustrations near the interface between water and base metal with crevice before and after crevice corrosion

12.5 Protection Against Corrosion

Protection against corrosion should be possible when the cause of the corrosion is removed. In this section, various methods for the protection against corrosion are introduced.

12.5.1 Protection by Environmental Control

Generally, corrosion occurs at the interface between water and base metals. Therefore, the removal of water is one of the most effective methods for protection. Dissolved oxygen in water affects the corrosion behavior as shown in Eqs. (12.7) and (12.8), so the removal of dissolved oxygen from water is also good for the protection. To remove dissolved oxygen from water, deaeration by nitrogen or argon bubbling, by boiling under reduced pressure, or chemical removal of oxygen using a certain deoxygenating agent is sometimes performed.

12.5.2 Cathodic Protection

The corrosion usually proceeds by electrochemical local cell mechanism so that the corrosion of base metals is suppressed when only the cathodic reaction occurs on the base metal and the anodic reaction occurs only on the other solid. This type of protection is called “cathodic protection,” such as “sacrificial anode method” and “impressed current method”.

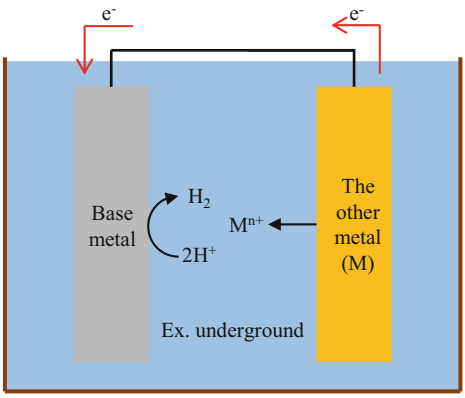

Fig. 12.10 Schematic illustration of the sacrificial anode method

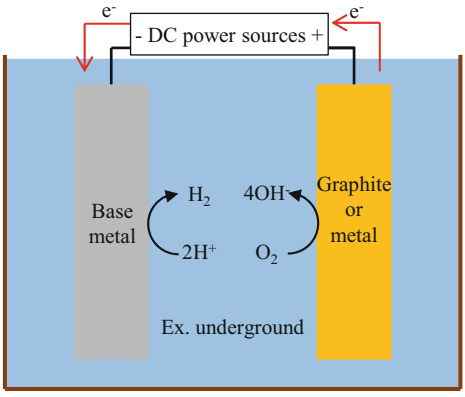

Fig. 12.11 Schematic illustration of the impressed current method

Figure 12.10 shows a schematic illustration of the sacrificial anode method. In this method, the base metal is connected with the other metal (M), called sacrificial anode, whose ionization tendency is higher than that of the base metal. The anodic reaction (the corrosion of metal) occurs only on the sacrificial anode, and only the cathodic reaction of hydrogen generation occurs on the base metal. As a sacrificial anode, zinc or magnesium is usually used.

Figure 12.11 shows a schematic illustration of the impressed current method. In this method, the base metal is connected with the stable electrode, such as graphite, and the voltage is impressed between the base metal as a cathode and the stable electrode as an anode. The anodic reaction occurs only on the stable electrode and only the cathodic reaction of hydrogen generation occurs on the base metal.

12.5.3 Protection by Surface Coating

Surface coating, such as metal coating, inorganic coating, organic coating, surface chemical treatment, and so on, is one of the protection methods.

When the base metal is coated with the other metal whose ionization tendency is higher than that of the base metal, the base metal is rarely corroded since the coated metal corrodes preferentially in the similar mechanism as the sacrificial anode method. However, the base metal might be corroded much more if there are pinholes and/or scratches on the coated metal when the base metal is coated with the other metal whose ionization tendency is lower than that of the base metal.

12.5.4 Formation of Corrosion Resistance Alloy

Alloy formation is one of the most effective methods for higher corrosion resistance. For example, iron is easily passivated by alloying with chromium and/or nickel. The steel containing less than 1.2 wt% of carbon and more than 10.5 wt% of chromium is called stainless steel, which has higher corrosion resistance than typical steel. The stainless steel can be classified into three: austenite stainless steel, ferrite stainless steel, and martensite stainless steel.

References

Armijo JS (1968) Intergranular corrosion of nonsensitized austenitic stainless steels. Corrosion 24 (1):24–30

Pourbaix M (1966) Atlas of electrochemical equilibria in aqueous solutions. National Association of Corrosion Engineers, Houston, TX

Rosenfeld IL, Marshakov IK (1964) Mechanism of crevice corrosion. Corrosion 20(4):115t–125t

Chapter 13
Microorganisms Inducing Microbiologically Influenced Corrosion

Takao Iino

13.1 Introduction

Metallic iron (Fe^0) and stainless steel corrosion causes a severe economic burden. The National Association of Corrosion Engineers (NACE) estimates that the annual cost of corrosion worldwide has been estimated to exceed 3% of the world's GDP (http://www.nace.org/uploadedFiles/Publications/ccsupp.pdf). Under aerobic conditions, molecular-oxygen-mediated corrosion may be predominant, whereas under anaerobic conditions, microbiologically influenced corrosion (MIC) is believed to be a major cause of corrosion-related failures. Corroding phenomena appeared to be caused by MIC was already observed for more than 100 years ago. In the early 1900s, sulfate-reducing bacteria (SRB) have been considered to be major causative microorganisms of MIC in anaerobic environments because FeS has frequently been observed as a major corrosion product (Enning and Garrelfs 2014). Besides SRB, culture-dependent approaches have elucidated that a variety of microorganisms such as methanogenic archaea (methanogens), sulfur-oxidizing bacteria, nitrate-reducing bacteria, iron-oxidizing bacteria, iodide-oxidizing bacteria, and acetogenic bacteria, which use Fe^0 as a sole electron donor and different respiratory substrates as electron acceptors, have been also implicated in MIC. Recent evidence has indicated that the direct electron transfer from Fe^0 to SRB via extracellular electron transfer was mediated by outer-membrane cytochromes (Beese-Vasbender et al. 2015; Deng et al. 2018; Dinh et al. 2004; Venzlaff et al. 2013). Some hydrogenic methanogens were shown to be capable of causing MIC on Fe^0 by secreting specific [NiFe] hydrogenase catalyzing the oxidation of Fe^0 to ferrous ion (Deutzmann et al. 2015; Tsurumaru et al. 2018). For effective prevention and control of MIC, the

T. Iino (✉)
Japan Collection of Microorganisms, RIKEN BioResource Research Center, Tsukuba, Ibaraki, Japan
e-mail: iino@riken.jp

M. Ishii, S. Wakai (eds.), *Electron-Based Bioscience and Biotechnology*,
https://doi.org/10.1007/978-981-15-4763-8_13

identification of causal microorganisms and the understanding of the mechanism of MIC by them are vital. This chapter provides an overview of representatives of iron-corroding microorganisms (Table 13.1), the phylogenetic relationships and biological features of them in the light of current prokaryotic systematics which is mainly based on the 16S rRNA gene phylogeny.

13.2 Sulfate-Reducing Bacteria

Sulfate-reducing bacteria (SRB) are specifically considered to be major causative microorganisms of MIC in anaerobic environments because FeS has frequently been observed as a major corrosion product. SRB accommodate to at least 60 genera containing 200 species or more. However, most corrosive SRB are in the class *Deltaproteobacteria*, while *Archaeoglobus fulgidus* may well contribute to corrosion in oil- and gas-producing facilities, particularly under conditions too hot to allow growth of their bacterial sulfidogenic counterparts. von Wolzogen Kühr and van der Vlugt (1934) described first the biological sulfate reduction by SRB, which were represented by *Desulfovibrio desulfuricans*, a.k.a. "*Spirillum desulfuricans*," "*Microspira desulfuricans*," and "*Vibrio desulfuricans*" as the cause of iron pipe failures in the ground in North Holland. The mechanism underlying MIC has been explained on the basis of the hydrogen consumption activity of sulfate-reducing bacteria (Fig. 13.1a). Fe^0 oxidation occurs at the anode:

$$Fe^0 \rightarrow Fe^{2+} + 2e^- \tag{13.1}$$

In anaerobic conditions, electrons at the cathode reduce the H^+ ions from water, and a hydrogen film is formed at the iron surface:

$$H_2O \rightarrow 2H^+ + 2OH^- \tag{13.2}$$

$$2H^+ + 2e^- \rightarrow H_2 \tag{13.3}$$

The cathodic hydrogen film is consumed by SRB, and the cathode is depolarized facilitating the transfer of the electrons from the anode to the cathode:

$$8H_2 + {SO_4}^{2-} \rightarrow S^{2-} + 4H_2O \tag{13.4}$$

The metabolic end product of SRB (S^{2-}) is deposited as FeS:

$$Fe^{2+} + S^{2-} \rightarrow FeS \tag{13.5}$$

This proposal was called as the cathodic depolarization theory and supported by followers (Butlin et al. 1949; Iverson 1966; Starkey 1947).

Table 13.1 List of iron-corroding microorganisms

Species	Strain no.	Other designations	Sources	Genome
Sulfate-reducing bacteria				
Desulfopila corrodens	IS4		Marine sediment in the North Sea near Wilhelmshaven, Germany	NA
Desulfovibrio ferrophilus	IS5	DSM 15579	Marine sediment in the North Sea near Wilhelmshaven, Germany	AP017378 (Chr), AP017379 (Plsm)
Desulfovibrio vulgaris	Hildenborough^T	ATCC 29579, CCUG 34227, CIP 107040, DSM 644, LMG 7563, NCAIM B.01489, VKM B-1760	Wealden clay in Kent, Hildenborough, UK	AE017285, AE017286 (plasmid), CABHLV000000000
Desulfovibrio sp.	HS2			NA
Methanogenic archaea				
Methanobacterium sp.	IM1		Marine sediment in the North Sea near Wilhelmshaven, Germany	NA
Methanococcus maripaludis	KA1	NBRC 102054	Oil sludge from a crude oil storage tank	AP011526, AP011527 (plasmid)
Methanococcus maripaludis	Mic1c10	NBRC 105639	Drain water of oil facility	NA
Methanococcus maripaludis	MM901		Unknown	NA
Methanococcus maripaludis	OS7	NBRC 103642	Bottom water of a crude oil storage tank at Osaka, Japan	AP011528
Sulfur-oxidizing bacteria				
Sulfurimonas sp.	CVO	NRRL B-21472	Water produced at the Coleville field in Saskatchewan, Canada	NA
Nitrate-reducing bacteria				
Geobacter sulfurreducens	PCA^T	ATCC 51573, DSM 12127	Surface sediment of a ditch in Norman, OK, USA	AE017180

(continued)

Table 13.1 (continued)

Species	Strain no.	Other designations	Sources	Genome
Prolixibacter denitrificans	MIC1–1^T	DSM 27267, JCM 18694, NBRC 102688	Crude oil from an oil well, Akita, Japan	BLAU00000000, PYGC00000000
Shewanella oneidensis	MR-1^T	ATCC 700550, BCRC 17276, CIP 106686, JCM 31522, LMG 19005, NCIMB 14063	Sediment from Oneida Lake, NY, USA	AE014299, AE014300 (plasmid)
Iron-oxidizing bacteria				
Mariprofundus sp.	GSB2		Iron oxide mat in a salt marsh on Great Salt Bay, Newcastle, ME, USA	NA
Iodide-oxidizing bacteria				
Iodidimonas sp.	MAT32		Brine in an iodine production facility, Japan	NA
Iodidimonas sp.	MAT33		Brine in an iodine production facility, Japan	NA
Iodidimonas sp.	MAT37		Brine in an iodine production facility, Japan	NA
Roseomonas sp.	Mat3		Brine in an iodine production facility, Japan	NA
Acetogenic bacteria				
Sporomusa sphaeroides	E^T	ATCC 35900, DSM 2875	Mud from Leine river, Germany	FCOW00000000, LSLJ00000000
Sporomusa sp.	GT1		Rice paddy field soil	NA

Abbreviations: ^{T} Type strain, *ATCC* American Type Culture Collection, *BCRC* Bioresources Collection and Research Center, *CCUG* Culture Collection, University of Göteborg, *CIP* Collection of Institut Pasteur, *DSM* German Collection of Microorganisms and Cell Cultures, *JCM* Japan Collection of Microorganisms at RIKEN, *LMG* Bacteria Collection at Belgian Co-ordinated Collections of Micro-organisms, *NBRC* Biological Resource Center at National Institute of Technology and Evaluation, *NCAIM* National Collection of Agricultural and Industrial Microorganisms, *NCIMB* National Collections of Industrial, Food and Marine Bacteria, *NRRL* Agricultural Research Service (ARS) Culture Collection, *VKM* All-Russian Collection of Microorganisms, *NA* not available

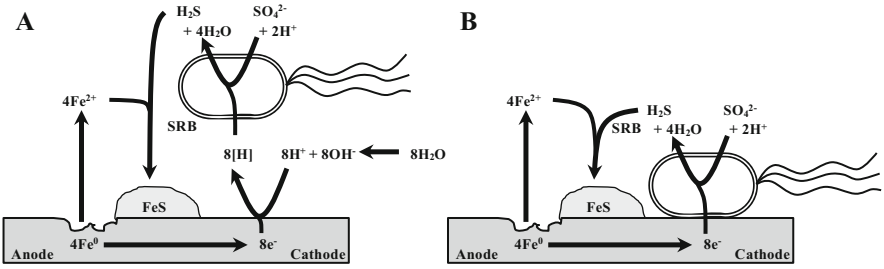

Fig. 13.1 Schematic model of iron corrosion by sulfate-reducing bacteria. (**a**) Iron corrosion caused indirectly through the production of corrosive chemical agent with hydrogen consumption activity; (**b**) iron corrosion caused directly via withdrawal of electrons by SRB

Since 1980s, role of the hydrogenase activity in the corrosion process has been accumulated using *Desulfovibrio vulgaris* strain Hildenborough (Pankhania 1988; Pankhania et al. 1986; Bryant and Laishley 1990; Bryant et al. 1991, 1993). Cells of *D. vulgaris* Hildenborough grown on cathodic hydrogen, which generated at an iron electrode surface, overexpressed two hydrogenases, the *hun-1* genes for [NiFe] hydrogenase 1 and the *hyd* genes encoding [Fe] hydrogenase, compared to that grown with gaseous hydrogen bubbling through the culture (Caffrey et al. 2008). The *hmc* genes for the high-molecular-weight cytochrome complex, which allows electron flow from the hydrogenases across the cytoplasmic membrane, were also overexpressed.

On the other hand, the validity of this theory has been questioned, as hydrogen sulfide from sulfate reduction was a cathodically active compound (Costello 1974; Spruit and Wanklyn 1951; Wanklyn and Spruit 1952) and as not all hydrogenotrophic microorganisms including acetogens, sulfate-reducing bacteria, and methanogens promoted iron corrosion (Enning et al. 2012; Mori et al. 2010).

In 2004, novel corrosive types of SRB, "*Desulfopila corrodens*" IS4, "*Desulfovibrio ferrophilus*" IS5, and *Desulfovibrio* sp. HS2 were isolated with metallic iron as the sole electron donor (Dinh et al. 2004). The direct electron transfer from an Fe^0 electrode to cells of the iron-corroding SRB, *Desulfopila corrodens* IS4, was experimentally demonstrated (Venzlaff et al. 2013) (Fig. 13.1b). Further electrochemical and infrared spectroelectrochemical analyses indicated that the direct electron transfer from Fe^0 to cells of strain IS4 occurred via *c*-type cytochromes located on the cell surface (Beese-Vasbender et al. 2015). The direct electron transfer from Fe^0 to the cells of another SRB, *Desulfovibrio ferrophilus* IS5, was also demonstrated (Deng et al. 2015, 2018). Currently, the iron corrosion caused directly via withdrawal of electrons by certain SRB is distinguished from that indirectly through a corrosive chemical agent. The former is termed electrical microbially influenced corrosion (EMIC), and the latter is chemical microbially influenced corrosion (CMIC), respectively (Enning et al. 2012).

13.2.1 Desulfopila *(Suzuki, Ueki, Amaishi, and Ueki 2007)*

Strictly anaerobic, mesophilic, and slightly alkaliphilic bacteria. Cells form rods with rounded ends. Gram-staining-negative, motile by a single polar flagellum and non-sporulating. Catalase- and oxidase-negative. Sulfate is used as alternative electron acceptor. Formate, pyruvate, lactate, fumarate, ethanol, propanol, butanol, and glycerol are used as alternative electron donors. The major respiratory quinone is MK-8. The major cellular fatty acids are $C_{16:0}$, $C_{16:1}\omega5c$, and $C_{16:1}\omega7c$. The G+C content of genomic DNA is 50–54 mol%. Represents a distinct phylogenetic lineage in the family *Desulfobulbaceae* and the order *Desulfobacterales* of the class *Deltaproteobacteria* based on 16S rRNA gene sequence analysis. At the time of writing (October 2019), the genus *Desulfopila* contains two species, *Desulfopila aestuarii* and *Desulfopila inferna* (Fig. 13.2). The type species is *Desulfopila aestuarii*.

13.2.2 Desulfovibrio *(Kluyver and van Niel 1936)*

Strictly anaerobic, mesophilic, and neutrophilic or alkaliphilic bacteria. Cells form vibrio, curved, or straight rods. Gram-staining-negative, non-motile, or motile by means of a single or lophotrichous polar flagellum. Sulfate, sulfite (most species), thiosulfate (most species), elemental sulfur (many species), nitrate (some species), Fe(III) (some species), and fumarate (some species) are used as alternative electron acceptor. Pyruvate, lactate, H_2 (most species), formate (most species), and primary alcohols (most species) are used as alternative electron donors. Fermentative growth is not observed (most species). The major respiratory quinone is MK-6 or MK-7. The major cellular fatty acids are $C_{14:0}$, iso-$C_{15:0}$, anteiso-$C_{15:0}$, $C_{16:0}$, $C_{16:1}\omega7c$, iso-$C_{17:0}$, anteiso-$C_{17:0}$, iso-$C_{17:1}\omega7c$, $C_{18:0}$, $C_{18:1}\omega7c$, and $C_{18:1}\omega9c$. The G+C content of genomic DNA is 36–69 mol%. Represents a distinct phylogenetic lineage in the family *Desulfovibrionaceae* and the order *Desulfovibrionales* of the class *Deltaproteobacteria* based on 16S rRNA gene sequence analysis. At the time of writing (October 2019), the genus *Desulvibrio* contains 55 species (Fig. 13.3). The type species is *Desulfopila desulfuricans*.

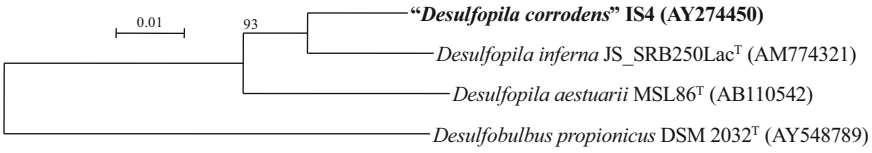

Fig. 13.2 Phylogenetic tree based on 16S rRNA gene sequences of sulfate-reducing bacteria belonging to the genus *Desulfopila*. The tree was constructed by using the neighbor-joining method. Numbers at nodes indicate bootstrap percentages derived from 1000 bootstrap replications. Bar, 0.01 substitutions per nucleotide position

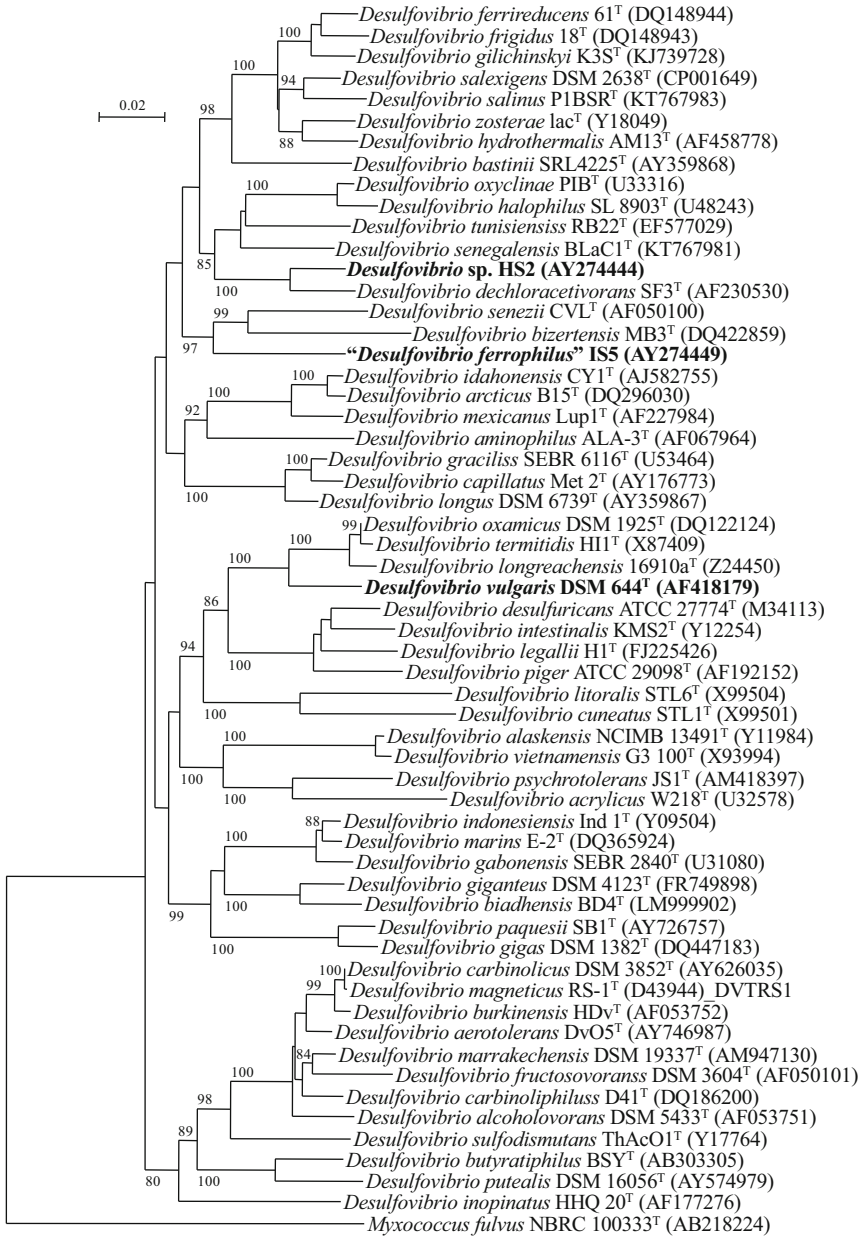

Fig. 13.3 Phylogenetic tree based on 16S rRNA gene sequences of sulfate-reducing bacteria belonging to the genus *Desulfovibrio*. The tree was constructed by using the neighbor-joining method. Numbers at nodes indicate bootstrap percentages derived from 1000 bootstrap replications. Bar, 0.02 substitutions per nucleotide position

13.3 Methanogenic Archaea (Methanogens)

Some of hydrogenotrophic methanogens that reduce carbon dioxide to methane (CO_2-respiration) cause iron corrosion under anaerobic conditions. These methanogens may be second only to SRB as the most common cause of MIC in anaerobic environments (Kip et al. 2017). Several methanogens have been shown to grow and produce methane in medium containing iron as the sole source of electrons (Daniels et al. 1987). The extent of the corrosion by these methanogens, however, was not substantial (Boopathy and Daniels 1991). *Methanobacterium* sp. strain IM1 produces methane more rapidly than does *Methanococcus maripaludis* DSM 2771 when cultured with iron granules (Dinh et al. 2004). *Methanococcus maripaludis* strains KA1, Mic1c10, MM901, and OS7 also corrode metallic iron at a rate significantly greater than the rate of an abiotic corrosion (Deutzmann et al. 2015; Mori et al. 2010; Tsurumaru et al. 2018; Uchiyama et al. 2010). The surface of the iron coupons from the KA1 culture was covered with crystalline deposits that consisted mainly of $FeCO_3$. Ferrous compounds have generally been dissolved as corrosion products in methanogen-mediated MIC.

Cell-free filtrates of spent cultures of the iron-corroding *M. maripaludis* MM901 accelerated H_2 generation from Fe^0, while filtrates of spent cultures of strain MM1284, which carried mutations in five hydrogenase genes and one dehydrogenase gene, did not accelerate it (Deutzmann et al. 2015). Since the activity in the filtrate of strain MM901 was thermolabile and proteinase-sensitive, they concluded that enzyme(s), most probably hydrogenase(s) secreted from strain MM901, catalyzed the electron withdrawal from Fe^0. *M. maripaludis* OS7 acquire electrons via direct electron transfer uptake using [NiFe] hydrogenase, catalyzing the oxidation of Fe^0 to ferrous ion: $Fe^0 + 2H^+ \rightarrow Fe^{2+} + H_2$ (Tsurumaru et al. 2018). The [NiFe] hydrogenase is excreted on the cell surface of *M. maripaludis* OS7 to obtain reducing equivalents. The genes encoding the large and small subunits of a [NiFe] hydrogenase and the TatA/TatC genes are necessary for the secretion of the [NiFe] hydrogenase.

13.3.1 Methanobacterium *(Kluyver and van Niel 1936)*

Strictly anaerobic, mesophilic or moderately thermophilic, and neutrophilic or slightly alkaliphilic. Cells form straight to irregularly crooked long rods often form filaments. Gram-staining variable. Most strains are non-sporulating. Produce methane by CO_2 reduction with H_2. Some strains produce methane from formate or secondary alcohols. The G+C content of genomic DNA is 29–61 mol%. Represents a distinct phylogenetic lineage in the family *Methanobacteriaceae* and the order *Methanobacteriales* of the class *Methanobacteria* based on 16S rRNA gene sequence analysis. At the time of writing (October 2019), the genus

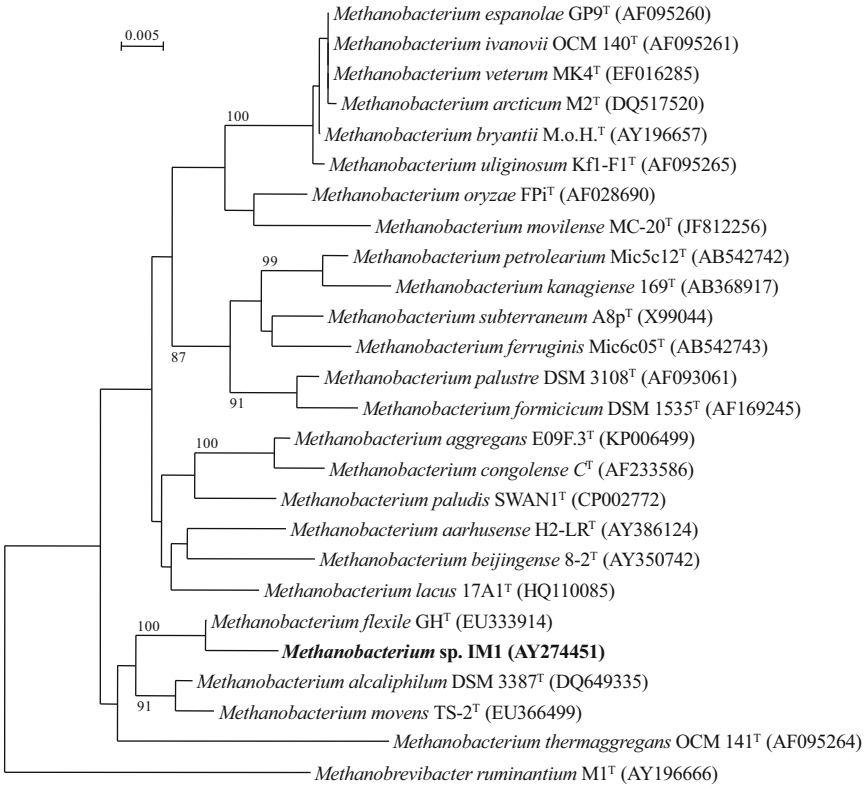

Fig. 13.4 Phylogenetic tree based on 16S rRNA gene sequences of methanogens belonging to the genus *Methanobacerium*. The tree was constructed by using the neighbor-joining method. Numbers at nodes indicate bootstrap percentages derived from 1000 bootstrap replications. Bar, 0.005 substitutions per nucleotide position

Methanobacterium contains 24 species (Fig. 13.4). The type species is *Methanobacterium formicicum*.

13.3.2 Methanococcus *(Kluyver and van Niel 1936)*

Strictly anaerobic, mesophilic, neutrophilic, and halophilic. Cells form cocci that occur singly or in pairs, while cells from older cultures are irregular. Cells lose integrity during Gram staining. Motile by polar tufts of flagella. Produce methane from H_2/CO_2 and formate. The G+C content of genomic DNA is 28–33 mol%. Represents a distinct phylogenetic lineage in the family *Methanococcaceae* and the order *Methanococcales* of the class *Methanococci* based on 16S rRNA gene sequence analysis. At the time of writing (October 2019), the genus *Methanococcus* contains four species (Fig. 13.5). The type species is *Methanococcus vannielii*.

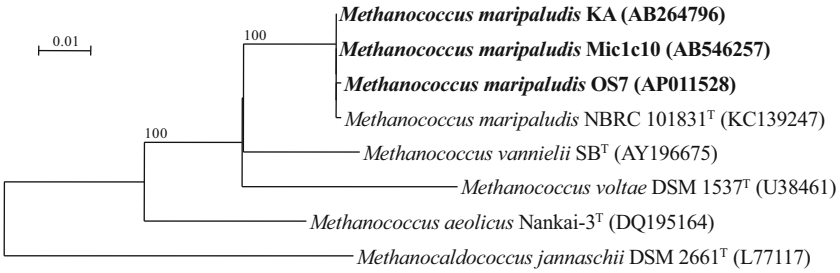

Fig. 13.5 Phylogenetic tree based on 16S rRNA gene sequences of methanogens belonging to the genus *Methanococcus*. The tree was constructed by using the neighbor-joining method. Numbers at nodes indicate bootstrap percentages derived from 1000 bootstrap replications. Bar, 0.01 substitutions per nucleotide position

13.4 Sulfate-Oxidizing Bacteria

Sulfurimonas sp. CVO corrode Fe^0 concomitantly with sulfide oxidation and nitrate reduction under anaerobic conditions (Lahme et al. 2019). When sulfide and nitrate were served under anaerobic conditions as an electron donor and a sole electron acceptor, respectively, the major corrosion products of Fe^0 formed in anaerobic cultures of *Sulfurimonas* sp. CVO is $Fe_3(PO_4)_2$.

13.4.1 Sulfurimonas *(Inagaki, Takai, Kobayashi, Nealson, and Horikoshi 2003)*

Microaerobic to facultatively anaerobic, mesophilic, neutrophilic, and chemolithoautotrophic bacteria. Cells form straight to slightly short rods, while cells form elongated rods and spiral under different culture conditions. Gram-staining-negative and non-motile or motile by means of a single polar flagellum or two flagella at opposite poles. Nitrate (most species), nitrite (many species), and O_2 (most species) are used as alternative electron acceptor. Sulfide (many species), elemental sulfur (most species), thiosulfate, and H_2 (many species) are used as alternative electron donor. The major cellular fatty acids are $C_{16:0}$, $C_{16:1}\omega7c$, and $C_{18:1}\omega7c$. The G+C content of genomic DNA is 33–37 mol%. Represents a distinct phylogenetic lineage in the family *Helicobacteraceae* and the order *Campylobacterales* of the class *Epsilonproteobacteria* based on 16S rRNA gene sequence analysis. At the time of writing (October 2019), the genus *Sulfurimonas* contains four species (Fig. 13.6). The type species is *Sulfurimonas autotrophica*.

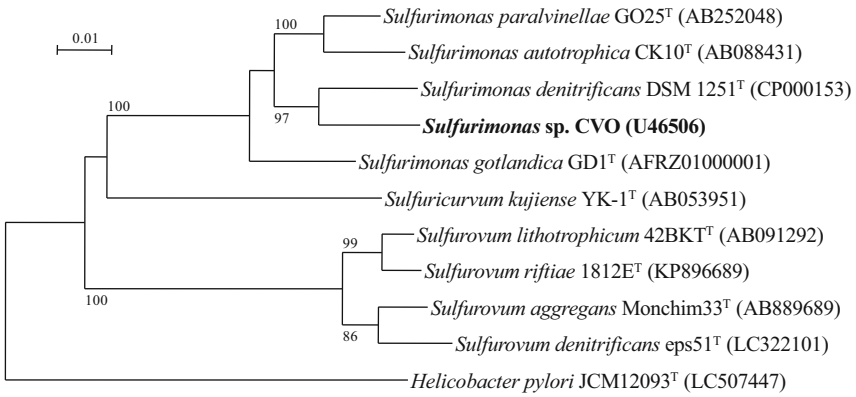

Fig. 13.6 Phylogenetic tree based on 16S rRNA gene sequences of nitrate-reducing bacteria belonging to the genus *Sulfurimonas* and related species. The tree was constructed by using the neighbor-joining method. Numbers at nodes indicate bootstrap percentages derived from 1000 bootstrap replications. Bar, 0.01 substitutions per nucleotide position

13.5 Nitrate-Reducing Bacteria

Nitrate-reducing bacteria (NRB)-assisted iron corrosion has been reported mainly in association with the remediation of nitrate-contaminated groundwater using granular Fe^0. The biological denitrification of groundwater by a combination of a hydrogenotrophic NRB and Fe^0 granules has been studied, and the addition of an NRB, such as *Paracoccus denitrificans* ATCC 17741^T, or an NRB-containing microbial consortium, generally resulted in faster nitrate removal and faster Fe^0 oxidation than in aseptic controls (Ginner et al. 2004; Kielemoes et al. 2000; Shin and Cha 2008; Till et al. 1998; Xiaomeng et al. 2009). Besides *Paracoccus denitrificans*, *Bacillus licheniformis* ATCC 14580 and *Pseudomonas aeruginosa* PA enhance the corrosion of carbon steel in the presence of nitrate (Jia et al. 2017; Xu et al. 2013). *Shewanella oneidensis* MR-1 and *Geobacter sulfurreducens* PCA notable for its diverse respiratory capabilities also stimulate iron corrosion through nitrate respiration (De Windt et al. 2003; Miller et al. 2018; Tang et al. 2019). As an iron-corroding NRB isolated from oil field with widespread internal corrosion problems, *Prolixibacter denitrificans* MIC1-1^T and *Sulfurimonas* sp. CVO corrode Fe^0 concomitantly with nitrate reduction under anaerobic conditions (Iino et al. 2015a, b; Lahme et al. 2019).

S. oneidensis MR-1 and *Geobacter sulfurreducens* PCA acquire electrons via direct electron transfer using, e.g., porin-*c*-type cytochrome complexes located on the cell surface (Breuer et al. 2015; Heidelberg et al. 2002; Liu et al. 2014; Logan et al. 2019; White et al. 2016; Xiong et al. 2006). *S. oneidensis* MR-1 possesses several complexes, one being the complex consisting of two decaheme cytochromes (MtrA and MtrC) and an outer-membrane β-barrel (MtrB), while paralogs of these proteins such as OmcA and MtrF (MtrC paralogs), MtrD (MtrA paralog), and MtrE

(MtrB paralog) are also encoded in its genome (Heidelberg et al. 2002; Xiong et al. 2006). Outer surface *c*-type cytochromes, OmcS, and OmcZ, were important for the extracellular electron transfer in *G. sulfurreducens* PCA on Fe^0 oxidation (Liu et al. 2014).

When Fe^0 and nitrate were served under anaerobic conditions as a sole electron donor and a sole electron acceptor, respectively, the major corrosion products of Fe^0 formed in anaerobic cultures of *Prolixibacter denitrificans* MIC1-1^T were $FePO_3$ and $FeCO_3$ (Iino et al. 2015b). The oxidation to ferric ion by MIC under anaerobic conditions was unusual because ferrous compounds have generally been detected as corrosion products in SRB- and methanogen-mediated MIC (Uchiyama et al. 2010; Widdel and Bak 1992; Xiaomeng et al. 2009). One explanation of the iron corrosion by NRB is the classic cathodic depolarization mechanism based on hydrogenophilic denitrification. However, given that nitrite was shown to be much more corrosive than nitrate (Lin et al. 2008), another possibility is that NRB indirectly stimulates iron corrosion through the production of nitrite. *Prolixibacter denitrificans* MIC1-1^T is not hydrogenophilic and thus may directly stimulate iron corrosion by abstracting cathodic electrons from the surface of Fe^0. The mechanism of MIC concomitantly with nitrate reduction by *Prolixibacter denitrificans* has been proposed based on biotic and abiotic chemical steps (Iino et al. 2015b). Fe^0 is oxidized primarily to ferrous ion by *P. denitrificans*:

$$Fe^0 + NO_3^- + 2H^+ \rightarrow Fe^{2+} + NO_2^- + H_2O \tag{13.6}$$

Given that *Prolixibacter denitrificans* MIC1-1 can use ferrous ions as an electron donor, ferrous ions formed by Eq. (13.6) are further oxidized to ferric ions:

$$2Fe^{2+} + NO_3^- + 2H^+ \rightarrow 2Fe^{3+} + NO_2^- + H_2O \tag{13.7}$$

In addition, chemical reactions that oxidize Fe^0 to ferrous ions concomitant with the reduction of nitrate to either nitrite (Eq. 13.6) or ammonium (Eq. 13.8) are known (Cheng et al. 1997; Choe et al. 2004).

$$4.5Fe^0 + NO_3^- + 10H^+ \rightarrow Fe^{2+} + NH_4^+ + 3H_2O \tag{13.8}$$

Chemical reactions that oxidize ferrous ions to ferric ions concomitant with the reduction of nitrate either to nitrite (Eq. 13.7) or to ammonium (Eq. 13.9) have also been reported (Rakshit et al. 2005).

$$9Fe^{2+} + NO_3^- + 10H^+ \rightarrow 9Fe^{3+} + NH_4^+ + 3H_2O \tag{13.9}$$

Thus, the reduction of nitrate to either nitrite or ammonium coupled with the oxidation of Fe^0 to Fe^{3+} is described as follows:

$$2/3Fe^0 + NO_3^- + 2\,H^+ \rightarrow 2/3Fe^{3+} + NO_2^- + H_2O \quad (13.10)$$

$$3Fe^0 + NO_3^- + 10H^+ \rightarrow 3Fe^{3+} + NH_4^+ + 3H_2O \quad (13.11)$$

Two-step chemical reactions that generate molecular hydrogen from Fe^0 are known. As shown in Eq. (13.12), Fe^0 undergoes ionization at the anode by a reaction whose rate is slow under anaerobic conditions at neutral pH:

$$Fe^0 \rightarrow Fe^{2+} + 2e^- \quad (13.12)$$

At the anode, electrons generated in reaction (13.12) are consumed to produce molecular hydrogen if no other electron acceptor is present:

$$2\,H^+ + 2e^- \rightarrow H_2 \quad (13.13)$$

Electrons and molecular hydrogen generated in the reactions shown by Eqs. (13.12) and (13.13) are largely consumed by the chemical reduction of nitrite to ammonium.

13.5.1 Geobacter *(Lovley, Giovannoni, White, Champine, Phillips, Gorby, and Goodwin 1995)*

Strictly anaerobic, mesophilic, neutrophilic and chemoorganotrophic bacteria. Cells form rods shape with rounded ends. Gram-staining-negative, non-motile or motile by means of a monotrichous polar flagellum and non-sporulating. Catalase-negative. Colonies are often pink, due to cytochrome accumulation. Elemental sulfur (many species), nitrate (some species), Fe(III), and Mn(IV) (most species) are used as alternative electron acceptor. H_2 (many species), formate (many species), acetate, pyruvate (many species), lactate (many species), primary alcohols (many species), and monoaromatic hydrocarbons (many species) are used as alternative electron donors. Fermentative growth is not observed. The major respiratory quinone is MK-8. The major cellular fatty acids are $C_{16:0}$ and $C_{16:1}\omega 7c$. The G+C content of genomic DNA is 50–61 mol%. Represents a distinct phylogenetic lineage in the family *Geobacteraceae* and the order *Desulfuromonadales* of the class *Deltaproteobacteria* based on 16S rRNA gene sequence analysis. At the time of writing (October 2019), the genus *Desulvibrio* contains 19 species and 2 subspecies (Fig. 13.7). The type species is *Geobacter sulfurreducens*.

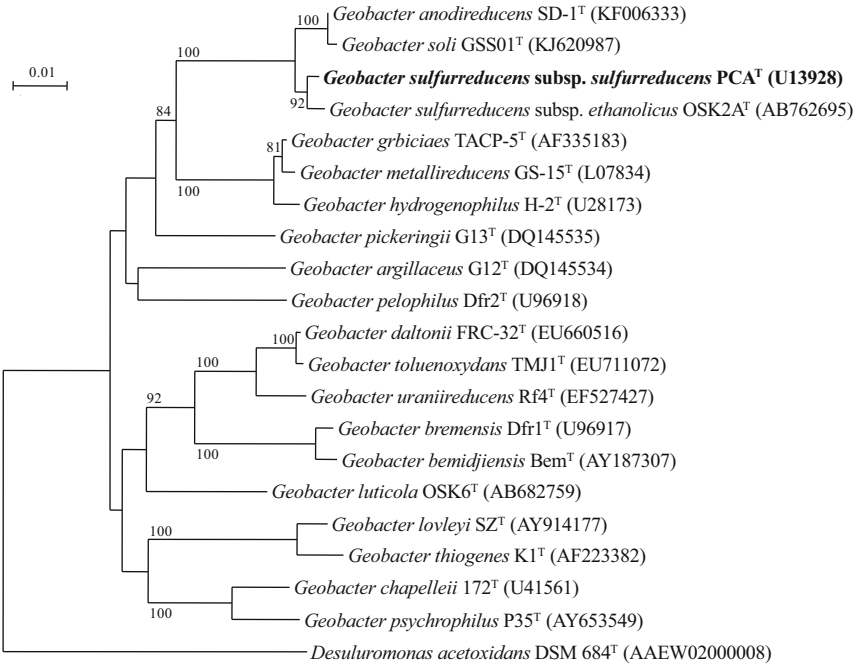

Fig. 13.7 Phylogenetic tree based on 16S rRNA gene sequences of nitrate-reducing bacteria belonging to the genus *Geobacter*. The tree was constructed by using the neighbor-joining method. Numbers at nodes indicate bootstrap percentages derived from 1000 bootstrap replications. Bar, 0.01 substitutions per nucleotide position

13.5.2 Prolixibacter *(Holmes, Nevin, Woodard, Peacock, and Lovley 2007)*

Facultatively anaerobic, mesophilic, neutrophilic, moderately halophilic, and chemoorganotrophic bacteria. Cells form long, filamentous, curved rods. Gram-staining-negative, non-motile, and non-sporulating. Catalase- and oxidase-positive. Nitrate (*P. denitrificans*) and O_2 are used as alternative electron acceptor. Fe (0) (*P. denitrificans*), Fe(II) (*P. denitrificans*), and L-cysteine are used as alternative electron donors. Fermentative growth is observed. The major respiratory quinone is MK-7. The major cellular fatty acids are iso-$C_{15:0}$ and anteiso-$C_{15:0}$. The major polar lipids are phosphatidylethanolamine, unidentified phospholipids, and unidentified lipids. The G+C content of genomic DNA is 42–45 mol%. Represents a distinct phylogenetic lineage in the family *Prolixibacteraceae* and the order *Marinilabiliales* of the class *Bacteroidia* based on 16S rRNA gene sequence analysis. At the time of writing (October 2019), the genus *Prolixibacter* contains two species, *Prolixibacter bellariivorans* and *Prolixibacter denitrificans* (Fig. 13.8). The type species is *Prolixibacter bellariivorans*.

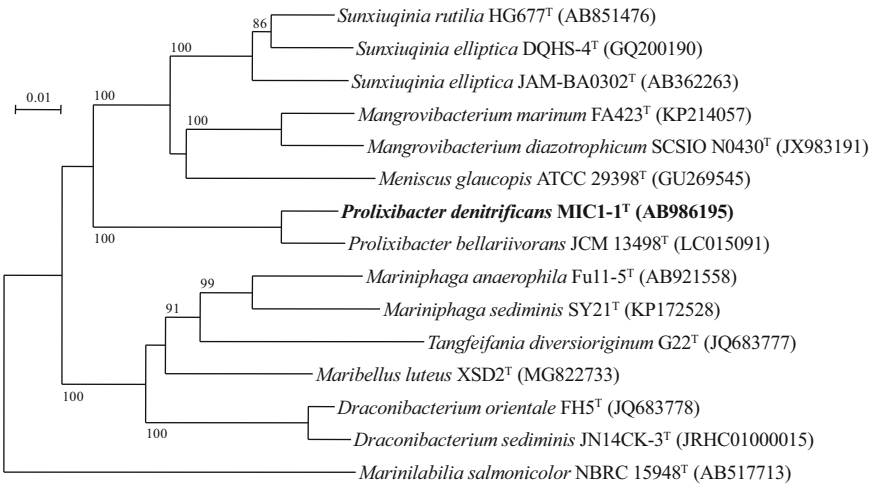

Fig. 13.8 Phylogenetic tree based on 16S rRNA gene sequences of nitrate-reducing bacteria belonging to the genus *Prolixibacter* and related species. The tree was constructed by using the neighbor-joining method. Numbers at nodes indicate bootstrap percentages derived from 1000 bootstrap replications. Bar, 0.01 substitutions per nucleotide position

13.5.3 Shewanella *(MacDonell and Colwell 1986)*

Facultatively anaerobic, mesophilic to psychrophilic, neutrophilic to moderately alkaliphilic, and chemoheterotrophic bacteria. Cells form straight or curved rods. Gram-staining-negative, motile by means of a single, unsheathed, polar flagellum, and non-sporulating. Catalase- and oxidase-positive. Colonies are often pale tan to pink-orange, due to cytochrome accumulation. Nitrate, nitrite, Fe(III), Mn(IV), and O_2 are used as alternative electron acceptor with organic carbon compounds or H_2 as the electron donor. Fermentative growth is observed (some species). The major respiratory quinone are Q-7, Q-8, and MK-7. The major cellular fatty acids are iso-$C_{13:0}$, $C_{14:0}$, $C_{15:0}$, iso-$C_{15:0}$, $C_{16:0}$, $C_{16:1}\omega7c$, and $C_{18:1}\omega7c$. The G+C content of genomic DNA is 38–54 mol%. Represents a distinct phylogenetic lineage in the family *Shewanellaceae* and the order *Alteromonadales* of the class *Gammaproteobacteria* based on 16S rRNA gene sequence analysis. At the time of writing (October 2019), the genus *Desulvibrio* contains 70 species (Fig. 13.9). The type species is *Shewanella putrefaciens*.

13.6 Iron-Oxidizing Bacteria

Mariprofundus is an obligate lithotroph whose only known energy source is Fe^{2+} oxidation coupled to respiration of oxygen (Emerson et al. 2007; McBeth et al. 2011). Stalk-forming iron-oxidizing *Mariprofundus* sp. GSB2, isolated from an iron

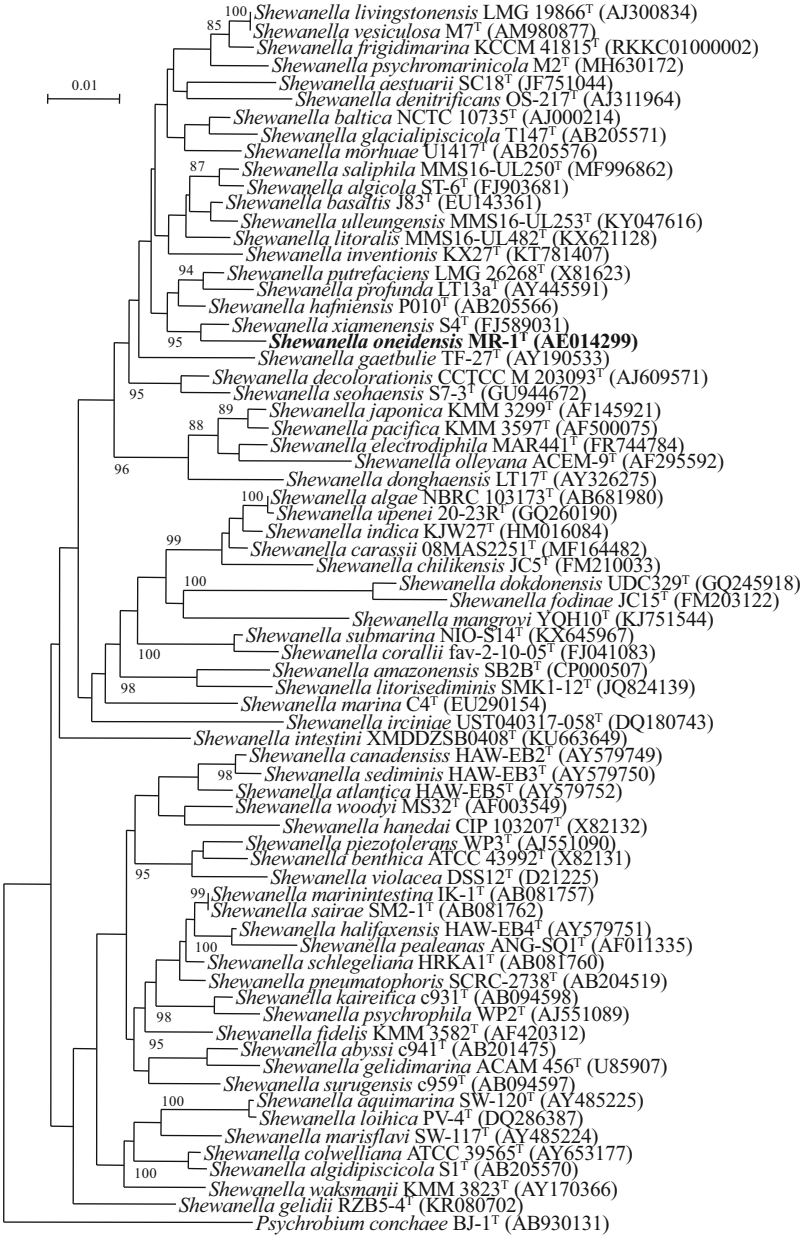

Fig. 13.9 Phylogenetic tree based on 16S rRNA gene sequences of nitrate-reducing bacteria belonging to the genus *Shewanella*. The tree was constructed by using the neighbor-joining method. Numbers at nodes indicate bootstrap percentages derived from 1000 bootstrap replications. Bar, 0.01 substitutions per nucleotide position

oxide mat in a salt marsh, enhances mild steel corrosion under microaerobic condition. This bacterium is able to grow by using mild steel, Fe^0 particle, FeS, and ferrous chloride as am Fe(II) source.

13.6.1 Mariprofundus *(Emerson, Rentz, Lilburn, Davis, Aldrich, Chan, and Moyer 2010)*

Microaerobic, mesophilic, neutrophilic, and obligately lithotrophic bacteria. Cells form curved rods. Gram-staining-negative. Catalase-negative. Fe(II) is used as alternative electron donors with O_2 as the electron acceptor. The major cellular fatty acids are $C_{16:0}$, iso-$C_{11:0}$-3OH, iso-$C_{17:0}$-3OH, and iso-$C_{18:1}$-H. The G+C content of genomic DNA is 54 mol%. Represents a monophyletic candidate lineage designated as "*Zetaproteobacteria*" based on 16S rRNA gene sequence analysis. At the time of writing (October 2019), the genus *Mariprofundus* contains a single species (Fig. 13.10). The type species is *Mariprofundus ferrooxydans*.

13.7 Iodide-Oxidizing Bacteria

Iodide-oxidizing bacteria (IOB) exhibit iodide-oxidizing ability by forming purple iodine-starch complexes on agar plates supplemented with soluble starch. IOB provoke iron corrosion in aerobic condition. The 16S rRNA gene sequence analysis showed that iron-corroding IOB were classified into two groups established two IOB groups, A and B (Amachi et al. 2005). Strain Mat3 was classified into group A comprising the genus *Roseovarius*, and strains MAT32, MAT33, and MAT37 were classified into group B comprising the genus *Iodidimonas* (Iino et al. 2016; Wakai et al. 2014). Each isolates from the two groups corrode iron in the presence of potassium iodide in a concentration-dependent manner. The following mechanism of IOB-mediated iron corrosion was proposed by Wakai et al. (2014). IOBs produce molecular iodine by oxidizing iodide ions:

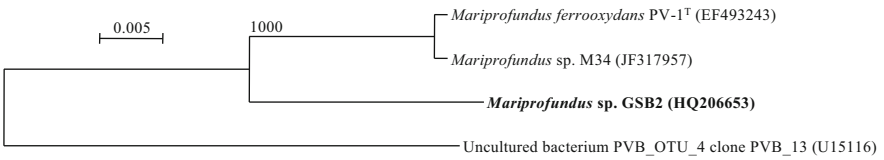

Fig. 13.10 Phylogenetic tree based on 16S rRNA gene sequences of iron-oxidizing bacteria belonging to the genus *Mariprofundus*. The tree was constructed by using the neighbor-joining method. Numbers at nodes indicate bootstrap percentages derived from 1000 bootstrap replications. Bar, 0.005 substitutions per nucleotide position

$$2I^- = I_2 + 2e^- \tag{13.14}$$

A water solubility of molecular iodine is significantly low, but it can be solubilized as triiodide ions (I_3^-) by combining with iodide ions:

$$I_2 + I^- = I_3^- \tag{13.15}$$

Since molecular iodine and triiodide ions are strong oxidizing reagents and corrode iron [11–13], iron is oxidized, and iodide ions are regenerated:

$$I_2 + Fe^0 = 2I^- + Fe^{2+} \tag{13.16}$$

$$I_3^- + Fe^0 = 3I^- + Fe^{2+} \tag{13.17}$$

Thus, in the presence of IOBs and iron, iodide ions are recycled to repeat the process of iron oxidation.

13.7.1 Iodidimonas *(Iino, Ohkuma, Kamagata, and Amachi 2016)*

Aerobic, mesophilic, neutrophilic, moderately halophilic, and chemo-organotrophic bacteria. Cells form rods. Gram-staining-negative, motile, and non-sporulating. Catalase- and oxidase-positive. Colonies are creamy white. Oxidizes iodide on Marine Agar 2216. Fermentative growth is not observed. The major isoprenoid quinone is Q-10. The major cellular fatty acids are $C_{18:1}\omega7c$ and $C_{16:1}\omega5c$. The major polar lipids are phosphatidylethanolamine, phosphatidylglycerol, diphosphatidylglycerol, and an unidentified aminolipid. The G+C content of genomic DNA is 58 mol%. Represents a distinct phylogenetic lineage in the family *Iodidimonadaceae* and the order *Iodidimonadales* of the class *Alphaproteobacteria* based on 16S rRNA gene sequence analysis. At the time of writing (October 2019), the genus *Iodidimonas* contains a single species (Fig. 13.11). The type species is *Iodidimonas muriae*.

13.7.2 Roseovarius *(Labrenz, Collins, Lawson, Tindall, Schumann, and Hirsch 1999)*

Aerobic, mesophilic, neutrophilic to alkaliphilic, and heterotrophic bacteria. Cells form rods. Gram-staining-negative and motile. Catalase- and oxidase-positive. Poly-β-hydroxybutyrate (PHB) are present. Bacteriochlorophyll *a* (bchl *a*) may be produced and colonies are pigmented. Fermentative growth is not observed. The

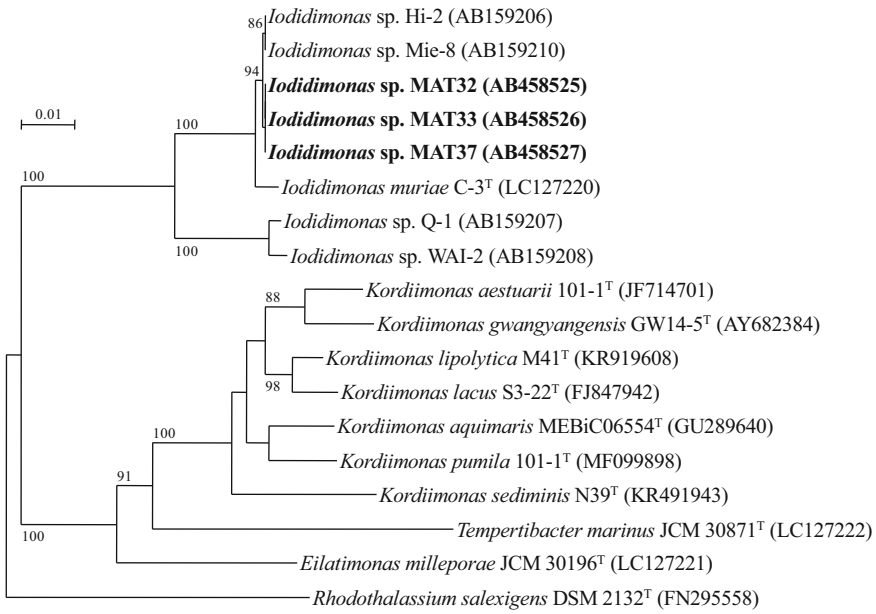

Fig. 13.11 Phylogenetic tree based on 16S rRNA gene sequences of iodide-reducing bacteria belonging to the genus *Iodidimonas* and related species. The tree was constructed by using the neighbor-joining method. Numbers at nodes indicate bootstrap percentages derived from 1000 bootstrap replications. Bar, 0.01 substitutions per nucleotide position

major isoprenoid quinone is Q-10. The major cellular fatty acids are $C_{16:0}$, $C_{18:0}$, $C_{16:1}$, $C_{18:2}$, $C_{12:0}$-2OH, and $C_{12:1}$-3OH. The major polar lipids are phosphatidylethanolamine, phosphatidylcholine, phosphatidylglycerol, diphosphatidylglycerol, an unknown phospholipid, and an unknown lipid. The G+C content of genomic DNA is 55–66 mol%. Represents a distinct phylogenetic lineage in the family *Rhodobacteraceae* and the order *Rhodobacterales* of the class *Alphaproteobacteria* based on 16S rRNA gene sequence analysis. At the time of writing (October 2019), the genus *Roseovarius* contains 26 species (Fig. 13.12). The type species is *Roseovarius tolerans*.

13.8 Acetogenic Bacteria (Acetogens)

Acetogenesis-assisted iron corrosion has been observed in microbial consortia derived from pipeline water samples of a water treatment facility (Mand et al. 2014). Acetogens conserve energy through acetogenesis.

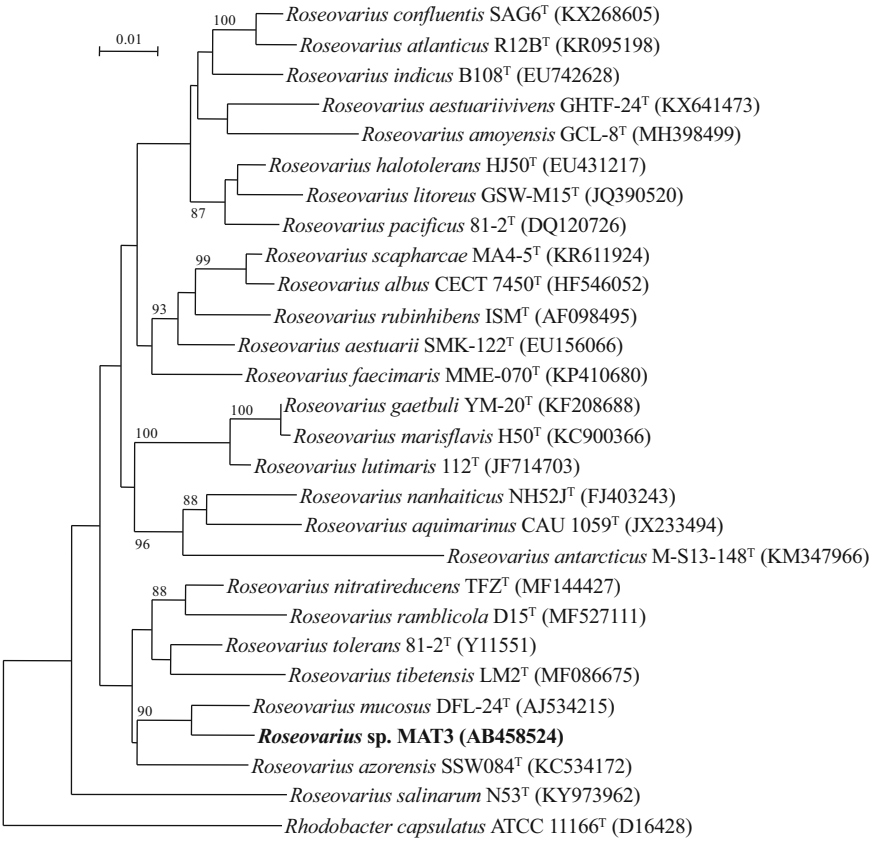

Fig. 13.12 Phylogenetic tree based on 16S rRNA gene sequences of iodide-reducing bacteria belonging to the genus *Roseomonas*. The tree was constructed by using the neighbor-joining method. Numbers at nodes indicate bootstrap percentages derived from 1000 bootstrap replications. Bar, 0.01 substitutions per nucleotide position

$$2HCO_3^- + 9H^+ + 8e^- = CH_3COO^- + 4H_2O$$

The resulting ferrous ions were precipitated in part with the sulfide produced, forming characteristic black iron sulfide. Therefore, this corrosion seems that the production of acetate by homoacetogens, such as *Acetobacterium*, resulted in iron corrosion by SRB which required acetate as a carbon source for the growth.

On the other hand, *Sporomusa* sp. GT1, which was isolated from rice paddy field soil and *Sporomusa sphaeroides* DSM 2875^T, grow acetogenetically with Fe^0 as the sole electron donor and enhanced iron corrosion (Kato et al. 2015).

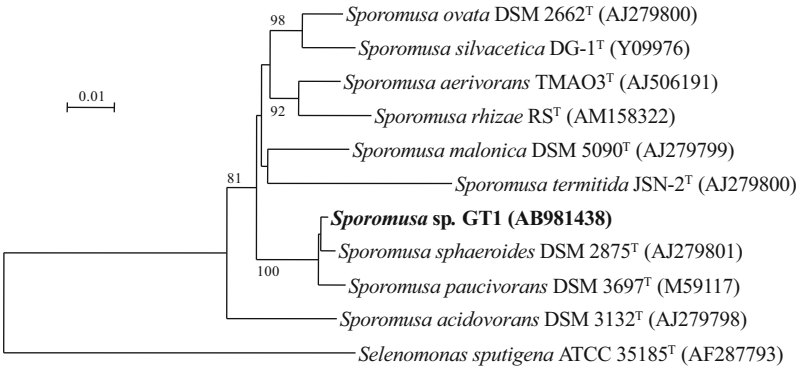

Fig. 13.13 Phylogenetic tree based on 16S rRNA gene sequences of acetogenic bacteria belonging to the genus *Sporomusa*. The tree was constructed by using the neighbor-joining method. Numbers at nodes indicate bootstrap percentages derived from 1000 bootstrap replications. Bar, 0.01 substitutions per nucleotide position

13.8.1 Sporomusa *(Möller, Ossmer, Howard, Gottschalk, and Hippe 1985)*

Strictly anaerobic, mesophilic, neutrophilic, chemoorganotrophic, and chemolithotropic bacteria using H_2 plus CO_2 as growth substrate. Cells form curved rods with tapered ends. Gram-staining-negative or weakly positive, motile by means of a monotrichous polar flagellum, and sporulating. Catalase-positive and oxidase-negative. Fermentative growth is observed. Acetate is the major end product. The G+C content of genomic DNA is 42–48 mol%. Represents a distinct phylogenetic lineage in the family *Sporomusaceae* and the order *Selenomonadales* of the class *Negativicutes* based on 16S rRNA gene sequence analysis. At the time of writing (October 2019), the genus *Sporomusa* contains nine species (Fig. 13.13). The type species is *Sporomusa sphaeroides*.

References

Amachi S, Muramatsu Y, Akiyama Y, Miyazaki K, Yoshiki S, Hanada S, Kamagata Y, Ban-nai T, Shinoyama H, Fujii T (2005) Isolation of iodide-oxidizing bacteria from iodide-rich natural gas brines and seawaters. Microb Ecol 49:547–557

Beese-Vasbender PF, Nayak S, Erbe A, Stratmann M, Mayrhofer KJJ (2015) Electrochemical characterization of direct electron uptake in electrical microbially influenced corrosion of iron by the lithoautotrophic SRB *Desulfopila corrodens* strain IS4. Electrochim Acta 167:321–329

Boopathy R, Daniels L (1991) Effect of pH on anaerobic mild steel corrosion by methanogenic bacteria. Appl Environ Microbiol 57:2104–2108

Breuer M, Rosso KM, Blumberger J, Butt JN (2015) Multi-haem cytochromes in *Shewanella oneidensis* MR-1: structures, functions and opportunities. J R Soc Interface 12:20141117

Bryant RD, Laishley EJ (1990) The role of hydrogenase in anaerobic biocorrosion. Can J Microbiol 36:259–264

Bryant RD, Jansen W, Boivin J, Laishley EJ, Costerton JW (1991) Effect of hydrogenase and mixed sulfate-reducing bacterial populations on the corrosion of steel. Appl Environ Microbiol 57:2804–2809

Bryant RD, Van Ommen Kloeke F, Laishley EJ (1993) Regulation of the periplasmic [Fe] hydrogenase by ferrous iron in *Desulfovibrio vulgaris* (Hildenborough). Appl Environ Microbiol 59:491–495

Butlin KR, Adams ME, Thomas M (1949) Sulphate-reducing bacteria and internal corrosion of ferrous pipes conveying water. Nature 163:26–27

Caffrey SM, Park HS, Been J, Gordon P, Sensen CW, Voordouw G (2008) Gene expression by the sulfate-reducing bacterium *Desulfovibrio vulgaris* Hildenborough grown on an iron electrode under cathodic protection conditions. Appl Environ Microbiol 74:2404–2413

Cheng IF, Muftikian R, Fernando Q, Korte N (1997) Reduction of nitrate to ammonia by zero-valent iron. Chemosphere 35:2689–2695

Choe C, Liljestrand HM, Khim J (2004) Nitrate reduction by zero-valent iron under different pH regimes. Appl Geochem 19:335–342

Costello JA (1974) Cathodic depolarization by sulphate-reducing bacteria. S Afr J Sci 70:202–204

Daniels L, Belay N, Rajagopal BS, Weimer PJ (1987) Bacterial methanogenesis and growth from CO_2 with elemental iron as the sole source of electrons. Science 237:509–511

De Windt W, Boon N, Siciliano SD, Verstraete W (2003) Cell density related H_2 consumption in relation to anoxic Fe(0) corrosion and precipitation of corrosion products by *Shewanella oneidensis* MR-1. Environ Microbiol 5:1192–1202

Deng X, Nakamura R, Hashimoto K, Okamoto A (2015) Electron extraction from an extracellular electrode by *Desulfovibrio ferrophilus* strain IS5 without using hydrogen as an electron carrier. Electrochemistry 83:529–531

Deng X, Dohmae N, Nealson KH, Hashimoto K, Okamoto A (2018) Multi-heme cytochromes provide a pathway for survival in energy-limited environments. Sci Adv 4:eaao5682

Deutzmann JD, Sahin M, Spormann AM (2015) Extracellular enzymes facilitate electron uptake in biocorrosion and bioelectrosynthesis. mBio 6:e00496-15

Dinh HT, Kuever J, Muβmann M, Hassel AW, Stratmann M, Widdel F (2004) Iron corrosion by novel anaerobic microorganisms. Nature 427:829–832

Emerson D, Rentz JA, Lilburn TG, Davis RE, Aldrich H, Chan C, Moyer CL (2007) A novel lineage of *Proteobacteria* involved in formation of marine Fe-oxidizing microbial mat communities. PLoS One 2:e667

Enning D, Venzlaff H, Garrelfs J, Dinh HT, Meyer V, Mayrhofer K, Hassel AW, Stratmann M, Widdel F (2012) Marine sulfate-reducing bacteria cause serious corrosion of iron under electroconductive biogenic mineral crust. Environ Microbiol 14:1772–1787

Enning E, Garrelfs J (2014) Corrosion of iron by sulfate-reducing bacteria: new views of an old problem. Appl Environ Microbiol 80:1226–1236

Ginner JL, Alvarez PJJ, Smith SL, Scherer MM (2004) Nitrate and nitrite reduction by Fe^0: influence of mass transport, temperature, and denitrifying microbes. Environ Eng Sci 21:219–229

Heidelberg JF, Paulsen IT, Nelson KE, Gaidos EJ, Nelson WC, Read TD, Eisen JA, Seshadri R, Ward N, Methe B, Clayton RA, Meyer T, Tsapin A, Scott J, Beanan M, Brinkac L, Daugherty S, DeBoy RT, Dodson RJ, Durkin AS, Haft DH, Kolonay JF, Madupu R, Peterson JD, Umayam LA, White O, Wolf AM, Vamathevan J, Weidman J, Impraim M, Lee K, Berry K, Lee C, Mueller J, Khouri H, Gill J, Utterback TR, McDonald LA, Feldblyum TV, Smith HO, Venter JC, Nealson KH, Fraser CM (2002) Genome sequence of the dissimilatory metal ion-reducing bacterium *Shewanella oneidensis*. Nat Biotechnol 20:1118–1123

Iino T, Sakamoto M, Ohkuma M (2015a) *Prolixibacter denitrificans* sp. nov., an iron-corroding, facultatively aerobic, nitrate-reducing bacterium isolated from crude oil, and emended

descriptions of the genus *Prolixibacter* and *Prolixibacter bellariivorans*. Int J Syst Evol Microbiol 65:2865–2869

Iino T, Ito K, Wakai S, Tsurumaru H, Ohkuma M, Harayama S (2015b) Iron corrosion induced by nonhydrogenotrophic nitrate-reducing *Prolixibacter* sp. strain MIC1-1. Appl Environ Microbiol 81:1839–1846

Iino T, Ohkuma M, Kamagata Y, Amachi S (2016) *Iodidimonas muriae* gen. nov., sp. nov., an aerobic iodide-oxidizing bacterium isolated from brine of a natural gas and iodine recovery facility, and proposals of *Iodidimonadaceae* fam. nov., *Iodidimonadales* ord. nov., *Emcibacteraceae* fam. nov. and *Emcibacterales* ord. nov. Int J Syst Evol Microbiol 66:5016–5022

Inagaki F, Takai K, Kobayashi H, Nealson KH, Horikoshi K (2003) *Sulfurimonas autotrophica* gen. nov., sp. nov., a novel sulfur-oxidizing ε-proteobacterium isolated from hydrothermal sediments in the Mid-Okinawa Trough. Int J Syst Evol Microbiol 53:1801–1805

Iverson WP (1966) Direct evidence for the cathodic depolarization theory of bacterial Corrosion. Science 151:986–988

Jia R, Yang D, Xu D, Gu T (2017) Electron transfer mediators accelerated the microbiologically influence corrosion against carbon steel by nitrate reducing *Pseudomonas aeruginosa* biofilm. Bioelectrochemistry 118:38–46

Kato S, Yumoto I, Kamagata Y (2015) Isolation of acetogenic bacteria that induce biocorrosion by utilizing metallic iron as the sole electron donor. Appl Environ Microbiol 81:67–73

Kielemoes J, De Boever P, Verstraete W (2000) Influence of denitrification on the corrosion of iron and stainless steel powder. Environ Sci Technol 34:663–671

Kip N, Jansen S, Leite MFA, de Hollander M, Afanasyev M, Kuramae EE, Van Veen JA (2017) Methanogens predominate in natural corrosion protective layers on metal sheet piles. Sci Rep 7:11899

Kluyver AJ, van Niel CB (1936) Prospects for a natural system of classification of bacteria. Zentralblatt fur Bakteriologie Parasitenkunde Infektionskrankheiten und Hygiene. Abteilung II 94:369–403

Labrenz M, Collins MD, Lawson PA, Tindall BJ, Schumann P, Hirsch P (1999) *Roseovarius tolerans* gen. nov., sp. nov., a budding bacterium with variable bacteriochlorophyll *a* production from hypersaline Ekho Lake. Int J Syst Bacteriol 49:137–147

Lahme S, Enning D, Callbeck CM, Menendez Vega D, Curtis TP, Head IM, Hubert CRJ (2019) Metabolites of an oil field sulfide-oxidizing, nitrate-reducing *Sulfurimonas* sp. cause severe corrosion. Appl Environ Microbiol 85:e01891–e01818

Lin KS, Chang NB, Chuang TD (2008) Fine structure characterization of zero-valent iron nanoparticles for decontamination of nitrites and nitrates in wastewater and groundwater. Sci Technol Adv Mater 9:0250151

Liu Y, Wang Z, Liu J, Levar C, Edwards MJ, Babauta JT, Kennedy DW, Shi Z, Beyenal H, Bond DR, Clarke TA, Butt JN, Richardson DJ, Rosso KM, Zachara JM, Fredrickson JK, Shi L (2014) A trans-outer membrane porin–cytochrome protein complex for extracellular electron transfer by *Geobacter sulfurreducens* PCA. Environ Microbiol Rep 6:776–785

Logan BE, Rossi R, Ragab AA, Saikaly PE (2019) Electroactive microorganisms in bioelectrochemical systems. Nat Rev Microbiol 17:307–319

Mand J, Park HS, Jack TR, Voordouw G (2014) The role of acetogens in microbially influenced corrosion of steel. Front Microbiol 5:268

McBeth JM, Little BJ, Ray RI, Farrar KM, Emerson D (2011) Neutrophilic iron-oxidizing "*Zetaproteobacteria*" and mild steel corrosion in nearshore marine environments. Appl Environ Microbiol 77:1405–1412

Miller RB II, Lawson K, Sadek A, Monty CN, Senko JM (2018) Uniform and pitting corrosion of carbon steel by *Shewanella oneidensis* MR-1 under nitrate-reducing conditions. Appl Environ Microbiol 84:e00790–e00718

Mori K, Tsurumaru H, Harayama S (2010) Iron corrosion activity of anaerobic hydrogen-consuming microorganisms isolated from oil facilities. J Biosci Bioeng 110:426–430

Pankhania IP (1988) Hydrogen metabolism in sulphate-reducing bacteria and its role in anaerobic corrosion. Biofouling 1:27–24

Pankhania IP, Moosavi AN, Hamilton WA (1986) Utilization of cathodic hydrogen by *Desulfovibrio vulgaris* (Hildenborough). J Gen Microbiol 132:3357–3365

Rakshit S, Matocha CJ, Haszler GR (2005) Nitrate reduction in the presence of wüstite. J Environ Qual 34:1286–1292

Shin KH, Cha DK (2008) Microbial reduction of nitrate in the presence of nanoscale zero-valent iron. Chemosphere 72:257–262

Spruit CJP, Wanklyn JN (1951) Iron sulphide ratios in corrosion by sulphate-reducing bacteria. Nature 168:951–952

Starkey RL (1947) Sulfate reduction and the anaerobic corrosion of iron. Antonie Van Leeuwenhoek 12:193–203

Suzuki D, Ueki A, Amaishi A, Ueki K (2007) *Desulfopila aestuarii* gen. nov., sp. nov., a Gram-negative, rod-like, sulfate-reducing bacterium isolated from an estuarine sediment in Japan. Int J Syst Evol Microbiol 57:520–526

Tang HY, Holmes DE, Ueki T, Palacios PA, Lovley DR (2019) Iron corrosion via direct metal-microbe electron transfer. mBio 10:e00303-19

Till BA, Weathers LJ, Alvarez PJJ (1998) Fe(0)-supported autotrophic denitrification. Environ Sci Technol 32:634–639

Tsurumaru H, Ito N, Mori K, Wakai S, Uchiyama T, Iino T, Hosoyama A, Ataku H, Nishijima K, Mise M, Shimizu A, Harada T, Horikawa H, Ichikawa N, Sekigawa T, Jinno K, Tanikawa S, Yamazaki J, Sasaki K, Yamazaki S, Fujita N, Harayama H (2018) An extracellular [NiFe] hydrogenase mediating iron corrosion is encoded in a genetically unstable genomic island in *Methanococcus maripaludis*. Sci Rep 8:15149

Uchiyama T, Ito K, Mori K, Tsurumaru H, Harayama S (2010) Iron-corroding methanogen isolated from a crude-oil storage tank. Appl Environ Microbiol 76:1783–1788

Venzlaff H, Enning D, Srinivasan J, Mayrhofer K, Hassel AW, Widdel F, Stratmann M (2013) Accelerated cathodic reaction in microbial corrosion of iron due to direct electron uptake by sulfate-reducing bacteria. Corros Sci 66:88–96

von Wolzogen Kühr CAH, van der Vlugt IS (1934) The graphitization of cast iron as an electrobiochemical process in anaerobic soil. Water 18:147–165

Wakai S, Ito K, Iino T, Tomoe Y, Mori K, Harayama S (2014) Corrosion of iron by iodide-oxidizing bacteria isolated from brine in an iodine production facility. Microb Ecol 68:519–527

Wanklyn JN, Spruit CJP (1952) Influence of sulphate-reducing bacteria on the corrosion potential of iron. Nature 169:928–929

White GF, Edwards MJ, Gomez-Perez L, Richardson DJ, Butt JN, Clarke TA (2016) Mechanisms of bacterial extracellular electron exchange. In: Advances in microbial physiology, vol 68. Academic Press, Cambridge, MA, pp 87–138

Widdel F, Bak F (1992) Gram-negative mesophilic sulfate-reducing bacteria. In: Balows A, Trüper HG, Dworkin M, Harder W, Schleifer K-H (eds) The prokaryotes, vol 6, 2nd edn. Springer, New York, pp 3352–3378

Xiaomeng F, Xiaohong G, Jun M, Hengyu A (2009) Kinetics and corrosion products of aqueous nitrate reduction by iron powder without reaction conditions control. J Environ Sci 21:1028–1035

Xiong Y, ShiL CB, Mayer MU, Lower BH, Londer Y, Bose S, Hochella MF, Fredrickson JK, Squier TC (2006) High-affinity binding and direct electron transfer to solid metals by the *Shewanella oneidensis* MR-1 outer membrane *c*-type cytochrome OmcA. J Am Chem Soc 128:13978–13979

Xu D, Li Y, Song F, Gu T (2013) Laboratory investigation of microbiologically influenced corrosion of C1018 carbon steel by nitrate reducing bacterium *Bacillus licheniformi*s. Corros Sci 77:385–390

Chapter 14
Electron Flow Rate in Microbiologically Influenced Corrosion and Its Applications

Satoshi Wakai

14.1 Introduction

In this chapter, the electron flow rate during corrosion by electron-utilizing microorganisms will be discussed. To date, many papers on iron-corrosive microorganisms have reported (Dinh et al. 2004; Uchiyama et al. 2010; Mori et al. 2010; McBeth et al. 2011; Wakai et al. 2014; Kato et al. 2015; Iino et al. 2015), some of which are proceeding by directly using electron; however little is known regarding corrosion reactions per unit area. Unfortunately, in many studies, experiments were conducted using iron granules with an unknown surface area, and corrosion was evaluated by relative weight loss. In addition, some researchers used excessive amounts of iron granules in cultivation, and excess amounts of metallic iron result in the constant generation of molecular hydrogen; therefore, hydrogen-consuming microorganisms can grow. Using a medium with an excessive amount of iron granules for the cultivation of hydrogen-utilizing, sulfate-reducing bacteria (SRB) results in the generation of hydrogen sulfide, from the bacterial consumption of molecular hydrogen, and this production of sulfide indirectly corrodes the metallic iron. Consequently, the interpretation of electron flow during corrosion becomes very complicated because the influence of certain sulfides must be subtracted. Therefore, it is necessary to follow the accelerated corrosion reaction, rather than chemical corrosion, while minimizing hydrogen generation. Similarly, a corrosion test whereby SRB is enriched and cultivated in a nutrient-rich medium would make it difficult to understand the corrosion ability of the cultivated SRB. Such corrosion involves a large amount of indirect chemical corrosion and is not likely the result of direct microbial corrosion.

S. Wakai (✉)
Institute for Extra-cutting-edge Science and Technology Avant-garde Research (X-star), Japan Agency for Marine-Earth Science and Technology (JAMSTEC), Yokosuka, Japan
e-mail: wakais@jamstec.go.jp

M. Ishii, S. Wakai (eds.), *Electron-Based Bioscience and Biotechnology*,
https://doi.org/10.1007/978-981-15-4763-8_14

Electrochemical tests may be useful for analyzing electron transfer per unit area. Recently, bio-based researchers have expanded their methods of analysis to include the use of electrochemical devices and techniques. Recently, cyclic voltammetry has been used to identify the redox properties of enzymes, and electrochemical analysis techniques, such as impedance measurements, have been incorporated into studies on microbial fuel cells. However, to perform an electrochemical test, an electrochemical device, as well as knowledge regarding electrochemical and experimental techniques, is required. Furthermore, impedance measurements cannot be performed with a conventional potentiogalvanostat device; therefore, an additional instrument is required. This makes it difficult for researchers, based on biochemistry and molecular biology, to get started. Therefore, this chapter also introduces experiments that can be performed using conventional apparatus. Additionally, the electron flow rate for the corrosion phenomenon of iron-corrosive methanogens, which, based on gas analysis, do not produce corrosive gases, will be discussed.

14.2 Corrosion by Iron-Corrosive Methanogen

Several strains have been reported as iron-corrosive methanogens; however, unlike the electron-utilizing SRB, the characteristics of the biomolecules related to corrosion are insufficiently understood.

14.2.1 Iron-Corrosive Methanogen IM1 Strain Isolated from Marine Sediments

In a study on novel corrosive anaerobic microorganisms, the emphasis was placed on SRB, but it also mentioned iron-corrosive methanogens (Dinh et al. 2004). Like iron-corrosive SRB, the corrosive methanogen was separated from marine sediments by a culture method using metallic iron as the sole energy source. Although the noncorrosive type, *Methanococcus maripaludis*, produced only methane, according to the amount of hydrogen generated from the chemical corrosion of metallic iron, the *Methanobacterium* sp. IM1 strain produced several times more methane. Unfortunately, no further detailed analyses have been conducted on the corrosive ability of this methanogen, and the biomolecules that lead to corrosion have never been identified.

14.2.2 Three Strains of Iron-Corrosive Methanogens Isolated from Petroleum Oil Storage Tanks

After the abovementioned report of corrosive methanogens was published, three strains of iron-corrosive methanogens were isolated from oil tanks in Japan, all belonging to *Methanococcus maripaludis*. Although metal corrosion by methanogens has been previously identified, most of the underlying mechanisms involved the consumption of hydrogen generated at the cathode, in association with the cathodic depolarization theory. The iron-corrosive type of *Methanococcus maripaludis*, reported by Uchiyama et al. (2010), clearly produced methane faster than expected as the actual yield exceeded the estimated amount, based on the amount of hydrogen generated by chemical corrosion, and a significant amount of ferrous ions was dissolved in the culture. In the enrichment culture, prior to isolation, the presence of *Desulfofustis glycolicus* was detected and a black corrosion product formed; therefore, corrosion was speculated to be caused by this SRB species. In contrast, since methanogens remain even after repeated subcultures, the possibility that methanogens are the actual causative microorganisms was concurrently speculated. The addition of 2-bromoethanesulfonate, which is an inhibitor of methanogenesis, clearly suppressed the dissolution of ferrous ions from the metallic iron, enabling methanogens to be recognized as the true causative microorganisms of corrosion. After isolation, the iron-corrosive methanogen was identified as *Methanococcus maripaludis* based on the 16S rRNA gene sequence analysis, and the sequence was 100% identical to that of *M. maripaludis*, strain JJ^T (type culture), which does not possess iron-corrosive abilities. This clearly indicates that there are differences in the presence or absence of corrosive ability among strains of *M. maripaludis* and that the corrosive ability could not be judged by 16S rRNA gene sequencing.

Similarly, Mori et al. (2010) reported the existence of iron-corrosive methanogens. In their study, they isolated hydrogen-consuming types of acetic acid bacteria, SRB, and methanogens from natural environments and evaluated their corrosive ability. They found that most of the hydrogen-consuming microorganisms resulted in corrosion comparable to that of chemical corrosion; thus, these microorganisms do not possess iron-corrosive abilities. However, one methanogen, namely, *M. maripaludis*, showed an accelerated dissolution rate of ferrous ions from metallic iron. Based on the cathodic depolarization theory, this result clearly disproves the long-standing belief that corrosion is accelerated by removing hydrogen generated at the cathode. Conversely, it demonstrated that iron-corrosive methanogens induced a more marked form of corrosion than SRB, which does not directly consume electrons. This finding is extremely important because it shows that hydrogen-consuming ability and iron-corrosive ability are independent of one another.

Later, the same iron-corrosive methanogen was isolated by Tsurumaru et al. (2018). Since the discovery of *Methanobacterium* sp. IM1 in 2004, three iron-corroding methanogens have been isolated from different oil storage tanks in

Japan and are all marine microorganisms belonging to *M. maripaludis*. Although there is no clear evidence to suggest the invasion route for marine methanogens in terrestrial oil tanks, all of the crude oil, contained in the Japanese storage tanks, was imported from overseas; therefore, the storage tanks may have been contaminated by making contact with seawater during production or tanker transportation. In addition, the presence of approximately 10^7 cells/mL of microorganisms, including hydrocarbon-degrading bacteria, anaerobic heterotrophic bacteria, and methanogens, was found in the water at the bottom of the oil tanks (Wakai et al. 2015). It is expected that crude oil *n*-alkanes are decomposed by hydrocarbon-degrading bacteria and that acetic acid, hydrogen, and carbon dioxide, produced by anaerobic heterotrophic bacteria, become energy sources for methanogens. Although the origin is not clear, some marine methanogens, belonging to *M. maripaludis*, possess iron-corrosive abilities; therefore, the distribution of corrosive methanogens in the marine environment is expected. Besides, iron-corrosive SRB, iron-corrosive methanogens, and neutrophilic iron-oxidizing bacterium have also been isolated from marine environments, indicating that there may be a strong correlation between iron-corrosive abilities and the marine environment (Dinh et al. 2004; McBeth et al. 2011).

14.2.3 Estimation of Electron Flow Rates from Gas Production Rates

Since methanogens do not produce corrosive metabolic by-products, unlike SRB and acid-producing bacteria, the amount of corrosion corresponds to the sum of the amount of electrons used by methanogens and the electrons consumed in the chemical generation of molecular hydrogen. A method of estimating the total amount of corrosion involves measuring the respective weight loss by removing the corrosion product from a test piece after performing a corrosion test, but this method does not factor in the timescale. Therefore, since the energy metabolism of iron-corrosive methanogens ends with methane production, we decided to estimate the amount of electrons lost using methane production rate.

As corrosion in an anaerobic environment is slow, the following reaction (Eq. 14.1) is observed:

$$Fe^0 + 2H^+ \rightarrow Fe^{2+} + H_2 \tag{14.1}$$

The abovementioned reaction consists of the following reactions:

$$Fe^0 \rightarrow Fe^{2+} + 2e^- \tag{14.2}$$

$$2H^+ + 2e^- \rightarrow H_2 \tag{14.3}$$

In contrast, the methanogenesis reaction is as follows:

$$HCO_3^- + 7H^+ + 8e^- \rightarrow CH_4 + 2H_2O \quad (14.4)$$

Therefore, the methanogenesis reaction with metallic iron can be represented as follows:

$$4Fe^0 + HCO_3^- + 7H^+ \rightarrow 4Fe^{2+} + CH_4 + 2H_2O \quad (14.5)$$

According to this reaction formula, the measured amount of methane corresponds to 1/4 moles of iron dissolved in the medium; however, the measured amounts of iron and methane did not correspond to each other. In fact, the iron-corrosive methanogen produced iron carbonate as the major corrosion product, which is represented by the following reaction:

$$4Fe^{2+} + 4HCO_3^- \rightarrow 4FeCO_3 + 4H^+ \quad (14.6)$$

In summary, the whole corrosion reaction, with regard to iron-corrosive methanogens, is as follows:

$$4Fe^0 + 5HCO_3^- + 5H^+ \rightarrow 4FeCO_3 + CH_4 + 3H_2O \quad (14.7)$$

Ferrous ions, liberated in the medium, reacted with carbonate ions to produce iron carbonate, and the amount of dissolved iron detected was less than the amount estimated from the amount of methane produced. In fact, in a previous study, iron carbonate was detected as a corrosion product using X-ray diffraction (XRD) analysis (Uchiyama et al. 2010). The early depletion of carbonate ions also affects its respective effectiveness as the methanogenic electron acceptor. Although iron-corrosive methanogens are cultured in a modified artificial seawater medium containing metallic iron with a N_2:CO_2 (80:20) gas mixture, when cultured with an arbitrary concentration of carbonate ions and pure N_2 gas, the final concentration of methane produced is significantly lower than that calculated using Eq. (14.4) (Fig. 14.1). The observed difference can be explained by the reaction in Eq. (14.6). Therefore, corrosion by iron-corrosive methanogens can be divided into two phases; the first phase consists of corrosion during methanogenesis, and the second phase involves corrosion during hydrogenesis, where the corrosion rate of each phase can be estimated from the production rate of each gas.

When 30 mM $NaHCO_3$ (600 μmol/20 mL of culture) is added, methane production stops in about 3 weeks and switches to hydrogen evolution. At this time, the amount of methane produced is only 150 μmol, corresponding to about 1/4 of the added $NaHCO_3$; therefore, methane production stops, due to the depletion of carbonate ions, as a result of iron carbonate formation. After the depletion of carbonate ions, the hydrogen generation rate is similar to the methane production rate during the early phase of cultivation and at the molar volume of gas. However, according to Eqs. (14.3) and (14.4), the electron flow rate calculated from the production rate of each gas clearly differs as the electron flow rate during

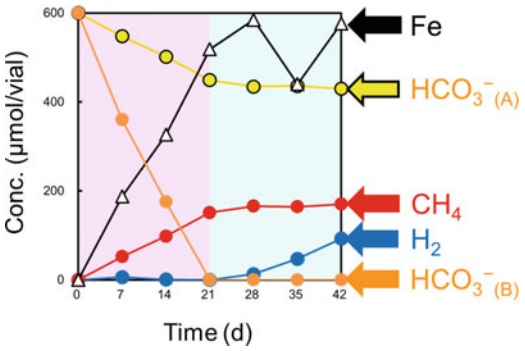

Fig. 14.1 Fe dissolution and gas productions during the cultivation of iron-corrosive methanogen. Fe, dissolved total iron (Fe^{2+}/Fe^{3+}) concentration measured by colorimetric method; CH_4 and H_2, produced methane and hydrogen measured by gas chromatography; $HCO_3^-{}_{(A)}$, estimated plot of remaining carbonate ion calculated from consumption of carbonate ions by methanogenesis; and $HCO_3^-{}_{(A)}$, estimated plot of remaining carbonate ion calculated from consumption of carbonate ions by methanogenesis and formation of iron carbonate as corrosion products

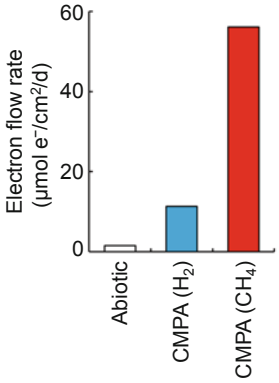

Fig. 14.2 Electron flow rates in the corrosion by iron-corrosive methanogen. Each electron flow rate was calculated from the gas production rate: abiotic, hydrogen production in the abiotic control culture; CMPA (H_2), hydrogen production in the culture iron-corrosive methanogen after depleting carbonate ions; and CMPA (CH_4), methane production in the culture iron-corrosive methanogen during methanogenesis

methanogenesis is faster than the electron flow rate during molecular hydrogen generation. Similarly, when the electron flow rate, in an abiotic control, is calculated from the gas generation rate and compared, the electron flow rate during methanogenesis is approximately 37-fold faster than that in the abiotic control (Fig. 14.2). The electron flow rate in corrosion occurring during methanogenesis cannot be explained by the associated change in surface area. Therefore, iron-corrosive methanogens clearly accelerate corrosion rate, and their energy metabolism, especially methanogenesis, evidently correlates to their corrosive behavior. The accelerated generation of molecular hydrogen in a spent culture medium of

M. maripaludis MM901 has previously been reported, with an observed rate several times faster than that of the abiotic control (Deutzmann et al. 2015). Moreover, this accelerated generation is similar to that after the depletion of carbonate ions during corrosion by the iron-corrosive methanogen *M. maripaludis* KA1. Therefore, the electron flow rates (electron equivalents) observed in the spent culture medium and after the depletion of carbonate ions demonstrated partial corrosion unrelated to energy metabolism in methanogens. Therefore, it is necessary to investigate the electron flow rate in corrosion during methanogenesis in order to understand the true corrosive ability of iron-corrosive methanogen.

14.2.4 Inhibition of Corrosion by an Iron-Corrosive Methanogen Using a Metal-Adhering Bacterium

From the calculation of the electron flow rate, it is evidenced that the iron-corrosive methanogen, *M. maripaludis* KA1, promotes electron flow at a considerably faster rate than abiotic corrosion under the same conditions. However, it has not yet been clarified whether the cells attached on the metal's surface or extracellularly secreted biological components promoted the electron flow during metallic iron corrosion by this iron-corroding methanogen. Deutzmann et al. (2015) reported a faster rate of hydrogen production than the abiotic control in experiments using the spent culture medium of *M. maripaludis*, but it is unclear whether the hydrogen generation was due to extracellularly secreted components or intracellular components because the spent culture medium contained both. The report by Tsurumaru et al. (2018) also demonstrated hydrogen production, evidenced in the filtrates of the culture supernatant for the iron-corrosive methanogen *M. maripaludis* OS7, but its rate was only about twice that of the control, and the influence of hydrogenase, derived from the cell lysate, cannot be ignored. Although the components in the spent culture medium and filtrate may contribute to accelerated electron loss, these relatively slow electron flow rates cannot explain the extremely fast electron flow rate in corrosion during methanogenesis by the iron-corrosive methanogen *M. maripaludis* KA1. Therefore, I hypothesized that corrosion, caused by iron-corrosive methanogens, requires electron transfer with adhesion, and in situations where the iron-corrosive methanogen could not contact the metal's surface, I examined whether the corrosion rate decelerated.

A colleague and I previously isolated microorganisms that rapidly adhered to metal surfaces, with an adhesion rate of about 1000 times that of other bacteria isolated from the same environment (Wakai and Harayama 2015). This metal-adhering bacterium can cover a metal's surface within about 10 min, given that there is sufficient cell density. We estimated that if adhesion to metal surfaces is essential for corrosion by iron-corrosive methanogens, then corrosion would be inhibited in the presence of a metal-adhering bacterium (Fig. 14.3). In fact, when an iron-corrosive methanogen and a metal-adhering bacterium were simultaneously

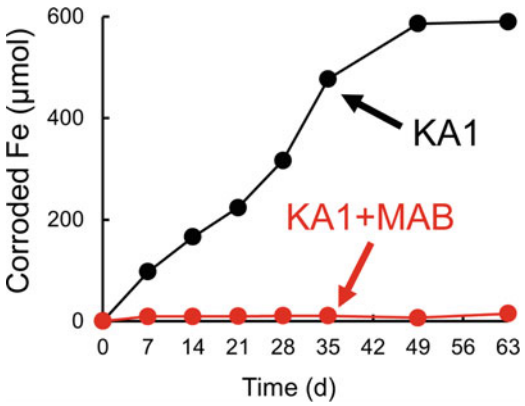

Fig. 14.3 Inhibition of the corrosion by metal adhesion bacterium. KA1: pure culture of iron-corrosive methanogen *M. maripaludis* KA1. KA1 + MAB: culture of iron-corrosive methanogen *M. maripaludis* KA1 co-inoculated with metal-adhering bacterium

inoculated into an artificial seawater medium containing metallic iron, corrosion by the iron-corrosive methanogen was almost completely suppressed. Contrastingly, the possibility remains that a metal-adhering bacterium may inhibit the growth of iron-corrosive methanogens. Therefore, I examined whether the coexistence of a metal-adhering bacterium is lethal for iron-corrosive methanogens. When both microorganisms were similarly inoculated into a medium, with hydrogen as the energy source, a sufficient amount of methane was produced by the utilization of hydrogen, therefore indicating that a metal-adhering bacterium does not inhibit the methanogenesis of iron-corrosive methanogens. These results strongly suggest that adhesion to the surface of metallic iron is essential for corrosion by iron-corrosive methanogens.

14.2.5 Proposed Corrosion Mechanisms Underlying Corrosion by Iron-Corrosive Methanogen

Tsurumaru et al. (2018) isolated a noncorrosive mutant, *M. maripaludis* OS7mut1, from a subculture of the iron-corrosive *M. maripaludis* OS7, and a comparative genome analysis of the corrosive and noncorrosive *M. maripaludis* strains led to the discovery of a MIC gene island possessing approximately 12 kbp and 14 genes, in the genome of the iron-corrosive methanogen. This MIC gene island encodes for a novel type of [NiFe] hydrogenase, including its secretory signals and maturation protease, Tat transport system, carbonic anhydrase, as well as other unknown genes. Similar MIC gene islands have been detected in the iron-corrosive methanogens *M. maripaludis* KA1 and Mic1c10. Furthermore, direct repeats, consisting of 221 bp, were detected at both ends of the MIC gene island; however, only the direct repeat sequence remained in the OS7mut1 strain. Therefore, the MIC gene island was expected to cause horizontal gene transfer based on gene deletion, due to looping out, or insertion by homologous recombination. Although a biochemical

demonstration of the corrosion mechanism has not been achieved, any or some combination of these 14 genes contributes to corrosive ability, because it is clearly affected by the presence or absence of this MIC gene island.

Of the 14 genes in the MIC gene island, the genes encoding for [NiFe] hydrogenase are the ones most likely to be associated with corrosion. The homology search of amino acid sequences, deduced from this MIC gene island, showed low similarities in comparison to well-known [NiFe] hydrogenases and high similarities with those of *Methanobacterium congolense*, *Methanobacterium* sp., and uncultured methanogens. Since some of the *Methanobacterium* sp. have previously been reported as iron-corrosive methanogens (Dinh et al. 2004), this novel type of [NiFe] hydrogenase may be a key enzyme involved in the corrosion induced by the iron-corrosive strains of *M. maripaludis* and *Methanobacterium* sp. There are several reports regarding hydrogen production from metallic iron, which is the electron donor, using hydrogenase; therefore, it is not difficult to consider the involvement of hydrogenase in corrosion. In contrast, when considering the location of the reaction, if the hydrogenase exists at the plasma membrane and in the cytosol, it cannot receive electrons from metallic iron as insoluble substrates are localized outside the cell. One of the major differences between well-known hydrogenases and the novel [NiFe] hydrogenase of iron-corrosive methanogens is that the novel hydrogenase contains a Tat signal motif, encoded in the MIC gene island, and is therefore transported extracellularly. Therefore, it is reasonable that the genes related to the secretion of [NiFe] hydrogenase and the Tat signal motif are encoded in clusters. In addition, as described in Sect. 14.2.4, it is essential that cells adhere to the metal's surface during corrosion caused by iron-corrosive methanogens. Therefore, it is presumed that the secreted [NiFe] hydrogenase is located on the outer surface of the cell, possibly at the S-layer.

14.3 Co-operative Corrosion by Iron-Corrosive Methanogen and SRB

As described in Chap. 11, corrosion, caused by iron-corrosive methanogens, is promoted by the presence of SRB. In this section, we will discuss the electron flow rate and the presumed mechanism of corrosion under conditions where iron-corrosive methanogens and SRB coexist.

Corrosion caused by coexisting iron-corrosive methanogens and SRB demonstrated about twice the amount of iron dissolution compared to that of iron-corrosive methanogens alone. When iron-corroding methanogens and SRB coexist, the color of the corrosion product is black, possibly indicative of iron sulfide, which differs from the gray color of the iron carbonate produced by iron-corrosive methanogens alone. In addition, the concentration of sulfate ions decreases slowly, indicating that SRB are living in this environment. In contrast, the amount of methane produced during corrosion, in conditions where iron-corrosive methanogens and SRB coexist,

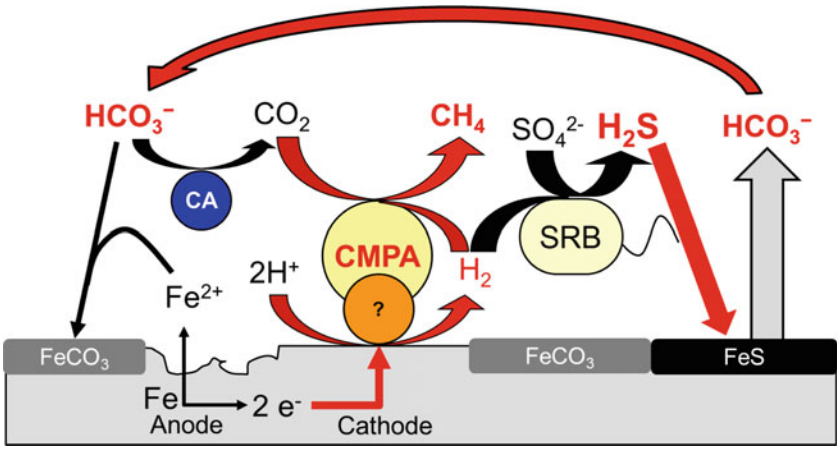

Fig. 14.4 Proposed mechanism of the cooperated corrosion by coexisting iron-corrosive methanogen and SRB. *CMPA* iron-corrosive methanogens, *SRB* hydrogen-consuming sulfate-reducing bacteria, *CA* carbonic anhydrase

is higher than that of the iron-corrosive methanogens alone. Therefore, it seems that SRB enhance the corrosive activity of the methanogens rather than directly taking part in corrosion.

Let us focus our attention on the electron flow rate during metallic iron corrosion, estimated from methane production, in the presence of iron-corrosive methanogens and SRB. The electron flow rate (electron equivalents) for methanogens alone was 56 μmol/2 cm^2/day, while it was 131 μmol/2 cm^2/day in conditions where iron-corrosive methanogens and SRB coexist. The corrosion product could provide an important clue regarding the enhanced corrosion rate observed when iron-corrosive methanogens and SRB coexist. Iron carbonate is the corrosion product produced by methanogens alone; however, when SRB are also present, iron sulfide is formed, from the reaction of ferrous ions with sulfide, and the released carbonate ions are used for methane production (Fig. 14.4; Eq. 14.8). Although this can explain the reason for increased amounts of methane produced, there is possibly another factor responsible for the increase in the electron flow rate per unit time:

$$FeCO_3 + H_2S \rightarrow FeS + HCO_3^- + H^+ \tag{14.8}$$

Alteration of the corrosion products may be important. The major difference between iron carbonate and iron sulfide is electrical conductivity, and iron sulfide is a much better conductor than iron carbonate. Therefore, when iron-corrosive methanogens are cultivated alone, the surface of the metallic iron is covered with iron carbonate (corrosion product), which may limit the electron flow rate due to its relatively low electrical conductivity. In contrast, in the co-cultivation system, the iron sulfide has a high conductivity; therefore, the electron flow rate is increased.

Based on these findings, the causative agent and enhancer of corrosion in the co-cultivation system are the iron-corrosive methanogen and SRB, respectively.

Previously, when severe corrosion was observed, accompanied by a hydrogen sulfide odor, the formation of iron sulfide, and the detection of SRB from microbial testing, SRB were the assumed causative agents of corrosion. However, the observed corrosion may have been caused by another causative microorganism, while SRB merely functioned as an enhancer, similar to relationship evidenced when iron-corrosive methanogens and SRB coexist. In a previous analysis, conducted by my colleagues and I, lab-scale corrosion tests were performed using environmental samples, and we observed that certain samples, despite containing the same type of SRB, demonstrated differing degrees of corrosion (Wakai et al. 2015). As a result of the subculture of corrosive samples, acetogen and SRB were mainly enriched, and the comparative analysis of the microbial communities strongly suggested that acetogen was a key role player in corrosion. Although SRB are easily detected in many corrosive environments, the actual function of the detected SRB and other microorganisms should be carefully assessed.

14.4 Potential Applications of Corrosion Abilities

MIC is a social problem and results in economic loss and environmental pollution. There are various types of microorganisms involved in MIC, and they are generally handled as harmful microorganisms. Contrastingly, many microorganisms have long been regarded from both negative and positive aspects in relation to human health and well-being, for example, rot and fermentation are related to both pathogenicity and drug production. Therefore, I considered the positive aspects of causative microorganisms in MIC.

For example, 40 million tons of scrap iron is generated in Japan annually, and inspired by the viewpoint of resource recycling, I considered whether this "scrap" could be used more effectively. If 25% (w/w) of the scrap iron was used as metallic iron, it would be possible to produce 300 million Nm^3 of hydrogen (Fig. 14.5a). This amount of hydrogen exceeds the supply required to promote the spread of hydrogen-fueled vehicles used in Japan. When trying to produce hydrogen by chemical reaction, a significant amount of hydrochloric acid is required; however, if iron-corrosive methanogens are used under carbonate depletion conditions, hydrogen can be produced under milder conditions. Although this reaction also produces a large amount of iron oxide, resource recycling may be possible by turning homogenous iron oxide to steel instead of low-grade ore. I am unsure whether this is actually economical as much of the infrastructure in modern society was constructed during periods of high economic growth and will eventually need replacing; therefore, how to efficiently deal with waste may be the next challenge (Fig. 14.5b). A social system in which next-generation energy and resource recycling can efficiently be performed would contribute to the formation of a sustainable society.

Iron-corrosive methanogens receive electrons by making contact with the surface of a solid substrate, and a large amount of the microbial cells, as well as the corrosion products, are attached to the surface. By taking advantage of this property, it could

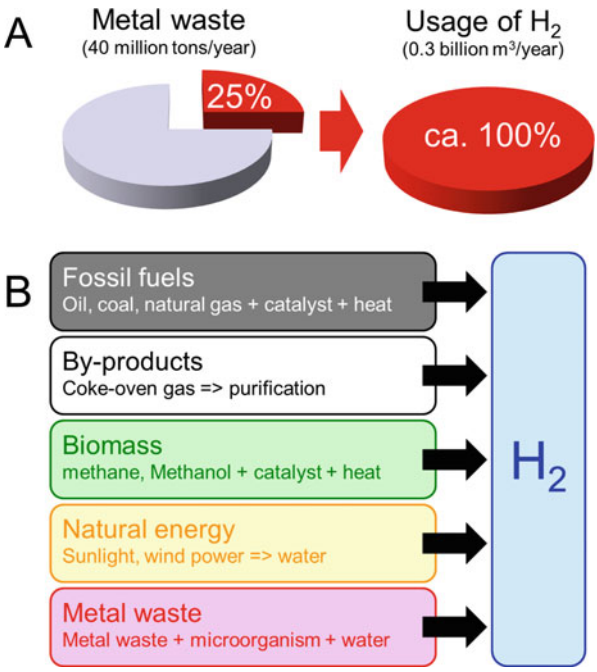

Fig. 14.5 Potential of hydrogen gas as clean energy by application of iron-corrosive activity. (**a**) Potential of biological hydrogen production from scrap iron. (**b**) Various methods for hydrogen production. To construct a sustainable society system, hydrogen production depending on fossil fuels must be replaced by methods depending on reproducible energy and waste recycling

be possible to immobilize cells on a corrosion-resistant conductive material and produce methane from carbon dioxide using electrical energy, such as a solar cell. In addition to simply producing methane, it is possible to construct a production system for useful chemicals using metabolic engineering, i.e., the genetic engineering of *M. maripaludis*, and by means of conversion from methane-utilizing, C1-compound-utilizing microorganisms. In fact, a technique for electrochemically producing formic acid, using an enzyme derived from a methanogen, has already been developed (Lienemann et al. 2018). Iron-corrosive nitrate-reducing bacteria and iron-corrosive acetogens have also been isolated and produce ammonia and acetic acid, respectively, during corrosion (Kato et al. 2015; Iino et al. 2015). The use of these iron-corrosive microorganisms, which use electrons directly, could be appealing in the development of new technologies for the formation of a sustainable society, such as using electrorefineries and electrosynthesis instead of oil refineries.

14.5 Concluding Remarks

Corrosion occurs as a result of the coupling of two kinds of electrochemical reactions, namely, anodic reactions, including iron dissolution, and cathodic reactions, involving the loss of electrons from metals, and these principles remain the same in MIC. When microorganisms directly use electrons at the cathode, they can directly cause MIC. One of these microorganisms is iron-corroding methanogens,

which can produce methane and molecular hydrogen using electrons from metallic iron. Although the biological and molecular mechanisms underlying corrosion caused by iron-corrosive methanogens are not fully understood, iron-corrosive methanogens can accelerate the electron flow rate. Understanding electron-based corrosive behavior would contribute to a better understanding of corrosion mechanisms. In addition, the production of molecular hydrogen and methane and their secondary production from biogas using biological electron-consuming systems are useful for the reasons described in this chapter. Other than iron-corrosive methanogens, iron-corrosive nitrate-reducing bacteria and iron-corrosive acetogens have been reported, and the electrochemical production of ammonia and acetic acid, respectively, is also useful. Understanding the biological and molecular mechanisms related to electron utilization could possibly enable the construction of a more sustainable society, based on the electro-biosynthesis of energy and compounds, by combining power generation systems that use renewable energy sources.

References

Deutzmann JS, Sahin M, Spormann AM (2015) Extracellular enzymes facilitate electron uptake in biocorrosion and bioelectrosynthesis. mBio 6:e00496-15

Dinh HT, Kuever J, Mußmann M, Hassel AW, Stratmann M, Widdel F (2004) Iron corrosion by novel anaerobic microorganisms. Nature 427:829–832

Iino T, Ito K, Wakai S, Tsurumaru H, Ohkuma M, Harayama S (2015) Iron corrosion induced by non-hydrogenotrophic nitrate-reducing *Prolixibacter* sp. MIC1-1. Appl Environ Microbiol 81:1839–1846

Kato S, Yumoto I, Kamagata Y (2015) Isolation of acetogenic bacteria that induce biocorrosion by utilizing metallic iron as the sole electron donor. Appl Environ Microbiol 81:67–73

Lienemann M, Deutzmann JS, Milton RD, Sahin M, Spormann AM (2018) Mediator-free enzymatic electrosynthesis of formate by the *Methanococcus maripaludis* heterodisulfide reductase supercomplex. Bioresour Technol 254:278–283

McBeth JM, Little BJ, Ray RI, Farrar KM, Emerson D (2011) Neutrophilic iron-oxidizing "Zetaproteobacteria" and mild steel corrosion in nearshore marine environments. Appl Environ Microbiol 77:1405–1412

Mori K, Tsurumaru H, Harayama S (2010) Iron corrosion activity of anaerobic hydrogen-consuming microorganisms isolated from oil facilities. J Biosci Bioeng 110:426–430

Tsurumaru H, Ito N, Mori K, Wakai S, Uchiyama T, Iino T, Hosoyama A, Ataku H, Nishijima K, Mise M, Shimizu A, Harada T, Horikawa H, Ichikawa N, Sekigawa T, Jinno K, Tanikawa S, Yamazaki J, Sasaki K, Yamazaki S, Fujita N, Harayama S (2018) An extracellular [NiFe] hydrogenase mediating iron corrosion is encoded in a genetically unstable genomic island in *Methanococcus maripaludis*. Sci Rep 8:15149

Uchiyama T, Ito K, Mori K, Tsurumaru H, Harayama S (2010) Iron-corroding methanogen isolated from a crude-oil storage tank. Appl Environ Microbiol 76:1783–1788

Wakai S, Harayama S (2015) Isolation of bacteria rapidly adhering on the surface of metallic iron. Mater Technol 30(B1):38–43

Wakai S, Ito K, Iino T, Tomoe Y, Mori K, Harayama S (2014) Corrosion of iron by iodide-oxidizing bacteria isolated from brine in an iodine production facility. Microb Ecol 68:519–527

Wakai S, Fujii S, Masanari M, Miyanaga K, Tanji Y, Sambongi Y (2015) Corrosion test using bottom water from oil-storage tank and microbial community analysis by next generation sequencer. Zairyo-to-Kankyo 64:540–544. (in Japanese); Corr Eng 64:460–465 (2015)

Chapter 15
Biocorrosion and Souring in the Crude-Oil Production Process

Kazuhiko Miyanaga

15.1 Introduction

To increase the productivity of crude oil from the oil well, the recovery methods have been developed. Waterflooding serves as a main oil recovery method to be applied whenever the geological pressure became inefficient, known as a secondary oil recovery (Plankaert 2005). In the secondary oil recovery process, seawater is commonly injected to enhance oil recovery; however, this method causes biological souring (i.e., sulfide production in oil reservoirs). The crude oil including more than 0.04 mol% of hydrogen sulfide is defined as "sour oil." Seawater contains a high concentration of sulfate (up to 27 mM) that can enhance the growth of sulfate-reducing bacteria (SRB) in the reservoir. Souring causes several problems, including microbiologically influenced corrosion of the tubing material and deterioration of crude oil (Gieg et al. 2011). Microbial sulfate reduction is an important metabolic activity in many petroleum hydrocarbon (PHC)-contaminated aquifers; contamination with mono-aromatic PHCs (e.g., benzene, toluene, ethylbenzene, and xylene) is a regulatory concern due to their solubility and toxicity. Because sulfate reduction can be coupled with the bacterial metabolism of mono-aromatic PHCs, it has received increasing attention as an intrinsic remediation process.

SRBs, which mostly belong to *Deltaproteobacteria* or *Firmicutes*, are among the microorganisms present in oil fields that induce souring. Although corrosion control measures can be used to remove oxygen from the injected water, these create an environment conducive to the growth of SRBs, which are obligate anaerobes. SRBs derive energy by coupling the oxidation of electron donors to the reduction of sulfate to sulfide. Previous studies have revealed that SRBs use volatile fatty acids (VFAs)

K. Miyanaga (✉)
School of Life Science and Technology, Tokyo Institute of Technology (Tokyo Tech), Yokohama, Japan
e-mail: kmiyanag@bio.titech.ac.jp

M. Ishii, S. Wakai (eds.), *Electron-Based Bioscience and Biotechnology*,
https://doi.org/10.1007/978-981-15-4763-8_15

and crude-oil components (e.g., toluene) as electron donors. The most common method to prevent souring is the injection of biocide, metabolic inhibitors such as nitrite or molybdate into reservoirs to inhibit SRB growth (Jayaraman et al. 1999; Nemati et al. 2001; Tang et al. 2009), and/or air injection to prevent anaerobic condition (Ochi et al. 1998), but these methods have yielded limited success. An alternative approach is nitrate injection, which seeks to promote the growth of nitrate-reducing bacteria (NRB) as competitors of SRB for the electron donors in the reservoir, such as volatile fatty acids (VFAs) (Agrawal et al. 2012). Thus, nitrate injection might be used to prevent and treat souring. Nitrate injection is an attractive solution to souring because nitrate is cost-effective and relatively nontoxic and can distribute evenly in the reservoir (Dunsmore et al. 2006; Gieg et al. 2011). However, so far, the effect of nitrate injection on the biocorrosion of carbon steel has not been well known.

In this chapter, the biological souring mechanisms and the prevention methods for souring are introduced. Moreover, the biocorrosion of carbon steel in the environment where the souring occurs and/or the prevention of souring is applied to the souring.

15.2 Identification of Crude-Oil Components and Microorganisms that Cause Souring Under Anaerobic Conditions

For biological souring, three factors are strongly related. They are sulfate as an electron acceptor, organic compounds as electron donors, and sulfate-reducing bacteria as biocatalyst. In the oil production process, the sulfate plentifully exists in the injection seawater. Therefore, to understand the mechanism of souring, the other two factors should be clarified. Various kinds of organic compounds, such as aromatics, hydrocarbons, and so on, are included in the crude oil, and a small amount of them is dissolved in the injection seawater.

To identify the preferential substrate for souring, the mixtures of the several crude-oil components (alkanes [AL], aromatics [AR], 2,4-dimethylxylenol [XY], naphthenic acids [NA]) and crude oil [CR] diluted 1:100 with biologically inert branched alkane 2,2,4,4,6,8,8-heptamethylnonane (HMN) were overlaid on the seawater supplemented with microorganisms from oil field water (OFW) taken from oil field (Akita, Japan) (Hasegawa et al. 2014). XY and NA were investigated as the organic compounds with the intramolecular oxygen, while ALs and ARs were investigated as dominant compounds in the crude oil. All of them were incubated in high-pressure vessels under 1 MPa at 28 °C for about 3 months. The components of crude oil that decomposed under anaerobic conditions were identified. Toluene, ethylbenzene, and alkanes (C_7–C_{17}) were selectively degraded. On the other hand, no change was observed for XY and NA. It is concluded that decomposition of aromatics [AR] and alkanes [AL] was accompanied by the production of acetate as an intermediate, followed by its oxidation. In XY and NA, no biological activity was

observed. It shows they are toxic to microorganisms, and the degradation of these compounds has not been well studied.

Biological conversion of crude-oil components to produce sulfide can be divided into two steps: oxidation of oil components to produce VFA (Step 1) and reduction of sulfate to sulfide coupled with oxidation of VFAs (Step 2). There are two possible degradation mechanisms of crude-oil components. One is the complete oxidation of crude-oil components to CO_2 by SRB. This mechanism is supported by the detection of *bssA* genes that were most likely the *bssA* gene of *Desulfobacula toluolica*. In this mechanism, toluene-degrading SRB is involved in both Step 1 and Step 2. The other is syntrophic oxidation. Detection of acetate indicated that the oil field microorganisms excreted acetate as a by-product, and the subsequent decreases indicated that other microorganisms such as SRB consume acetate and produce sulfide. Production of sulfide in AL was much less than in AR, although acetate was produced in both vessels. Moreover, toluene and ethylbenzene were completely degraded, and *bssA* affiliated with SRB was detected in AR. The metagenomic analysis of 16S rRNA gene sequencing revealed that *Desulfotignum* spp. detected in AR were affiliated with the toluene-degrading SRB, *D. toluenicum*. Although it remains unclear whether alkanes were degraded by SRB, it seems that degradation of aromatic hydrocarbons mainly toluene contributes significantly to souring.

Community analysis revealed that abundant classes in day 49 were distributed among *Deltaproteobacteria*, *Gammaproteobacteria*, and *Clostridia*. Specifically, the proportions of *Deltaproteobacteria* and *Clostridia* were increased in AL, AR, and CR after 49 days. Many SRBs, including *Desulfotignum* spp., belong to *Deltaproteobacteria*. The dominant *Clostridia* were *Fusibacter* spp., a genus of anaerobic fermenting bacteria. Although the proportion of *Fusibacter* was lower than in AL and CR, *Fusibacter* spp. were also detected in AR. *Fusibacter paucivorans*, isolated in an oil-producing well, can transform glucose to acetate by fermentation (Ravot et al. 1999). Therefore, *Fusibacter* spp. detected in this experiment might be involved in acetate production by fermentation. Minor phylotypes were distributed within the *Bacteroidetes*. The involvement of *Bacteroidetes* in hydrocarbon degradation has been investigated (Zrafi-Nouira et al. 2009; Popp et al. 2006). *Acinetobacter* spp., which belong to *Gammaproteobacteria*, were also detected in AL, AR, and CR. Abboud et al. (2007) reported that some strains of *Acinetobacter* spp. are involved in biodegradation of crude-oil components.

15.3 The Effect of Nitrate Injection on the Biological Souring Under the Presence of Sulfate-Reducing Bacteria (SRB) and Nitrate-Reducing Bacteria (NRB)

As described in the introduction, to prevent souring, the nitrate addition is applied to the oil-producing process. Kamarisima et al. (2018) revealed that the nitrate addition at the beginning could suppress the biological souring by chemical analysis and by

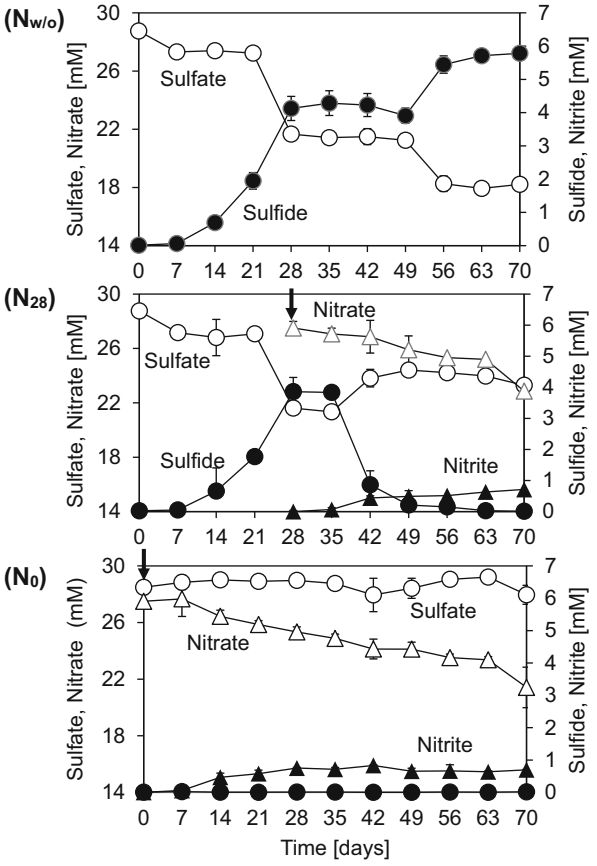

Fig. 15.1 Effect of nitrate addition on sulfide production and sulfate reduction. Arrows indicate the nitrate addition (Kamarisima et al. 2018)

biological analysis. By chemical analysis, it was revealed that without the addition of nitrate ($N_{w/o}$) to the artificial souring environment using the 2% of crude oil in the 2,2,4,4,6,8,8-heptamethylnonane (HMN) as a substrate, the sulfide production and sulfate consumption were simultaneously observed in the seawater medium (Fig. 15.1). Moreover, after souring occurred by SRB derived from the oil field water, the nitrate addition at day 28 (N_{28}) was also effective for the decrease of sulfide production and suppression of sulfate reduction. On the other hand, when 27 mM of nitrate at the same level of sulfate (27 mM) in the seawater was added from day 0 (N_0), no sulfide production occurred for 70 days. According to the results of biological analysis based on 16S rRNA gene sequences shown in Fig. 15.2, in the conditions of $N_{w/o}$ and N_{28}, the relative abundance of *Desulfotignum* sp., one of the representative SRBs suspected to be the primary degrader of toluene, became dominant after 28-day incubation. It was thought that this SRB caused souring for the initial stage of incubation. Moreover, in the condition of N_{28}, the dominant *Desulfotignum* sp. did not disappear till the end of incubation, even though the sulfide production was suppressed after nitrate addition at day 28. In the case of N_0

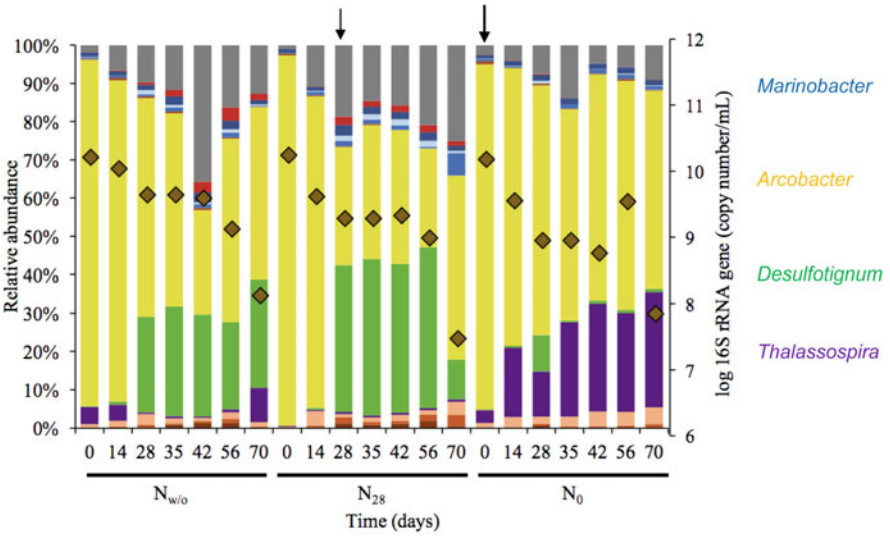

Fig. 15.2 Bacterial community profile in 70 days of incubation. The symbols of diamond and arrows indicate 16S rRNA gene copy number and time of nitrate addition, respectively (Kamarisima et al. 2018)

condition, instead of *Desulfotignum* sp., *Thalassospira* sp. became dominant as the incubation period. *Thalassospira* is known as the heterotrophic nitrate-reducing bacteria (hNRB). Therefore, it is reasonable that the NRB abundance increased instead of SRB after nitrate addition to the microbial mixture. SRB and hNRB might share similar sources of electron donors, such as the hydrocarbon fraction (especially toluene) in crude oil.

However, in the condition of N_{28}, *Thalassospira* sp. did not become dominant, although a small relative abundance of *Marinobacter* sp., also one of the NRB, appeared at the final stage. In all conditions, *Arcobacter*, considered as nitrate-reducing and sulfide-oxidizing bacteria (NR-SOB) (De Gusseme et al. 2009), were the most dominant species. NR-SOB are chemoautotrophic bacteria that can oxidize sulfide coupled to reduction of nitrate. Oxidation of sulfide under denitrifying condition could lead to the formation of sulfur or sulfate. This is the reason why under the N_{28} condition the sulfide was not observed at the later culture period even though hNRB was not dominated after nitrate addition. The bacterial community could be divided into four groups (Fig. 15.3): (1) fermentative bacteria, (2) hNRB, (3) NR-SOB, and (4) SRB. Each group was thought to play a unique role in biological souring under each condition. Considering these relationships, at the limiting nitrate concentration to suppress SRB activity, 1 mM, SRB could coexist with NRB and promote a more diverse bacterial community (Kamarisima et al. 2019).

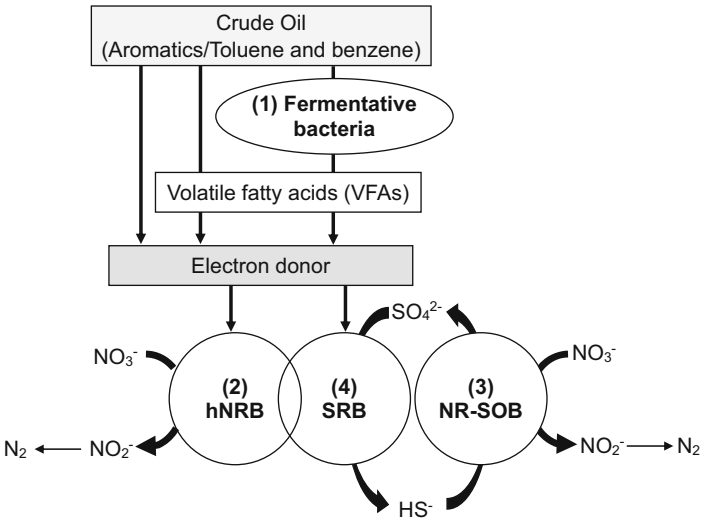

Fig. 15.3 Possible microbial interactions based on possibility of their preference electron donor and electron acceptor under microbial souring following nitrate injection (Kamarisima et al. 2018)

15.4 The Effect of Nitrate Addition on Microbiologically Influenced Corrosion (MIC)

In oil and gas industrial appliances, corrosion contributes to an increase in the cost due to corrosion control and mitigation. Microbiologically influenced corrosion (MIC) has been reported to accelerate the corrosion process more than 50-fold compared to sterile conditions as reported elsewhere (Koch et al. 2001; Kruger 2011). Several groups of bacteria have been reported and proved to play a role in MIC, such as SRB (Enning and Garrelfs 2014), NRB (Iino et al. 2015), acid-producing bacteria (Gu 2012), methanogen (Uchiyama et al. 2010), and iron-oxidizing bacteria (Emerson 2018). Among them, SRB was proposed as the primary player not only of microbial souring in the crude oil but also of MIC in oil and gas industry appliances.

MIC in the oil and gas industry often occurs during or after water injection to increase the yield of oil production. The treatment for MIC is varied among the places, which includes chemical and physical treatment. The most known chemical treatment for MIC control is the application of biocide, which then turns up that it has a high cost and toxic to the environment (Skovhus et al. 2017). Since one of the leading groups of bacteria in MIC is SRB, then a similar approach for SRB control was applied to MIC as well, which is nitrate treatment. Hydrogen sulfide was known as a corrosive agent which is produced by SRB. Various studies of nitrate treatment show successful results of controlling the production of hydrogen sulfide (Gieg et al. 2011; Hubert et al. 2005; Kamarisima et al. 2018; Voordouw et al. 2009). To date, however, the application of nitrate treatment for MIC control was limited. Only

several studies are available in the monitoring of nitrate treatment for MIC in the past 10 years. In this section, one example of nitrate-treatment effect on MIC is introduced.

Nitrate addition was proved to inhibit souring caused by SRB. However, the addition of nitrate can have contributed to cause severe corrosion. Based on bacterial community analysis, the bacterial community was different in the condition without and with nitrate addition as well as in the planktonic and biofilm sample of both conditions. In general, nitrate addition has increased the diversity of bacterial community in both planktonic and biofilm zone. There was no domination of specific bacteria in the planktonic zone of condition with nitrate addition until 90 days, and then *Arcobacter* became dominant for the later time. The common bacteria found in planktonic and biofilm site on condition with nitrate addition were identified as *Arcobacter*, *Marinobacterium*, *Acetobacterium*, *Marinobacter*, *Rhodospirillaceae* (f), *Tindallia*, *Halomonas*, *Fusibacter*, and *Bacteriodales*. Most of these bacteria were classified as NRB. Thus, it proved the enhancement of NRB in the condition of nitrate addition. In the biofilm attached to the surface of carbon steel coupon, these bacteria may produce various kinds of metabolites, especially volatile fatty acids, and provoke the pitting corrosion. The corrosion behavior of condition amended with nitrate was characterized by the formation of pitting corrosion as the localization of acid-bacteria and extracellular polymeric substance (EPS)-forming bacteria. Moreover, surface roughness was also contributed for more extensive pitting corrosion. The rougher the surface, the more pit was formed.

15.5 The Effect of Alkaline Addition on Souring and Microbiologically Influenced Corrosion (MIC)

Seawater injection into oil reservoirs for secondary oil recovery is frequently accompanied by souring (increased sulfide concentrations) in crude oil. The hydrogen sulfide produced by microbiological sulfate reduction in the seawater causes various problems, including corrosion of tubing materials and deterioration of crude oil. Sulfate-reducing bacteria (SRBs) play major roles in souring. However, under high pH (>9), most microbes (including SRBs) cannot grow. Moreover, it is known that iron corrosion is theoretically negligible under the alkaline condition. To investigate new approaches to simultaneously control souring and metal corrosion, Miyanaga et al. (2017) analyzed souring and metal corrosion under high-pH conditions (Fig. 15.4). NaOH was added to adjust the pH clean seawater (ca. pH 8) to 11 or 13. Then, a carbon steel test coupon was incubated for 123 days and supplemented with microbes separated from oil field water (OFW) and crude oil. At pH 11 and pH 13, the corrosion rate of the test coupon was decreased. Additionally, souring did not occur at pH 11 and 13, although it took place at pH 8 with microbes. Next-generation sequencing analysis of the 16S rRNA gene revealed drastic changes in the microbial consortia for pH 8 after incubating for 111 days.

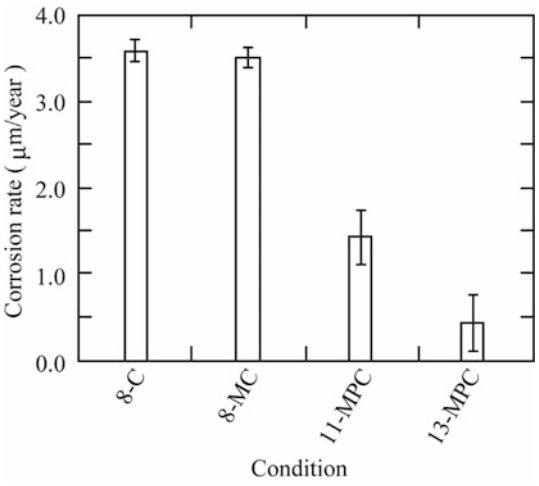

Fig. 15.4 Corrosion rate of the carbon steel coupons. Each number indicates pH value. M and P indicate with microbes and precipitate, respectively (Miyanaga et al. 2017)

Desulfotignum, which shows a high identity compared to that of toluene-utilizing SRB, became dominant. It is thought to contribute a biological souring by utilizing toluene in the crude oil at pH 8. On the other hand, at pH 11, the microbial consortia did not change significantly after 111 days of incubation. At pH 13, the microbial consortia drastically changed compared with that of initial condition (OFW) due to cell lysis. That is, even under strict conditions (e.g., pH 13), some bacteria are not lysed, increasing their relative ratio without growth. Alkaline addition could inhibit not only metal corrosion but also biological souring.

References

Abboud MM, Khieifat KM, Batarseh M, Taraeneh KA, Al-Mustafa A, Al-Madadhah M (2007) Different optimization conditions required for enhancing the biodegradation of linear alkylbenzosulfonate and sodium dodecyl sulfate surfactant by novel consortium of *Acinetobacter calcoaceticus* and *Pantoea agglomerans*. Enzym Microb Technol 41:432–439

Agrawal A, Park HS, Nathoo S, Gieg LM, Jack TR, Miner K, Ertmoed R, Benko A, Voordouw G (2012) Toluene depletion in produced oil contributes to souring control in a field subjected to nitrate injection. Environ Sci Technol 46:1285–1292

De Gusseme B, De Schryver P, De Cooman M, Verbeken K, Boeckx P, Verstraete W, Boon N (2009) Nitrate-reducing, sulfide-oxidizing bacteria as microbial oxidants for rapid biological sulfide removal. FEMS Microbiol Ecol 67:151–161

Dunsmore B, Youldon J, Thrasher D, Vance I (2006) Effects of nitrate treatment on a mixed species, oil field microbial biofilm. J Ind Microbiol Biotechnol 33:454–462

Emerson D (2018) The role of iron-oxidizing bacteria in biocorrosion: a review. Biofouling 34:989–1000

Enning D, Garrelfs J (2014) Corrosion of iron by sulfate-reducing bacteria: new views of an old problem. Appl Environ Microbiol 80:1226–1236

Gieg LM, Jack TR, Foght JM (2011) Biological souring and mitigation in oil reservoirs. Appl Microbiol Biotechnol 92:263–282

Gu T (2012) Can acid producing bacteria be responsible for very fast MIC pitting? Paper no. C2012-0001214, CORROSION, Salt Lake City, UT, 11–15 Mar 2012

Hasegawa R, Toyama K, Miyanaga K, Tanji Y (2014) Identification of crude-oil components and microorganisms that cause souring under anaerobic conditions. Appl Microbiol Biotechnol 98:1853–1861

Hubert C, Nemati M, Jenneman G, Voordouw G (2005) Corrosion risk associated with microbial souring control using nitrate or nitrite. Appl Microbiol Biotechnol 68:272–282

Iino T, Ito K, Wakai S, Tsurumaru H, Ohkuma M, Harayama S (2015) Iron corrosion induced by nonhydrogenotrophic nitrate-reducing *Prolixibacter* sp. strain MIC1-1. Appl Environ Microbiol 81:1839–1846

Jayaraman A, Mansfeld FB, Wood TK (1999) Inhibiting sulfate-reducing bacteria in biofilms by expressing the antimicrobial peptides indolicidin and bactenecin. J Ind Microbiol Biotechnol 22:167–175

Kamarisima, Hidaka K, Miyanaga K, Tanji Y (2018) The presence of nitrate- and sulfate-reducing bacteria contributes to ineffectiveness souring control by nitrate injection. Int Biodeterior Biodegradation 129:81–88

Kamarisima, Miyanaga K, Tanji Y (2019) The utilization of aromatic hydrocarbon by nitrate- and sulfate-reducing bacteria in single and multiple nitrate injection for souring control. Biochem Eng J 143:75–80

Koch GH, Brongers MPH, Thompson NG, Virmani YP, Payer JH (2001) Corrosion cost and preventive strategies in the United States. FHWA-RD-01-156. CC Technologies Laboratories, NACE International, Dublin, OH

Kruger J (2011) Cost of metallic corrosion. In: Revie RW (ed) Uhlig's corrosion handbook, 3rd edn. Wiley, Hoboken, NJ, pp 15–20

Miyanaga K, Hasegawa R, Tanji Y (2017) Addition of sodium hydroxide to seawater inhibits sulfide production (souring) by microbes in oil field water. J Chem Eng Jpn 50:850–856

Nemati M, Mazutinec TJ, Jenneman GE, Voordouw G (2001) Control of biogenic H_2S production with nitrite and molybdate. J Ind Microbiol Biotechnol 26:350–355

Ochi T, Kitagawa M, Tanaka S (1998) Controlling sulfide generation in force mains by air injection. Water Sci Technol 37:87–95

Plankaert M (2005) Oil reservoir and oil production. In: Ollivier B, Magot M (eds) Petroleum microbiology. ASM, Washington, DC, pp 123–142

Popp N, Schlomann M, Mau M (2006) Bacterial diversity in active stage of a bioremediation system for mineral oil hydrocarbon- contaminated soils. Microbiology 152:3291–3304

Ravot G, Magot M, Fardeau M, Patel BKC, Thomas P, Garcia J, Ollivier B (1999) *Fusibacter paucivorans* gen. nov., sp. nov., an anaerobic, thiosulfate-reducing bacterium from an oil-producing well. Int J Syst Bacteriol 49:1141–1147

Skovhus TL, Eckert RB, Rodrigues E (2017) Management and control of microbiologically influenced corrosion (MIC) in the oil and gas industry—overview and a North Sea case study. J Biotechnol 256:31–45

Tang K, Baskaran V, Nemati M (2009) Bacteria of the sulphur cycle: an overview of microbiology, biokinetics and their role in petroleum and mining industries. Biochem Eng J 44:73–94

Uchiyama T, Ito K, Mori K, Tsurumaru H, Harayama S (2010) Iron-corroding methanogen isolated from a crude-oil storage tank. Appl Environ Microbiol 76:1783–1788

Voordouw G, Grigoryan AA, Lambo A, Lin S, Park HS, Jack TR, Coombe D, Clay B, Zhang F, Ertmoed R, Miner K, Arensdorf JJ (2009) Sulfide remediation by pulsed injection of nitrate into a low temperature Canadian heavy oil reservoir. Environ Sci Technol 43:9512–9518

Zrafi-Nouira I, Guermazi S, Chouari R, Safi NMD, Pelletier E, Bakhrouf A, Saidane-Mosbahi D, Sghir A (2009) Molecular diversity analysis and bacterial population dynamics of adapted seawater microbiota during the degradation of Tunisian zarzatine oil. Biodegradation 20:467–486

Chapter 16
Effect of Metallurgical Factors on Microbial Adhesion and Microbiologically Influenced Corrosion (MIC)

Yasuyuki Miyano and Sreekumari Kurissery

16.1 Microbial Adhesion and MIC

Colonization of wet surfaces by bacteria generally leads to the formation of biofilms. However, the microbial adhesion on metal surfaces could sometimes lead to serious problems known as microbiologically influenced corrosion (MIC). MIC causes problems in various industries such as chemical plants, power generation facilities, water and oil pipelines, water tanks, and ship hulls (Borenstein 1994; Licina 1998; Kikuchi and Sreekumari 2002; Miyano and Kikuchi 2008). MIC on metal surfaces once initiated can proceed at a rate of several mm/year; MIC can even occur on corrosion-resistant materials, such as stainless steel.

Stainless steel is one of the major structural materials which have superior corrosion resistance, but there have been many reports on severe local corrosion associated with microbial activity, i.e., MIC. Many corrosion case analyses for stainless steel in which MIC is suspected tend to show the welds or heat-affected zone (HAZ) gets higher bacterial adhesion leading to higher corrosion risk (Enos and Taylor 1996; Borenstein and Lindsay 1987; Borenstein 1991). For this reason, the effect of metallurgical factors, such as changes in metallographic microstructure due to welding heat cycle and manufacturing specifications, has been studied on microbial adhesion (Obukwe et al. 1981; Walsh et al. 1994; Little et al. 1996). Although stainless steel is originally a material with excellent corrosion resistance, if exposed to thermal cycles during welding process, its microscopic properties such as the

Y. Miyano (✉)
Graduate School of Engineering Science, Akita University, Akita, Japan
e-mail: y.miyano@gipc.akita-u.ac.jp

S. Kurissery
Department of Sustainability Sciences, Lakehead University, Orillia, ON, Canada

Department of Biology, Lakehead University, Thunder Bay, ON, Canada
e-mail: skurisse@lakeheadu.ca

M. Ishii, S. Wakai (eds.), *Electron-Based Bioscience and Biotechnology*,
https://doi.org/10.1007/978-981-15-4763-8_16

metallic structure or the presence of alloying elements can easily be altered. Although solidification segregation is just an example of such a thermal impact that leads to deterioration of corrosion resistance, heterogeneity of alloying elements like this is suspected to be involved in inducing microbial attachment. The idea that such changes in metallurgical properties not only may contribute to the deterioration of corrosion resistance of materials but also increase the susceptibility to MIC is currently gaining researchers' attention.

In the following section, the authors refer to some cases of MIC of stainless steel and outline the correlation between MIC and microbial adhesion.

16.2 MIC in Stainless Steel Welds

MIC has been reported as the cause for various structural damages in industries. This unexpected corrosion failure and rapid increase in corrosion rate in stainless steel structures exceed the material risk assessment, and this makes MIC a matter of considerable concern in material engineering. To make matters worse, corrosion damage is concentrated in the vicinity of stainless steel welds in many cases. Although the reason has not been elucidated until now, it is known that both bacterial adhesion at the welded portion and the incidences of MIC in and around welds are high.

Figure 16.1 shows a SUS304 steel joint (weld) used in a wastewater treatment plant (Kikuchi and Sreekumari 2002). Large corroded area is confirmed around the weld area. This corrosion incidence has been reported within a few months after being put into use. Although the corrosion resistance of the material to the environment was considered to be sufficient at the design phase and construction stages, both the corrosion dimension and rate were extremely larger than corrosion engineering assumptions. It was confirmed that the possibility of poor welding was infinitely zero during the failure analysis. This was one of the major factors for suspecting the possibility of MIC occurrence.

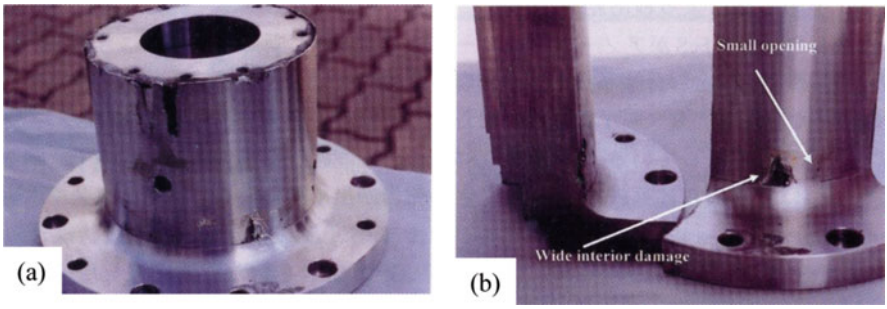

Fig. 16.1 Figure showing suspected MIC in a SUS304 piping fitting units used in a wastewater treatment plant. (**a**) Appearance of piping fitting units. (**b**) Enlarged image of the corrosion site

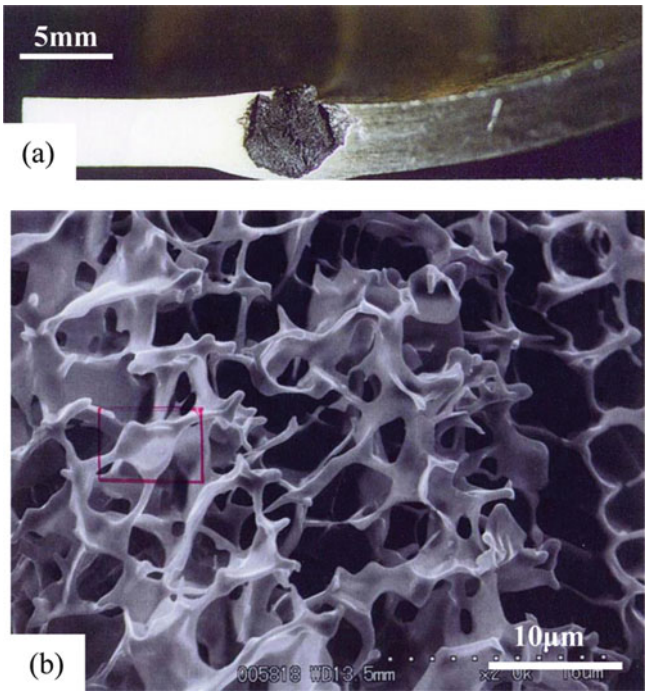

Fig. 16.2 A suspected MIC case occurred on a SUS316 cooling water piping in a power plant. (**a**) Cross-sectional image of corrosion part around welds. (**b**) SEM micrograph of corrosion site. (The tendency of selective corrosion of austenitic phase was confirmed by EDX)

Another failure case analysis involved SUS316L from a cooling water piping system in an energy plant. Figure 16.2 shows a cross-sectional image of corrosion failure part in the welds perpendicular to the welding direction (Miyano and Kikuchi 2008). In visual observation, significant corrosion damage was confirmed at the inner surface contacting the cooling water around weld and the HAZ regions. Observation of these parts under a scanning electron microscope (SEM) showed selective corrosion dissolution of the austenitic phase. Since the cooling water flowing through the pipe was neutral and at room temperature, the corrosion risk was considered to be low from the corrosion engineering viewpoint. However, a water leak was discovered within a few months after construction of the plant and starting its operations. This is the reason why mechanical welding defects were initially suspected during the initial inspection, but a detailed re-examination concluded that the possibility of construction failure was extremely low.

The samples from the above incidence were brought back to the laboratory, and by using simulation experiments, the risk posed by MIC was examined (Miyano et al. 2004). As shown in Fig. 16.3a, the SEM images showed remarkable bacterial attachment and biofilm formation on the SUS316 weld test pieces exposed to the bacterial culture for 56 days. Figure 16.3b shows the results of SEM observation

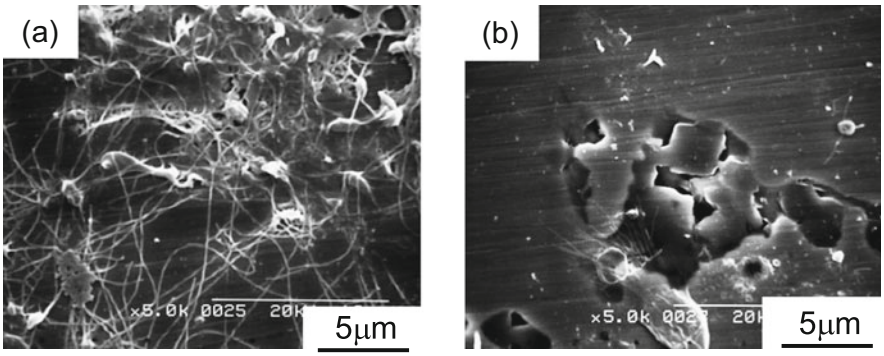

Fig. 16.3 Figures showing MIC in laboratory simulation tests. (**a**) Biofilms formed on the surface of a SUS316 weld specimen by exposure test in a flask. (**b**) Pitting corrosion confirmed in the same field of view as (**a**) after the removal of biofilms

performed on the same field of view but after removing the biofilm. Corrosion pits generated below biofilms were clearly confirmed. The extend of bacterial attachment was observed to be more in stainless steel welds where MIC incidence was remarkably higher than in the base metal.

Similar rate of microbial adhesion was observed on polished surfaces of stainless steel in the areas of welds. There are many reports showing that a large amount of microorganisms adheres to the stainless steel welds even after polishing to a smooth surface finish. This shows stainless steel welds can easily attract microorganisms. However, there is not much data available as to why the microbial adherence is predominant on stainless steel welds. In the following section, the authors would like to mention the available information on this issue from a material engineering viewpoint.

16.3 Lab Study on Microbial Adhesion on Stainless Steel Welds

As previously mentioned, there is a correlation between bacterial adhesion and occurrence of MIC. The process begins by the adhesion of bacteria on the wet material surface leading to biofilm formation and initiation of MIC. Metal surfaces to which microbes are adhered have different properties than those of glass, resin, etc. The metal microstructure includes grain boundaries and precipitates, i.e., a disorder of the atomic arrangement or a nonuniform part. These metallurgical factors characterize the physical and chemical properties of metal surfaces.

The following results show the effect of macroscopic morphologies of metal surface on the bacterial adhesion. Figure 16.4 shows results of numerical analysis at a two-dimensional laminar flow field that is showing macroscopic (mm-order scale)

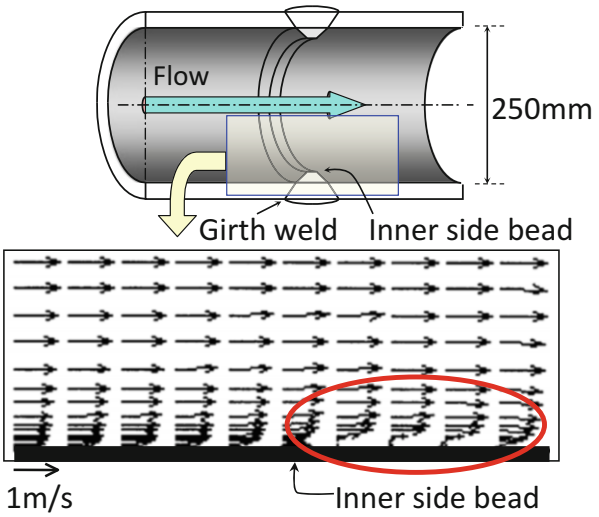

Fig. 16.4 Results of the numerical analysis at a two-dimensional laminar flow field around the inner side of welded pipes

geometry near stainless steel (SUS304) welds that assist microbial adhesion and induce corrosion (Amaya et al. 2001). When a weld shape is present in a flow field such as a cooling water pipe, there may be flow velocity variation around the weld part compared to the non-weld (base metal) part. The concept is that this slowing down of flow near the weld surface assists the adhesion of microbes and, as a result, MIC initiation. As shown in Fig. 16.5, bacterial adhesion is significantly higher near the weld area where the flow velocity is slow. From the uniaxial flow field reproduced by the numerical calculation of the flow field, the tendency of increased microbial adhesion around the convex part of the weld (the toe (Toe) and the heat-affected zone (HAZ)) has been confirmed.

Figure 16.6 shows the correlation between the initial microbial adhesion (within 2 h from the start) and the microstructure, i.e., grain boundary or phase interface, of a SUS304 base metal and welds (Sreekumari et al. 2001). The images were obtained by a superimposing method using two types of images. One type is fluorescence micrographs from microbial adhesion tests on mirror-polished test specimens (tested bacteria are appearing as orange spots); another is an optical microscopy image acquired after crystal grain boundaries are revealed by etching (same field of view as fluorescence microscope observation for bacterial adhesion). The tendency for preferential bacterial attachment to grain boundaries or phase interfaces is clearly confirmed. More interestingly, although the specimens were mirror finished to eliminate the effect of the surface morphology on bacterial adhesion, the weld specimen shows larger amount of adhesion and proliferation of tested bacteria than the base metal. To summarize the observation here, in the case of stainless steel, the amount of bacterial adhesion increases as the microstructure becomes finer and the microbial adhesion to the weld is larger than that of the base metal possibly because of more grain boundaries and inclusions. However, the reason has not been clearly identified yet.

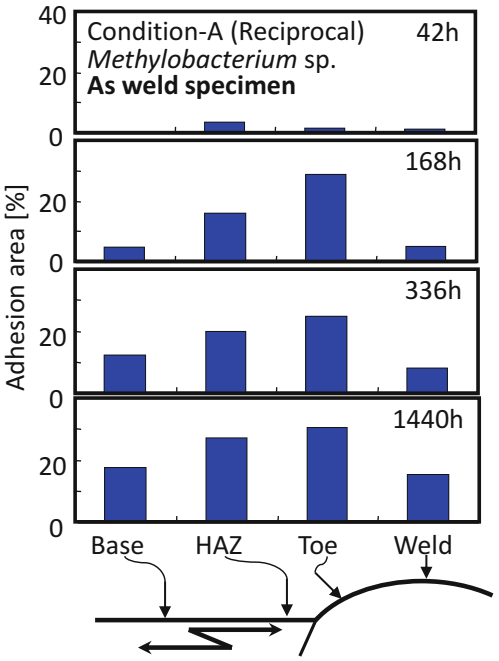

Fig. 16.5 Comparison of adhesion area of bacteria on as-weld specimen in laboratory simulation tests

Certainly, the microstructure of stainless steel welds forms fine solidification structure with fine phase interface at high density due to quick heating and quenching during welding process. Generation of grain boundary segregation and sensitized structure also occur in this process. In previous studies on the correlation between microstructure and bacterial adhesion, the possibility that the localization of surface energy, the precipitation including elements with high affinity for bacteria, and the grain boundary energy inducing the bacterial adhesion are discussed (Sreekumari et al. 2001). In the field of material science, how the metallurgical factors such as the ones mentioned above affect the bacterial adhesion has become a challenging research theme and is attracting attention. From this point of view, the authors would like to introduce the results of investigation on the effects of alloying elements on bacterial repellency, i.e., alloying elements which have antibacterial properties, on the attachment of microorganisms.

16.4 Bacterial Adhesion on Antibacterial Stainless Steel

It is well known that metals such as Cu or Ag suppress the growth of microorganisms. Although not originally developed for suppressing MIC, materials that are classified as antibacterial stainless steels are manufactured by adding Cu or Ag as alloying elements. Here, the authors would like to introduce some results of

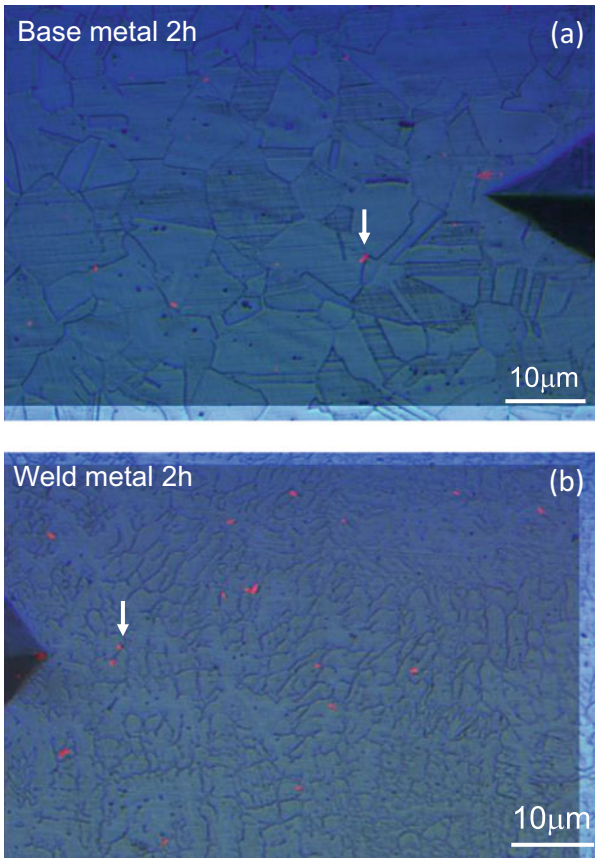

Fig. 16.6 Correlation between initial bacterial adhesion and stainless steel microstructure, i.e., grain boundary in the base metal or phase interface formed by ferrite and austenite phases in welding materials. (**a**) Base metal surface. (**b**) Weld metal surface

interaction of microorganisms and antibacterial materials. Figure 16.7 shows the results of bacterial adhesion on copper-containing antibacterial stainless steel and general stainless steel SUS304 (Sreekumari et al. 2005). The orange color spots indicate bacteria attached on the material surface. It can be seen that the bacterial adhesion on antibacterial stainless steel is significantly lower compared to the general stainless steel. Figure 16.8 shows the result of a similar study performed on silver-containing antibacterial stainless steel and general stainless steel SUS304 (Kikuchi and Sreekumari 2002). Similar to the previous study, the bacterial adhesion was significantly lower in the silver-containing antibacterial stainless steel. These studies were conducted in the laboratory using isolated pure cultures of corrosive bacteria. Further studies were carried out to evaluate the performance of silver-containing antibacterial stainless steel exposed to natural microbial flora in a fresh-water pond. Although the evaluation period was only 30 days, as shown in Fig. 16.9, the antibacterial stainless steel significantly reduced the natural biofilm formation (Kikuchi and Sreekumari 2002).

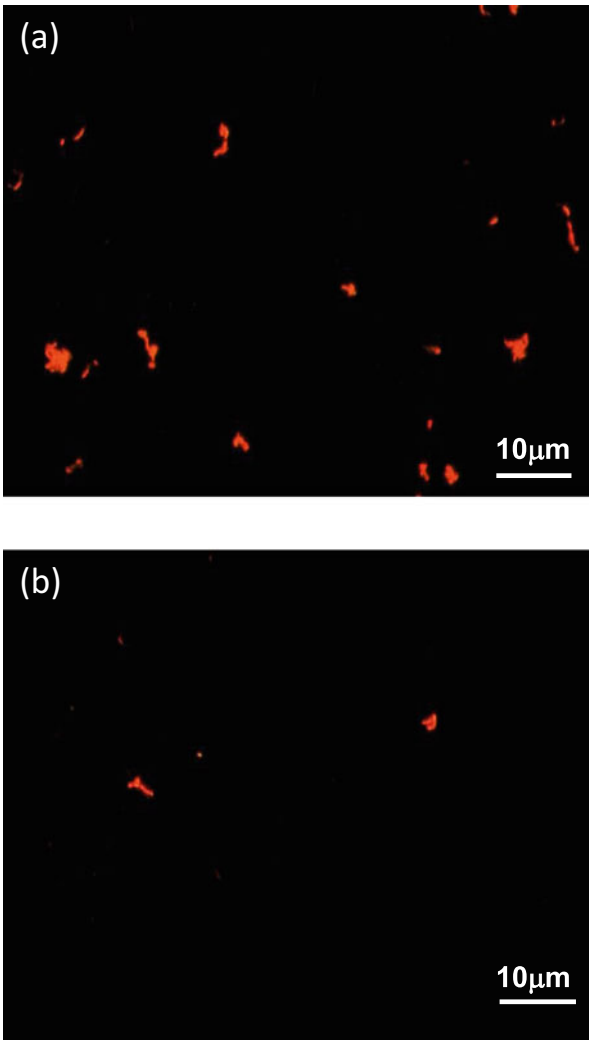

Fig. 16.7 Images of copper-containing antibacterial stainless steel in a laboratory study. (**a**) General stainless steel. (**b**) Copper-containing antibacterial stainless steel

Before these materials can be used commercially, we need more intense studies to understand the effectiveness of these materials to prevent biofilm formation on a longer period. However, biofilm formation or biofouling prevention function of these materials proposes new possibilities for industrial application. Recently, one of the practical strategies for using antibacterial materials to control MIC, the choice of copper as over pack barrier materials for geological treatment of radioactive waste (METI Database 2018), attracted attention.

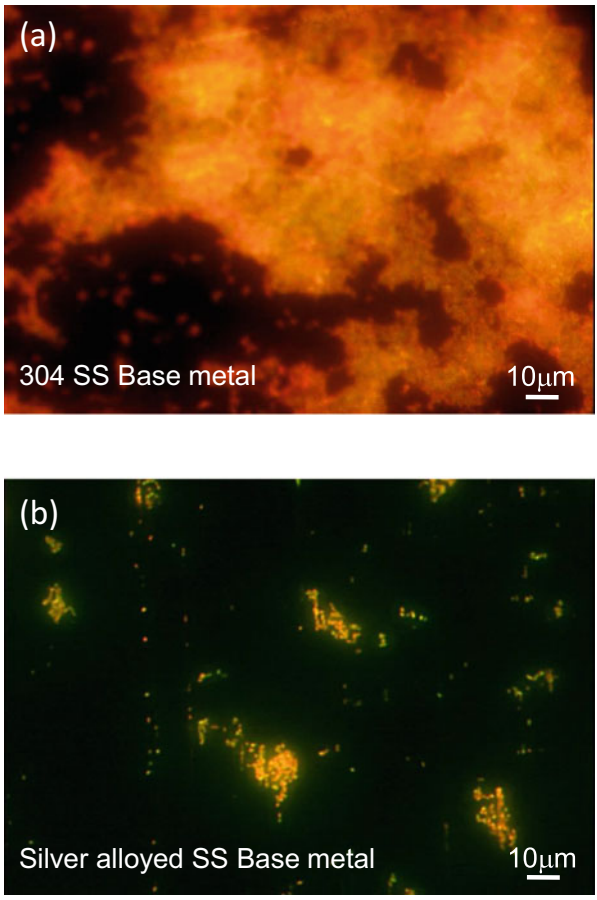

Fig. 16.8 Images of silver-containing antibacterial stainless steel in a laboratory study. (**a**) General stainless steel. (**b**) Silver-containing antibacterial stainless steel

16.5 Research Prospects for Material Microbe Interactions

The authors have reviewed the relationship between metal surfaces and adhesion of microorganisms. However, it is clear that various metallurgical factors that can affect the adhesion of microorganisms have been unexplored. It is very difficult to study the factors influencing the material microbe interactions in a comprehensive way as it needs both metallurgy and microbiology expertise. This is thought to be a major factor hindering the progress of research in this field. Here, the authors would like to introduce a pioneering result of in situ observation of MIC initiation process on stainless steel welds by COCRM (Miyano et al. 2015). Figure 16.10 shows the results of continuous observation at a fixed point on SUS303 steel weld surface exposed to natural seawater for 15 h. Figure 16.10a shows a mirror-finished initial surface by buff polishing using diamond paste after wet polishing with emery paper. Although there are some fine damages due to embedding of abrasive particles, a

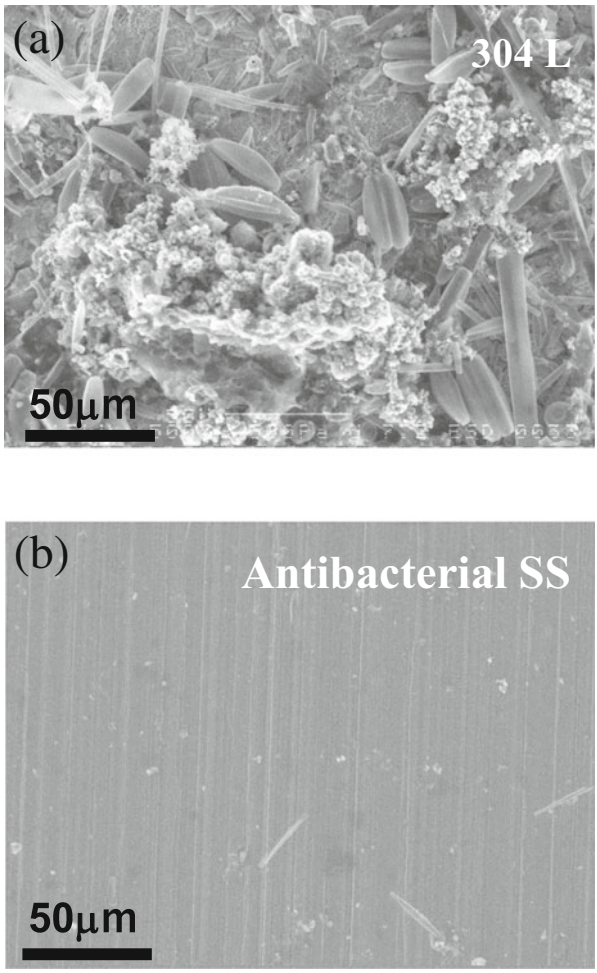

Fig. 16.9 Images of silver-containing antibacterial stainless steel exposed in a freshwater pond. (**a**) General stainless steel. (**b**) Silver-containing antibacterial stainless steel

sound initial surface without substantial irregular morphology can be clearly confirmed. Figure 16.10a–e are time lapse images of the surface of the test specimen during 15-h exposure test. This results show the beginning of bacterial attachment leading to the formation of biofilm and its impact on the changes of surface morphology of the test specimen. Figure 16.10f is a synthesized image of the fluorescence microscope image and the COCRM one acquired immediately after the image acquisition of Fig. 16.10e. The dye staining operation was performed during microscopic observation. The localization of the microbial cells identified by the green color is almost corresponding to the state of the test material shown in Fig. 16.10e. Note the fact that the microbial adhesion is localized, even though the initial surface was almost evenly smooth. This result suggests that the attachment of the microorganism to the metal and its subsequent growth are affected by

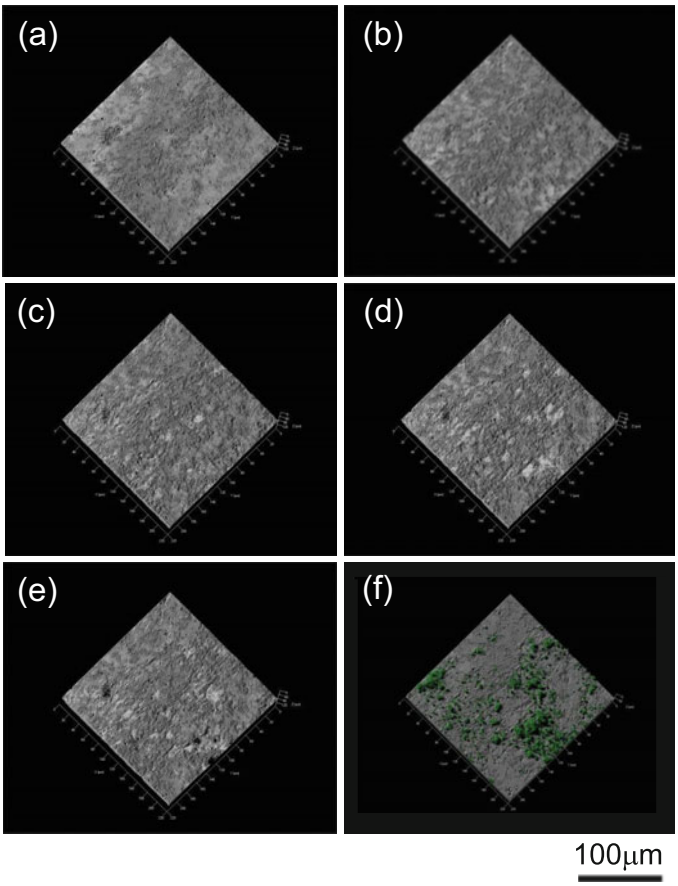

Fig. 16.10 15-hours fixed-point continuous observation results for in situ metal/microbial simultaneous observation designed to analyze biofilm formation and corrosion initiation process. The observation surface is mirror-finished SUS303 welds exposed in fresh marine water. (**a**) 0 h (immediately after exposure) and (**b**) 4 h, (**c**) 8 h, (**d**) 12 h, and (**e**) 15 h (immediately before the end of exposure test) and (**f**) a synthesized image of the fluorescence observation image and the COCRM one acquired immediately after the image acquisition of (**e**)

microstructure such as uneven distribution of elements on the metal surface. This research achievement has been evaluated as a breakthrough result of simultaneous in situ observation for microbial behavior and metal surface changes.

Similar studies on microbial attachment on metal surfaces using COCRM have been conducted on stainless steel base metals and its two welds types (Miyano et al. 2015). Figure 16.11 shows the difference of bacterial adhesion in each of these samples. Although the surface of the test specimen was smooth-finished by polishing, in SUS303 weld which has welding solidification structure and contains higher P and S content compared with SUS304, a large amount of bacterial adhesion

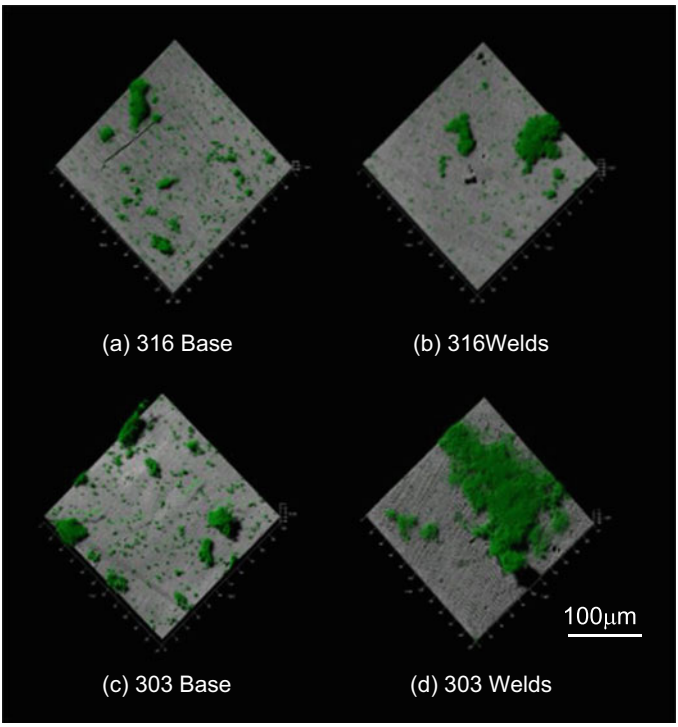

Fig. 16.11 Synthesized image of the fluorescence micrograph and the in situ metal/microbial simultaneous observation after 12-h exposure test in fresh marine water. (**a**) SUS316 steel base metal, (**b**) SUS316 steel weld metal, (**c**) SUS303 steel base material, (**d**) SUS316 steel weld metal. The surface of each specimen was mirror finished with diamond paste

was confirmed. Previous studies have shown that microbial adhesion to welds tends to be significantly greater than the base metal and that the reason for this is considered to be the effect of alloying elements to which microbes have some affinity. The results presented here indicate that the alloying element concentration influences the initial bacterial adhesion and thereby the biofilm formation. These results indicate the potential for acquiring new knowledge based on dynamic analysis of bacterial behavior to metals by applying new technologies such as COCRM. The authors hope that research related to the interaction between microorganisms and metals will be further expanded, starting from the analysis of MIC, and may result in the prevention of MIC.

References

Amaya H, Kikuchi Y, Ozawa M, Miyuki H, Takeishi Y (2001) Effect of adherent bacteria on microbially influenced corrosion (MIC) of stainless-steel welded joints. Quart J Jpn Weld Soc 19(2):345–353

Borenstein SW (1991) Microbiologically influenced corrosion of austenitic stainless-steel weldments. Mater Perform 30(1):62

Borenstein SW (1994) Microbiologically influenced corrosion handbook. Woodhead Publishing Ltd., New York, pp 1–50

Borenstein SW, Lindsay PB (1987) Microbiologically influenced corrosion failure analysis. In: Proceedings of NACE international annual conference, Houston, Texas, United States, Paper no. 381

Enos DG, Taylor SR (1996) Influence of sulfate-reducing bacteria on alloy 625 and austenitic stainless-steel weldments. Corrosion 52(11):831–842

Kikuchi Y, Sreekumari KR (2002) Microbially influenced corrosion and biodeterioration of structural metals. Tetsu-to-Hagane 88(10):620–628

Licina GJ (1998) Sourcebook for microbiologically influenced corrosion in nuclear power plants. Electric Power Research Institute Report, pp 1–22

Little BJ, Wagner PA, Hart KR, Ray RI (1996) Spatial relationships between bacteria and localized corrosion. In: Proceedings of NACE international annual conference, Denver, USA, Paper no. 278

Miyano Y, Kikuchi Y (2008) Microbiologically influenced corrosion on metal welds. J Jpn Weld Soc 77(7):650–657

Miyano Y, Yamamoto M, Watanabe K, Oomori A, Kikuchi Y (2004) Corrosion behavior of stainless-steel welds by microbes in marine water. Quart J Jpn Weld Soc 22(3):443–450

Miyano Y, Inaba T, Nomura N (2015) Visualization of microbiologically influenced corrosion by an in-situ investigation technique for metal/microbial simultaneous observation. Zairyo-to-Kankyo 64(11):492–496

METI Database (2018). http://www.meti.go.jp/committee/kenkyukai/energy_environment/chisou_shobun_chousei/pdf/003_03_00.pdf

Obukwe CO, Westlake DWS, Cook FD, Costerton JW (1981) Surface changes in mild steel coupons from the action of corrosion-causing bacteria. Appl Environ Microbiol 41(3):766–774

Sreekumari KR, Nandakumar K, Kikuchi Y (2001) Bacterial attachment to stainless steel welds: significance of substratum microstructure. Biofouling 17(4):303–316

Sreekumari KR, Sato Y, Kikuchi Y (2005) Antibacterial metals—a visible solution for bacterial attachment and microbiologically influenced corrosion. Mater Trans 46(7):1636–1645

Walsh D, Willis E, Van DT, Sanders J (1994) The effect of microstructure on microbial interaction with metals accent welding. In: Proceedings of NACE international annual conference, Baltimore, USA, Paper no. 612